Development of an uncertainty analysis framework for model-based consequential life cycle assessment

Document status and date:
Published: 20/04/2021

Document Version:
Publisher's PDF, also known as Version of Record (includes final page, issue and volume numbers)

Please check the document version of this publication:

• A submitted manuscript is the version of the article upon submission and before peer-review. There can be important differences between the submitted version and the official published version of record. People interested in the research are advised to contact the author for the final version of the publication, or visit the DOI to the publisher's website.
• The final author version and the galley proof are versions of the publication after peer review.
• The final published version features the final layout of the paper including the volume, issue and page numbers.

Link to publication

Download date: 05. Oct. 2023

Development of an uncertainty analysis framework for model-based consequential life cycle assessment.

Application to
activity-based modelling and life cycle assessment of multimodal mobility.

PROEFSCHRIFT

ter verkrijging van de graad van doctor aan de Technische Universiteit Eindhoven, op gezag van de rector magnificus prof.dr.ir. F.P.T. Baaijens, voor een commissie aangewezen door het College voor Promoties, in het openbaar te verdedigen op dinsdag 20 april 2021 om 13:30 uur

door

Paul Martin Baustert

geboren te Friesach, Oostenrijk

Dit proefschrift is goedgekeurd door de promotoren en de samenstelling van de promotiecommissie is als volgt:

voorzitter: prof.dr.ir. T.A.M. Salet
1^e promotor: prof.dr.ir. S. Rasouli
2^e promotor: prof.dr.ir. H.J.P. Timmermans
copromotor(en):   dr. E. Benetto (Luxembourg Institute of Science and Technology)
leden: prof.dr.ir. B.J.E. Blocken
                       dr. R. Heijungs (VU)
                       prof.dr. G.C. de Jong (Leeds University)

Het onderzoek of ontwerp dat in dit proefschrift wordt beschreven is uitgevoerd in overeenstemming met de TU/e Gedragscode Wetenschapsbeoefening.

Acknowledgements

When I first though about becoming an engineer, I imagined my future with precision. I imagined smooth surfaces and sharp edges. There was no doubt in my mind, that all things could be measured and all behaviours understood. The present dissertation marks the end of my journey from precision to uncertainty — the irony is not lost on me.

Following my application to the Luxembourg Institute of Science and Technology (LIST) for an open Ph.D. position, I quickly received an e-mail from Dr. Enrico Benetto inviting me to a first interview. A second interview followed, where I first met Dr. Tomás Navarrete Gutiérrez. On the 30th of May 2015 I ran my first (and to this day only) half marathon. On the 2nd of June I could barely walk the stairs up to office D1.01, which became my regular workplace until March of 2020.

I started to work on the CONNECTING project, which was launched upon my arrival at LIST, in collaboration with the Luxembourg Institute of Socio-Economic Research (LISER). The beginning of my Ph.D. was also the end of five and a half years abroad in Zurich. LIST is five minutes away from the primary school I attended and the house I grew up in. It all felt oddly familiar and thanks to Tomás, Antonino, Thomas (Gibon), Laurent, Florin, Alessio, Sameer, Kahina and my intern Paul, office D1.01 has always been more than just a room to me. They have all helped me in one way or another to reach my goals at LIST. I feel this especially now that I am forced to work in my kitchen/dining/living room due to the sanitary crisis.

On the 14th of July 2015 I met Prof. Harry Timmermans and Prof. Soora Rasouli and in September 2015 I was formally admitted as a Ph.D. student at the Eindhoven University of Technology (TU/e). Over the course of my Ph.D. project, my visits in Eindhoven have always marked important inflection points. My first audit was a kind reminder of what was expected and that a Ph.D. project requires a bit more preparation than a half marathon. Meetings with Prof. Harry Timmermans and Prof. Soora Rasouli always helped me to narrow down the subject, deepen my understanding of what was important, and open my mind up to new and interesting avenues.

During the first years of my Ph.D. I slowly adjusted to the topic and the project plan. Yet, early on there were warning signs that some key work packages I depended on would not be completed within the foreseen timespan. This marked the beginning of a challenging period and at times I was doubtful if I would be able to finish my work in time. I took on more responsibilities within the project to speed up the process, while participating in side projects with my fellow Ph.D. students Benoit Othoniel and Rodolphe Meyer. Looking back, I now know that these were very productive years, which allowed me to expand my horizon and refine my coding skills – those came in handy later on.

Following the prolongation of my contract for the fourth and final year, I was finally starting to catch up and to implement the core parts of the present work. However, at this point my funding was stating to dry up and I still had to produce results and write the manuscript. In May of 2019 I had the opportunity to apply for an engineering/post-doc position at LIST and on

the 31st of May I signed my new contract. While this provided me with some additional time to plan the final work on my dissertation, it added additional tasks on three projects with a wide range of topics. The time since has been a back and forth between working on the new projects and dedicating every hour I could carve out to finalising the present work.

The past years have allowed me to be close to my mother Irene and father John. I feel deep gratitude for their endless patience and unconditional support. While my brother Mathias has been living abroad for many years now, I always appreciate when we find the time to meet or video call, and I admire his honesty and wit. Finally, I would like to thank my wife Dominique for all her love and support.

Dippach, 2021

To Dominique — my love
and
To my son Mathis — who's light brightens even the darkest days.

Summary

Transportation is fundamental to fulfilling our human needs and travel demand is widely understood to be derived from the demand for activity participation. Transportation, much like all other economic processes, consumes energy (and other resources) and causes environmental interventions. The transport sector is a major contributor to Greenhouse Gas (GHG) emissions and in consequence to global climate change. The transport sector is also an emitter of many air pollutants causing respiratory and cardiovascular diseases among the affected populations which may lead to premature mortality.

These impacts have caught the attention of policy makers, who have tried to avoid or mitigate them using various policy options at their disposal. Often a broad range of transport policy options exist including economic measures (e.g., taxes and subsidies), regulatory measures (e.g., emissions standards) or infrastructural measures (e.g., public transport infrastructures). These decisions however come at a price (e.g., economic costs, ensuring enforcement etc.) and economic pressures force policy makers to take decisions that are both effective and efficient. Policy makers therefore desire an assessment of their alternative policy instruments and disciplines such as transportation planning and Industrial Ecology (IE) have emerged to provide adequate modelling approaches.

The CONNECTING project has taken on the challenge of proposing a modelling approach to provide scientific information on environmental impacts for various future transport policy scenarios. The project has led to the development of an Activity-Based Model (ABM) coupled to a Life Cycle Assessment (LCA), where the ABM allows to simulate a Daily Activity Pattern (DAP) for each individual of a population, while the LCA allows to assess the environmental impacts of a range of available transport modes from a life cycle perspective. The coupling allows to assess the environmental impacts of a population's travel demand (derived from the need to participate in daily activities) and is applied to a case study of French Cross-Border Commuters (CBCs) working in Luxembourg.

However, without a thorough and systematic analysis of the uncertainties of such a large and complex model, policy makers cannot be sure if the CONNECTING model's results are meaningful. Given this relevance and importance of Uncertainty Analysis (UA), the CONNECTING project dedicates a work package – of which the present thesis is the result – to the development of a framework towards UA of ABM/LCA coupled models. The aims of the present thesis are thus to develop a framework to systematically identify where uncertainty is present in an ABM/LCA coupled model and propagate the relevant uncertainties throughout the model to quantify the uncertainty of the model outputs. This framework is then applied to the specific case study of the CONNECTING project.

A first contribution of the present thesis is thus a new classification of uncertainty locations for ABM/LCA coupled models, building on the results of a systematic literature review. At the highest level the following uncertainty locations are distinguished: experimental frame, inputs, model and outputs. Each of these locations is further broken down into more specific locations

relating to parts of an ABM/LCA coupled model.

A second contribution of the present thesis is a set of three stochastic propagation schemes (and various sub-schemes) building on Monte Carlo (MC) sampling. These schemes are formulated for the two most widely addressed uncertainty locations of ABMs and LCA models (simulation error and model parameters) to propagate uncertainty from each location individually, as well as to perform joint propagation. The schemes, which are the first attempt to propagate uncertainty throughout ABM/LCA coupled models, allow to make several novel and relevant analyses operational, including assessing the magnitude of uncertainty stemming from both sub-models, the propagation of uncertainty from individual choice facets of the ABM (i.e., activity type, scheduling, location and mode choices) and accounting for dependencies among technosphere and biosphere exchanges in the Life Cycle Inventory (LCI). Finally, the application of the framework to the CONNECTING case study builds on the state-of-the art of uncertainty communication for comparative LCA, for several distinct policy scenarios.

The results of the case study allow to draw several relevant conclusions with regard to uncertainty analysis of ABM/LCA coupled models: (1) the conclusions of the model can be affected by uncertainty, where uncertainty communication measures suggest that there might be trade-off situations between different policy options (2) simulation error of the ABM part of the model contributes marginally compared to the contribution of the LCA measured parameters; (3) even though uncertainty stemming from the ABM part of the model is small, running the model stochastically (versus deterministic results) can both affect the median model outputs as well as the extent to which uncertainty potentially affects policy decisions.

Contents

List of Figures

List of Tables

Glossary of acronyms

A-LCA Attributional Life Cycle Assessment. 16

ABM Activity-Based Model. v, vi, 1, 3–7, 16–20, 22–32, 34, 36, 41–47, 49, 60, 62, 68, 69, 75–78, 82, 83, 85, 86, 88–90, 93, 94, 96–99, 106, 108–110, 113, 115, 117, 139, 140, 144, 145, 148, 151–156

AEIO Agents, Environment, Interactions and Organisation. 20

AgBM Agent-Based Model. 6, 7, 16, 19–24, 34, 68, 75, 76, 156

BEV Battery Electric Vehicle. 71

C-LCA Consequential Life Cycle Assessment. 4, 5, 16, 23, 151, 156

CBC Cross-Border Commuter. v, 4, 49–51, 55, 69–74, 79, 82, 94–96, 99, 106, 107, 117, 122, 127, 132, 140, 145, 151

CF Characterisation Factor. 9, 13, 15, 30, 36, 51, 61, 62, 75, 76

CI Confidence Interval. 47

CTV Contribution To Variance. 34, 156

CV Coefficient of Variation. 35, 47, 89, 97–100, 102–104, 106–111, 113, 116–118, 121, 123, 127–129, 131–134, 137, 140–142, 144–146, 154, 155

DAP Daily Activity Pattern. v, 3, 4, 17–20, 22, 23, 43, 50, 51, 53–55, 62–68, 75, 77, 94, 99, 107, 151, 152, 154

DQI Data Quality Indicator. 33, 34, 78, 79, 115

EF Environmental Footprint. 50

EoL End-of-Life. 2, 3, 8, 12, 22, 35, 60

EU-28 European Union (including the United Kingdom). 1–3

EV Electric Vehicle. 2, 4, 35, 37–39, 50, 82, 94–96, 120, 128, 147

GHG Greenhouse Gas. v, 2, 4, 13, 38, 51, 94, 95

GSA Global Sensitivity Analysis. 34, 156

GSD Geometric Standard Deviation. 80, 82

GTFS General Transit Feed Specification. 56, 57, 71

HEV Hybrid Electric Vehicle. 2, 4, 35

ICEV Internal Combustion Engine Vehicle. 2, 3, 35, 37, 50, 137

IE Industrial Ecology. v, 3, 4, 7, 20, 21

IIA Independence of Irrelevant Alternatives. 77

ISIC International Standard Industrial Classification of all economic activities. 80

LCA Life Cycle Assessment. v, vi, 1, 3–11, 13, 15, 16, 19–31, 33–38, 41, 42, 46, 47, 49, 50, 58, 59, 68, 69, 75–79, 82, 83, 85–90, 94, 106, 115, 119, 136, 137, 139, 140, 144, 145, 148, 151–156

LCC Life Cycle Costing. 8

Chapter 1

Introduction

This chapter will provide an introduction to the content of the present thesis, as well as the larger context it is embedded in. The aim is to establish the need for new and reliable modelling approaches to quantify environmental impacts of transport systems, by relating human travel demand to some of the most challenging environmental issues of our times. The thesis constitutes a distinct work package of the CONNECTING project. While the CONNECTING project aims at coupling an Activity-Based Model (ABM) and Life Cycle Assessment (LCA), the thesis is focussed on developing an appropriate Uncertainty Analysis (UA) framework for the CONNECTING model. The CONNECTING project is part of the FNR CORE program (C14/SR/8330766).

In the following, section 1.1 will present the broader context, section 1.2 will present the background of the CONNECTING project and the need for UA, before section 1.3 will elaborate on the aims of the thesis and its structure.

1.1 General context

1.1.1 Passenger transport and environmental impacts

Transportation is fundamental to fulfilling our human needs. Jones (1983) links the motivations for our daily behaviour (i.e., participation to activities) to the satisfaction of our various needs. Our daily activities (working, eating, recreational activities, etc.) in turn cause a need to travel between them, if these activities are taking place in different locations and their utility exceeds the travel dis-utility plus the utility from activities involving no travel (Jones, 1983; Bowman and Ben-Akiva, 2001). The travel demand on an individual level and the observed transport flows on the level of a population can thus be related to these activities and the utility gained from them.

The travels between our daily activities are enabled by various *transport modes*, which encompass the means of movement in space between different activity locations. Various categories of passenger transport modes can be distinguished, e.g., air, water, and land transport. Focusing on land transport modes, they can be further classified: with regard to their source of energy (human, animal, fuels, electricity, etc.); whether these sources are renewable or non-renewable; whether they are individual or collective; and with regard to the required infrastructure (e.g., rail or road transport). According to Eurostat (2017a), in the European Union (including the United Kingdom) (EU-28) in 2014 over 80% of inland passenger-kilometres (pkm) were travelled by means of passenger cars on roads. Road transport (passenger and freight) was responsible for

1

roughly one third of the final energy consumption (defined as the total energy consumed by end users) in the EU-28 in 2015, while other transport modes accounted for around 8%. While the share of renewable energy sources in the transport sector as a whole has been gradually increasing, in 2016 it still only reached 6.7% in the EU-28.

The processes involved in satisfying transport needs thus consume energy and much like all economic processes they also cause *environmental interventions* (Hensher and Button, 2003). These interventions can be defined as interactions between the economy (or technosphere) and the environment (or biosphere), and include, e.g., emissions (to air, water, and soil), resource extractions (mining minerals, drilling for oil, cutting down forests, etc.) and land use (urban, agricultural, forestry, etc.) (EC, 2010). Road transport is a major source of Greenhouse Gas (GHG) emissions (IPCC, 2015), atmospheric pollution (EEA, 2018a) and noise emissions (Fritschi et al., 2011). However, the environmental interventions are not limited to the transport use, but include the processes necessary for the production of the transport modes, such as resource extraction and processing (e.g., steel, plastics and glass), and recycling and waste disposal once a transport mode is no longer in use. The environment interventions thus occur during the entire *life cycle* of transport modes and are not limited to their use phase.

The undesirable impacts of these interventions are usually classified as environmental, human health or resource depletion impacts. Metals, rare-earth elements (i.e., neodymium or dysprosium used in electric motors) and other valuable materials needed for the production contribute to the scarcity of these resources. At the use phase fuel consumption contributes to the fossil fuel depletion, while air pollution due to exhaust and tire wear emissions (i.e., nitrogen oxides, ozone and particulate matter) cause respiratory and cardiovascular diseases among the effected populations and may lead to premature mortality (EEA, 2018a). Finally, at the End-of-Life (EoL) phase of transport modes, they cause waste generation and the release of hazardous substance contributing to environmental and human health impacts (Vermeulen et al., 2011).

1.1.2 Activity-based modelling and the life cycle perspective

All along the life cycle, carbon dioxide emissions thus contribute to anthropogenic climate change which increases pressures on many ecosystems diminishing their delivered services (IPCC, 2018). According to EEA (2018b) emissions from the EU-28 transport sector (including road and aviation) have increased since 2014, while average CO_2 emissions of newly registered passenger cars in its territory have increased since 2017[1]. Evaluating potential solutions, (e.g., electric mobility) from a life cycle perspective allows to quantify not only the potential benefits in one life cycle stage, (e.g., use phase) but also to take into account a possible burden shifting to other phases, (i.e., to the production or EoL phases) or from one to other impact categories.

Some of these impacts have caught the attention of policy makers, who have tried to avoid or mitigate them. Active policy instruments can be classified as information, economic and regulatory (Vedung, 2017). Governments use information campaigns and platforms to encourage the use of transport modes associated with lower impacts (e.g., the European Local Transport Information Service (ELTIS)[2]). Economic instruments include taxes (e.g., most EU-28 member states apply CO_2 taxes to vehicle ownership/registration according to the European Automobile Manufacturers' Association) and incentives or subsidies (e.g., offering an incentive to purchase a lower CO_2-emitting vehicle such as a Hybrid Electric Vehicle (HEV) or an Electric Vehicle (EV) instead of an Internal Combustion Engine Vehicle (ICEV)). Regulatory instruments include emission standards, control of technologies or operation and production standards (most prominently the European emission standards have been introduced in 1992 and stricter limits have been

---

[1] https://www.eea.europa.eu/data-and-maps/data/co2-cars-emission-18
[2] http://www.eltis.org/

introduced regularly since). Besides these policy instruments, infrastructural measures (e.g., charging stations and Public Transport (PT) infrastructures) are key to render transport modes associated with lower impacts competitive with individual mobility using ICEVs.

These decisions however come at a price (e.g., economic costs, ensuring enforcement etc.) and economic pressures force policy makers to take decisions that are both effective and efficient. Policy makers therefore desire an assessment of their alternative policy instruments (e.g., potential environmental benefits). Several research disciplines have evolved to produce such an assessment, such as urban, regional and transportation planning (studying the urban land use in connection with transportation systems and the impacts of policies on, e.g., economic, social and environmental aspects), and Industrial Ecology (IE) (studying material and energy flows through industrial systems and the related impact on the environment). In fact these two research fields are complementary when faced with research questions on sustainable transitions of mobility, where urban and transportation planning can link human decision making to transportation policies and planning aspects of cities, while IE can answer questions about the environmental interventions and impacts of these decisions.

In particular ABMs (having their roots in transportation planning) and LCA (stemming from IE) have emerged as appropriate modelling approaches for policy support in their respective domains. ABMs tackle the challenge of quantifying travel demand from a household or individual perspective as the decision unit, taking into account interdependencies between various factors underlying a Daily Activity Pattern (DAP) and allowing for higher temporal and spatial resolutions than conventional (i.e., four-step) models (Rasouli and Timmermans, 2014a). In practice, ABMs allow to assess a wide range of policy measures and scenarios related to the urban environment. These policy measures and scenarios can range from more imminent ones, such as new parking policies or toll strategies, to more long term ones, such as demographic change or shorter workdays (Davidson et al., 2007).

LCA, following an internationally standardised method (ISO, 2006b; ISO, 2006a), has emerged as an approach allowing to quantify all relevant emissions and resources consumed associated to a good or service over its life cycle (from "cradle-to-grave"), and is used to evaluate environmental policies (EC, 2010; Finnveden et al., 2009). This is achieved, by explicitly modelling the processes responsible for resource extraction ("cradle"), production, use phase and disposal or EoL ("grave"). Valuable policy recommendations regarding transport modes can be found in recent publications, e.g., Hawkins et al. (2013) and Bauer et al. (2015) on the life cycle impacts of passenger vehicles, where the importance of assessing potential burden shifting (by taking into account all life cycle phases), as well as considering a range of scenarios regarding key assumptions have been emphasized.

While both methodologies have their respective strength regarding policy support, their use in practice depends on the trust decision makers can put in their results. One way to establish such a trust is to thoroughly investigate all uncertainties potentially affecting the model conclusions relevant to the policy decision. Possible outcomes and their associated probabilities of occurrence are typically presented as a result of UA, in contrast to only having one single model outcome, allowing to take decisions regarding the most effective policy measure based on such additional information.

1.1.3 The case of Luxembourg

The Grand Duchy of Luxembourg situated between Germany, France and Belgium is confronted to a particular situation with regard to passenger transport and urbanization. Luxembourg has a high proportion of its workforce travelling each day across national borders (approximately 45% according to STATEC (2018)), while at the same time having the lowest share of its popu-

lation living in cities (causing additional rural-urban commuting from the resident population). Luxembourg also exhibited the fastest population growth between 2004 and 2014 among the EU-28 (3.1% per year on average) (Eurostat, 2017b; Eurostat, 2017a). As such, the travel behaviour of the commuting population is central to the mobility situation in Luxembourg and the strong population growth is likely to cause additional mobility related challenges.

The main transport mode for commuters working in Luxembourg city is the car (Eurostat, 2017b). A recent study conducted among the resident and Cross-Border Commuter (CBC) population shows that the car accounts for 73% of all home-work commutes (61% drivers and 12% passengers), while PT accounts for only 19% and slow mobility for 8% (MDDI, 2018).

In 2011 road transport in Luxembourg was responsible for 76% of nitrogen oxides emissions, 59% of fine particulate matter emissions and 56% of GHG emissions (Eurostat, 2014).

International obligations (e.g., the Paris climate agreement[3]), European directives (e.g., the National Emission Ceilings Directive (NECD)[4]) and national goals to improve air quality and reduce GHG emissions have sparked policy action to foster PT use, as well as increase the share of EVs in the car fleet. Specifically, two objectives were set for 2020: 40'000 EVs in circulation and 19% of all travel conducted by PT (MDDI, 2012). More recently new objectives for 2025 have been formulated, e.g., to achieve 22% home-work travels to be conducted by PT and to increase the occupation rate of cars from 1.2 passengers per car (as measure for 2017) to 1.5 passengers per car. Several infrastructural projects have been launched to reach these objectives, such as the extension of the new tramway in the city of Luxembourg connecting multi-modal nodes, new charging infrastructures and incentives for HEVs and EVs, and the digitalization of the PT and car pooling offer[5] (MDDI, 2018).

Considering the high investments (especially of infrastructural measures), the question arises which policy actions are most promising to reach such objectives to reduce environmental interventions and avoid or mitigate the related impacts. The CONNECTING project – FNR CORE program (C14/SR/8330766) – has taken on this challenge by proposing a modelling approach to provide scientific information on environmental impacts for various future policy scenarios.

1.2 Background

1.2.1 CONNECTING project

At the core the CONNECTING project is at the nexus of behavioural science and IE. Its purpose is to assess the mobility policies of the Luxembourgish government with a specific focus on CBCs living in the French border region, by quantifying environmental impacts related to satisfying their transportation demand. The study period ranges from 2015 until 2025, for a set of policy scenarios including: the business as usual (BAU) scenario considering the most plausible policy action and the $GREEN$ scenario investigating policies in favour of a more sustainable development.

The innovative aspects of the CONNECTING project include the development of an ABM to simulate the population's DAPs and the coupling of that ABM to a LCA of the available transport modes. The developed ABM part of the model is composed of 4 sub-models generating the daily activities, forecasting activity durations, activity locations and mode choices for the commuting population. In order to assess the environmental impacts related to individual DAPs, the outputs of the ABM are transformed into a demand for products and services from the transport system.

---

[3]https://unfccc.int/process-and-meetings/the-paris-agreement/the-paris-agreement
[4]https://www.eea.europa.eu/themes/air/national-emission-ceilings
[5]https://www.copilote.lu/

The LCA part of the model allows to assess the environmental impacts from a life cycle perspective of this demand for products and services, where the system specific processes are modelled using regional data and projections. Overall, the CONNECTING model follows a Consequential Life Cycle Assessment (C-LCA) approach in a broad sense, as outlined by Marvuglia et al. (2013).

1.2.2 The need for uncertainty analysis

In general, the role of models in the context of policy making is to assess the likely reactions of the system to policy instruments under behavioural and structural constraints (Boulanger and Bréchet, 2005). CONNECTING is no exception to this, where the results are planned to be used in workshop settings as a planning tool, allowing for bi-directional feedback, e.g., feedback to policy makers regarding the impacts of their policy measures as well as feedback to the modellers regarding the realism of their approach. UA can play valuable roles in such a process. In this section some of these roles, relevant in the context of the CONNECTING project, are presented.

As a first, UA can increase the trust decision makers place in a presented model and ultimately lead to its use in practice. As argued in Cash et al. (2003), scientific information in environmental assessments is likely to influence decisions when it is credible (scientifically adequate), legitimate (respectful of divergent values) and salient (relevant to the decision-maker). One way to address scientific adequacy and achieve high scientific quality is to perform UA, allowing users of information to "assess its strength relevant to their purposes" (Funtowicz and Ravetz, 1990). In practice, this means that during CONNECTING workshops model results will be presented along with the associated uncertainty, taking into account the level of expertise of the target audience, e.g., building on a progressive disclosure of information (Kloprogge et al., 2007).

As a second, UA can help to guide model design, refinement and data collection during the iterative process of model development and use (Morgan et al., 1990). The modelling process with its UA is of iterative cyclic nature (Refsgaard et al., 2007; Baustert et al., 2018; Kolkman et al., 2005). The results of one iteration (e.g., model development, case study results, UA and Sensitivity Analysis (SA)) are used in subsequent iterations. When specific model components are identified as contributing largely to the uncertainty of the outcome, hindering the modeller and ultimately the decision-maker to draw relevant conclusions, additional or more specific data can be collected or additional model refinements can be made to reduce the uncertainty from these components. In the case of CONNECTING, this can be a valuable outcome of a workshop or stakeholder interaction, especially if stakeholders have access to relevant data sources.

Finally, as a third, uncertainty estimates can constitute valuable information during the decision making process itself. Policy makers provided with the probability of occurrence for each possible outcome, rather than one single model outcome, can make informed decisions potentially hedging away from undesirable outcomes.

Given the relevance and importance of UA, the CONNECTING project dedicates a work package – of which the present thesis is the result – to the development of an UA framework for ABM/LCA coupled models.

1.3 Aims and objectives of the Ph.D. project

The lack of an UA framework for sophisticated and complex C-LCA modelling approaches (such as the CONNECTING model) is a recognized obstacle to their application (Whitefoot et al., 2011). The aim of the present thesis is to address this challenge for ABM/LCA coupled models. The CONNECTING model and scenarios will serve as a case study in this endeavour and the work will thus focus on ABM/LCA coupled models in the context of mobility policies in

Luxembourg.

The specific research question derived from the CONNECTING project proposal is:

How to quantify uncertainty of ABM and LCA, and how to perform the uncertainty propagation for the coupling of these two models, in the context of mobility policy support?

The thesis aims at providing the state-of-the-art on the type of modelling approaches and respective UA methodologies. Further, the thesis aims at providing an uncertainty propagation framework suitable for the specificities of the CONNECTING model. Finally, the developed framework will be applied to the CONNECTING model.

Chapter 2 will present a literature review on both modelling approaches (ABM and LCA) and on attempts to couple an Agent-Based Model (AgBM) to LCA. This work is partially based on Baustert and Benetto (2017), but has been updated and elaborated on for the present thesis. The aim of the chapter is to provide a broad background to readers unfamiliar with either ABMs, LCA or both, and to establish the state-of-the-art on coupling attempts.

Chapter 3 will present a review on UA, both in general and focussed on ABMs and LCA. While the chapter is partially based on Baustert and Benetto (2017) and Baustert et al. (2018), it will introduce new uncertainty classifications for ABM/LCA coupled models and provide a focussed quantitative review of UA efforts in both fields.

Building on the review of chapter 2, chapter 4 will present the CONNECTING model and case study. This chapter is partially based on Mariante (2017) describing the development of the ABM of CONNECTING, and Baustert et al. (2019) describing the coupling of the ABM part and the LCA part of the CONNECTING model.

Building on the classifications and reviews of chapter 3, chapter 5 will present the advanced UA framework and conducted analyses for the present thesis. The focus is set on addressing uncertainty from all model parts (both separately and simultaneously) and communicating model output uncertainties to experts and decision makers.

Chapters 6-8 will present the results of this thesis, following the application of the methodologies advanced in chapter 5. While chapter 6 is concerned with uncertainty stemming from the ABM part of CONNECTING, chapter 7 focusses on uncertainty from the LCA part. Finally, chapter 8 combines uncertainties from both model parts.

Finally, chapter 9 will provide a discussion and the conclusions to the present thesis.

Chapter 2

Review of LCA, ABMs and their coupling

2.1 Introduction

Before reviewing the state-of-the-art of UA and describing the CONNECTING model in detail, a better understanding of the applied modelling approaches and general modelling paradigms needs to be established. The present chapter thus aims at providing a review on existing LCA and ABM approaches. LCA is an internationally standardised methodology building on a framework of distinct phases for which different computational methods and modelling approaches exist. ABMs are models that share some features, yet differ in their rich variety of computational structures and modelling approaches, and do not build on a common standardised framework. As both *activity-based modelling* and *agent-based modelling* are relevant to this chapter (and the thesis as a whole) it needs to be made clear that throughout this thesis, the acronym *ABM* will be used for activity-based model as the specific approach used in the CONNECTING model, while for the more general agent-based model paradigm the acronym *AgBM* is used.

When introducing LCA and ABMs, different approaches will be taken. For LCA the aim is to deepen the understanding of the existing standardised framework and give an overview of computational methods and modelling approaches. For ABMs, which have emerged as alternatives to conventional trip-based approaches, the aim is to establish some common features and provide an overview of existing modelling approaches.

Next, this chapter goes beyond the state-of-the-art by providing insights into the coupling of ABMs and LCA. To this end, a more general stance will be taken by relating ABMs to the AgBM paradigm. This will allow to review how AgBMs have emerged in IE and have been coupled to LCA. The coupling of AgBMs and LCA is described in terms of the type, degree and computational structure. The promises of coupling AgBMs and LCA are synthesised from literature and a focussed review of coupling efforts similar to the CONNECTING model is presented.

The structure of the chapter is as follows: section 2.2 introduces LCA; section 2.3 introduces ABMs; and section 2.4 reviews the coupling of AgBMs with LCA. A short summary is provided at the end of the chapter in section 2.5.

2.2   Life cycle assessment

LCA is an internationally standardised method (ISO, 2006b; ISO, 2006a) which allows to quantify all relevant emissions and resources consumed, and the related environmental impacts, health impacts and resource depletion issues, that can be associated to a good or service over its life cycle (EC, 2010).

The history of assessing the impacts of consumer products dates back to the late 1960s and early 1970s (Guinée et al., 2010). It coincided with an increasing awareness about finite raw materials and energy resources as well as environmental deterioration and predictions of climate change. This was illustrated by the formation of the club of Rome and publications such as Meadows et al. (1972). It was recognized that large shares of the environmental impacts occur during the production, transportation and disposal of products, and not only during their use. Thus the life cycle perspective for product comparison gained traction, with an ever broadening scope of considered impacts and increasing depth with regard to the sophistication of the underlying modelling (Guinée et al., 2010).

However, until the 1990s there was still a lack of a standardised approach and terminology leading to large variations in results of studies with similar objectives, hampering a wider application (Guinée et al., 2010). Thus, in the 1990s a number of guidelines and handbooks were published (e.g., Heijungs et al. (1992) and Vigon et al. (1993)) which ultimately led to the Society of Environmental Toxicology and Chemistry (SETAC) "Code of Practice" (Consoli, 1994) and the involvement of the International Organization for Standardization (ISO) to formally standardize the LCA "principles and framework" (ISO, 2006a) and "requirements and guidelines" (ISO, 2006b).

It needs to be specified that the focus of the CONNECTING project as well as of this thesis is environmental LCA and not social LCA (Jørgensen et al., 2007), Life Cycle Costing (LCC) (Swarr et al., 2011) or Life Cycle Sustainability Assessment (LCSA) (Finkbeiner et al., 2010). Therefore, the aim is not to address the economic or social aspects of a product or service, but only the environmental pillar of sustainability.

A second point that needs to be clarified is the definition of the life cycle, which in the CONNECTING project as well as the thesis follows a *cradle-to-grave* perspective (from resource extraction over production and use phases to the EoL phase). Specific implications of *cradle-to-gate* (from resource extraction to factory gate) or pure *cradle-to-cradle* (where the EoL phase is a recycling process) perspectives are not discussed here.

2.2.1   Terminology

A *product* is any good (e.g., vehicle) or service (e.g., transport). Products are provided by *unit processes*, the smallest elements transforming inputs into outputs, or *product systems* which are collections of unit processes. In the case of passenger transport, the product systems providing the service of transporting people from one location to another encompass many unit processes, such as vehicle production, assembly, use, maintenance and disposal.

The *system boundary* specifies which unit processes are part of a product system and which are not. The extraction and refining of fuel or production of electricity are usually viewed as part of different product systems, which however provide necessary products for passenger transport.

If a unit process or product system provides two or more products they are referred to as *co-products*. While nowadays such multi-output processes or product systems are less common in the domain of transport, an historic example is a mixed train transporting both passengers and goods.

Inputs and outputs can be characterised as: (1) *elementary flows* which are directly drawn

from (or released to) the environment without previous (or subsequent) human transformation; (2) *intermediate flows* which are product, material or energy flows occurring between unit processes; (3) *product flows* occurring between product systems. Examples of elementary flows are tailpipe emissions of vehicles such as carbon dioxide or nitrogen oxides. Intermediate flows occur, e.g., between unit processes contributing to vehicle component production and vehicle assembly. Product flows occur, e.g., between product systems providing fuel and electricity to the transport product system. The distinction between intermediate flows and product flows can however be subjective at times as product systems can be subdivided into smaller product systems or aggregated into larger ones depending on the specific context.

The *functional unit* allows for the quantification of the product performance and is the reference unit. The *reference flow* is the output of a product system required to deliver the functional unit. The functional unit can be defined as *the provision of transport services to a specific population in a region for a period of time*, while the reference flow quantifies the passenger-kilometres for each transport mode necessary to provide these transport services. LCA is a relative approach structured around this functional unit, often used in *comparative assertions* comparing the environmental performance of competing products (and their product systems) delivering the same functions.

LCA focusses on environmental impacts of a product system (with economic and social impacts considered out of the scope of LCA) aiming at considering all aspects of natural environment, human health and resources. These impacts are categorized in so-called *impact categories* representing environmental issues of concern (e.g., global warming potential, air pollution or fossil depletion). For each elementary flow relevant to an impact category a corresponding Characterisation Factor (CF) (derived from a characterisation model) allows to determine the impact in units of *impact category indicators*.

Four LCA phases are distinguished in ISO (2006a): the *goal and scope definition phase*, the *inventory analysis phase* (hereafter referred to as LCI), the *impact assessment phase* (hereafter referred to as LCIA) and the *interpretation phase*. Sometimes the goal and scope definition phase is treated as two separate phases: a goal definition phase and a scope definition phase (EC, 2010).

2.2.2 Four phases of LCA

The goal definition clearly states the intended application, reasons for carrying out the study and target audience. A study can for example present new methodological advances for the scientific community or investigate alternative processes to inform an industrial consortium about the most environmental friendly options. The scope definition identifies and defines the object of study in detail by defining, e.g., the product system and its functions, the functional unit, the system boundary, the chosen impact categories and methods, the required data (type, quality and sources), limitations and assumptions. When the object of study is a transport system, the product system includes all transport processes contributing to providing the functional unit. The relevant impact categories for a transport system could be respiratory disease and climate change related. Finally, the type of modelling is defined distinguishing the attributional and consequential approach. Section 2.2.5 will focus on both modelling approaches in more detail. The goal and scope definition phase thus frames the rest of the LCA study and subsequent phases.

During the LCI phase, data collection, system modelling and calculations are done in line with the goal definition and the requirements derived in the scope definition phase. This is done by describing the product system as a collection of unit processes. Each unit process is characterized by its inputs and outputs (or intermediate, product and elementary flows). Then, the collected data is related to these unit processes and scaled to the reference flow of the functional unit after validation, allowing to generate the results of the LCI analysis for the defined functional unit.
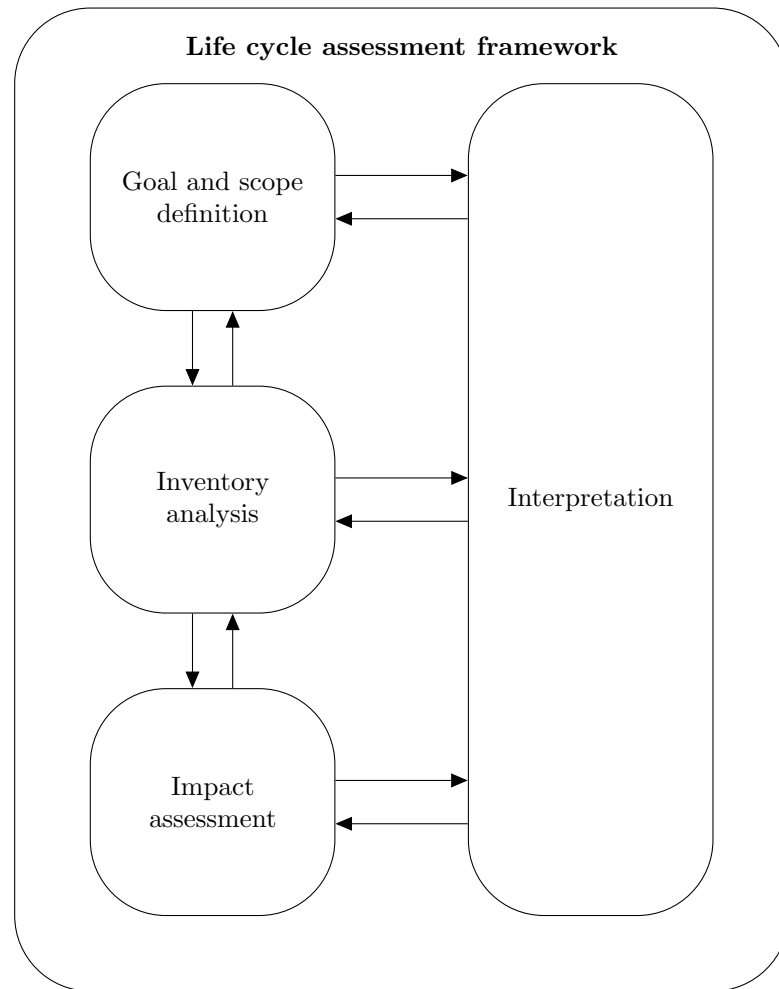
Figure 2.1: ISO flowchart of LCA framework (ISO, 2006b)

Following the LCI phase, the LCIA phase relates the LCI results to the impact categories selected in the scope definition phase and their impact category indicators. This is done by assigning LCI results to impact categories and calculating their impacts in terms of units of impact category indicators using Characterisation Factor (CF)s.

The existing computational methods for the LCI and LCIA phases will be introduced in sections 2.2.3-2.2.4.

Finally, during the interpretation phase the results of the LCI and LCIA phases are considered and conclusions, limitations and recommendations are provided, which are consistent with the goal and scope definitions. It should be acknowledged that LCA is a relative approach intended for comparison on the basis of the functional unit and indicating potential environmental effects.

The interpretation phase, together with all other LCA phases are embedded in an iterative framework allowing for feedback between phases and modifications of the original goal and scope, inventory, impact assessment and interpretation as shown in figure 2.1.

2.2.3 Process flow diagram

To arrive at the life cycle impacts of a product or service, two different computational problems have to be solved. First, the so-called *inventory problem* has to be solved, which is defined as "the task of scaling all unit processes in the system in such a way that they exactly produce the reference flow [...]" (Heijungs, 2010). Second, the environmental interventions and related impacts of this system of scaled unit processes need to be assessed.

Two computational methods have coexisted for LCA. While early LCA studies relied primarily on the *process flow diagram* (or sequential) approach, upon the emergence of the *matrix inversion* approach, the latter has become increasingly popular and is used in many LCA software (e.g.,

Table 2.1: Unit process stand-alone data.

Process		Amount	unit
Raw material extraction			
	Inputs		
	Raw material	1	kg
	Outputs		
	Raw material	1	kg
	Carbon dioxide	10	kg
Energy provision			
	Inputs		
	fossil fuel	0.02	kg
	Outputs		
	Energy	1	MJ
	Carbon dioxide	0.06	kg
Product manufacturing			
	Inputs		
	Raw material	1	kg
	Energy	100	MJ
	Outputs		
	Product	1	kg
Product use			
	Inputs		
	Product	0.1	kg
	Outputs		
	Waste	0.1	kg
	Product function	1	unit
Product disposal			
	Inputs		
	Energy	5	MJ
	Waste	1	kg
	Outputs		
	Carbon dioxide	5	kg
	Methane	2	kg
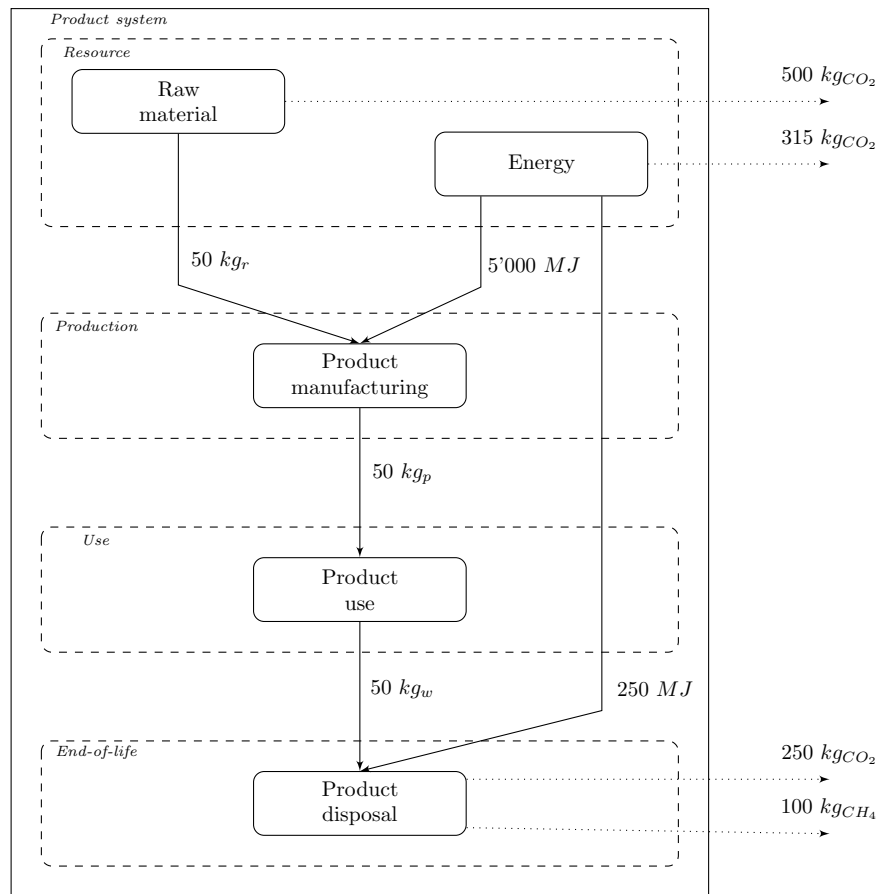
Figure 2.2: Process flow diagram of toy example.

openLCA[1] or brightway2[2]). While the matrix inversion approach has been applied before, Heijungs and Suh (2002) introduce the first comprehensive and coherent overview. While this section introduces the process flow diagram approach, the next section will introduce the matrix inversion approach.

The process flow diagram approach consists of representing the system as a directed graph where unit processes are represented as nodes and flows are represented as arrows. Next, the unit process data is transformed into *stand-alone data* (e.g., inputs and outputs are scaled for a standard unit of output for each sub-system), before sequentially moving upstream the graph while scaling the inputs and outputs of each unit process to the amounts required by downstream unit processes, until the entire product system exactly provides the functional unit (Lesage and Muller, 2017). To illustrate the approach a very simple set of unit process stand-alone data is listed in table 2.1.

To solve the inventory problem, each input and output in table 2.1 needs to be scaled in order for the entire product system to produce a reference flow. Assuming that the functional unit is "the provision of 500 product usages", one can scale all flows for the entire life cycle of

---

[1]https://www.openlca.org/
[2]https://brightwaylca.org/

the toy example using plain algebra to arrive at the values in figure 2.2. Figure 2.2 thus shows a simple process flow diagram, where each box (or node) corresponds to one unit process and each arrow corresponds to a flow. The cradle-to-grave life cycle perspective is illustrated by regrouping unit processes according to four life cycle phases (resource extraction, production, use and EoL). The intermediate flows are represented by continuous arrows while the elementary flows are represented by dotted arrows. For reasons of simplicity only carbon dioxide and methane emissions are shown in figure 2.2 and not all elementary flows.

Now, the cumulative environmental interventions can be calculated. This is done by summing the environmental intervention for each scaled unit process. In case of the toy example the life cycle carbon dioxide emission can be assessed by summing all elementary carbon dioxide flows over the life cycle in figure 2.2 resulting in 1065 kg_{CO_2}. Using the same approach, the life cycle emissions of methane arrive at 100 kg_{CH_4}. It is apparent that in case of a large number of unit processes and considered elementary flows this becomes an impractical task. However more recently, this graph based approach has received new attention in order to make dynamic full temporalization of LCA calculations operational (Pigné et al., 2019).

Several complications might arise, which are not covered in this simplistic example. For unit processes that have more than one function, producing two or more co-products, multifunctionality issues arise. These issues can be solved using one of three approaches: (1) *sub-division* into smaller unit processes each having only one function; (2) *partitioning* (or allocation) of process flows based on coefficients (e.g., mass-based, economic value-based, energy content-based, etc.); (3) *substitution* where the impact of alternative processes yielding unused co-products (or similar products) is subtracted from the impact of the unit processes. Once all multifunctionality issues of a process diagram are solved, the cumulative environmental interventions can be computed as shown above. Another issues occurs when the process flow diagram is not a directed acyclic graph (DAG) and exhibits feedback loops. In such cases, the solution can be approached iteratively or solved using infinite geometric progression as shown in Suh and Huppes (2005).

The second problem (computing the environmental impacts of the total environmental interventions) can be solved by multiplying the LCI results with the respective CFs to arrive at the environmental impacts for a specific impact category. In the toy example, to arrive at the global warming potential impact measured in $kg_{CO_2 equivalents}$, the life cycle emissions for each GHG (e.g., carbon dioxide or methane) need to be multiplied with the corresponding CFs (e.g., 1 $\frac{kg_{CO_2 equivalents}}{kg_{CO_2}}$ or 37 $\frac{kg_{CO_2 equivalents}}{kg_{CH_4}}$). Taking into account both the carbon dioxide and methane emissions of the toy example one arrives at a score of 4765 $kg_{CO_2 equivalents}$ for the chose functional unit.

2.2.4 Matrix inversion approach

The matrix inversion approach builds on a matrix representation of the product system, which resembles input-output analysis (e.g., Leontief (1986) and Duchin (1992)) as first presented in Heijungs (1994) and further developed by Heijungs and Suh (2002). To this end unit process stand-alone data are formulated as vectors, where process flows **a** and elementary flows **b** are distinguished:

$$\begin{pmatrix} \mathbf{a} \\ \mathbf{b} \end{pmatrix} = \begin{pmatrix} a_1 \\ \vdots \\ a_k \\ \vdots \\ a_m \\ b_1 \\ \vdots \\ b_q \\ \vdots \\ b_r \end{pmatrix}$$

The convention is that inputs are negative and outputs are positive. All unit processes of a product system can be represented as vectors, while the entire product system can be represented as a matrix, where $\mathbf{A}$ is referred to as the technosphere matrix and $\mathbf{B}$ the intervention matrix, containing the stand-alone data. The general form is presented by the left side matrix, while the right side matrix contains the flows of the toy example presented in table 2.1:

$$\begin{bmatrix} \mathbf{A} \\ \mathbf{B} \end{bmatrix} = \begin{bmatrix} a_{1,1} & \cdots & a_{1,l} & \cdots & a_{1,n} \\ \vdots & & \vdots & & \vdots \\ a_{k,1} & \cdots & a_{k,l} & \cdots & a_{k,n} \\ \vdots & & \vdots & & \vdots \\ a_{m,1} & \cdots & a_{m,l} & \cdots & a_{m,n} \\ b_{1,1} & \cdots & b_{1,l} & \cdots & b_{1,n} \\ \vdots & & \vdots & & \vdots \\ b_{q,1} & \cdots & b_{q,l} & \cdots & b_{q,n} \\ \vdots & & \vdots & & \vdots \\ b_{r,1} & \cdots & b_{r,l} & \cdots & b_{r,n} \end{bmatrix} = \begin{bmatrix} 1 & 0 & -1 & 0 & 0 \\ 0 & 1 & -100 & 0 & -5.0 \\ 0 & 0 & 1 & -0.1 & 0 \\ 0 & 0 & 0 & 1.0 & 0 \\ 0 & 0 & 0 & 0.1 & -1.0 \\ 10 & 0.06 & 0 & 0 & 5.0 \\ 0 & 0 & 0 & 0 & 2.0 \\ 1 & 0 & 0 & 0 & 0 \\ 0 & 0.02 & 0 & 0 & 0 \end{bmatrix}$$

For a given functional unit, the final demand vector $\mathbf{f}$ contains the reference flows. Again the final demand vector of the toy example is presented containing as a reference flow the 500 product usages:

$$\mathbf{f} = \begin{pmatrix} f_1 \\ \vdots \\ f_k \\ \vdots \\ f_m \end{pmatrix} = \begin{pmatrix} 0 \\ 0 \\ 0 \\ 500 \\ 0 \end{pmatrix}$$

The matrix inversion approach allows to solve the inventory problem through inversion of the technosphere matrix and multiplication with the final demand vector to yield the scaling vector $\mathbf{s}$ which contains the amounts needed of each reference product to provide the functional unit. Formula 2.1 holds true for squared technosphere matrices, where the number of processes (or number of columns n) is equal to the number of products (or number of rows m). This is

equivalent to solving the inventory problem in the process flow diagram, yet much more convenient in case of a large amount of data.

$$\mathbf{s} = \mathbf{A}^{-1}\mathbf{f} \tag{2.1}$$

The inversion of the technosphere matrix of the toy example yields:

$$\mathbf{A}^{-1} = \begin{bmatrix} 1 & 0 & 1 & 0.1 & 0.0 \\ 0 & 1 & 100 & 10.5 & 5.0 \\ 0 & 0 & 1 & 0.1 & 0.0 \\ 0 & 0 & 0 & 1.0 & 0.0 \\ 0 & 0 & 0 & 0.1 & 1.0 \end{bmatrix},$$

and the scaling vector of the toy example can be derived by multiplication with the final demand vector following equation 2.1. The values in the scaling vector $\mathbf{s}$ correspond to the values in the process flow diagram figure 2.2. However, $\mathbf{s}$ contains the aggregated amounts across in the whole product system, i.e., the second element is the sum of all energy consumptions needed to provided the function unit, including the 5'000 MJ for manufacturing and 250 MJ for disposal:

$$\mathbf{s} = \begin{pmatrix} 50 \\ 5250 \\ 50 \\ 500 \\ 50 \end{pmatrix}$$

By multiplying the intervention matrix with the scaling vector one can arrive at the results of the LCI (the cumulative environmental interventions), where $\mathbf{g}$ is the intervention vector:

$$\mathbf{g} = \mathbf{Bs} \tag{2.2}$$

In case of the toy example one can thus solve the inventory problem using equation 2.2:

$$\mathbf{g} = \begin{pmatrix} 1065 \\ 100 \\ 50 \\ 105 \end{pmatrix},$$

where the first element corresponds to the life cycle carbon dioxide emissions, the second element to the life cycle methane emissions, the third element ot the life cycle raw material consumption and the final element to the life cycle fossil fuel consumption.

Finally, using the characterisation matrix $\mathbf{Q}$ which contains the CFs for all chosen LCIA methods and all elements in the intervention vector, the impact vector $\mathbf{h}$ can be calculated. The intervention vector contains the life cycle environmental impacts of each chosen impact category the functional unit:

$$\mathbf{h} = \mathbf{Qg}, \tag{2.3}$$

where for the toy example only the global warming potential impact category is considered. $\mathbf{Q}$ thus contains the CFs for carbon dioxide and methane, while containing zeros for elementary flows with no impact on climate:

$$\mathbf{Q} = \begin{bmatrix} 1 & 37 & 0 & 0 \end{bmatrix},$$

and the final LCA results can be computed using equation 2.3:

$$\mathbf{h} = 4765$$

Similar to what has been mentioned above, in case of processes with multiple co-products a multifunctionality problems arises, which can be solved through allocation. This is of special importance to the matrix inversion approach, as multifunctionality causes the technosphere matrix to be rectangular. Specifically, as each process in the technosphere matrix is represented as a column and each product as a row, a process producing two co-products causes an imbalance of rows and columns thus leading to a non-squared matrix. Such a matrix cannot be inverted as written in equation 2.1 and partitioning, substitution or more advanced solutions to invert non-squared matrices are needed (see e.g., Marvuglia et al. (2009)).

While the occurrence of feedback loops pose a challenge to the process diagram approach, the matrix inversion approach remains valid as long as the technosphere matrix is squared. However, similar to multifunctional processes, some loops in the product system (e.g., closed loop recycling) can lead to non-squared matrices also requiring, e.g., partitioning, substitution or the use of pseudo-inverse in equation 2.4 (see, e.g., Heijungs and Frischknecht (1998)):

$$\mathbf{s} = (\mathbf{A}^T\mathbf{A})^{-1}\mathbf{A}^T\mathbf{f} \tag{2.4}$$

2.2.5   Attributional versus consequential approach

Two modelling approaches have emerged in literature and in the practice: Attributional Life Cycle Assessment (A-LCA) and Consequential Life Cycle Assessment (C-LCA) (Weidema, 2003). The approaches differ in the research question they address, where A-LCA addresses questions about the responsibility for a portion of the total environmental impact generated by a product system (e.g., the impact of a specific product), C-LCA addresses questions about the environmental consequences of a decision affecting a product system (e.g., purchasing an additional product). A-LCA thus looks at products at a particular point in time for a given amount of the functional unit (Rebitzer et al., 2004) and describes the environmentally relevant physical flows to and from its life cycle and subsystems (Curran et al., 2005; Ekvall and Weidema, 2004; Russell et al., 2005). An A-LCA is suited for cases where the steady-state assumption applies and the system can be described by average data in the technosphere matrix (Russell et al., 2005), because the existing market remains unaffected by the studied LCA (fully elastic market) (Marvuglia et al., 2013). As a consequence, the results scale linearly with the functional unit (Rebitzer et al., 2004). However, when the LCA is supposed to inform on the consequences of a change in demand for the functional unit underlying a decision process, A-LCA fails to describe the direct and indirect related impacts (Weidema et al., 1999).

To overcome this limitation, C-LCA includes the impacts generated by all the systems affected by the change in demand of the functional unit, also including processes affected through market relationships and not through physical ones (Dandres et al., 2011; Vázquez-Rowe et al., 2013; Marvuglia et al., 2013; Weidema, 1993). Also, C-LCA implies the integration of marginal technology data in the LCI instead of average data, a concept first formulated by (Weidema, 1993) and further developed in several studies, e.g., (Ekvall and Weidema, 2004; Weidema, 2003; Weidema et al., 1999). As a result, the LCA outcomes are no longer linearly dependent on the functional unit due to the expansion of the system, which takes into account indirect effects that occur outside of the original life cycle made of physical relationships between unit processes (Ekvall, 2000). These indirect effects can even surpass the direct ones in some cases (Fargione et al., 2008; Searchinger et al., 2008). This change oriented approach is argued to be better suited to evaluate the environmental consequences of decisions (Tillman, 2000), especially when faced with large scale decisions (Brandão et al., 2014).

Recently it is argued that market-based C-LCA falls short in cases of large systems affected by non-marginal variations or systems exhibiting dynamics mainly driven by human behaviour, that cannot be properly described by economic theory alone (Dandres et al., 2011; Marvuglia et al., 2013). In these cases, methodologies are required that detach C-LCA from a purely market-based approach and constitute the convergence of LCA with complex economic models and/or behaviour-oriented methodologies (Earles and Halog, 2011; Marvuglia et al., 2013; Vázquez-Rowe et al., 2013). The original market-based C-LCA is considered a special case of this broader interpretation (Marvuglia et al., 2013). It is in this context that AgBM is seen as a promising modelling paradigm, allowing to make behaviourally realistic approaches operational and capturing marginal effects relevant for C-LCA studies. It is this broader definition of C-LCA modelling that is adopted in this thesis and that is at the core of the CONNECTING project.

2.3 Activity-based modelling

This section is concerned with ABMs allowing to estimate travel demand. First, the fundamental flaws of traditional trip-based approaches, which led to the development of the activity-based approach, will be briefly touched upon. Next features and promises of ABMs will be introduced. Finally, the different modelling approaches of ABMs will be discussed building on existing classifications.

2.3.1 Flaws of conventional trip-based approaches

It is difficult to introduce the activity-based approach, without building on the criticism of trip-based approaches which ultimately led to the development of many ABMs as conceptually superior approaches to estimate travel demand. While an exhaustive review of these criticisms is beyond the scope of these thesis, the synthesis of more fundamental works (Jones, 1983), as well as recent reviews (Rasouli and Timmermans, 2014a) can help to gain the necessary insights.

The classic four step-modelling approach has been based on a sequence of largely independent sub-models, and has been described as a special application of spatial interaction models (Rasouli and Timmermans, 2014a). The four steps usually include (1) trip generation, (2) trip distribution, (3) modal split and (4) traffic assignment.

Jones (1983) lists several simplifications of trip-based approaches such as four-step models: (1) the daily context of travel is lost as trips are treated separately from others events; (2) the order of travel is lost due to strong temporal aggregation; (3) the direction of travel is lost by using production and attraction rather than specific origins and destinations; and (4) the linkage between trips is lost (Jones, 1983). Similarly, Rasouli and Timmermans (2014a) formulate several fundamental criticisms of four step-modelling including (1) the lack of integrity, (2) assumption of independence between sub-models, (3) strong aggregate nature both in time and space, and (4) lack of behavioural realism.

Theses flaws and simplifications potentially lead to biases when trying to forecast complex behavioural responses to specific transport policy measures such as congesting pricing, teleworking and ride sharing incentives (Jones, 1983; Rasouli and Timmermans, 2014a). It is in this context that the activity-based approach was introduced to address these criticisms.

2.3.2 Features of ABMs

While there is no one framework and computational structure of ABMs, one can establish a set of features encountered among such modelling efforts. The following set of features is based on a qualitative selection, aiming at introducing such features of ABMs.

A first feature of ABMs is that travel demand is derived from the demand for activity participation (Damm, 1979; Wigan and Morris, 1981; Pas, 1985; Kitamura, 1988; McNally, 1996; Ben-Akiva and Bowman, 1998; Bhat and Koppelman, 1999; Rasouli and Timmermans, 2014a). Jones (1983) describes the role of travel as a "space-shifting mechanism" which allows people to move between sites where they take part in activities. Activity participation in turn arises from more fundamental human needs and desires, for which activities (a more tangible concept) serve as a reasonable proxy in order to understand the derived travel behaviour (Jones, 1983). Many ABMs ultimately aim at accounting for decisions of whether, where, when, for how long and with whom an activity is conducted, which in turn affects the demand for travel (Axhausen and Gärling, 1992; McNally and Rindt, 2007). A common example is the pursuit of employment, which in many cases accounts for a large share of the daily activities of the active population. With some exceptions (e.g., self-employment, home office or teleworking) the participation in work related activities implies leaving the usual residence location to travel to the usual work location. Besides work or other mandatory activities (e.g., sleeping and eating), people participate in other discretionary activities (e.g., recreation) which might cause a demand for travel. Similar to Davidson et al. (2007) and Davidson et al. (2011) this feature will be referred to as the *activity-based platform* of ABMs.

A second feature of ABMs is the accounting for interdependencies of activities and travels, forming tours and ultimately DAPs (Damm, 1979; Pas, 1985; Bhat and Koppelman, 1999; McNally and Rindt, 2007; Chu et al., 2012; Rasouli and Timmermans, 2014a). Subsets of trips between activities can be grouped together (often referred to as trip chaining) to form single entities (or tours) beginning and ending in the same location, and providing a sequence, location and timing of activities and travels. These tours become the basic elements of analysis (Golob and Golob, 1982; Jones, 1983; Davidson et al., 2007; Pinjari and Bhat, 2011). The sequence of tours and activities between tours (e.g., time at home) form the DAP (Jones, 1983; Davidson et al., 2007). More or less complex interdependencies can be accounted for, such as dependencies between different elements of the DAP, between elements of the DAP and the environment, or consistencies, e.g., of transport modes within tours (Rasouli and Timmermans, 2014a). Similar to Davidson et al. (2007) and Davidson et al. (2011) this feature will be referred to as the *tour-based structure* of ABMs.

A third feature of ABMs is the focus on the individual or the household as the decision making unit (Kitamura et al., 2000; Bradley and Bowman, 2006; Davidson et al., 2007; Davidson et al., 2011; Rasouli and Timmermans, 2014a). Outcomes are based on behaviourally valid autonomous decision structures on a micro level, assuring consistent and feasible individual or household activity patterns (Jones, 1983; Kitamura et al., 2000; Davidson et al., 2007; Rasouli and Timmermans, 2014a). Each decision unit (e.g., an individual) can be uniquely identified, has individual attributes (e.g., age, gender or marital status) and makes crisp activity and travel related decision (e.g., whether and where to participate in an activity) among discrete choices based on deterministic or stochastic rules (Bradley and Bowman, 2006; Davidson et al., 2007; Davidson et al., 2011). This usually implies using a population of decision units (e.g., individuals or households) to model and simulate their individual complex travel behaviour, giving rise to their collective travel behaviour on a contiguous temporal scale (Kitamura et al., 2000; Bowman, 2004). Similar to Davidson et al. (2007) and Davidson et al. (2011) this feature will be referred to as the *micro-simulation modelling* of ABMs.

A fourth feature of ABMs is the explicit consideration of various constraints that channel activity and travel behaviour (Jones, 1983; McNally, 1996; Ben-Akiva and Bowman, 1998; Chu et al., 2012; Rasouli and Timmermans, 2014a). Hägerstrand (1970) first introduced a time-space geography framework, formulating three groups of constraints: (1) channelling the individual day paths within space-time prisms (the time-space volume within the reach of an individual

given posterior commitments and available transport modes, called *capability constraints*); (2) by grouping several day paths to form bundles (defining where, when and for how long individuals have to align their day paths to other paths, called *coupling constraints*); and (3) by passing through or evading domains of restricted access (determined by individual access rights to locations for specific periods of time called *authority constraints*). Individuals thus face their choices in the context of such objective and additional subjective constraints acting on their sets of options (or choice sets) by limiting them and ultimately shaping the possible individual DAP (Jones, 1983). ABMs include such constraints to identify feasible/unfeasible DAPs or to limit choice sets, e.g., of possible activity locations using space-time prisms (Rasouli and Timmermans, 2014a). This feature will be referred to as the *constraint consistency* of ABMs.

A fifth feature of many ABMs is the high temporal and spatial resolution (Jones, 1983; Rasouli and Timmermans, 2014a). Besides the high resolution of ABMs with regard to the representation of individuals in a population, many ABMs also allow for a high integrity and resolution in terms of scheduling activities in time and space (Ben-Akiva and Bowman, 1998; Bhat and Koppelman, 1999; Rasouli and Timmermans, 2014a). The temporal resolution of ABMs can achieve continuous representation of time while spatial resolution typically is zip code areas but can achieve parcel-level (Rasouli and Timmermans, 2014a). This feature will be referred to as the *spatio-temporal resolution* of ABMs.

Finally, a sixth less common feature of ABMs is the accounting for the interdependencies between behaviours of different individuals (Damm, 1979; Jones, 1983; Pas, 1985; Kitamura, 1988; Axhausen and Gärling, 1992; McNally, 1996; Bhat and Koppelman, 1999; Bradley and Bowman, 2006; Rasouli and Timmermans, 2014a). This feature entails viewing the individual's travel behaviour in the context of the DAPs of others sharing the same fixed locations (e.g., usual residence or work location) of the individual (Damm, 1979; Jones, 1983). Jones (1983) discusses three categories of inter-personal linkages mainly from a household perspective where (1) *greater role specialisation* occurs as individuals in a household take on the burden of some tasks for the entire household (e.g., for grocery shopping) or have to take on additional responsibilities for other individual (e.g., for children); (2) *competition for resources* occurs as some household resources (e.g., household car) can be scarce and their availability to an individual is subject to bargaining; and finally (3) *joint activity participation* causes tighter constraints on activity scheduling as activity type, place and time have to be agreed upon, and a feasible common block of discretionary time has to be found (e.g., due to coupling constraints). Such interdependencies in travel decisions can be made operational in ABMs through specific variables (e.g., describing the household composition) or more complex mechanisms (e.g., by modelling choices of one individual conditional on those of another individual) (Kitamura, 1988; Bradley and Bowman, 2006). This feature will be referred to as the *inter-personal linkage* of ABMs.

2.3.3 Modelling approaches

A final aspect to shed light on is the modelling approach to implement the choice models and constraints in an ABM. Rasouli and Timmermans (2014a) distinguish three different modelling approaches: *constraints-based models*, *utility-maximizing models* and *computational process models*.

Rather than predicting individual DAPs, constraints-based models check the feasibility of a DAP in a space-time context (Rasouli and Timmermans, 2014a). These models receive a list of activities as inputs and using the space-time context (e.g., institutional constraints such as opening/closing hours of potential locations or available transport modes and travel times) return all possible activity agendas. An early example of such a constraints-based model is the Program Evaluating the Set of Alternative Sample Paths (PESASP) model which is the first attempt to operationalize the time-space geography framework advanced by Hägerstrand (1970). This model

works with the DAPs of individuals and the environment described in time and space (including e.g., authority constraints), and proceeds by estimating the number of possible trajectories of the DAPs within the environment (Lenntorp, 1979). Another example is the Combinatorial Algorithm for Rescheduling Lists of Activities (CARLA) which is similar to PESASP, but proceeds by decomposing a DAP and examining the number of feasible ways to re-assemble it under a set of constraints (Jones, 1983). Overall, constraints-based models are considered to be behaviourally weak, especially with regard to their sensitivity to policies, while being well adapted to identify infeasible DAPs in changing environments.

Utility-maximizing models are based on the premise that individuals maximize utility in choosing alternative DAPs. While trip based approaches already include utility-maximizing models, e.g., for mode choice, for ABMs falling under this category the complexity of these discrete choice models is extended by accounting for interdependencies among choice facets at the individual level. One example of such an utility-maximizing model is the Comprehensive Econometric Micro-simulator of Daily Activity-Travel Patterns (CEMDAP), which constitutes an econometric modelling systems for activity-travel pattern generation (Bhat et al., 2004). The model proceeds by first predicting the participation in activities for individuals to satisfy individual and household needs. Next, the predicted activities are scheduled to form complete DAPs. Choice facets are implemented through econometric modelling such as regression, hazard duration, multinomial logit or ordered probit models. These models can be combined with concepts of constraints-based models, e.g., space–time prisms, to constraint the choice sets. Taking a more general stance, utility-maximizing models could also be replaced by alternative behavioural models (e.g., regret-minimizing models).

Finally, computational process models relax the strict and behaviourally unrealistic assumption of utility-maximizing behaviour by including rule-based models to depict decision heuristics. These models aim at mimicking the underlying decision-making process. The so-called A Learning Based Transportation Oriented Simulation System (Albatross) is such a computational process model, which predicts DAPs subject to various constraints (Arentze and Timmermans, 2004). The system builds on a rule-based formalism (rather than utility maximizing theory) proceeding through sequence of steps, each represented by a decision tree representing the heuristic decision-making. While computational process models are usually associated with high behavioural realism, some of their assumptions may built on a priori rather than empirical data (e.g., sequence of choice facets) (Rasouli and Timmermans, 2014a).

The ABM part of the CONNECTING model is an utility-maximizing model, which will be outlined in chapter 4. The coupling of the ABM part to a LCA is one of the main innovations of the CONNECTING project, building on prior work of coupling AgBMs and LCA. In the following, the literature on coupling such models will be reviewed.

2.4   Coupling AgBMs and LCA

The CONNECTING project is the first to aim at coupling ABM with LCA and thus no prior example of such a coupling exists in literature. In contrast, examples of previous attempts linking LCA and AgBM can be found. Therefore, an overview of the integration of AgBM and LCA is presented.

2.4.1   Agent-based modelling

Agent-based modelling defines a class of simulations models that share a common modelling paradigm. In contrast to LCA and ABMs, AgBMs can not be related to a specific field, instead agent-based approaches have emerged in many disciplines including IE (Dijkema and Basson,

2009; Dijkema et al., 2015) and urban planning (Perez et al., 2017). In general, agent-based modelling is advocated as a modelling paradigm appropriate for complex systems, where the following definition of complex systems is adopted:

"A system in which large networks of components with no central control and simple rules of operation give rise to complex collective behaviour, sophisticated information processing, and adaptation via learning or evolution (Mitchell, 2009)."

This definition suits as a description for the source system of CONNECTING, where a large number of individuals take decisions regarding their DAPs. Their individual choices and interactions with each other, as well as the physical transportation environment gives rise to the complex transport flows on a regional level, while individuals are capable of adapting their behaviour when confronted with changing conditions. It can thus be concluded that the aim of the CONNECTING project is to model and simulate this complex system. While the specific modelling approach of the CONNECTING project is an ABM (coupled with LCA), it can be argued that all ABMs (exhibiting several of the features above) follow (at least in part) an AgBM paradigm. To support this claim, first a short description of the AgBM paradigm is provided.

AgBMs allow for direct representation of agents, their interactions with each other and the environment (Gilbert, 2008). They allow to model individual heterogeneity (e.g., in terms of decision rules or attributes) and conduct experiments under condition of isolation without the ethical or financial constraints encountered with human source systems (Gilbert, 2008). Demazeau (1995) identifies four basic components of the AgBM paradigm: Agents, Environment, Interactions and Organisation (AEIO) and describes these components as follows. Agents have simple or more complex architectures and can be reactive, cognitive or both (hybrid). The nature of the environment depends on the specific case but is often spatial. Interactions can range from speech acts to interactions of physical nature. The organisation can be dynamic or governed by laws. Macal and North (2005) further describe a typical AgBM using three elements:

- A set of *agents*, their attributes and behaviours.

- A set of agent *relationships* and methods of interaction: An underlying topology of connectedness defines how and with whom agents interact.

- The agents' *environment*: Agents interact with their environment in addition to other agents.

These three elements are clearly related to some of the features of ABMs, such as the micro-simulation modelling. Other features of ABMs (the tour-based structure of travel and activity-based platform) are specific examples of agent behaviours. A clear link can also be drawn to agent relationships and interactions, where some ABMs model not only where, when and for how long household members participate in activities, but also with and for whom they do so, thus accounting for interactions between household members (inter-personal linkage). One can thus conclude that ABMs falls (at least in part) under the AgBM paradigm.

Using AgBMs in contexts of relevance to IE originated in the 1990s. Axtell et al. (2001) argue that AgBMs should explicitly model the incentives that realistic agents behaviourally face in empirically credible environments, which is at the core of the phenomena studied in IE. Following the call from Kraines and Wallace (2006) to apply AgBMs in LCA several authors present studies of AgBM/LCA coupled models.

The challenge of studying complex systems in IE using AgBMs remains a relevant topic, e.g., Dijkema and Basson (2009), yet more recently a decrease of AgBMs in IE literature has been

noticed, attributed to the difficult compatibility of AgBMs with material flow analysis and LCA (Dijkema et al., 2015).

2.4.2   Coupling options

To address the challenges of coupling AgBMs and LCA, several authors have reviewed coupling efforts and categorized different coupling options of both models, with Baustert and Benetto (2017) suggesting: an AgBM feeding information to a LCA (*AgBM enhanced LCA*); a LCA feeding information to an AgBM (*LCA enhanced AgBM*); a coupling where information flows in a loop between both models (*AgBM/LCA symbiosis*).

More recently Micolier et al. (2019) further conceptualise the type and degree of AgBM/LCA coupling, distinguishing three types of coupling: *model integration* where one unique and larger model is created; *hybrid analysis* where both models exchange data between each other; and *complementary use* where two separate models are used in combination calculating results separately. Further three degrees of coupling are distinguished: *soft-coupling* where aggregated AgBM results at the end of the simulation are used as inputs to LCA; *tight-coupling* where AgBM results are used at each time step as inputs to LCA; and *hard-coupling* where data is exchanged between both models at each time step.

2.4.3   Computational structures

Baustert and Benetto (2017) details two computational structures of coupling options that are found in literature, focussing on the LCA matrix approach described above.

On one side, authors such as Davis et al. (2009) see technology adopters (e.g., emerging in a market) as agents. The authors draw the comparison of the LCI matrices and AgBM network structures and conclude that they are fundamentally the same. As a consequence, rows and columns (representing unit processes and reference products respectively) are added to the technosphere matrix of the LCI foreground to represent these agents and their exchanges. The technosphere matrix can grow and shrink in accordance with the number of agents, creating dynamic supply chains. This extends the conventional LCI implementation which views the supply chains and markets as being composed of fixed connections. Therefore, this computational structure seems to be appropriate to address research questions about the impacts of structural changes of markets and values chains.

On the other side, authors such as Querini and Benetto (2015) and Navarrete Gutiérrez et al. (2015b) see actors (or users) as agents in a changing market or affected by an emerging technology. These agents are not perceived as components in the computational structure of the LCI. The role of the AgBM is to compute the demand of the system under the investigated scenarios, thus rendering part of the final demand vector a function of the AgBM output. This extends the current LCI implementation by simulating behavioural components and heuristic aspects. This computational structure seems appropriate to answer questions about a change in demand within a changing market or due to an emerging technology where the change is mainly driven by the behaviour of the users. As a result, the computational structure of the LCI is not significantly modified as the AgBM intervenes by providing more accurate scenarios of the future evolution of the system following the change.

2.4.4   Promises

Several promises have been voiced with regard to the coupling of AgBMs and LCA, as reviewed in Baustert and Benetto (2017). A first promise is that AgBMs can *solve data scarcity*

issues, e.g., for emerging products or systems for which the necessary LCA data cannot be gathered (Alfaro et al., 2010; Heairet et al., 2012; Bichraoui-Draper et al., 2015). This promise is not specific to AgBMs, as it would also relate to any other modelling paradigms appropriate for the specific source system. AgBMs however allow to model and simulate future supply chains following the first computational structure; or the emergence of a product or service use among a human population of agents following the second computational structure presented in the previous section.

A second promise is that AgBMs can *account for the micro-scale variability* (e.g., for non-homogeneous spatial conditions or among individuals of a populations) which is usually missed by LCA (Bichraoui-Draper et al., 2015; Heairet et al., 2012; Querini and Benetto, 2013; Querini and Benetto, 2014; Querini and Benetto, 2015). This can be related to the variability of preferences and choices in the demand for product or services within a human population of agents, as well as the variability of local production conditions for technology agents.

Finally a third promise is that AgBMs *allow for the consideration of human-driven consequential effects*, especially when human behaviour is driving consequential effects relevant to a LCA (Querini and Benetto, 2014). This can be related to ABMs, where besides the intended policy impacts on the individual DAPs (e.g., higher share of PT usage among commuters), secondary reinforcing or rebounding effects can occur in other parts of the DAPs (e.g., changing car availability for other household members).

2.4.5   Review of AgBM/LCA coupled models

For a comprehensive review of efforts of coupling AgBMs and LCA both Baustert and Benetto (2017) and Micolier et al. (2019) should be consulted. In this section a review of AgBM/LCA coupled models is presented, focussing on modelling efforts that resemble the CONNECTING model. Therefore, first the CONNECTING model is defined in terms of the three criteria: *coupling type*, *coupling degree* and *computational structure*.

The coupling type of the CONNECTING model follows the hybrid analysis as described in Micolier et al. (2019). While the CONNECTING model will still be composed of two distinguishable sub-models (the ABM part and the LCA part), both models will interact in a flexible combination. The flow of information however will be purely one directional, where the outputs of the ABM are used as inputs to the LCA part. With regard to the degree of coupling the CONNECTING model will follow a tight coupling, where for each time step of the ABM a LCA will be conducted. Finally the computational structure will follow modelling efforts where both sub-models interface at the final demand vector, describing human agents and their demand for mobility services.

Out of the articles reviewed in Baustert and Benetto (2017) only few adopt a comparable approach, with the work of Querini and Benetto (2013), Querini and Benetto (2014), and Querini and Benetto (2015) focussing on the emergence of electric mobility among the commuting population in Luxembourg, and the related environmental impacts of their mobility needs. In contrast to CONNECTING, no ABM approach is chosen to determine travel demand for different transport means and the focus of the model is on the long term choice of car ownership and competing powertrains. LCA is used to describe each car type (in terms of car segment and powertrain) from a life cycle perspective where a distinction is made between production, use phase and EoL impacts. A hybrid analysis type of coupling is adopted using pre-calculated LCA impacts. The coupling degree is a tight coupling, where on a monthly basis agents evaluate whether or not to replace their current car and which car to buy based on a decision tree (taking range constraints into account) and daily travel demands are determined based on assumptions. The AgBM results are aggregated on a yearly scale in terms of the production of new and

disposal of old vehicles and vehicle use for each car type, thus determining the reference flows and ultimately the final demand vector of the LCA part. Using the pre-calculated LCA impacts, the yearly impacts are computed.

A second effort that resembles the CONNECTING model in terms of the three criteria is described in Navarrete Gutiérrez et al. (2015a), Navarrete Gutiérrez et al. (2015b), and Marvuglia et al. (2016) simulating the evolution of the Luxembourgish agriculture sector, where the agents perceive the results of a LCA and use them during the farm planning. Similar to the CONNECTING model a hybrid analysis and tight-coupling is adopted. Farmer agents decide on planting crops under the constraint of their assigned crop rotation scheme and according to three types of behaviour: pure profit maximization, pure environmental concern (taking LCA results into account, focussing on reducing CO_2 emissions) and a mixture of the previous two. In the LCA part of the model agricultural processes are described for each crop type planted in the study region. For a subsidy scenario the variations in the cultivated area of each crop compared to a reference scenario are determined on a yearly basis. These variations in the cultivated area determine the system's changes in demand for agricultural processes, which correspond to the reference flows and ultimately the elements in the final demand vector.

While these two efforts are the most similar to the CONNECTING model, a wide range of modelling efforts exist, covering most combinations of the presented coupling types, degrees and computational structures. Most noticeably is the work of Davis et al. (2008), Davis et al. (2009), and Davis et al. (2010), Nikolić (2009) and Miller et al. (2013) which are the first authors to couple an AgBM to LCA and serve as an example of a hard-coupling following the first computational structure. The main difference to the present work is their definition of agents as "technology agents" in contrast to the human agents of the CONNECTING project.

2.5   Summary

The AgBM paradigm can be related to ABMs, where AgBM describes a modelling paradigm with a broad range of applications, with some ABMs following this paradigm. However, ABMs cannot be reduced to a specific application of the AgBM paradigm, as a rich variety of such models can be encountered in literature (as shown in the review of this chapter), of which many diverge from the AgBM paradigm.

Following the review of the relevant literature on the coupling of AgBMs and LCA, several promises of this modelling approach have been identified and the types of coupling have been distinguished. The CONNECTING model constitutes an ABM enhanced LCA, with a computational structure where the system's final demand is generated by the ABM and the LCA describes the processes contributing to the required products and services to satisfy this demand and the related environmental impacts. This constitutes a C-LCA approach, where the consequential aspect is driven by the ABM comparing different scenarios, along with the non-marginal consequences (i.e., travel mode switches).

Using an ABM to model the commuting behaviour in CONNECTING builds on several of the promises of coupling AgBMs and LCA identified in the reviewed literature. Related to the first promise (data scarcity), the ABM part allows to simulate input data in a bottom-up manner for the subsequent LCA. The transport demand (for the various scenarios) are emergent from the individual agent choices, defining the demand of the system for processes. Related to the second promise (micro scale variability), the ABM allows to take into account variabilities on an individual agent scale (e.g., generating individual DAPs), thus accounting explicitly for variabilities in the commuter population, such as contrasting rural and urban areas both in the demographic and physical transport environment. Finally, related to the third promise (human

driven consequential effect), the ABM part of the CONNECTING model allows to model the source system in great detail thus exhibiting strong explanatory power retracing environmental impacts to individual or group decisions and potential interactions among agents.

The specific coupling type adopted in the CONNECTING projects also has some implications for the analysis of uncertainty and thus for the present thesis. In fact the propagation of uncertainty through the resulting integrated model is bound to follow the direction of the information flow between both models. However as shown in the review, different AgBM/LCA coupling types can be distinguished by the direction of the information flow. The specific coupling type is thus relevant for the UA, more specifically the uncertainty propagation, where uncertainty propagates along with the information flow. In CONNECTING this means that uncertainty propagates from the ABM to the subsequent LCA and not vice-versa.

The next chapter will be concerned with presenting the concepts of uncertainty and UA before reviewing the relevant literature on UA of ABMs and LCA with a focus on transport modes.

Chapter 3

Uncertainty analysis review

3.1 Introduction

Uncertainty occurs at the limits of our knowledge, where our information is either imperfect or lacking. As uncertainty is a description of our state of information and by extension of our knowledge, it refers to an epistemic situation. The study of uncertainty can be dated back as far as the work ancient Greek philosophers such as Plato (and perhaps even further), who described our incapacity to grasp the true nature of reality in his allegory of the cave. Ever since, scholars have touched upon the subject, such as Descartes, Kant or Laplace. While A full review of these historic efforts is beyond the scope of this thesis, Popper (1962) provides an invaluable contribution on this subject.

The present chapter has a more narrow focus: uncertainty in modelling and simulation. More specifically, the interest will be on the analysis of uncertainty in the model and on estimating its effect on the simulation outcome. In contrast to a philosophical interest in uncertainty, practical implications are at the centre of attention, stemming from the deep conviction that uncertainty is becoming of increasing importance for science in general and sustainability assessment in particular. The fourfold challenge that sparked the post-normal scientific movement, "facts uncertain, values in dispute, stakes high and decisions urgent" (Funtowicz and Ravetz, 1990), describes this new environment where science has to find ways to manage and communicate uncertainty.

After providing an overview of the concept of uncertainty and UA, this chapter will propose a novel classification of uncertainty for ABM/LCA coupled models, building on existing classifications of both fields. Next, systematic literature reviews are conducted to establish the state-of-the-art of current UA practices applied to ABMs and LCA.

The chapter will take the following structure. Section 3.2 will give a brief overview of uncertainty and introduce the new classification. In section 3.3 the purpose and steps of UA are introduced. In the following two sections 3.4 and 3.5 the systematic literature reviews are presented. Finally in section 3.6 the main content of the chapter is summarised.

3.2 Uncertainty

Uncertainty is generally understood to be "any departure from the (unachievable) ideal of complete determinism" (Walker et al., 2003). More formally, an event Y is uncertain if the Probability $P(Y) \in \left]0, 1\right[$.
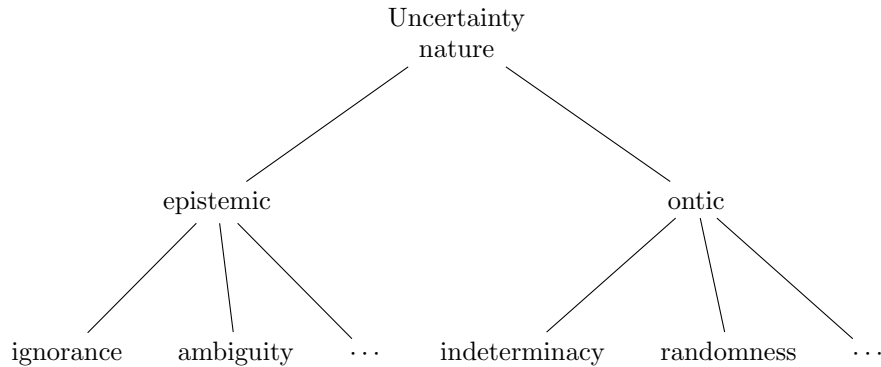
Figure 3.1: Classification of uncertainty natures

Going beyond this definition, several efforts have been made to distinguish various dimensions of uncertainty with respect to modelling and simulation. Starting with Walker et al. (2003) three distinct dimensions have been proposed in the *W&H framework*:

- *Nature* - how the source of uncertainty relates to reality

- *Location* - where the uncertainty manifests itself within the model

- *Level* - what degree can be attributed to the uncertainty

Building on this initial work, several new and adapted classifications have been proposed, e.g., Refsgaard et al. (2007) and Kwakkel et al. (2010). In the following, the three dimensions will be rendered more tangible, by relating them to ABM/LCA coupled models. Of particular interest will be the dimension termed "location" since several scholars have proposed specific classifications of so-called uncertainty sources (often containing both locations and natures in a single classification) for LCA and ABMs respectively.

3.2.1 Uncertainty nature

The first and most widely acknowledge dimension of uncertainty is the nature of uncertainty. Usually two different uncertainty natures are distinguished, where uncertainty is either *epistemological* (or epistemic) or it is *ontological* (or ontic). The former refers to uncertainty due to imperfect or lacking knowledge about reality and can be reduced (at least in principle), e.g., by gathering more information; while the latter refers to uncertainty due to the inherent indeterminacy or randomness of reality itself and can not be reduced. For both uncertainty natures subsets of manifold uncertainty sources can be defined, however an exhaustive and consensual list of such sources does not exist.

In literature various other pairs of terms can be found. Epistemological uncertainty is sometimes referred to as "knowledge uncertainty" or simply "uncertainty", while ontological uncertainty is referred to as "variability uncertainty", "aleatory uncertainty" or simply "variability". Throughout this thesis the pair *epistemic* and *ontic* is used, as these terms agree best with definitions focussed on the relation to reality and in consequences its reducibility.

In addition to these two natures of uncertainty, a third nature has been proposed by Warmink et al. (2010): ambiguity. However an argument can be made that ambiguity is a subset of epistemic uncertainty. Figure 3.1 gives an overview of the retained classification of uncertainty natures, where for each, two examples of uncertainty sources are provided.

Determining uncertainty as epistemic or ontic can be useful in several ways. As a first, when guiding data collection efforts, steering these towards sources of epistemic uncertainty can allow to efficiently reduce uncertainty of the outputs. Especially in the field of sustainability assessment, where ever more complex models are employed, efficient data collection is becoming of increasing importance. As a second, understanding the nature of uncertainty can have relevant implications for the modelling itself, where ontic uncertainty might require stochastic modelling while epistemic uncertainty could be dealt with UA of a deterministic model.

The most widely applied classification for managing uncertainty in LCA was proposed by Huijbregts (1998) and later updated and extended by Björklund (2002) and Hauschild et al. (2017). The classifications implicitly distinguished between epistemic (e.g., lack of data, relevance or mistakes) and ontic uncertainty sources (e.g., spatial variability, temporal variability or variability between sources and objects). Lack of data can be associated with, e.g., emerging technologies for which LCI data might not exist, or might be proprietary and unavailable. Relevance uncertainty refers to environmental relevance, accuracy or representativeness of an indicator towards an area of protection, while mistakes include modelling wrong substances, processes or units. Spatial variability occurs, e.g., due to variability of environmental states in space relevant to the LCIA, such as population density, water availability or regional variability of LCI production conditions. Temporal variability includes seasonal, weakly and daily variability in emission profiles and the corresponding environmental burden. Variability between sources and objects occurs, e.g., due to difference in technological processes serving the same function, or variability in ecosystem and human characteristics causing variability in their sensitivity to substances.

Among the classifications for ABMs, Rasouli and Timmermans (2012) provide an extensive description of various uncertainty sources, which can divided into epistemic sources (e.g., sampling bias, survey design, mistakes or incomplete information) and ontic sources (e.g., inherent variability). Sampling bias can occur, e.g., when travel behaviour of non-respondents strongly diverges from those captured by the survey. Inadequate survey design may cause random or systematic error, by failing to capture the relevant explaining factors of travel. Mistakes can occur, e.g., due to ambiguous labelling of travel locations. Many model quantities can exhibit variability, e.g., travel times can vary from day to day.

3.2.2   Uncertainty location

The second dimension of uncertainty, uncertainty location is concerned with where uncertainty manifests itself within the model. Classifications of such locations can be both field specific, e.g., specific to travel demand modelling (de Jong et al., 2007) and LCA (Hauschild et al., 2017), or more general as the classification by Walker et al. (2003). In the following first the general classification is introduced, before relating it to the more field specific ones.

A first location of uncertainty is the modelling context and experimental frame (or simply *context and frame*) (Walker et al., 2003). This location encompasses the definition of the conditions under which the source system is observed and modelled. It includes, e.g., the definition of the system boundary, time frame and each Quantities of Interest (QOI). The modelling context and frame requires inevitable and uncertain modelling choices.

Most models are directed systems, which take in a set of inputs and produce a set of outputs. These model *inputs* and *outputs* are locations of uncertainty, where the uncertainty in model outputs stems from the uncertainty in other locations (Walker et al., 2003). Model inputs represent, e.g., the state of the model environment, decision variables or other drivers of the modelled system, which could be static or follow a scenario.

The term "model uncertainty" is used as an umbrella term for uncertainty locations within the system boundary, encompassing the *model structure*, *model parameters* and *model variables*.
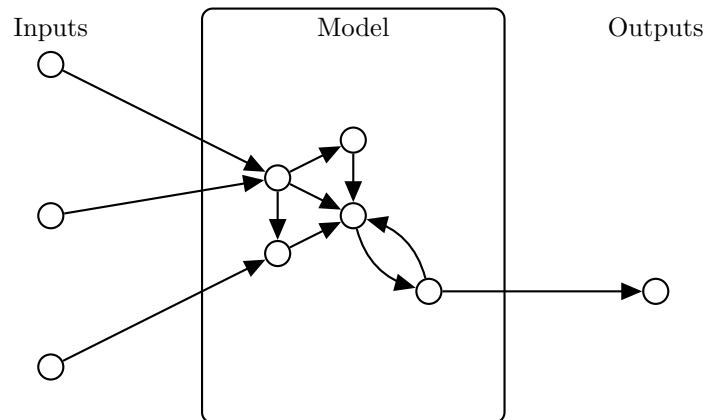
Figure 3.2: Inputs, outputs, parameters and variables are represented as circles. The model structure is represented by edges. Contextual choices such as the system boundary are represented as a rectangle with rounded edges.

Model structure designates the relationships formulated in the model between model quantities (i.e., inputs, parameters, variables and outputs) and it is a location of uncertainty in case there is doubt about the true model structure (Walker et al., 2003; Morgan et al., 1990). This structure can be hierarchical, where each sub-model can form relationships among sub-model quantities and at a higher scale of aggregation a model structure forms relationships among sub-model inputs and outputs (Klir, 2013). Model parameters describe states of the modelled system assumed to have a true value, while model variables describe states of the modelled system which are assumed to be random, usually modelled stochastically causing simulation variability McKay et al. (1999).

Inputs, parameters, variables and outputs are sometimes described with the umbrella term "model quantities" with Morgan et al. (1990) proposing an alternative classification of such quantities proposing the following classes: empirical parameters, defined constants, decision variables, value parameters, index variables, model domain parameters and output criteria. While this classification is useful to determine how to characterise uncertainty of quantities and which quantities are uncertain at all (constants and index variables are certain by definition) they do not specify distinct locations. This classification is thus complementary to the one provided here.

Figure 3.2 shows a representation of a model, where the uncertainty locations introduced above can be related to elements in the graph. Circles represent potentially uncertain quantities (inputs, model parameters, model variables and outputs), arrows represent the model structure, and contextual and framing choices such as the system boundary are represented by the rectangle with rounded edges separating the model from its environment.

The classifications proposed for LCA usually include classes corresponding more or less to those of general classifications (Huijbregts, 1998; Björklund, 2002; Lloyd and Ries, 2007; Hauschild et al., 2017). A first uncertainty location is uncertainty due to (normative) choices, usually occurring in the goal and scope definition phases of a LCA study (e.g., during the definition of the functional unit and system boundaries or the choice of allocation procedures and LCIA methods). A second, but less acknowledged location of uncertainty in LCA is model inputs, i.e., the quantities in the final demand vector, which can be defined in the goal and scope definition, derived from policy scenarios or generated from other models (i.e., by an ABM). Parameter uncertainty encompasses all quantities in the technosphere, biosphere and characterisation matrices, as well as LCIA weighting factors. Model (structure) uncertainty concerns uncertainty about the best

Experimental
frame _____ Goal
& Scope

Final
demand

Socio
demographic

Inputs

Service
level

Functional
form

Uncertainty Model
location specification
Parameter
& variable sets

Measured
parameters

Model Model
estimation
Calibrated
parameters

simulation _____ Error
error terms

Quantities
Outputs of interest
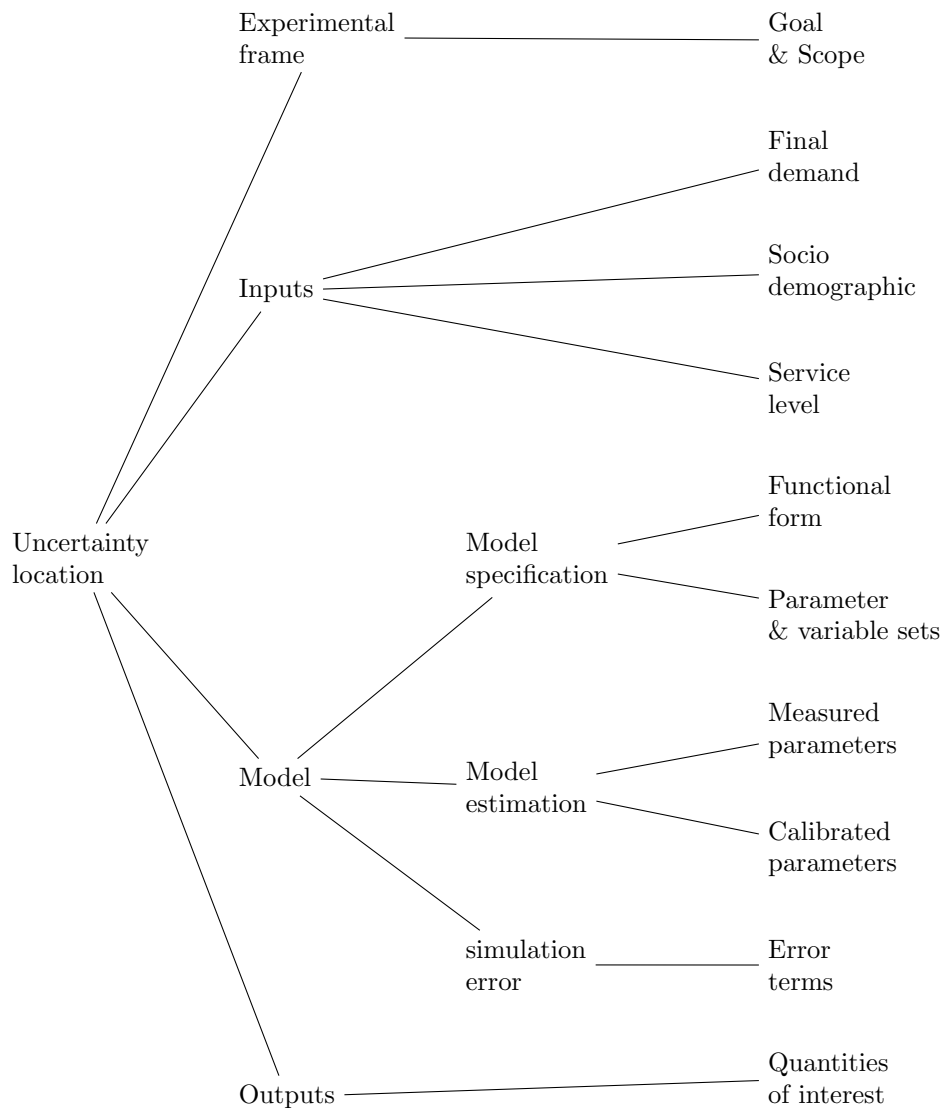
Figure 3.3: Classification of uncertainty locations in ABM/LCA coupled models

functional form of the LCI and LCIA modelling, as well as the impact of conscious simplifications (e.g., linearisation of non-linear or threshold dependent phenomena in the LCIA, or strong spatial and temporal aggregation in the LCI modelling). While most classifications also include various types of variability, these do not constitute specific locations in the model, but are rather sources of ontological nature.

The classifications of uncertainty proposed for ABMs usually distinguish two broad location classes: input uncertainty and model uncertainty (Hugosson, 2005; Cools et al., 2011; Rasouli and Timmermans, 2012; Petrik et al., 2018). Input uncertainty is most concerned with the data used as inputs to the ABM model such as socio-demographic and service level data. The second broad category is model uncertainty, which in most classifications is used as an umbrella term for several sub-classes. A first is model specification, which encompasses uncertainty about the

Uncertainty level

shallow   medium   deep   recognized
uncertainty   uncertainty   uncertainty   ignorance
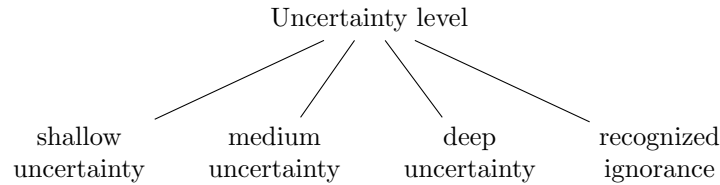
Figure 3.4: Classification of uncertainty levels

functional form of the model, uncertainty from omitted variables and the simulation error. A second sub-class is the model estimation, which describes the uncertainty about the true values of the model parameters (which are usually estimated only for a sample and not the entire population). Some authors classify the stochastic nature of ABMs causing simulation error as separate class (Petrik et al., 2018), while others include it as a sub-class of the specification error.

To build a classification for ABM/LCA coupled models, the relevant locations for both modelling approaches need to be identified and related to more general location classes both models share. To this end, the general locations of: *experimental frame*, *inputs*, *model* and *outputs* are selected as building blocks. Figure 3.3 shows these building blocks at the first level.

The location of model uncertainty is subdivided into the more specific sub-classes of *model specification*, *model estimation* and *simulation error*. These sub-classes are shown at the second level of figure 3.3.

At the last level of figure 3.3 the model specific locations of uncertainty are shown. The goal & scope definition phase of an ABM/LCA coupled model is where the experimental frame of the study is defined by taking many normative choices such as the definition of the functional unit, system boundary, etc. This phase also includes choices regarding the ABM, such as the appropriate synthetic population sample size.

The inputs to both models encompass the system's final demand (which includes, e.g., ABM outputs or policy scenario variables), as well as socio-demographic and service level inputs to the ABM.

The model specification includes the functional form of the ABM (e.g., the chosen functional form of the mode choice model), LCI (e.g., structure of the product system processes) and LCIA modelling approaches, and the higher level integrating structure of the ABM sub-models and ABM/LCA coupling. The second sub-class of model specification includes the parameter and variable selection for ABM sub-models. The model estimation encompasses the calibrated parameters of ABM sub-models (e.g., coefficients of the mode choice model), as well as the measured parameters of the technosphere (e.g., transport mode fuel or electricity consumption), biosphere (e.g., transport mode carbon dioxide emissions) and characterisation matrices (e.g., CFs to evaluate effects of nitrogen oxide emissions on human health). Finally, model uncertainty includes uncertainty from random draws of individual choices.

3.2.3   Uncertainty level

The third and final dimension of uncertainty is the uncertainty level suggested by Walker et al. (2003). More recently this dimensions has been subject to some adaptations by Kwakkel et al. (2010) and it is generally understood to be the degree or severity of uncertainty ranging from deterministic knowledge to total ignorance.

Linked to concepts such as the definition of risk and uncertainty by Knight (1921), the basic idea is that some uncertainty is controllable and quantifiable, and some is not. Kwakkel et al. (2010) introduce four levels of uncertainty to update the taxonomy of Walker et al. (2003), which

are ultimately related to the scales of measurement introduced by Stevens (1946).

Level 1 or *shallow uncertainty* is described as uncertainty where both alternative states and their likelihoods can be determined. This level is related to the ratio scale of measurement. Shallow uncertainty can usually be described using probabilities, e.g., by attributing a probability to an outcome or determining a probability distribution for a parameter.

Level 2 or *medium uncertainty* is described as uncertainty where alternative states can be determined and their perceived likelihood can be ordered by rank. This level is related to the ordinal scale of measurement. Medium uncertainty is sometimes described by developing rank ordered scenarios, e.g., a median scenario and several outlier scenarios.

Level 3 or *deep uncertainty* is described as uncertainty where only alternative states can be determined, but no likelihoods can be attached to these states (probability measure ignorance Baustert et al. (2018)). This level is related to the nominal scale of measurement. Deep uncertainty is sometimes described by developing scenarios (or story lines) perceived as equally likely.

Level 4 or *recognized ignorance* is described as uncertainty where no alternative states can be determined (sample space ignorance (Giang, 2015)). No scale of measurement can be attached to this level. Figure 3.4 shows the classification of levels of uncertainty found in literature.

3.3 Uncertainty analysis

3.3.1 Goal

The analysis of uncertainty is concerned with locating, identifying, characterising, treating and communicating uncertainty of a model. Modern UA is conducted in an iterative and participatory fashion, where modellers and stakeholders work closely together. Figure 3.5 gives an overview of UA as a process.

Depending on the purpose of the model, UA can take different forms, where for proof-of-concept and developing models it might be more interesting to investigate individual uncertainty locations and their influence on the model outputs to guide future model development, once models become decision support tools, UA aims at quantifying the confidence decision makers can place in different options. The importance of UA is emphasized by Morgan et al. (1990) stating that "without thorough and systematic modeling and analysis of the uncertainty of the problem we can not be sure that the results of a model, especially a very large and complex one, mean anything at all".

UA usually starts with locating and identifying uncertainty in the model, by describing it, e.g., building on the three dimensions suggested by Walker et al. (2003). Building on this description, uncertainty locations of interest are characterised quantitatively by assigning a mathematical structure (e.g., a probability distribution) or qualitatively (e.g., building on scenario development). Once uncertainty is characterized, uncertainty treatment (i.e., uncertainty propagation or SA) allows to determine how the uncertainty locations affect the model outputs. Finally, uncertainty needs to be communicated to stakeholders.

In the following, each of the distinguishable steps of UA depicted in 3.5 will be introduced in more detail, each time referring to specific practices in both fields (ABMs and LCA).

3.3.2 Uncertainty location and identification

This steps relies on the main concepts introduced in section 3.2. The aim is the determine the relevant uncertainty locations of the model to the specific goal of the study.

In LCA this usually relies on the classification of uncertainty sources, where the classification advanced by Huijbregts (1998) is the most broadly applied. More recently, the "uncertainty
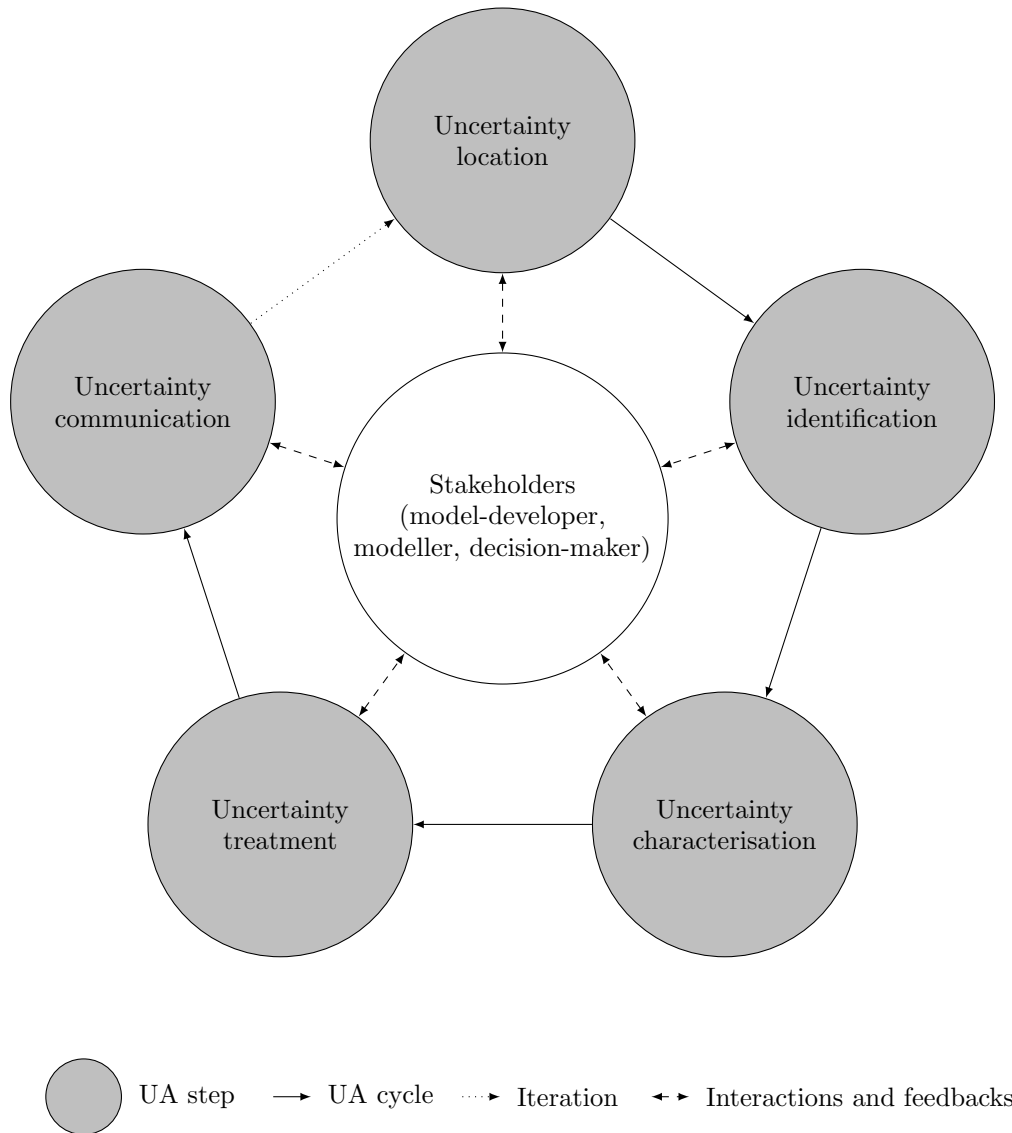
Figure 3.5: Distinguishable steps of UA, considered as a participatory and iterative process. Note that depending on the context, some steps or interactions might not be necessary. Adapted from Baustert et al. (2018).

matrix" of Walker et al. (2003) was adapted for LCA purposes by Igos et al. (2018). The classification of uncertainty locations and natures of Walker et al. (2003) are applied to three of the four LCA phases (goal and scope definition, LCI and LCIA). Another example is the issue matrix first introduced by Heijungs (1996), which maps uncertainty locations according to their uncertainty level and sensitivity. Figure 3.6 shows the key issue matrix adapted from Hauschild et al. (2017). While originally, it is used for parameters, it is argued to be generally applicable to all locations.

The classification of uncertainty sources (e.g., Rasouli and Timmermans (2012)) introduced
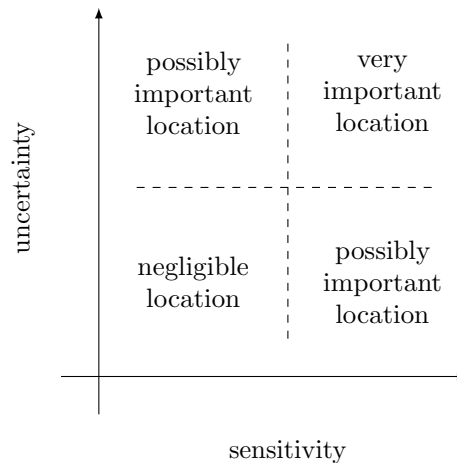
Figure 3.6: Key issue matrix adapted from Hauschild et al. (2017).

in section 3.2 corresponds to the state-of-the-art regarding uncertainty location and identification of ABMs. In addition, Manzo et al. (2015) discusses the taxonomy of uncertainty proposed by Walker et al. (2003) for transport models in general.

3.3.3   Uncertainty characterisation

Once uncertainty is located and identified, in order to perform the subsequent steps of uncertainty treatment it needs to be described either in quantitative (numeric) or qualitative (verbal) terms. The former entails representing the state of knowledge by assigning a mathematical structure (e.g., a probability density function) to the uncertainty and specifying its parameters (Roy and Oberkampf, 2012). The latter is applied in case the uncertainty cannot be captured in such a mathematical structure (Refsgaard et al., 2007; Warmink et al., 2010; Bastin et al., 2013; Beven et al., 2015).

The most widely applied quantitative language to represent uncertainty is probability theory (Aven, 2010). Other quantitative theories can be found in literature, such as evidence theory, possibility theory, set theory and quantitative scenarios (Helton et al., 2004; Chowdhury et al., 2009; Aven and Zio, 2011). One prominent methodology of qualitative uncertainty characterisation is the pedigree matrix of the Numeral, Unit, Spread, Assessment and Pedigree (NUSAP) scheme, built on a set of linguistic criteria and expert judgement (Funtowicz and Ravetz, 1990). Qualitative scenarios describe different possible outcomes in the form of consistent storylines allowing for stakeholder involvement (Refsgaard et al., 2007; Beven et al., 2015), such as the concept of Shared Socioeconomic Pathway (SSP) scenarios used for climate change research (O'Neill et al., 2014).

The appropriate characterisation usually depends on the location, nature and level of the uncertainty. Morgan et al. (1990) provide an elaborate description for various locations arguing, e.g., that uncertainty about the model structure should not be modelled probabilistically, while uncertainty about quantities can be modelled in various ways depending on the specific nature of uncertainty (e.g., epistemic uncertainty due to linguistic imprecision can be modelled using fuzzy set theory).

In LCA, besides the appropriate characterisation of uncertainty locations, the high number of measured parameters and inputs poses an additional challenge. The key issue matrix presented shown in figure 3.6 caters to this by highlighting the most important locations of uncertainty and

focussing on their characterisation. It is sometimes argued to characterize uncertainty iteratively, where broad initial characterisations are updated for identified key issues (Huijbregts et al., 2001).

A second instrument broadly applied in the field of LCA is the pedigree approach which is based on the NUSAP scheme. Data Quality Indicators (DQIs) are used in qualitative and quantitative assessments of uncertainty, where quantitative distributions are derived from the DQIs (Björklund, 2002). Two sorts of uncertainty and corresponding DQIs are distinguished: "basic" uncertainty related to all sampled data (e.g., measurement error) and "additional" uncertainty related to the data quality (i.e., reliability, completeness, temporal correlation, geographical correlation, further technological correlation) (Weidema and Wesnæs, 1996). The appropriateness of the quantitative use of the DQIs however may still be questioned (Henriksson et al., 2014).

For ABMs, the characterisation of uncertainty does not yet follow such standardised approaches. However, for utility-maximization models the concepts of random utility theory often apply, allowing for a characterisation of uncertainty for individual choice models.

3.3.4   Uncertainty treatment

Two broad groups of methods of uncertainty treatment can be distinguished: *uncertainty propagation* and *sensitivity analysis* (SA). Both types of analysis complement each other: uncertainty propagation tries to quantify how uncertain an inference is, while SA estimates where this uncertainty is coming (Saltelli and Annoni, 2010).

Uncertainty propagation allows to assess the cumulative effect of numerous uncertainty locations on the model outputs. This usually relies on having a simulator, which allows to execute model calculations. This simulators can be numerical or physical and potentially cause some additional uncertainty. Methods to perform uncertainty propagation include analytical propagation (e.g., using Taylor series expansion (Hong et al., 2010)), sampling methods which can build on probability theory (e.g., such as Monte Carlo (MC) simulation), fuzzy set theory (Baustert and Benetto, 2017) or set theory (e.g., factorial design based methods).

According to Hamby (1994) models can be sensitive to parameters in two ways: (1) the contribution of the parameter uncertainty to the overall output variability; and (2) the change in the output resulting from a change in the parameter value. Following these two possible sensitivities, two applications of SA can be distinguished: (1) Contribution To Variance (CTV) to quantify how much each uncertain parameter contributes to the output variance; and (2) Screening to determine the significant parameters. While CTV tells the practitioner which parameters to focus on, in order to efficiently reduce the uncertainty of the output and thereby improve the model, screening can help to simplify the model itself or to reduce the number of parameters in the UA (Björklund, 2002). Often the following two concepts are distinguished: Local Sensitivity Analysis (LSA) that varies the parameters One-at-a-Time (OAT) while the others are fixed at their nominal value; Global Sensitivity Analysis (GSA) that takes into account interactions by varying parameters at the same time (Hamby, 1994; Saltelli et al., 2000).

A broad range of uncertainty treatment methods have been applied to LCA, and several reviews have been published, e.g., Lloyd and Ries (2007), Baustert and Benetto (2017), and Igos et al. (2018). These reviews show that uncertainty propagation based on MC simulations (or more advanced sampling schemes such as Latin Hypercube Sampling (LHS) McKay et al. (1979) or quasi random sampling based on Sobol or Halton sequences) is mostly applied, followed by some methods of analytical uncertainty propagation and fuzzy set theory. In some cases uncertainty propagation is complemented by SA, either to identify key issues before uncertainty characterisation or to assess the CTV after uncertainty propagation.

Similar to LCA, MC simulations (or more advanced sampling schemes) are being applied to ABMs. Rasouli and Timmermans (2012) reviews the efforts. Unlike in LCA, the range of

applied methods is more narrow. This can be explained by the nature of many ABMs, for which closed form expressions are often impractical (and in some cases impossible) to derive. As noted in Baustert and Benetto (2017) the same applies to many AgBMs, making it difficult to apply analytical approaches.

3.3.5   Uncertainty communication

A final step of one iteration of performing UA is uncertainty communication. This step aims at synthesising the key findings of the uncertainty treatment results for the model stakeholders. Different forms of uncertainty communication are distinguished in literature: verbal (e.g., high or low), numerical (e.g., an interval or Coefficient of Variation (CV)), graphical (e.g., error bars) or a combination of these (Wardekker et al., 2008; Petersen et al., 2013). The target audience and their needs with regard to uncertainty information can influence the choice of a communication form.

LCA as a relative approach is generally used in comparative assessments. Uncertainty communication of comparative LCA is a of high interest and several measures have been proposed and tested Mendoza Beltran et al. (2018a) and Heijungs (2021). Igos et al. (2018) further review uncertainty communication frameworks for LCA such as the one proposed by Gavankar et al. (2015).

3.4   Review: uncertainty analysis of LCA

The scope of review of UA in LCA is set to include studies that apply UA to LCA of passenger transport systems (ranging from individual modes and their fuel cycles to the usage of modes within larger systems). The review process is both quantitative and qualitative.

The literature search is initiated by keyword searches and complemented by first level backward and forward searches of references, authors and keywords. Figure 3.7 shows the resulting corpus of literature by date of publication and means of article identification in the literature search.

3.4.1   Type of LCA

A majority of studies is focussed on private transport with only a few studies focussing on PT modes (e.g., alternative bus fuel and engine types (Ercan and Tatari, 2015; Dreier et al., 2018; Harris et al., 2018), bus fleet operation (Bi et al., 2018; Harris et al., 2020)) or other more diverse topics (e.g., highway projects (Verán-Leigh et al., 2019) or large scale mobility scenarios (Spielmann et al., 2005; Spielmann and Althaus, 2007; Spielmann et al., 2008)).

When looking in more detail at the studies focussing on private transport, the large majority is focussed on investigating the impacts of alternative fuels (e.g., biofuels (Edwards et al., 2004; Hsu et al., 2010)) or EVs and HEVs (e.g., Cox et al. (2018), Samaras and Meisterling (2008)). A few studies focus on vehicle materials (e.g., lightweighting by replacing heavy materials with lighter options (Geyer, 2008; Kelly et al., 2015; Pryshlakivsky and Searcy, 2017)) and one study investigates the longevity of vehicles (Spielmann and Althaus, 2007).

As outline in chapter 2 at least two types of LCA can be distinguished: attributional and consequential. Figure 3.9 summarizes the share of these LCA types within the corpus. The majority of studies can be classified as attributional (building on average data, e.g., average electricity mixes), with only four studies following a consequential approach.

Consequential aspects that are investigated include car replacement pathways in the Swiss passenger car fleet (Spielmann and Althaus, 2007) and in Luxembourg (Querini and Benetto,
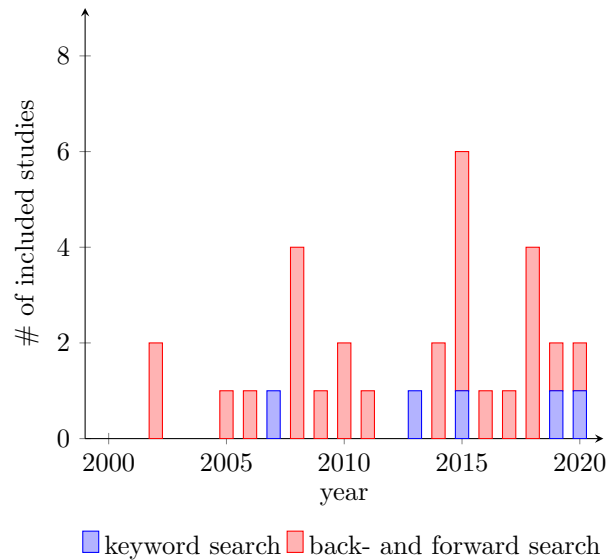
Figure 3.7: Number of included studies per year and for both search means.

2015), as well as changes in the modal split of transport systems and rebound effects (Spielmann et al., 2008). Geyer (2008) uses consequential system expansion to model scrap recycling in the EoL phase.

As for the LCI phase, figure 3.10 shows that almost every study covers the use phase, thus taking into account fuel or electricity consumptions and direct emissions relevant to, e.g., climate change and air quality related impacts. The only study that does not explicitly cover the use phase (Pryshlakivsky and Searcy, 2017) focusses on the material composition of vehicles.

Raw material and production phases are covered by 50% and 44% of studies respectively. These phases can be of particular interest, e.g., when the impact of vehicle lightweighting is assessed (Geyer, 2008; Kelly et al., 2015; Pryshlakivsky and Searcy, 2017) or when comparing conventional ICEVs to alternative powertrains (Querini and Benetto, 2015; Cox et al., 2018).

Finally, the EoL phase is covered by only 28% of studies. The relative lower rate of coverage of this phase is both due to the definition of the functional unit of many studies (e.g., focussing on different fuel life cycles and omitting the EoL phases if they are identical for all options) and studies claiming that this phase is of low relevance with regard to the impact categories of interest (e.g., McCleese and LaPuma (2002) anticipate that the EoL phase has low air emissions and energy consumption).

A final aspect of specific relevance to LCA studies of transport modes concerns the modelling of the fuel life cycle. Specifically, one distinguishes Well-to-Tank (WTT) describing the life cycle emissions occurring during the extraction of crude oil, the refining and provision at the pump), Tank-to-Wheel (TTW) describing direct emissions occurring during the use of the transport mode) and Well-to-Wheel (WTW) comprising both WTT and TTW. Studies only considering WTT fuels cycles are not considered as they usually are focussed on fuel life cycles without considering the actual transport modes. Most studies (94%) consider the broader WTW system boundary, with only one study taking into account only TTW (or direct) emissions. As seen above, one study does not consider the transport mode use phase.

LCA - Study subject   **Share of studies**
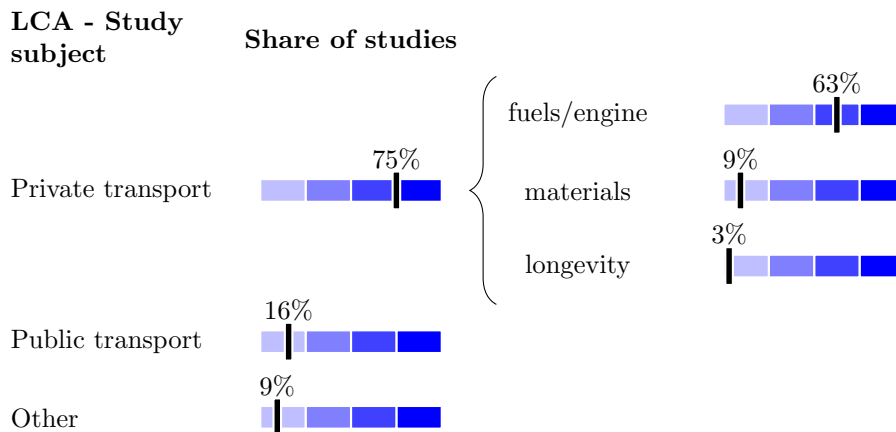
Figure 3.8: Share of studies for LCA of different transport modes.

LCA - Modelling approach   **Share of studies**
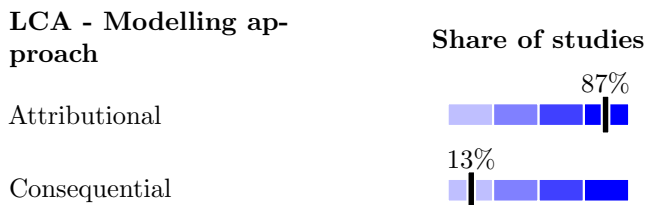
Figure 3.9: Share of studies for different LCA modelling types.

3.4.2   Uncertainty location and identification

Regarding uncertainty locations, figure 3.12 shows the share of studies addressing uncertainty at each of the locations of the proposed classification for ABM/LCA coupled models. Note, that some studies are dealing with uncertainty at multiple locations. There is a strong tendency to deal with uncertainty in the model estimation part (specifically measured parameters in the LCI), with only few other locations being addressed.

The high share of studies dealing with uncertainty in measured parameters, could be explained by several factors, including the relatively easy and wide spread approaches to characterise uncertainty in these locations (i.e., the pedigree approach), and its application to commercial databases (i.e., ecoinvent[1]). With regard to model specification and simulation error, the fact that they are not being addressed can be explained by the consensual function form of many LCA studies and ISO standardisation, as well as the absence of randomness in textbook LCA studies.

Staring with studies that focus on the experimental frame, in Spielmann and Althaus (2007) "ambiguous methodological decisions" regarding open-loop recycling are investigated, by testing study results for multiple allocation approaches (cut-off versus system expansion). Messagie et al. (2019) investigate the robustness of their comparison of different vehicle technologies towards the usage of individualist, egalitarian and hierarchist based world view scenarios (Thompson et al., 2018) for CFs of the "recipe" method (Huijbregts et al., 2017).

---

[1]https://www.ecoinvent.org/

LCA - LCI phase   **Share of studies**

Raw material

Production

Use

End-of-life
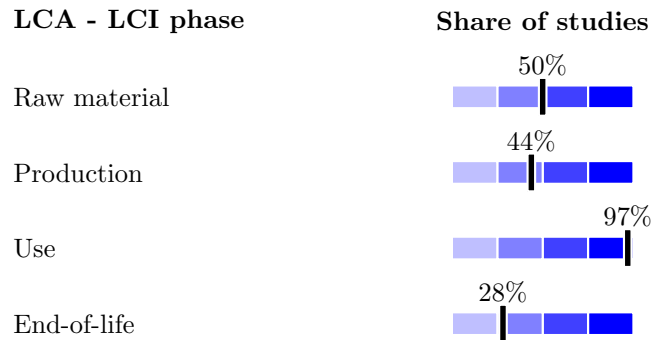
Figure 3.10: Share of studies for different LCI phases.

LCA - Fuel cycle   **Share of studies**

Well-to-Tank

Tank-to-Wheel

Well-to-Wheel
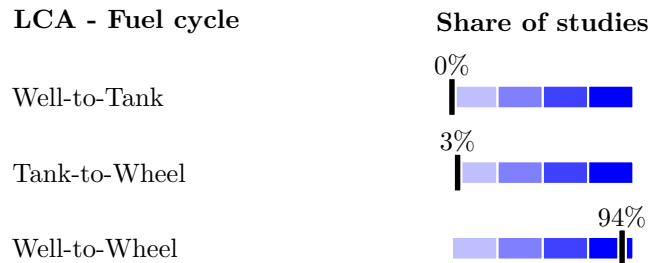
Figure 3.11: Share of studies for different fuel cycle modelling approaches.

Studies investigating uncertainty from model inputs focus on the demand side (final demand vector) of the LCI. Spielmann et al. (2005) take into account uncertainty regarding so-called mobility life styles, and the effect on the mobility demand for bus transport. Spielmann et al. (2008) investigate uncertainty of the transport demand for different modes stemming from daily mobility pattern in their study of high speed trains in Switzerland. Noshadravan et al. (2015) use UA to compare conventional ICEVs and EVs under a broad range of use-phase scenarios. Similarly Querini and Benetto (2015) take into account the variability of vehicle usage in their study of EV market penetration. Dreier et al. (2018) account for a range of operation conditions for conventional, hybrid-electric and plug-in hybrid-electric city buses as LCA inputs for their study of bus routes in Curitiba, Brazil. Finally, Bi et al. (2018) assess the impact of uncertainty in the operation (e.g., charging times) of an optimized charging infrastructure for electric buses in Michigan, U.S..

Finally, the large majority of identified studies investigate uncertainty in measured parameters, i.e., elements in the technosphere and biosphere matrices (in case the matrix inversion approach is applied) and in general measured parameters of the modelled processes.

Several studies investigate the uncertainty within the fuel life cycle (often building on the GREET model[2]) (Wang, 2002; Edwards et al., 2004; Wu et al., 2006; Subramanyan et al., 2008; Hsu et al., 2010; Cai et al., 2013; Cai and Wang, 2014; Huo et al., 2015; Lu et al., 2016) for various fuel and engine types taking into account uncertainty with regard to the provision of fuel

---

[2]https://greet.es.anl.gov/

LCA - Uncertainty location

Share of studies

Experimental frame

6%

Inputs

19%

Specification

0%

Model

Estimation

91%

Simulation error

0%
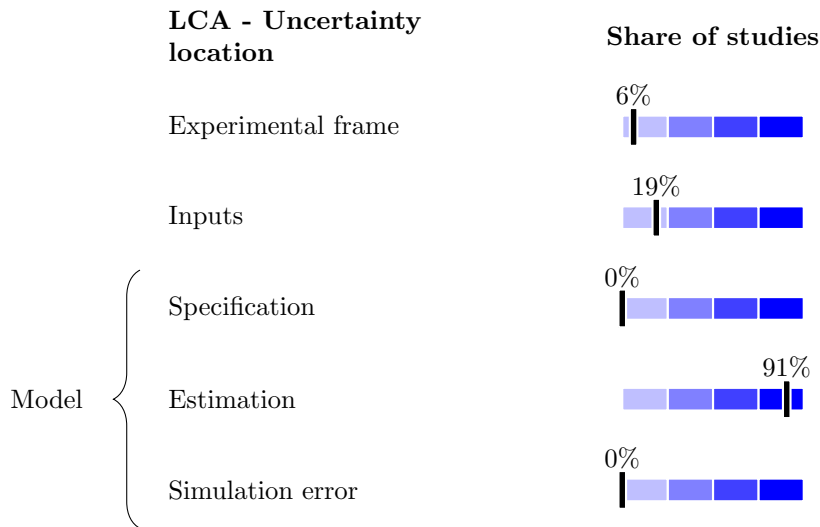
Figure 3.12: Share of studies addressing different uncertainty locations.

(WTT) and the usage (TTW). With the introduction of the second version of GREET other phases of the vehicle life cycle are added and uncertainty is analysis by Abdul-Manan (2015) and Ercan and Tatari (2015). Several other studies take into account the uncertainty in LCA modelling parameters affecting use phase interventions (e.g., fuel consumption, vehicle weight and tailpipe emissions) (Boureima et al., 2009; Messagie et al., 2010; Messagie et al., 2014; Messagie et al., 2019).

In a series of publications, Spielmann et al. (2005), Spielmann and Althaus (2007), and Spielmann et al. (2008) investigate the impact of uncertainty regarding future technology mixes (e.g., car fleet composition) and electricity mixes on large scale transport systems.

Two connected publications, Cox et al. (2018) focussing on electric and autonomous mobility and Mendoza Beltran et al. (2018b) focussing on electric mobility, account for uncertainties about the future impacts of these transport modes. Cox et al. (2018) account for current and future uncertainty with regard to EV weight, lifetime, aerodynamics, powertrain efficiency, battery mass and other parameters. In Mendoza Beltran et al. (2018b) future electricity mixes are adjusted according to large scale simulations of the IMAGE model (PBL, 2014).

With regard to electric mobility, uncertainty about two groups of parameters are broadly accepted to be influential and treated. The first group of parameters relates to battery production (e.g., mass, raw material composition, life time and production emissions) (McCleese and LaPuma, 2002; Cox et al., 2018; Harris et al., 2018). The second group of parameters relates to the electricity production (e.g., GHG intensity and composition of future electricity mixes) (Samaras and Meisterling, 2008; Noshadravan et al., 2015; Mendoza Beltran et al., 2018b).

Finally, several studies dealing with vehicle material composition and lightweighting analyse uncertainty of LCA parameters such as material emission-intensity (i.e., emissions per weight) (Geyer, 2008; Pryshlakivsky and Searcy, 2017), material substitution ratios and fuel reduction values (Kelly et al., 2015).

LCA - Uncertainty characterisation

Share of studies

Probability theory

69%

Set theory

16%

Scenarios

19%

LCA - Uncertainty treatment

Only uncertainty analysis

66%

Uncertainty and sensitivity analysis

34%
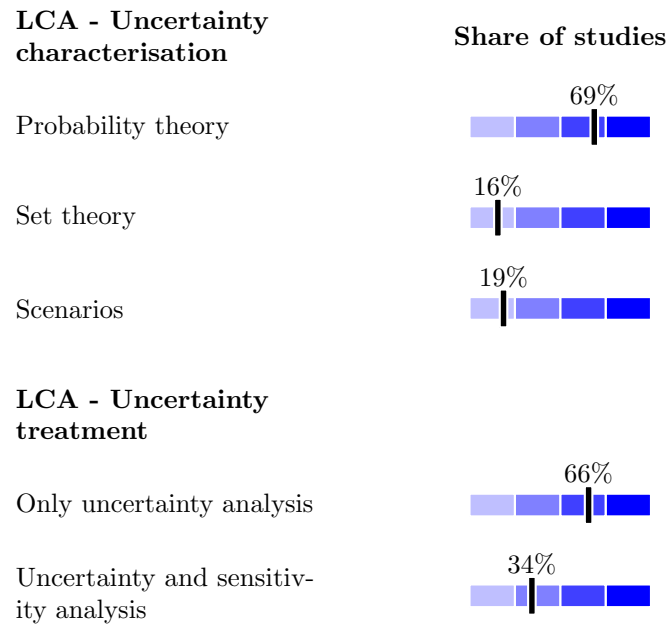
Figure 3.13: Share of studies applying uncertainty treatment

3.4.3   Uncertainty characterisation and treatment

The large majority of studies use probability theory to describe and treat uncertainty in parameters, with only a few studies using set theory (e.g., minimum and maximum values). Scenario analysis is often used to describe uncertainty about inputs or the experimental frame (Spielmann et al., 2005; Spielmann and Althaus, 2007; Spielmann et al., 2008).

Figure 3.13 shows the share of studies for the different characterisation options and distinguishes studies that only apply uncertainty propagation from studies that apply both UA and SA. Note that studies applying only SA without assessing the uncertainty in the model output were excluded.

Regarding uncertainty propagation, another interesting aspect is the computational burden of the stochastic modelling approaches. Figure 3.14 shows the reported number of iterations for each study applying stochastic modelling (e.g., MC sampling) in case it is reported. The number of iterations is plotted against the publication date of the study and ranges from 8 to 12'000. Computation times can depend on the size of the LCI model, i.e., if the matrix inversion approach is applied, the number of rows and columns.

Another relevant aspect with regard to stochastic modelling is that LCI parameters of transport modes can exhibit more or less complex dependencies. As acknowledged by Boureima et al. (2009) fuel consumption is strongly correlated to vehicle weight as well as carbon dioxide and sulphur dioxide tailpipe emissions, while showing no satisfying correlation with other tailpipe emissions (e.g., nitrogen oxides or carbon monoxide). Similarly Cox et al. (2018) acknowledge strong correlations among vehicle design parameters of EVs (e.g., battery mass and efficiencies) and their energy consumption. Such correlations are either dealt with using multivariate sampling (Subramanyan et al., 2008) or by explicitly modelling parameters dependencies among elements of the technosphere and biosphere matrices where, e.g., fuel-related tailpipe emission values become
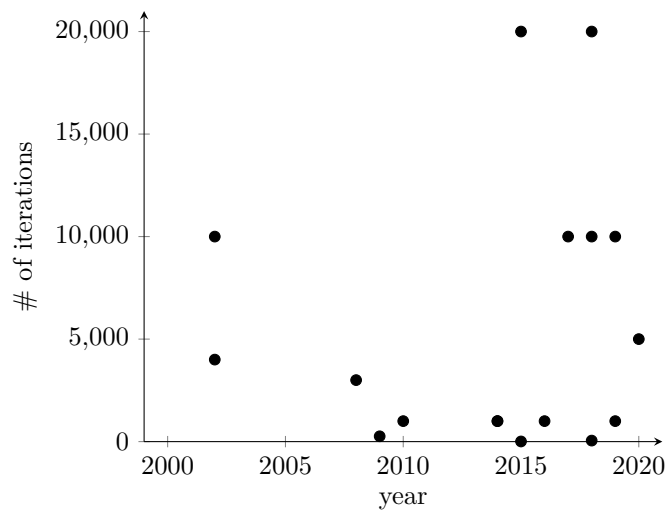
Figure 3.14: Number of stochastic modelling iterations for studies investigating simulation error from stochastic choice models.
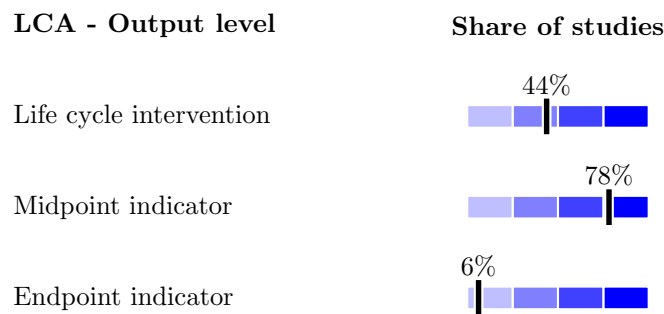
Figure 3.15: Share of studies applying uncertainty treatment

a function of the sampled fuel consumption values.

3.4.4   Model outputs and uncertainty communication

Finally, uncertainty can be characterised for three different levels of output aggregation: *life cycle interventions* (i.e., the intervention vector computed according to equation 2.2), *midpoint indicators* (i.e., the impacts vector computed according to equation 2.3) and *endpoint indicators* (usually computed from midpoint indicators using a weighting process). While life cycle interventions will be affected by uncertainty from parameters in the technology and biosphere matrix, they are unaffected by uncertainty from characterisation methods applied in the LCIA phase. Midpoint and endpoint indicators however accumulate the uncertainty both from the LCI and LCIA phases. However only one study explicitly treats uncertainty of the LCIA phase (Messagie et al., 2019), although most studies report results at the midpoint level.
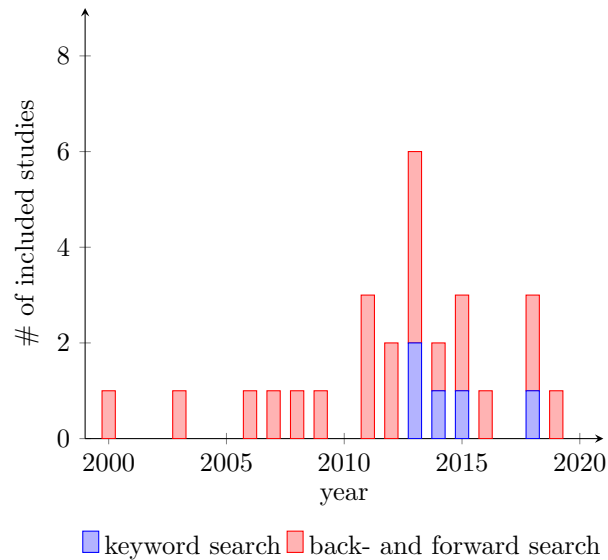
Figure 3.16: Number of included studies per year and for both search means.

3.5   Review: uncertainty analysis of ABMs

The scope of the review was set to include studies that apply UA to ABMs. The literature search and article selection follows the same systematic approach outlined for LCA in the previous section. Figure 3.16 shows the identified studies by date of publication and means of identification in the literature search. While more recent years suggest that there has been a cooling off regarding the topic, there are still several new contributions since 2015 that could be identified.

3.5.1   Type of ABM

A first criteria to investigate is the repartition of ABM types among the identified studies. Figure 3.17 shows the repartition among utility-based models, rule-based model and other models (i.e., models that are more difficult to categorise). The corpus is skewed towards studies performing UA for rule-based models.

In fact, most of these studies are focussed on uncertainty in the Albatross model Arentze and Timmermans (2004) followed by studies of the Feathers model (Janssens et al., 2007) (which in fact incorporates the core of the Albatross model) and one of the Ramblas model (Veldhuisen et al., 2000b). For utility-based models, each of the five identified studies deals with a different model, including the "San Francisco model"(Jonnalagadda et al., 2001), SacSim (Bradley et al., 2010), the "Tel Aviv ABM" (Shiftan et al., 2004), the "New York activity-based microsimulation model" and SimMobility (Adnan et al., 2016). Finally, for models which were not clearly in one of the first two categories MATsim (Axhausen et al., 2016) and TRANSIMS (Smith et al., 1995) are the most prominent models for which two studies each have been identified, followed by a study of the Danish National Transport Model (NTM) (Rich et al., 2010). No studies could be found for purely constraint-based models.

ABM - Modelling approach

Share of studies

Constraint-based

0%

Utility-based

22%

Rule-based

57%

Other

22%
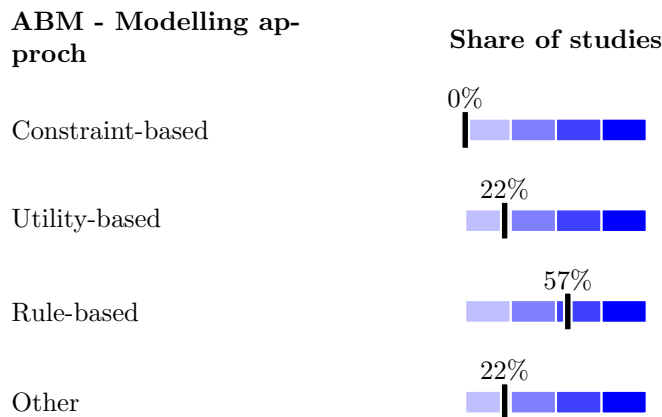
Figure 3.17: Share of studies for different ABM types.

3.5.2 Uncertainty location and identification

Regarding uncertainty locations, figure 3.18 shows the share of studies addressing uncertainty for each of the locations of the proposed classification for ABM/LCA coupled models. Note, that some studies are dealing with uncertainty of multiple locations. While there is a strong tendency for studies to address the simulation error, other locations are much less addressed. Several studies deal with uncertainty from the experimental frame (all of which address the sampling error due to running the model with only a fraction of the population) (Kwak et al., 2012; Bekhor et al., 2014; Petrik et al., 2018). A couple of studies address input uncertainty (e.g., uncertainty of travel time data) (Rasouli and Timmermans, 2014b; Manzo et al., 2015), while only one study addresses uncertainty of the model estimation (i.e., the estimated parameters) (Petrik et al., 2018). No study dealing with uncertainty of the model specification (e.g., the functional form) was found.

The high share of studies dealing with the micro simulation error could be explained by the relative easy means to address this location. Some ABMs are stochastic by nature where, e.g., random draws of individual choices are already in place causing the simulation error. Uncertainty in other locations (e.g., the model specification) can be more challenging to characterise (e.g., requiring the modelling of alternative model structures prior to running simulations) or a consensual characterisation framework might not exist for the specific location (e.g., model estimation). Another explanation could be, that stochastic models are argued to require multiple simulation runs to reach stability and UA (or at least stability analysis) becomes an integral part of the model results. This however should ultimately hold true for all relevant uncertainty locations.

Studies exploring uncertainty in the experimental frame all focus on the so-called sampling error. Kwak et al. (2012) investigate running the ALBATROSS model for 25%, 50% or 100% of the internal population, and 2% or 4% for the external population. Bekhor et al. (2014) use the Tel Aviv ABM to run simulations for sample sizes of 10%, 50% and 100% making the observation that the sample size has an affects on the "stationary point" of results and showing that the sampling error is proportional to the inverse of the square root of the sample size. Rasouli (2016) runs the ALBATROSS model for sample sizes of 10%, 30% and 50% to investigate the uncertainty in a range of outputs, concluding that an increase in sample size can dramatically reduce the uncertainty. Finally, Petrik et al. (2018) use SimMobility to run simulations for sample sizes

ABM - Uncertainty location

Share of studies

Experimental frame   17%

Inputs   13%

Model {

Specification   0%

Estimation   4%

Simulation error   91%
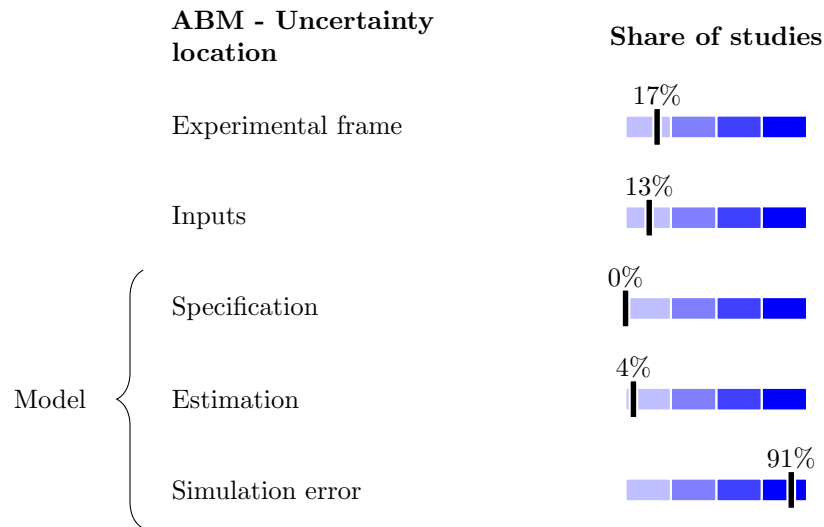
Figure 3.18: Share of studies treating different uncertainty locations.

of 5%, 10%, 20%, 30% and 50% of the total population, confirming the results of Bekhor et al. (2014) regarding the relationship between error and sample size. Both Rasouli (2016) and Petrik et al. (2018) find that the "elbow" of the curve is achieved around 30% of the total population, where an additional increase in sample size allows to reduce uncertainty only to a lesser extent.

Input uncertainty is addressed by three studies. Rasouli (2016) investigates uncertainty in land-use data (i.e., employment data), and Rasouli and Timmermans (2014b) investigate the effect of uncertainty in service level data (i.e., travel times for selected routes), both for the Albatross model. Manzo et al. (2015) focusses on large scale socio-economic drivers such as population size, gross domestic product, employment, and fuel prices in the Danish National Transport Model. Only Petrik et al. (2018) investigate uncertainty in the model estimation. Their analysis is performed for 817 parameters of the 22 discrete choice models of Preday model, which is part of the SimMobility framework. Following parameter screening, only the 100 most influential parameters are included in the UA.

The largest share of studies investigate the simulation error. In utility-based ABMs the randomness is coming from the error terms of discrete choice models, while for stochastic rule-based ABMs it is coming from e.g., probabilistic decision tables. The earliest study found investigating this location is Veldhuisen et al. (2000a) for the Ramblas model, where marginal and conditional probability matrices are used to predict DAPs. Similar studies have since been performed for the Albatross (Rasouli and Timmermans, 2013b) and Feathers models (Cools et al., 2011). With regard to utility-based models Castiglione et al. (2003) investigate the uncertainty stemming from the individual choice models of the San Francisco model and several studies since have performed similar analyses Bowman et al. (2006), Vovsha et al. (2008), Bekhor et al. (2014), and Petrik et al. (2018).

3.5.3   Uncertainty characterisation and treatment

Uncertainty characterisation is dealt with in a very homogeneous manner, with all studies applying probability theory.

Figure 3.19 shows the uncertainty treatment methods applied, distinguishing studies that

ABM - Uncertainty characterisation

Share of studies

Probability theory

100%

Set theory

0%

Scenarios

3%

Uncertainty treatment

Only uncertainty analysis

87%

Uncertainty and sensitivity analysis

13%
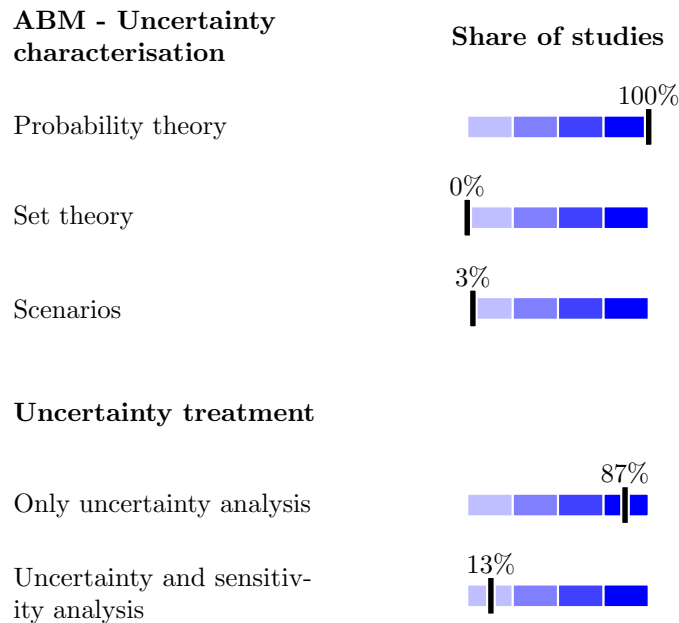
Figure 3.19: Share of studies applying uncertainty treatment

only apply uncertainty propagation from studies that apply both UA and SA. Note that studies applying only SA without assessing the uncertainty in the model output were excluded according to the criteria.

Among the large share of studies that apply only uncertainty propagation, all of them apply some form of stochastic modelling (e.g., MC simulations), where sampling is conducted on inputs, parameter or model variables. Only three studies conduct SA as a complement to the uncertainty propagation. Most notability Petrik et al. (2018) use regression models to identify the most influential parameters of the Preday model of the SimMobility framework.

Regarding uncertainty propagation, another interesting aspect is the computational burden of the stochastic modelling approaches. Figure 3.20 shows the reported number of iterations for each study investigating the simulation error. The number of iterations is plotted against the publication date of the study and ranges from a couple of iterations to one thousand, with the large majority of studies reporting 100 iterations or less. There can be a trade-off between the necessary number of iterations to reach convergence of the model results and the computational burden. Since the duration of a simulation, as well as the model convergence rate can vary between different ABMs, it is not surprising that the number of simulations varies as well.

While all studies apply some form of stochastic modelling, a relevant difference among studies reported is the specific sampling technique applied. Three relevant aspects of sampling will be highlighted in the following.

As a first, taking into account dependencies between uncertain quantities. This usually builds on sampling from a multivariate distribution which preserves correlations, rather than sampling from each quantity independently. Assuming normal distributions Manzo et al. (2015) use multivariate sampling for the Danish National Transport Model, taking into account statistically significant correlations between model inputs (e.g., population size, gross domestic product, employment, and fuel prices), which are determined from historic data. Petrik et al. (2018) apply
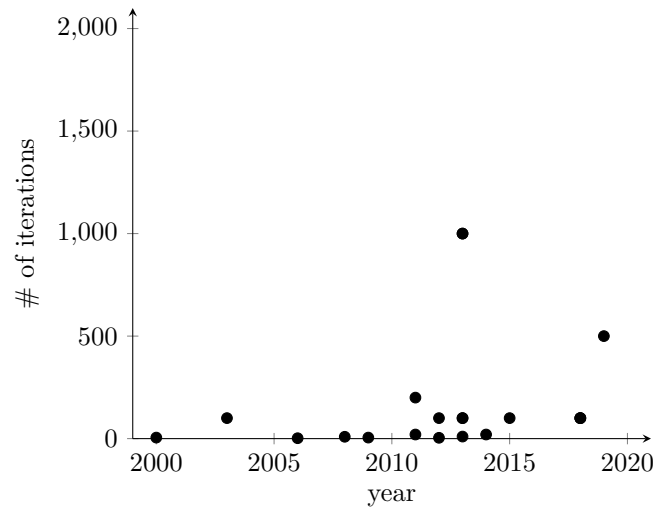
Figure 3.20: Number of stochastic modelling iterations for studies investigating simulation error from stochastic choice models.

multivariate sampling for the Preday model within the SimMobility framework, for parameters of discrete choice models building on parameter estimates, their standard errors and correlations, yielded by model calibration.

As a second, some sampling methods can cover the sampling space in a more efficient manner, which usually aims at increasing the convergence rate of the UA and thus to have stable model outputs and uncertainty measures with a lower number of model runs. This is especially important for models with long computation times, such as ABMs. Manzo et al. (2015) and Petrik et al. (2018) use LHS, a method of stratified pseudo-random sampling, for input and parameter sampling respectively. Rasouli (2016) applies Halton draws, a method of quasi-random sampling, to sample sequentially from nodes of the probabilistic decision tables of the Albatross model. Rasouli (2016) also compares the outcome to those of a similar experimental design which uses regular MC sampling, concluding that Halton draws allow to substantially reduce the required runs to get stable results.

As a third, when performing UA for comparative assertions (e.g., when comparing the effect of two or more policy scenarios) the difference in predictions should be a consequence of differences in the compared scenarios and not due to the pseudo-random numbers. This implies some level of "coordination" of the sampling procedures applied across scenarios. Specifically, with regard to random number seeds, care has to be taken that a sampled input, parameter or specific decision (e.g., the mode choice to arrive at the jth activity of the ith individual) is always based on the same identical seed across scenarios for the same iteration, while varying across iterations. This does not mean that the sampled input, parameter value or choice is the same, since the difference in the compared scenarios can cause a difference in the quantity's distribution parameters (e.g., higher or lower mean value) or in modelled utilities and explanatory variables of the discrete choice model (e.g., the available transport mode and their travel times). This challenge and potential solutions have been acknowledged by Bowman et al. (2006) and Vovsha et al. (2008). Vovsha et al. (2008) discuss storing random seeds for each choice of each individual and re-use the stored seeds for different scenarios. Bowman et al. (2006) assess the impact of this random seed coordination, concluding that much of the simulation error for comparative assertions can be removed by coordination.

ABM - Output level   **Share of studies**
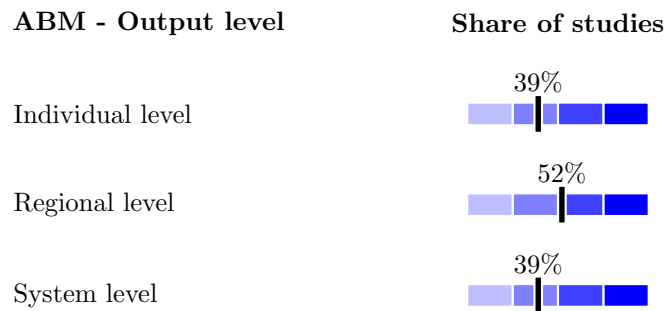
Figure 3.21: Share of studies applying uncertainty treatment

3.5.4   Model outputs and uncertainty communication

As acknowledged in Petrik et al. (2018), the level of output aggregation for which uncertainty is characterised can differ among studies performing UA and is of specific interest to ABM/LCA coupled models, where ABM outputs can become LCA inputs.

Three levels of outputs are distinguished: *individual* level outputs, *regional* level outputs and *system* level outputs, such as the total amount of vehicle kilometres travelled.

Figure 3.21 gives an overview of the output levels for which uncertainty is characterised and communicated in the reviewed articles.

Individual level outputs for which uncertainty is characterised include the average number of trips (Castiglione et al., 2003; Cools et al., 2011; Bao et al., 2013; Bao et al., 2015; Rasouli and Timmermans, 2014b; Petrik et al., 2018), distances travelled Cools et al. (2011), Rasouli et al. (2012), Bao et al. (2013), and Bao et al. (2015), activity durations and travel times (Rasouli and Timmermans, 2014b) observed per individual. Regarding uncertainty communication, most noticeably is the work of Rasouli and Timmermans (2013c) who suggest a multidimensional extension of the Levenshtein distance to measure uncertainty in predicted activity travel sequences. Most of the other studies rely on statistical measures such as e.g., Standard Deviation (SD), Coefficient of Variation (CV) or Confidence Interval (CI).

Regional levels for which uncertainty is characterised include the number of trip between origins and destinations (Veldhuisen et al., 2000a; Castiglione et al., 2003; Vovsha et al., 2008; Rasouli and Timmermans, 2013b; Rasouli and Timmermans, 2013c) or the number of trips passing through network sections (e.g., in case traffic assignment is done) (Vovsha et al., 2008; Lawe et al., 2009; Ziems et al., 2011; Kwak et al., 2012; Bekhor et al., 2014; Paulsen et al., 2018). In terms of uncertainty measures and communication, graphical representations, e.g., using zonal boundaries and colour scales to represent uncertainty levels as done by Rasouli and Timmermans (2013b), can be a valuable tool to highlight spatial heterogeneities in uncertainty levels.

Finally, at the system level uncertainty is characterised, e.g., for the number of trips (Bowman et al., 2006; Rasouli and Timmermans, 2013a; Manzo et al., 2015; Petrik et al., 2018), travelled distances (Manzo et al., 2015; Bao et al., 2018; Petrik et al., 2018), travel durations (Bekhor et al., 2014) or mode shares (Bowman et al., 2006; Rasouli and Timmermans, 2014b; Petrik et al., 2018) at population level within the studied region.

3.6   Summary

After reviewing the general classifications of uncertainty natures, locations and levels a new classification for uncertainty locations of ABM/LCA coupled models is proposed in the first part of this chapter. The classifications of both fields are therefore related to more the general framework of Walker et al. (2003). The following uncertainty locations are distinguished: experimental frame, inputs, model and outputs. For each of these locations, more specific sub-classes are specified. The purpose of this new classification is to support systematic UA of ABM/LCA coupled models.

Next, a broad review on the distinguishable steps of UA is presented, introducing the concepts of uncertainty location, identification, characterisation, treatment and communication. This provides the background knowledge for the following review of UA conducted for LCA and ABMs, as well as for the subsequent chapters introducing the CONNECTING model and the proposed methodology of UA.

Two separate reviews of UA conducted for LCA of transport systems and ABMs are presented. This approach is chosen, as currently no study exists conducting UA of an ABM/LCA coupled model. The review of LCA conducted for 32 identified studies reveals that the large majority of studies is focussed on individual transport modes and performs UA for parameter uncertainty. Only few studies are focussed on other subjects (e.g., PT) and other uncertainty locations (e.g., experimental frame or inputs). The review of ABMs conducted for 23 identified studies reveals that UA has been conducted for both rule-based and utility-based models. A large share of the identified studies focusses on the simulation error caused by stochastic choice models. With regard to the applied methods, stochastic modelling (e.g., MC simulations) is by far the most popular, both for LCA and ABMs. However, there is a significant disparity with regard to the number of iterations that are applied, which tends to be higher in LCA studies.

Chapter 4

CONNECTING Model

4.1 Introduction

The CONNECTING project takes on the challenge of proposing a modelling framework to provide scientific evidence of environmental impacts of future mobility policy scenarios in Luxembourg, focussing on French CBCs. This chapter will elaborate on this modelling approach, which was briefly introduced in section 1.2. The present chapter provides the most extensive description of the CONNECTING model so far. The model constitutes a collaborative effort, where the ABM part has originally been developed by Mariante (2017), while the LCA part and coupling is presented by Baustert et al. (2019).

LCA introduced in chapter 2 is an internationally standardized approach and as such has clear documentation requirements described in ISO (2006b) and ISO (2006a). This standard defines the reporting requirements for the four LCA phases: the *goal and scope definition phase*, *inventory analysis phase*, *impact assessment phase* and *interpretation phase*. While the final interpretation phase will be covered in chapters 6-8, this chapter is concerned with reporting on the first three phases.

However, as the CONNECTING project does not constitute a pure LCA study but aims at advancing the LCA framework, simply following the ISO standard would insufficiently describe the CONNECTING model especially, the ABM part and model integration. In order to both report the essential parts of the ISO standard reporting requirements and adequately describe the CONNECTING model, there will be a dedicated section to the ISO reporting, prior to describing the CONNECTING model. The dedicated section will only include aspects not covered in the following model description (i.e., the goal and scope definition phase).

Section 4.2 will present the ISO reporting on the goal and scope definition phase. Section 4.3 will describe all model variables and data sources, being followed by sections 4.4-4.5 presenting the ABM and LCA structures respectively. Finally, section 4.7 will briefly introduce the scenarios that will be investigated in the present thesis.

4.2 ISO reporting

In the following the goal and scope definitions for the LCA study will be discussed. This is done according to the ISO standards of LCA (ISO, 2006b; ISO, 2006a). The description of the LCI and LCIA phases are provided in sections 4.3.4-4.3.5 respectively.

4.2.1   Goal of the study

The intended application of the CONNECTING model is to quantify environmental impacts, with regard to air quality and climate change, of mobility policies from a life cycle perspective taking into account uncertainty. The reason for carrying out the study is the novelty of the proposed framework, which allows to couple individual DAPs to life cycle impacts. The intended audiences are policy makers interested in comparing different policy scenarios towards a more sustainable mobility system and scholars interested in the proposed modelling framework and its systematic UA. Finally, results are intended to be used in comparative assertions and disclosed to the public by means of peer-reviewed publications.

4.2.2   Scope of the study

The product system being studied is the trans-border transportation system (including individual car and PT options) between France and Luxembourg.

The function of the trans-border transportation system is the provision of transport services to all individuals within the CBC population and for all their activities conducted during a regular work day. The provision of transport services for other populations (e.g., Luxembourgish residents or commuters from other countries) is omitted.

The functional unit is to "meet the daily travel demand by French commuters working in Luxembourg for 2015–2025". The reference flow is derived by aggregation of the passenger-kilometres (pkm) for each transport mode for a single work day over the commuting population.

The system boundary, determining the selection of included unit processes, encompasses all motorized transport modes (individual car, train and bus) from cradle-to-grave (excluding slow mobility as their impact is considered negligible compared to motorized mobility). In addition the projected change of electricity mixes (the shares of different energy sources contributing to the power grid) for Luxembourg and France are modelled (see section 4.7) for the study period. For individual cars, fleet shares of different powertrains (diesel, gasoline, hybrid and electric cars) are distinguished, as well as different emission standards for ICEVs (EURO3 and older, EURO4, EURO5 and EURO6).

There is no particular allocation procedure necessary for the description of the product system, as there are no co-products to be considered.

The selection of impact categories is consistent with the goal definition. The Environmental Footprint (EF) (2013/179/EU) method derived from the International Life Cycle Data system (ILCD) scheme, developed by the European Commission, is chosen. The specific impact categories chosen are (1) the climate change global warming potential (GWP100) midpoint indicator, measured in kilogram CO_2-equivalents and; (2) respiratory inorganics human health effects associated with exposure to $PM_{2.5}$ midpoint indicator, measured in disease incidences. These measures are the QOIs for decision makers produced by the CONNECTING model. The climate change related effects will be simply referred to as *GWP100*, while the respiratory effects related impacts will be referred to as *R-E*.

The interpretation is focused on the comparison of different mobility policy scenarios with regard to the QOIs over the study period. The effectiveness of different types of policy investment will be tested.

Data sources include manufacturer data for the production, emission standards, technical reports and real-world measurements for the use phase, and existing databases for the disposal of each transport mode. Prior LCA studies and databases serve as references. Strategic policy documents are sources for the predictions of future car fleet shares and electricity mixes.

Several assumptions have to be highlighted for each product system. These assumptions include production location, used electricity mixes (e.g., for charging EVs), lifetimes, occupancy

rates and average fuel (or electricity) consumption rates.

There are several limitations regarding the LCI modelling. As a first, in reality electricity mixes vary in time (e.g., solar power production is usually limited to the day and varies across seasons) and different shares of electricity production sources imply different environmental impacts. However, the CONNECTING model does not include a module to predict individual charging patterns or hourly/seasonal electricity mixes, but relies on yearly average data. The same issue relates to electric buses. A second limitation relates to the lack of regional specific data for the LCIA. While CFs distinguish "urban" and "non-urban" emissions for *R-E*, the aggregated nature of generated DAPs and the fact that no traffic assignment is performed, makes it difficult to match elementary flows and CFs. This limitation does however not affect the GWP100 scores as the impact of GHG emissions is usually independent of the location of emissions.

Data quality requirements include the temporal, technological and geographical coverage of data. Especially the use phase of transport modes is relevant for the chosen QOIs, thus data for fuel consumptions and emissions should be as recent as possible and the focus of data collection efforts. With regard to geographical coverage, whenever possible data should be collected for the French and Luxembourgish study region, especially regarding the CBC car fleet and the electricity mix. Finally, the technologies covered should include the dominant transport modes used within the study region, including PT modes and private vehicles. Overall, the collected data for the CONNECTING case study is deemed representative using recent and regional specific sources for fuel consumption, electricity mixes and car fleet composition (as described in section 4.3). The used ecoinvent database covers all relevant transport modes, while recent publications are used to complement (i.e., for hybrid cars). Chapter 5 will further detail the approaches applied to characterise the uncertainty of all LCI data sources.

4.3 Variables and data

Five groups of variables are distinguished. These groups include variables related to the commuting population, the Travel Analysis Zones (TAZs), the transport system, the transport modes (constituting the LCI) and the environment (described by the LCIA). Each variable will be given an unique identifier, as well as a short description. To avoid confusion, in subsequent sections the unique identifier will often be complemented by a description of the variable. For each variable a "domain" summarizing all possible states will be provided. Finally all data sources are disclosed.

4.3.1 Commuting population

The commuting population is described by a set of variables related to individual and household characteristics (*hh*), work characteristics (*w*) and their individual activity pattern (*ap*). The following tables 4.1-4.3 summarize all variables.

First, individual and household variables are listed in table 4.1. These variables describe the socio-demographic characteristics of the commuting population on the household level and are assumed to be relevant predictors of their commuting behaviour. Most variables are of nominal or ordinal scale, while the monthly household income is of interval scale, and age and the number of cars per household are of ratio scale.

The education level variable builds on the French school system where "sec. tech./gen." designates graduation from "enseignement secondaire technique ou général", "sec. prof." designates graduation from "enseignement secondaire professionnel", "bac tech./gen." designates a "Baccalauréat technique ou général", "bac prof." designates a "Baccalauréat professionnel", "B+3" designates "Baccalauréat + 1 to 3 years of higher education (e.g., DUT, DEUG, BTS

or Licence)" and "B+4" designates "Baccalauréat + at least 4 years of higher education (e.g., Master degree, maîtrise, doctoral degree or degree from a grande école)". The classification used for the settlement type variable is based on commonly used terms, e.g., terminology used by the National Institute of Statistics and Economic Studies (INSEE), classifying settlement types ordinally by population size. Respondents ultimately classify their settlement based on these provided classes.

Table 4.1: Individual and household variables. In the variables domains "NA" is used to designates "No Answer". C is a set containing an identifier for each TAZ in the study region (i.e., each commune).

ID	Description	Domain
hh_1	Gender	1: male
		2: female
		3: NA
hh_2	Age	$x \in \mathbb{N}$
hh_3	Marital status	0: not married
		1: married
		2: NA
hh_4	Children	0: No
		1: Yes
		2: NA
hh_5	Education level	1: primary
		2: sec. tech./gen.
		3: sec. prof.
		4: bac tech./gen.
		5: bac prof.
		6: B+3
		7: B+4
		8: other
		9: NA
hh_6	Settlement type	1: hamlet
		2: village
		3: town
		4: city
		5: big city
		6: NA
hh_7	Occupancy status	1: owner or co-owner
		2: tenant
		3: parents/friends
		4: other
		5: NA
hh_8	Number of cars	$x \in \mathbb{N}$
hh_9	Monthly household income [€]	1: $x \leq 2000$
		2: $2000 < x \leq 3000$
		3: $3000 < x \leq 4000$
		4: $4000 < x \leq 6000$
		5: $6000 < x \leq 8000$
		6: $x > 8000$
		7: NA
hh_{10}	Household location	$c \in C$

In table 4.2 the work related variables are listed for the commuting population. These variables describe the usual work location and employment characteristics. Again most variables are of nominal or ordinal scale, with the exception of working hours which are specified per week on a ratio scale.

The parking availability variable was derived from several survey questions and is based on the respondents perception, where no quantification of what constitutes "close by" was given in the survey. The travel reimbursement variable distinguishes three answers, where either travel expenses are not reimbursed ("No"), the employee have access to a "company car" or the employee is at least partially reimbursed for his travel expenses by PT or private car ("reimbursement").

Finally in table 4.3 the DAP related variables are listed for the commuting population. These variables describe what activities the commuters are engaged in, for how long, travel times between these activities, locations and transport modes. Activity duration and travel time, as well as the available time budget and total number of daily travels are of ratio scale, the departure time is of ordinal scale, and activity types, locations and transport modes are of nominal scale. Activity and travel durations are derived from time indications (departure and arrival times) recorded in the survey. The time budget is a calculated variable, recording the remaining amount of time until midnight in minutes.

"PT" is public transport, which is a multi-modal combination of bus and train (where slow

Table 4.2: Work related variables. In the variables domains "NA" is used to designates "No Answer". C is a set containing an identifier for each location in the study region (i.e., each commune).

Variable	Description	Domain
w_1	Working hours	1: Defined by employee
		2: Defined by employer
		3: Defined jointly
		4: NA
w_2	hours/week	$x \in \mathbb{N} : 1 \leq x \leq 40$
w_3	Type of profession	1: senior manager
		2: engineer
		3: armed forces
		4: middle mgmt.
		5: administration
		6: service providers
		7: agriculture
		8: industry
		9: assembly workers
		10: non-qualified
		11: NA
w_4	Parking availability	1: at work
		2: close by
		3: no availability
		4: NA
w_5	Travel reimbursement	1: No
		2: company car
		3: reimbursement
		4: NA
w_6	Workplace location	$c \in C$

mobility is assumed as mode to reach the main mode and for transfers). "car+PT" is the same as "PT", with the exception that the mode car is used to reach the stop of the first PT mode. The activity type variable distinguished 10 categories, with "leisure" activities including e.g., sport or cultural activities, "service" activities including e.g., doctor visits, bank related activities or taking part in training courses, and "work" activities also including work related travels. The "end" state designates that no subsequent activity is conducted. Finally, in the model the total number of daily trips $ap_{j,8}$ corresponds to the number of trips conducted by an individual and is capped to a maximum of 6 (corresponding to a maximum of 7 activities since the first daily activity does not require a prior trip to reach it). This maximum of 6 trips was chosen because the large majority of DAPs observed in the survey are composed of 6 trips of less.

The main data source for this group of variables is the survey data stemming from the

Table 4.3: Activity pattern related variables. Where j is the index indicating the activity. In the variables domains "NA" is used to designates "No Answer". C is a set containing an identifier for each TAZ in the study region (i.e., each commune).

Variable	Description	Domain
$ap_{j,1}$	Activity type	0: end
		1: pick up/drop off
		2: at home
		3: work
		4: outside meal
		5: shopping
		6: service
		7: visit friends/family
		8: go for a walk
		9: leisure activity
		10: other
		11: NA
$ap_{j,2}$	Activity duration [min]	$x \in \mathbb{N}$
$ap_{j,3}$	Activity location	$c \in C$
$ap_{j,4}$	Travel duration [min]	$x \in \mathbb{N}$
$ap_{j,5}$	Transport mode	1: car
		2: bus
		3: train
		4: slow mobility
		5: car+PT
		6: PT
		7: other
		8: NA
$ap_{j,6}$	Time budget [min]	$x \in \mathbb{N} : 0 \leq x \leq 1440$
$ap_{j,7}$	Departure category	1: $00:00 \leq x < 06:00$
		2: $06:00 \leq x < 08:00$
		3: $08:00 \leq x < 10:00$
		4: $10:00 \leq x < 16:00$
		5: $16:00 \leq x < 18:00$
		6: $18:00 \leq x < 20:00$
		7: $20:00 \leq x < 24:00$
		8: NA
$ap_{j,8}$	Total number of trips	$x \in \mathbb{N} : 1 \leq x \leq 6$

"Enquête Mobilité des Frontaliers (EMF)" conducted between November 2010 and January 2011 by CEPS/INSTEAD in collaboration with the university of Strasbourg (Schmitz et al., 2012; Schmitz and Gerber, 2011). The survey constitutes a representative spatially stratified sample conducted among CBCs from all neighbouring regions of Luxembourg, where initially 40'000 surveys were sent out. This first phase was focussed on the socio-demographic characteristics (e.g., housing, household composition and level of education) of the CBC population, as well as characteristics related to daily travels (e.g., daily activities, car park and travel distance). This first phase had 7'235 respondents, for which a second survey phase was conducted to deepen the understanding of their mobility to which roughly half of the initial responds replied [1].

Using the survey, the values of the variables described in tables 4.1-4.2 are determined, where each ith survey respondent is characterized by a vector describing his household (HH_i) and work (W_i) related variables:

$$HH_i = [hh_1, hh_2, hh_3, \cdots, hh_{10}]$$

$$W_i = [w_1, w_2, w_3, \cdots, w_6]$$

Next a matrix describing the DAPs for each respondent is used, where each row corresponds to the jth activity and each column to a variable describing the DAP for a maximum of 7 activities (note that travel related variables such as travel duration are not defined for $j = 7$, as there is no subsequent travel to activity 7):

$$AP_i = \begin{bmatrix} ap_{1,1} & \cdots & ap_{1,8} \\ \vdots & & \vdots \\ ap_{j,1} & \cdots & ap_{j,8} \\ \vdots & & \vdots \\ ap_{7,1} & \cdots & ap_{7,8} \end{bmatrix}$$

4.3.2 Travel analysis zones

The TAZs are characterized by a set of variables describing the attractiveness characteristics (tz) of each zone (i.e., commune) in the study region.

Table 4.4 shows the attractiveness related variables for the TAZ. These variables describe e.g., the number of available establishments to conduct certain activity types as well as the more general population density. All variables are of ratio scale. Where the service index is a normalised score accounting for, e.g., public, health care, child care or leisure related services at the communal level.

The data related to these variables is based on multiple sources. To derive the population density the population data [population/commune] for each commune is based on census data for

Table 4.4: Variables describing the TAZ.

Variable	Description	Domain
tz_1	Number of restaurants	$x \in \mathbb{N}$
tz_2	Number of supermarkets	$x \in \mathbb{N}$
tz_3	Service index	$x \in \mathbb{N}$
tz_4	Population density	$x \in \mathbb{R} \mid x > 0$

---

[1] https://statistiques.public.lu/catalogue-publications/cahiers-CEPS/2012/hors-serie-FR.pdf

Luxembourg[2] conducted by Institute of Statistics and Economic Studies of the Grand Duchy of Luxembourg (STATEC) and for France[3] conducted by INSEE. Commune surface data is derived from GIS based calculations using the Luxembourgish open data platform[4] and ADMINEXPRESS data[5] for French communes. Commune coordinates (longitudes and latitudes) are based on their centroids derived from GIS data. The number of restaurants, supermarkets and the service index are based on the "base permanentes des équipements"[6] for France and the "Observatoire du Développement Spatial"[7] for Luxembourg.

All communes c in C of the study region are characterized by a set TZ_c:

$$TZ_c = [tz_1, tz_2, tz_3, tz_4]$$

Figure 4.1 shows all TAZs of the study region and their respective population density.

4.3.3   Transport system

The transport system is described by a set of variables (ts) related to travel times and travel distances between location pairs for all transport modes. Table 4.5 shows the variables for each of the motorized transport modes. Again "PT" and "car+PT" describe the multi-modal options, where travel distances are further subdivided by mode. These variables describe performance of the transport system for the different transport modes available to the commuting population. All variables are of ratio scale.

Data sources for variables in table 4.5 for the PT system are described using General Transit Feed Specification (GTFS) data provided by the Luxembourgish open data platform[8] and the French Multimodal Information System of French region Grand Est called "Fluo"[9] and the supporting agencies of the Lorraine. These GTFS files include detailed time table and stop locations for all public transport modes in the study region. The files from both data sources

Table 4.5: Variables describing the transport system.

Variable	Description	Domain
ts_1	Travel time car [min]	$x \in \mathbb{N}$
ts_2	Travel distance car [km]	$x \in \mathbb{N}$
ts_3	Travel time bus [min]	$x \in \mathbb{N}$
ts_4	Travel distance bus [km]	$x \in \mathbb{N}$
ts_5	Travel time train [min]	$x \in \mathbb{N}$
ts_6	Travel distance train [km]	$x \in \mathbb{N}$
ts_7	Travel time PT [min]	$x \in \mathbb{N}$
ts_8	Travel distance PT [km]	$x \in \mathbb{N}$
ts_9	Travel time car+PT [min]	$x \in \mathbb{N}$
ts_{10}	Travel distance car+PT [km]	$x \in \mathbb{N}$

---

[2] http://www.statistiques.public.lu/fr/population-emploi/rp2011/caracteristiques-personnelles/index.html
[3] https://www.insee.fr/fr/statistiques/1280956
[4] https://data.public.lu/fr/datasets/limites-communales-historiques-1/
[5] http://professionnels.ign.fr/donnees
[6] https://www.insee.fr/fr/metadonnees/source/serie/s1161/
[7] https://amenagement-territoire.public.lu/fr/strategies-territoriales/observatoire-developpement-spatial.html
[8] https://data.public.lu/en/search/?q=gtfs
[9] https://www.fluo.eu/

Figure 4.1: Study region with population density of all TAZs.

(from Luxembourg and France) have been combined for the CONNECTING project to describe the cross-border PT system.

To describe the road network the tool "geofabrik"[10] is used which provides the openstreetmap[11] data for the study region.

Travel times and distances between each possible Origin-Destination (OD) pair and for each transport mode (private car, single PT modes and multi-modal modes) are calculated using an opentripplanner (otp)[12] which uses the created GTFS files and road network.

Each OD pair of the communes c in the study region C is characterized by a set of values $(TS_{o,d})$ (where o is the identifier of the origin commune and d the identifier of the destination commune):

$$TS_{o,d} = [ts_1, ts_2, ts_3, ..., ts_{10}]$$

---

[10]https://www.geofabrik.de/
[11]https://www.openstreetmap.org/
[12]http://www.opentripplanner.org/

The transport system as a whole can be described by multiple OD matrices (one for each variable in table 4.5), where each row represents an origin and each column a destination. As an example, the matrix for car travel times (ts_1) can be written as follows:

$$OD_{ts_1} = \begin{bmatrix} ts_{1_{1,1}} & ts_{1_{1,2}} & \cdots & ts_{1_{1,d}} & \cdots \\ ts_{1_{2,1}} & ts_{1_{2,2}} & \cdots & ts_{1_{2,d}} & \cdots \\ \vdots & \vdots & & \vdots & \\ ts_{1_{o,1}} & ts_{1_{o,2}} & \cdots & ts_{1_{o,d}} & \cdots \\ \vdots & \vdots & & \vdots & \end{bmatrix}$$

4.3.4   Transport modes

The transport modes are characterised by a set of variables describing their production, use and disposal, as well as interventions with the environment. The following table exemplifies the variables for one product system considered in CONNECTING, describing domains for a generic "individual car" product system.

All variables can be scaled to relate to 1 life cycle, 1 vehicle-kilometre (vkm) or 1 passenger-kilometres (pkm), where assumptions have to be made about the life cycle performance (e.g., total travelled distance, average occupancy, etc.). In case of the CONNECTING LCI all transport modes are scaled to relate to 1 vkm before being aggregated to car or PT fleets. Once aggregated to the fleet level, unit processes are scaled to relate to 1 pkm.

Variables such as car maintenance (or assembly) are provided as unit processes (marked with unit [-] in table 4.5) for 1 life cycle (or for the assembly of 1 car). Variables for car components such as the powertrain, glider or battery are provided per kilogram produced (assuming a certain composition of metals, plastics etc.).

To further illustrate the life cycle perspective and embedding of product systems in the technosphere, figure 4.2 shows the product system presented in table 4.6, where product/waste flows between unit processes within the car product system and between the car product system and other product systems are represented by arrows. Elementary flows between the car product system and the biosphere (i.e., b_1, b_2, b_3, etc.) are represented by dashed arrows. The system boundary of the car product system is shown as well as the three life cycle phases. As the product system includes are large number of unit processes and flows, it is impractical to show a comprehensive product system here.

The LCI modelling thus encompasses all data needed for the processes of each transport product system (e.g., bus or train) from a life cycle perspective, as well as the upstream and downstream product systems which provide the inputs to or receive outputs from these transport product systems.

Specifically, the car inventories are based on the ecoinvent LCA database[13], where fuel consumptions and related emissions have been updated using regional specific data from the Luxembourgish data platform[14]. In addition, fuel consumption data (which is determined from official driving cycle data) is corrected using the correction factors published in the most recent report issues by the International Council on Clean Transportation (ICCT)[15]. For hybrid electric cars the inventories from ecoinvent were adapted according to Raykin et al. (2012). Car fleet composition is modelled based on a cohort model (where a cohort is modelled for all powertrains and emission standards) the modelling effort first presented in Baustert et al. (2019) will be outlined in section 4.7. The bus inventories are based on specific manufacture data from (Transport

---

[13]https://www.ecoinvent.org/
[14]https://data.public.lu/
[15]https://theicct.org/

& Environment, 2018). Finally the train LCI data relies on the existing ecoinvent LCA database[16]. To describe the upstream product system (e.g., primary energy production, resource mining etc.) the ecoinvent version 3.5 "cutoff" database is used.

Following the notation of Heijungs and Suh (2002), the LCI data is structured in two matrices, the technosphere matrix $\mathbf{A}$ containing the technosphere exchanges (e.g., a_1 of table 4.6) and biosphere matrix $\mathbf{B}$ containing the biosphere exchanges (e.g., b_1 of table 4.6). These matrices contain the exchanges both for the transport product system data described above as well as the data from ecoinvent.

Table 4.6: Car inventory variables. Where under *Prod.* production inputs; under *Use* use phase inputs; under *Disp.* disposal/emission outputs to the technosphere; and under *Air*, *Water* and *Soil* the outputs to the biosphere are listed.

| Variable	Description	Domain
Prod.		
a_1	Car powertrain [kg]	$x \in \mathbb{R}$
a_2	Car glider [kg]	$x \in \mathbb{R}$
a_3	Car battery [kg]	$x \in \mathbb{R}$
a_4	Car assembly [-]	$x \in \mathbb{R}$
...		
Use		
a_5	Maintenance [-]	$x \in \mathbb{R}$
a_6	Fuel [kg]	$x \in \mathbb{R}$
a_7	Road [m·year]	$x \in \mathbb{R}$
...		
Disp.		
a_8	Manual dismantling [-]	$x \in \mathbb{R}$
a_9	Used car powertrain [kg]	$x \in \mathbb{R}$
a_{10}	Used car glider [kg]	$x \in \mathbb{R}$
a_{11}	Used car battery [kg]	$x \in \mathbb{R}$
a_{12}	Used tyre [kg]	$x \in \mathbb{R}$
...		
Air		
b_1	Carbon dioxide [kg]	$x \in \mathbb{R}$
b_2	Particulates, $< 2.5\ \mu$m [kg]	$x \in \mathbb{R}$
b_3	Nitrogen oxides [kg]	$x \in \mathbb{R}$
...		
Water		
b_4	Cadmium [kg]	$x \in \mathbb{R}$
b_5	Chromium [kg]	$x \in \mathbb{R}$
b_6	Lead [kg]	$x \in \mathbb{R}$
...		
Soil		
b_7	Cadmium [kg]	$x \in \mathbb{R}$
b_8	Chromium [kg]	$x \in \mathbb{R}$
b_9	Lead [kg]	$x \in \mathbb{R}$
...		

---

[16]https://www.ecoinvent.org/
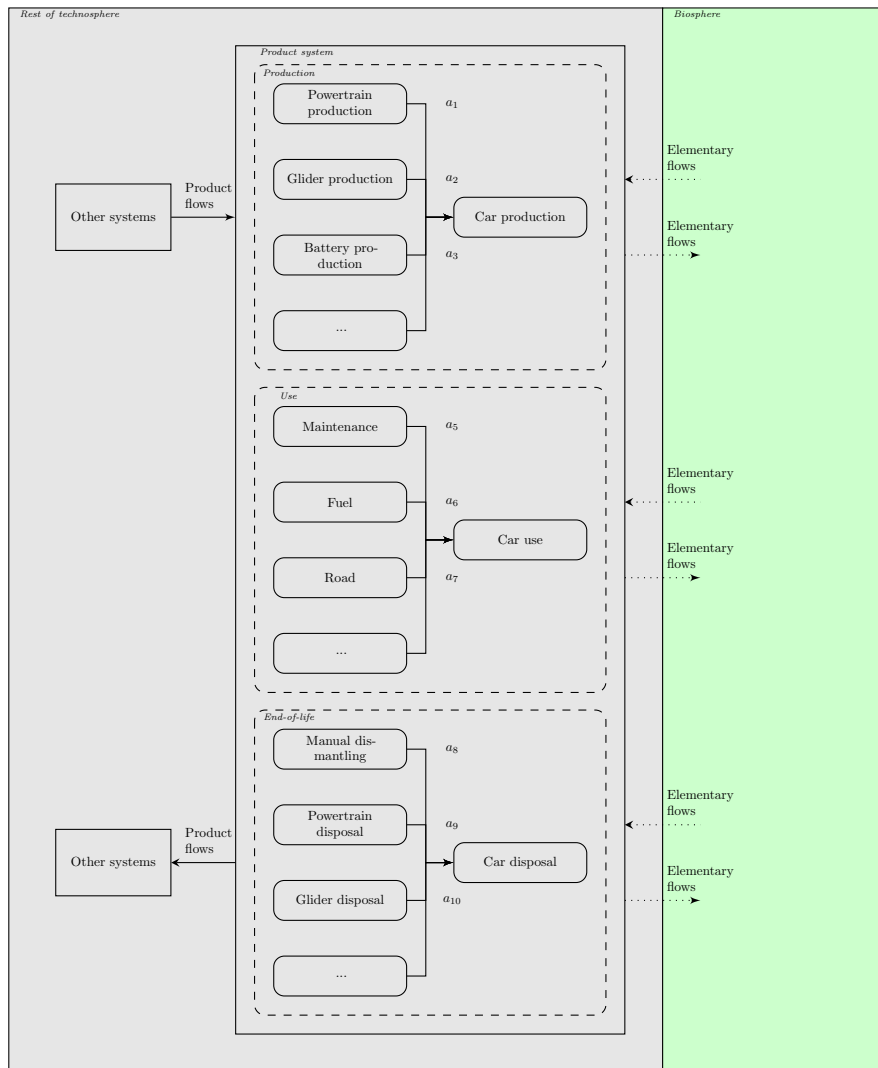
Figure 4.2: Life cycle perspective of the car product system. The car product system is composed of a set of unit processes (e.g., powertrain production) which spread over the three life cycle phases (production, use and EoL). The product system takes input product flows from other product systems which are upstream of the value chain (e.g., raw material extraction processes). The product system has some output flows (e.g., intermediate products) which can be used by downstream processes. Elementary flows can enter a product system (e.g., crude oil) or leave a product system (e.g., emissions to air, water and soil) from or to the biosphere.

Section 2.2.4 introduces the generic notation for the matrix inversion approach which was adapted from Heijungs and Suh (2002) (only changing indexation to avoid confusion with other indices of the ABM sub-model). In the technosphere matrix $\mathbf{A}$ each column corresponds to a technosphere unit process and each row to the reference product, where element $a_{k,l}$ is the exchange between the kth process and the lth process. In the case of CONNECTING there is only one reference product for each unit process, leading to a squared matrix with n rows and columns.

While the ecoinvent database includes 16'022 unit processes, the CONNECTING foreground includes 64 additional unit processes leading to $n=16'086$.

$$\mathbf{A} = \begin{bmatrix} a_{1,1} & \cdots & a_{1,l} & \cdots & a_{1,n} \\ \vdots & & \vdots & & \vdots \\ a_{k,1} & \cdots & a_{k,l} & \cdots & a_{k,n} \\ \vdots & & \vdots & & \vdots \\ a_{n,1} & \cdots & a_{n,l} & \cdots & a_{n,n} \end{bmatrix}$$

In $\mathbf{B}$ each column describes the intervention of a unit process with the biosphere, where each column in $\mathbf{B}$ corresponds to a column in $\mathbf{A}$, together representing one unit process such as the one shown in table 4.6. Each row in $\mathbf{B}$ corresponds to an elementary flow (e.g., CO_2) from or to the environment. Element $b_{q,l}$ is the qth elementary flow of the lth process from or to the biosphere. The total number r of elementary flows (and rows of $\mathbf{A}$) depends on the specific LCI and its coverage of environmental interventions. In case of CONNECTING 4'321 elementary flows are covered leading to $r=4'321$.

$$\mathbf{A} = \begin{bmatrix} b_{1,1} & \cdots & b_{1,l} & \cdots & b_{1,n} \\ \vdots & & \vdots & & \vdots \\ b_{q,1} & \cdots & b_{q,l} & \cdots & b_{q,n} \\ \vdots & & \vdots & & \vdots \\ b_{r,1} & \cdots & b_{r,l} & \cdots & b_{r,n} \end{bmatrix}$$

Finally, the demand of the transport system for processes is formulated in the final demand vector, which in case of the CONNECTING model contains the distances of each modelled transport mode (as well as potentially the demand for every other reference product in $\mathbf{A}$):

$$\mathbf{f} = \begin{pmatrix} f_1 \\ \vdots \\ f_k \\ \vdots \\ f_n \end{pmatrix}$$

where element f_k is the demand for the kth reference product in $\mathbf{A}$, and $\mathbf{f}$ has the same length as $\mathbf{A}$ (i.e., one demand for each product in $\mathbf{A}$). In case of CONNECTING there is an element f_k for each transport mode (i.e., car, bus and train) containing the system's demand in pkm. Since in the case of the CONNECTING model the functional unit only considers the satisfaction of transport needs all other elements in $\mathbf{f}$ are equal to zero.

4.3.5   Environment

The environment is described by the CFs, which describe the sensitivities to the emissions of the transport system. The term environment is used here in a broad sense similar to the term biosphere. Section 4.2 details which specific impact methods are chosen.

Focusing on GWP100 table 4.7 presents the variables describing the CFs of this impact category. While there are more than 100 such variables (according to the IPCC), only the most relevant for mobility are listed here.

For the two midpoint impact categories chosen for this thesis ($\mathbf{ic}$) two vectors $\mathbf{ic_1}$ and $\mathbf{ic_2}$ can be defined, each vector containing a CFs for each qth elementary flow (cf_q).

Taking the example of GWP100 from table 4.7, $\mathbf{ic_1}$ contains the a cf for each elementary flow in $\mathbf{B}$ (where some of the 4321 elementary flows will have no effect on climate change and thus have a values of zero):

$$\mathbf{ic_1} = \begin{pmatrix} cf_1 & \cdots & cf_q & \cdots & cf_r \end{pmatrix}$$

The CFs for both chosen methods ($GWP100$ and $R-E$) can be combined in the characterisation matrix $\mathbf{Q}$ (in our case two rows, one for each method):

$$\mathbf{Q} = \begin{bmatrix} \mathbf{ic_1} \\ \mathbf{ic_2} \end{bmatrix}$$

4.4   ABM model structure

In this section the functional form of the ABM part of the CONNECTING model will be introduced describing how the variables are related to each other. The ABM part of CONNECTING is based on a collection of sub-models which together allow to generate the DAP of an agent in the synthetic population. Originally this was developed in Mariante (2017) for the CONNECTING project. In the following a summary of the original description is provided.

First the generation of the synthetic population is described. Next the choice models are introduced. First, the ABM generates a schedule of activity types, their durations and durations of travels among these activities. This schedule constitutes the sequence of activities and the time allocated for each activity and each travel. The activity type and duration models introduced in the following are executed alternately, where activity type models take as inputs the outputs predicted by activity and travel duration models and vice versa.

Building on the schedule of activities and travels, next a location choice model generates the activity locations taking into account the allocated times for activities and travel. Finally, a mode choice model is used to predict the mode choice for each travel to complete the activity pattern AP_i of each ith individual.

At the end of this section the CONNECTING ABM is qualified with regard to the ABM features introduced in chapter 2.

Table 4.7: Environment variables (CFs) describing the climate change global warming potential (GWP100) of various environmental interventions. The unit for all listed CFs is kilogram CO_2-equivalents per kilogram emitted substance

Variable	Description	Domain
Air		
cf_1	Carbon dioxide	$x \in \mathbb{R}$
cf_2	Methane	$x \in \mathbb{R}$
cf_3	Dinitrogen monoxide	$x \in \mathbb{R}$
...		

4.4.1 Synthetic population

The basic idea of generating the synthetic population data is to get the variable values for the commuting population (for variables in tables 4.1-4.2) by sampling from multivariate probability distributions of a representative sample preserving essential statistical features of the population data.

For the CONNECTING model, the approach to generate the synthetic population was developed by Mariante (2017). The R package "synthpop" (Nowok et al., 2016) is used to perform the sampling of all work and household related variables, with the exception of the home and usual work locations. To determine these locations, a list of locations pairs (home-work locations) is created based on the survey, from which locations are bootstrapped with replacement for each individual in the synthetic population. The synthetic population is generated for the year 2015 and updated yearly to account for population growth.

4.4.2 Activity type

The activity type generation is based on Multi-Nominal Logistic (MNL) models. To this end MNL models for each jth activities ($ap_{j,1}$, where index 1 denotes that activity type is the first column in AP_i of the ith individual) are estimated. $ap_{1,1}$, the first activity, is always assumed to be of state "Home". The following equation shows the general formula of the MNL models used to estimate subsequent activity types:

$$
\begin{aligned}
U_{ap_{j,1}=at} = \ &\beta_{j,0,at} + \sum_{id \in AT_{j,hh}} \beta_{j,hh_{id},at} \cdot hh_{id} \\
&+ \sum_{id \in AT_{j,w}} \beta_{j,w_{id},at} \cdot w_{id} \\
&+ \alpha_{j,1,at} \cdot ap_{j-1,1} \\
&+ \alpha_{j,2,at} \cdot ap_{j-1,2} \\
&+ \alpha_{j,3,at} \cdot ap_{j,6} \\
&+ \epsilon_{j,at}
\end{aligned}
\tag{4.1}
$$

where $ap_{j,1}$ is the type of the jth activity (which correspond to the domain of $ap_{j,1}$ in table 4.3 excluding 'NA'). To make the selection of household (hh_{id}) and work related variables (w_{id}) explicit the sets $AT_{j,hh}$ and $AT_{j,w}$ are used (where AT_j specifies that these are the sets for the activity type model of the jth activity).

$AT_{j,hh} = \{1, 2, 3, 4, 5, 6, 7, 8, 9\}$, indicating that gender (hh_1), age (hh_2), marital status (hh_3), children (hh_4), education level (hh_5), settlement type (hh_6), occupancy status (hh_7), number of cars (hh_8) and monthly household income (hh_9) are all chosen as predictors for the jth activity type of the ith individual.

$AT_{j,w} = \{2, 3, 5\}$, indicating that number of working hours per week (w_2), the type of profession (w_3) and the travel reimbursement (w_5) were retained as relevant predictors as well.

Finally, the activity type of the previous activity in the sequence of predicted activity types ($ap_{j-1,1}$), duration of the previous activity ($ap_{j-1,2}$ estimated by the activity duration models presented in section 4.4.3) and the current time budget ($ap_{j,6}$) are predictors stemming from the already predicted facets of an individual's DAP.

All α and β are coefficients, where one set of coefficients is estimated for each jth activity type model, each predictor variable (e.g., hh_1) and each activity type at. Finally, $\epsilon_{j,at}$ designates the error term.

4.4.3   Activity duration

The activity duration models are based on Cox proportional-hazard models (Cox, 1972). In contrast to the activity type models, the response of these models are not discrete but a continuous durations predicted for each jth activity ($ap_{j,2}$, where index 2 denotes that activity duration is the second column in AP_i of the ith individual). This will be expressed in terms of a transition hazard from state a (i.e., current activity) to state b (i.e., next travel), as a function of time t and explanatory variables:

$$\lambda_{ab}(t, HH_i, W_i, AP_i) = \lambda_{0ab}(t) \cdot \exp(\beta_{j,0} + \sum_{id \in AD_{j,hh}} \beta_{j,hh_{id}} \cdot hh_{id}$$
$$+ \sum_{id \in AD_{j,w}} \beta_{j,w_{id}} \cdot w_{id}$$
$$+ \alpha_{j,1} \cdot ap_{j,1} \tag{4.2}$$
$$+ \alpha_{j,2} \cdot ap_{j-1,4}$$
$$+ \alpha_{j,3} \cdot ap_{j,6}$$

The transition from an activity to the subsequent trip marks the end of the activity episode and the time interval between the start of the activity and the transition is the activity duration. λ_{0ab} is the unspecified baseline hazard function.

Similarly to the activity type model, the sets $AD_{j,hh}$ and $AD_{j,w}$ containing the indices for the specific household and work related variables chosen as predictors are defined (where AD_j specifies that these are the sets for the activity duration model of the jth activity). Ultimately, the selection of household and work related variables is the same as for the activity type models introduced in the previous section.

In addition several predictors from the DAPs have shown to be significant: the current activity type ($ap_{j,1}$), the previous travel duration ($ap_{j-1,4}$) and the current time budget ($ap_{j,6}$).

All α and β are coefficients representing the relative risk against the baseline hazard, where one set of coefficients is estimated for each jth activity duration model and each predictor variable (e.g., hh_1).

4.4.4   Travel duration

The travel duration models are defined similarly, expressing a transition hazard from state b (i.e., current travel) to state a (i.e., next activity) as a function of time t and explanatory variables to predict for travel from each jth activity ($ap_{j,4}$, where index 4 denotes that travel duration is the fourth column in AP_i of the ith individual):

$$\lambda_{ba}(t, HH_i, W_i, AP_i) = \lambda_{0ba}(t) \cdot \exp(\beta_{j,0} + \sum_{id \in TD_{j,hh}} \beta_{j,hh_{id}} \cdot hh_{id}$$
$$+ \sum_{id \in TD_{j,w}} \beta_{j,w_{id}} \cdot w_{id}$$
$$+ \alpha_{j,1} \cdot ap_{j,1} \tag{4.3}$$
$$+ \alpha_{j,2} \cdot ap_{j+1,1}$$
$$+ \alpha_{j,3} \cdot ap_{j,2}$$
$$+ \alpha_{j,4} \cdot ap_{j,6}$$

The transition from a travel to the subsequent activity marks the end of the travel episode

and the time interval between the start of the travel and the transition is the travel duration. λ_{0ba} is the unspecified baseline hazard function.

Similarly to the activity type and duration models, the sets $TD_{j,hh}$ and $TD_{j,w}$ containing the indices for the specific household and work related variables chosen as predictors are defined (where TD_j specifies that these are the sets for the travel duration model for travels departing from the jth activity). Ultimately, the selection of household and work related variables is the same as for the activity type and duration models introduced in the previous sections.

In addition several predictors from the DAPs have shown to be significant: the activity type at the travel origin ($ap_{j,1}$), the activity type at the travel destination ($ap_{j+1,1}$), the activity duration at the travel origin ($ap_{j,2}$) and the current time budget ($ap_{j,6}$).

All α and β are coefficients representing the relative risk against the baseline hazard, where one set of coefficients is estimated for each travel duration model and each predictor variable (e.g., hh_1).

In both cases (activity and travel duration models) survival functions can be derived as follows:

$$P(ap_{j,2} > t) = \exp(-\Lambda_{ab}(t)) \tag{4.4}$$

$$P(ap_{j,4} > t) = \exp(-\Lambda_{ba}(t)) \tag{4.5}$$

where Λ_{ab} and Λ_{ba} are cumulative hazard functions:

$$\Lambda_{ab}(t) = \int_0^t \lambda_{ab}(x)dx \tag{4.6}$$

$$\Lambda_{ba}(t) = \int_0^t \lambda_{ba}(x)dx \tag{4.7}$$

4.4.5 Activity location

Different conditional logistic models (called conditional since utilities are expressed in terms of characteristics of the alternative locations rather than attributes of the individuals) are estimated for four state categories of activity types ($ap_{j,1}$): (1) *outside meal*, (2) *shopping*, (3) *service* (including the states *service* and *leisure activity*) and (4) *other* (including the states *pick up/drop off*, *friends/family*, *go for a walk* and *other*). Note that the other activity types are assumed to have fixed locations, where for each individual i *work* activities are assumed to take place at w_6, while *home* activities are assumed to take place at hh_{10} (both the usual work w_6 and home location hh_{10} are generated during the synthetic population generation). The first activity type is always *home*, thus the first location is always hh_{10}.

In the following the utility functions for these four models are presented. For each model, the utility of each possible destination $c \in C_j$, for the travel from the jth activity, is a function of alternative specific variables. Note that for each location model presented in this section, the choice set C_j is constrained, where based on the variables in TZ_c only those communes c are retained, that allow that activity type $ap_{j,1}$ is conducted (e.g., C_j for *outside meal* excludes communes where $tz_1 = 0$).

First, the model for *outside meal* activities uses the number of restaurants (tz_1), as well as car travel times (ts_1) from the previous location o (or $ap_{j-1,3}$) to each alternative c of the choice set C_j, and from each location to the location of the next fixed activity (nf). The next fixed activity is defined as the next activity in the sequence of predicted activities, which is either of type "at home" or "work". If there is no subsequent fixed activity the location hh_{10} is assumed.

Car travel times are used here as a proxy for the detour of each location from the home-work trajectory of the ith individual. The resulting utility function is:

$$U(ap_{j,3} = c) = \beta_1 \cdot tz_{1,c} + \beta_2 \cdot ts_{1_{o,c}} + \beta_3 \cdot ts_{1_{c,nf}} + \epsilon_{j,c} \qquad (4.8)$$

Second, the model for *shopping* activities uses the number of supermarkets (tz_2), as well as car travel times (ts_1) from the current location o (or $ap_{j-1,3}$) to each alternative c of the choice set, and from each alternative to the location of the next fixed activity (nf) as explanatory variables. In addition it uses the *available time* as an explanatory variable, which is calculated from the travel and activity durations (ap_2 and ap_4) predicted by the duration models introduced in sections 4.4.3-4.4.4, as well as the resulting travel times for each alternative (ts_1). The resulting utility function is:

$$\begin{aligned}
U(ap_{j,3} = c) = {} & \beta_1 \cdot tz_{2,c} + \beta_2 \cdot ts_{1_{o,c}} \\
& + \beta_3 \cdot ts_{1_{c,nf}} \\
& + \beta_4 \cdot (ap_{j,2} + ap_{j-1,4} + ap_{j,4} - ts_{1_{o,c}} - ts_{1_{c,nf}}) \\
& + \epsilon_{j,c}
\end{aligned} \qquad (4.9)$$

Third, the model for *service* activities uses the services index (tz_3), as well as car travel times (ts_1) from the current location to each alternative of the choice set, and from each alternative to the next fixed activity as explanatory variables. Similar to the model for shopping activities the available time is used as predictor. The resulting utility function is:

$$\begin{aligned}
U(ap_{j,3} = c) = {} & \beta_1 \cdot tz_{3,c} + \beta_2 \cdot ts_{1_{o,c}} \\
& + \beta_3 \cdot ts_{1_{c,nf}} \\
& + \beta_4 \cdot (ap_{j,2} + ap_{j-1,4} + ap_{j,4} - ts_{1_{o,c}} - ts_{1_{c,nf}}) \\
& + \epsilon_{j,c}
\end{aligned} \qquad (4.10)$$

Finally, the model for *other* activities uses the population density (tz_4), car travel times (ts_1) from each alternative to the next fixed activity and the available time as an explanatory variable. The resulting utility function:

$$\begin{aligned}
U(ap_{j,3} = c) = {} & \beta_1 \cdot tz_{4,c} + \beta_2 \cdot ts_{1_{o,c}} \\
& + \beta_3 \cdot ts_{1_{c,nf}} \\
& + \beta_4 \cdot (ap_{j,2} + ap_{j-1,4} + ap_{j,4} - ts_{1_{o,c}} - ts_{1_{c,nf}}) \\
& + \epsilon_{j,c}
\end{aligned} \qquad (4.11)$$

For all models, the choice probability of a specific activity location *loc* can be estimated as follows:

$$P(ap_{j,3} = loc) = \frac{exp(U(ap_{j,3} = loc))}{\sum_{c \in C_j} exp(U(ap_{j,3} = c))} \qquad (4.12)$$

4.4.6   Travel mode

The final models used to generate the individual DAPs are the mode choice models, for the six potential travels. The following equation shows the general formula of these models:

$$
\begin{aligned}
U_{(ap_{j,5}=mo)} = \beta_{j,0,mo} &+ \sum_{id \in MO_{j,hh}} \beta_{j,hh_{id},mo} \cdot hh_{id} \\
&+ \sum_{id \in MO_{j,w}} \beta_{j,w_{id},mo} \cdot w_{id} \\
&+ \alpha_{j,1,mo} \cdot ap_{j,1} \\
&+ \alpha_{j,2,mo} \cdot ap_{j+1,1} \\
&+ \alpha_{j,3,mo} \cdot ap_{j,5} \\
&+ \alpha_{j,4,mo} \cdot ap_{j,7} \\
&+ \alpha_{j,5,mo} \cdot ap_{j,8} \\
&+ \alpha_{j,6,mo} \cdot ts_{mo_{o,d}} \\
&+ \epsilon_{j,mo}
\end{aligned}
\tag{4.13}
$$

where $ap_{j,5}$ is the used travel mode from the travel origin location ($ap_{j,3}$ or o) to the destination activity location ($ap_{j+1,3}$ or d) out of the possible travel modes mo defined (which correspond to the domain of $ap_{j,5}$ in table 4.3 excluding 'NA'). $ap_{j,1}$ is the activity type at the travel origin and $ap_{j+1,1}$ is the activity type at the travel destination. To make the selection of household (hh_{id}) and work related variables (w_{id}) explicit, the sets $MO_{j,hh}$ and $MO_{j,w}$ are used (where MO_j specifies that these are the sets for the mode choice model of the travel departing from the jth activity).

$MO_{j,hh} = \{1, 2, 3, 4, 6, 8, 9\}$, indicating that gender (hh_1), age (hh_2), marital status (hh_3), children (hh_4), settlement type (hh_6), number of cars (hh_8) and monthly household income (hh_9) are chosen as predictors.

$MO_{j,w} = \{1, 2, 4, 5\}$, indicating that the flexibility of working hours, (w_1), number of working hours per week (w_2), parking availability at the work location (w_4) and the travel reimbursement (w_5) were retained as relevant predictors.

$ap_{1,5}$ is the mode chosen for the first travel, $ap_{j,7}$ is the departure category, $ap_{j,8}$ is the total number of travels conducted and $ts_{mo_{o,d}}$ is the travel time of transport mode mo from the location of the origin o (or $ap_{j,3}$) to the activity location of the destination d (or $ap_{j+1,3}$).

All α and β are coefficients, where one set of coefficients is estimated for each transport mode models, each predictor variable (e.g., hh_1). Finally, $\epsilon_{j,mo}$ designates the error term.

4.4.7 Distance generation model

A small part of the CONNECTING model is concerned with deriving travel distances from the population's DAPs. For each recorded travel in the DAP of the ith individual (AP_i) starting from the jth activity, the origin o corresponds to $ap_{j,3}$ and the destination d corresponds to $ap_{j+1,3}$. Using the mode $ap_{j,5}$ the travelled distance can be recovered from the corresponding distance OD matrix (e.g., for travels by car $ts_{2_{o,d}}$).

A final demand vector $\mathbf{f}_i$ can be derived for the ith individual by aggregating travelled distances for each mode across all travels in AP_i, where $\mathbf{f}_i$ is a function of the individual's DAP AP_i and the transport system $TS_{o,d}$: $\mathbf{f}_i(AP_i, TS_{o,d})$. $\mathbf{f}$ corresponds to the system's demand for transport processes, and can be derived by aggregating over the entire population:

$$
\mathbf{f} = \sum_{i \in POP} \mathbf{f}_i(AP_i, TS_{o,d})
\tag{4.14}
$$

where POP is the entire commuting population.

4.4.8   Model classification

Building on the review of chapter 2 and the introduced ABM features, the CONNECTING ABM is classified as a simple modelling effort exhibiting some of the basic features of an ABM. Specifically, the model clearly builds on an activity-based platform, deriving travel from the demand for activity participation. The model first schedules activities prior to determining locations and transport modes. Then, the travelled distances are derived from each individual DAP. The model also accounts for some simple interdependencies of activities and travels, e.g., accounting for a time budget or detours from the home-work axis. The model can be classified as a micro-simulation model, viewing individual commuters as the decision making unit. While the spatial resolution is rather low (based on administrative bounds of communes), the temporal modelling is high (in minutes). However, two of the features mentioned in chapter 2 are less pronounced as the model does not show a strong set of constraints and does not feature inter-personal linkage (e.g., among household members). With regard to the AgBM paradigm, the CONNECTING ABM can not be classified as a full fledged AgBM. Specifically, the model does model a set of agents and their attributes (commuters in the synthetic population). The model also has an environment (i.e., the transport system) within which agents exhibit their behaviours (i.e., generating individual DAPs). However, while agents interact with the environment, there is no interaction among agents themselves and thus a key element of the AgBM paradigm is missing.

4.5   LCA model structure

In the following a brief description of the structure of the LCA part of CONNECTING is provided, building on the structure of the ABM part and its outputs.

4.5.1   Life cycle inventory model

Once the final demand vector $\mathbf{f}$ has been determined, the LCI model of CONNECTING can be executed. The matrix inversions approach presented in chapter 2 allows to solve the inventory problem as follows:

$$\mathbf{g} = \mathbf{B}\mathbf{A}^{-1}\mathbf{f} \tag{4.15}$$

4.5.2   Life cycle impact assessment model

Finally the LCIA model of CONNECTING can be executed, yielding the QOIs to the decision makers in vector $\mathbf{h}$:

$$\mathbf{h} = \mathbf{Q}\mathbf{g} \tag{4.16}$$

The LCA model is implemented using the python package brightway2 (Mutel, 2017).

4.6   Limitations

The CONNECTING model has several limitations that need to be acknowledged. These limitations related to the available data, simplifications with regard to the ABM and LCA and limitations with regard to the coupling of both model parts.

A first limitations relating to the survey data, is that there is no distinction between car driver and car passenger in the travel diaries. This limitation of particular relevance for the LCI

modelling, since the share of drivers and passengers in the population could allow to estimate car occupation rates. In the present model occupations rates are based on literature values (i.e., MDDI (2018)) and remain static for the study period.

A second limitations relating to the travel time data, is that travel times are often dependent on the time of day (e.g., peak hour travel times by car are usually longer). Such detailed and dynamic travel time data was however unavailable for the study region. Only car travel times account for congestion, but remains static. This limitation also extends to the modelling of travel duration, where the CONNECTING ABM estimates the allocated time towards travel between two activities based on a range of predictors.

A third limitations, is that no travel cost data was collected for the study region. Travel cost is usually a predictor of mode choice. This also to some extend limited the scenario modelling, where policy action on the cost of public transport could not be included in the scenario modelling.

A fourth limitations relating to the mode and location choice modelling, is that the CONNECTING model performs this sequentially, rather than jointly modelling this in a hierarchical manner, as suggested by some scholars (Castiglione et al., 2015).

A fifth limitation relating to coupling is the aggregated nature, where at this point only aggregated travelled distances are used as inputs to the LCA part of the CONNECTING model.

4.7 Future scenarios

Two classes of scenarios are distinguished here: (1) scenarios which represent large scale changes outside of the control of transportation policy makers such as the population growth or change in electricity mixes in the study regions; (2) policy scenarios within control of transportation policy makers including the evolution shares of different powertrains in the private car fleet and the evolution of travel times within the PT system.

4.7.1 Population growth

The evolution of CBCs in the study region has been studied by the National Institute of Statistics and Economic Studies of the Grand Duchy of Luxembourg (STATEC) over the past decades. Building on medium and long term macroeconomic projections of STATEC Baustert et al. (2019) builds three population scenarios to be used by CONNECTING model.

Projections which are based on medium term demographic modelling STATEC (2019) until 2023 and long term macroeconomic projections Haas and Peltier (2017) until 2060. The share of French commuters is assumed to remain stable (around 50%). The scenarios used from Haas and Peltier (2017) assume a yearly economic growth rate of 3% and a yearly increase of the workforce of around 10'000. Varying shares of the CBC population in the workforce (33%, 50% and 66%) are applied to arrive at low, baseline high projections. For the purpose of this thesis, only the baseline scenario is considered, not considering high and low scenarios.

Figure 4.3 shows the strong increase of CBC population projected by STATEC, with the number of commuters from France increasing from around 85'000 in 2015 to around 120'000 in 2025.

4.7.2 Electricity mix

A second factor, considered exogenous is the electricity mix within the study region, which influences the environmental impacts of all transport modes relying on electricity from the grid (e.g., trains, electric buses and electric cars).
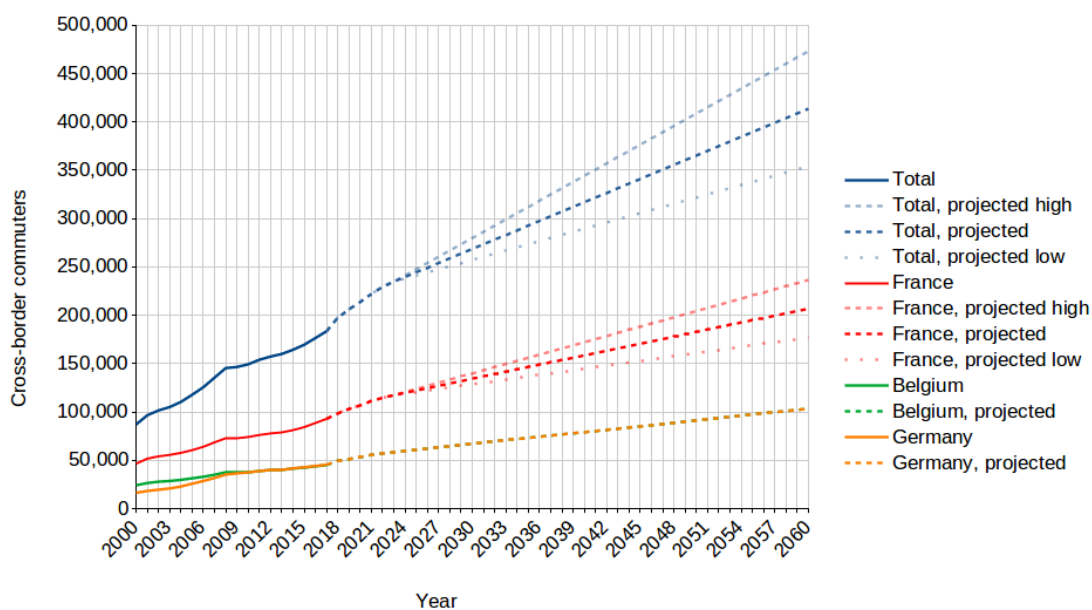
Figure 4.3: Projections of CBC population working in Luxembourg by country of residence from 2000 projected until 2060 Baustert et al. (2019).

The current and future electricity mixes for Luxembourg and France are shown in table 4.8 and are assumed to evolve linearly between 2015 and 2025. The initial values of 2015 are extracted directly from the ecoinvent database. The final values of 2025 are derived based on several expert assumptions.

In Luxembourg an increase in natural gas and wind power generation is observed domestically, while imports (namely from the coal-intensive German mix) are decreasing. In France the objective of reducing nuclear power to 50% in the national mix is reached in 2030, entailing a share of about 64.5% in 2025 from this source, which is assumed to be replaced by wind and hydro power.

Table 4.8: Projected evolution of electricity mixes from 2015 to 2025 as presented in Baustert et al. (2019).

Country	Luxembourg		France	
Electricity Source (%)	2015	2025	2015	2025
Photovoltaics	0.0	0.0	0.8	0.8
Coal	0.0	0.0	1.6	0.0
Hydro	12.2	12.0	12.9	19.8
Natural gas	0.0	20.0	0.6	0.0
Oil	0.0	0.0	0.1	0.0
Wind	0.8	10.0	3.0	14.9
Nuclear	0.0	0.0	78.5	64.5
Combined Heat and Power	13.9	15.0	1.1	0.0
Imports	73.1	43.0	1.5	0.0

4.7.3 Fleet shares

The two scenarios for the emergence of electric mobility have been modelling in Baustert et al. (2019), following a stock-flow cohort modelling approach presented in Fridstrøm et al. (2016) and building on French fleet data published by the Portail statistique de la Grande-Région[17]. Given an initial age distribution in year y of vehicles for each powertrain (and emissions standard) type ct and 30 age classes ac (vehicles are assumed to be decommissioned after 30 years), the stock of vehicles A for each combination of ac and ct for year $y+1$ can be derived as follows:

$$A_{ct,ac+1}^{y+1} = A_{ct,ac}^{y}[1 + \gamma_{ct,ac+1}],$$ (4.17)

where γ is derived based on the cumulative survival probability curves published in Fridstrøm et al. (2016) based on historic car fleet data.

As inputs to the model, projected yearly market shares of all different powertrain types ct are used. These market shares determine the stocks of new vehicles $A_{ct,ac=0}$ for each ct, entering the car fleet each year. Equation 4.17 is then applied to each of these stocks for sub-sequent years. For these market shares two scenarios are developed following (1) the French Environment and Energy Management Agency (*ADEME*) and (2) the Third Industrial Revolution initiative (*TIR*) of Luxembourg.

The results of the cohort model are align to the available ct classes in the CONNECTING LCI, as both scenarios provided a higher level of detail with regard to powertrains than present in the LCI database. Figure 4.4 shows the resulting fleet shares building on historical data starting in 2010 and projecting future fleet shares until 2050. For each year y on the x axis, the share of a each A_{ct}^{y} (sum across all age classes) corresponds to the thickness of the corresponding coloured area with the sum of all shares summing to 100% in each year. (e.g., in 2050 the *TIR* scenario projects a that 84% of the car fleet are Battery Electric Vehicles (BEVs), 14% are Plug-in Hybrid Electric Vehicles (PHEVs) and the remaining shares are diesel and gasoline cars).

While the outcomes for both scenarios strongly differ by 2050, for the study period of the CONNECTING project (2015-2025), both scenarios only start to differ somewhat towards the end, with the *TIR* showing a stronger increase of BEVs and PHEVs compared to the *ADEME* scenario. Another significant difference between both scenarios is the phase-out of diesel vehicles, which progresses much faster for the *TIR* scenario, while the *ADEME* scenario projects a still significant share of diesel vehicles in 2050.

4.7.4 Public transport evolution

The second dimension of policy scenarios concerns the PT system variables ts.

Building on the original OD matrices developed for 2015 based on the data sources (i.e., GTFS data) introduced in section 4.3.3 two separate trajectories until 2025 are modelled. These trajectories model additional direct trans-border bus lines (requiring no transfer) to cover rural areas of the French region and connect them to the city of Luxembourg and Esch-sur-Alzette (the two major centres of attractions in Luxembourg), and Bettembourg and Foetz which are locations of co-working hubs targeting French commuters.

In addition, express bus lines (without intermediate stops) are added to connect communes with a high number of CBCs to the city of Luxembourg and Esch-sur-Alzette. These additional bus lines affect the "bus" mode, as well as the multi-modal "PT", and "car+PT" mode partially based on bus transfer. The implementation of both the higher coverage of rural areas and express bus lines is spread evenly (adding roughly the same amounts of bus lines each year) over the study

---

[17] http://www.grande-region.lu/
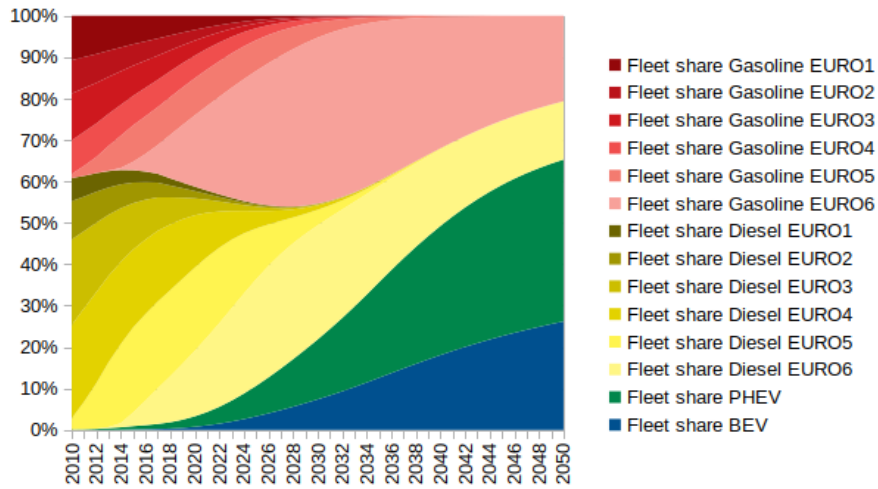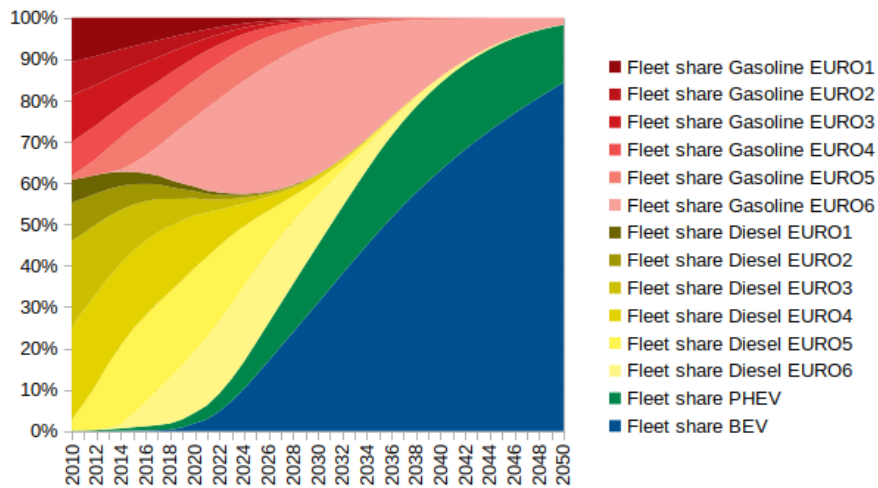
Figure 4.4: Evolution of fleet shares for different engine types for the CBC population. (a) shows the evolution for the *ADEME* scenario. (b) shows the evolution for the *TIR* scenario. Baustert et al. (2019) further details the scenarios and modelling approach.

period. Bus lines for communes with a high shares of CBCs are prioritised, based on STATEC data[18] shown in table 4.9.

Specifically, the first trajectory is the business-as-usual (or *BAU*) scenario which aims at representing an average policy investment affecting travel times and distances in each OD matrix. This scenario applies additional trans-border bus lines for all communes with at least 450 CBCs (table 4.9), while applying express bus lines for communes with at least 1'000 CBCs.

The *GREEN* scenario aims at representing a policy in favour of a more sustainable development (e.g., a broader coverage of the study region with trans-border bus lines and express bus

---

[18]https://data.public.lu/fr/datasets/r/b69301c0-8b67-46d6-9746-924f73652bd3

Table 4.9: Number of CBCs per French commune in 2015 for communes with at least 450 CBCs.

Commune	Number of commuters
Thionville	6'500
Metz	3'660
Yutz	2'400
Villerupt	2'290
Longwy	2'190
Hettange-Grande	2'140
Audun-le-Tiche	2'110
Hayange	2'110
Fameck	1'550
Florange	1'540
Mont-Saint-Martin	1'150
Terville	1'060
Algrange	950
Hussigny-Godbrange	930
Ottange	850
Hagondange	790
Herserange	780
Réhon	760
Guénange	750
Amnéville	720
Lexy	700
Volmerange-les-Mines	700
Nilvange	660
Maizières-lès-Metz	600
Uckange	600
Cosnes-et-Romain	580
Aumetz	560
Haucourt-Moulaine	550
Cattenom	550
Mondelange	540
Gorcy	530
Boulange	530
Rombas	510
Talange	510
Serémange-Erzange	510
Tressange	500
Longuyon	480
Audun-le-Roman	470
Saulnes	470
Zoufftgen	460
Longlaville	450
Thil	450
Bertrange	450
Fontoy	450

lines). For this scenario trans-border bus lines are applied for all communes in the study regions with express bus lines being applied for all communes with more than 450 CBCs (table 4.9).

Chapter 5

Methodology

5.1 Introduction

In this chapter the methodologies applied to characterise, treat and communicate uncertainty of the CONNECTING model are presented. Together with the classification of uncertainty introduced in chapter 3 this builds the core of the UA framework developed in this thesis. The formulation of the methodology aims at being applicable not only to ABM/LCA coupled models, but also AgBM/LCA coupled models.

No prior study has addressed the topic of UA in ABM/LCA coupled models. Knowledge about the relevant uncertainty locations is thus limited and the literature review in chapter 3 was conducted for UA of ABMs and LCA separately. However, findings of the literature review indicate which locations are most addressed in both fields and which characterisation and treatment options can be considered appropriate and feasible.

The most addressed uncertainty locations revealed by the literature review are the simulation error and measured parameters for ABMs and LCA respectively. The proposed framework will aim at prioritising these locations. This choice is motived by the fact that in both fields there are established methods to address these locations and that the present framework aims at catering to the broad audience of practitioners attempting similar modelling efforts. However, the treatment of all locations is discussed.

Uncertainty characterisation will be based on probability theory. This choice is motivated both by the findings of the review where for both ABMs and LCA probabilistic approaches are well established. Since in the case of the CONNECTING model it is impractical to derive a closed form expression (Rasouli and Timmermans, 2013a), this limits the choice of feasible uncertainty treatment methods (excluding e.g., analytical uncertainty propagation). Since ABMs are usually stochastic by nature, stochastic modelling approaches (i.e., MC simulations) are also appropriate to treat uncertainty in ABM/LCA coupled models in general. The challenge that arises is: how to combine model runs of both sub-models to propagate uncertainty systematically.

ABMs exhibit uncertainty in outputs at different levels of spatial and temporal resolution (e.g., at the level of individual DAPs, more aggregated OD matrices and TAZs, or system level outputs) (Petrik et al., 2018). In case of the CONNECTING model the ABM and LCA part intersect only at system level (where ABM outputs at system level become LCA inputs) (Baustert et al., 2019). The proposed framework will thus focus at this type of coupling.

With regard to LCA this thesis is focused on the LCI phase and its impact on the uncertainty of outputs at midpoint indicator level, with uncertainty of the LCIA phase considered out of the scope. While uncertainty of CFs can be relevant, uncertainty information is scarce with many

LCIA methods only publishing single value CFs. If the underlying LCIA model to derive these factors in unavailable, it becomes near to impossible to derive reasonable estimates of uncertainty information to make UA for the LCIA phase operational.

In the following, section 5.2 will provide a nomenclature for ABM/LCA coupled models to formally describe the research design. Section 5.3, 5.4 and 5.5 will introduce the framework and research design including uncertainty characterisation, propagation and communication. Finally, section 5.6 summarised the key findings of the chapter.

5.2 Nomenclature

In this section a new nomenclature is introduced to relate uncertainty locations and their characterisation to both parts of the CONNECTING model. Similar efforts can be found for AgBMs (e.g., Navarrete Gutiérrez (2012)) to organize simulations and are applied here in the context of UA. A *concrete instance* of a model (and its sub-models) is defined as a model for which uncertainty locations have a determined state. Specifically this means that the model has a defined functional form and that all parameters (measured and calibrated) take defined values. Similarly, a concrete instance can be defined for model inputs and the experimental frame.

A special case of a model's concrete instances is one, where the chosen functional form represents a reference case and parameters take their so-called nominal value. This concrete instance is referred to as *nominal concrete instance* and provides a reference to which results of other concrete instances can be compared to. Similarly, nominal concrete instances can be defined for model inputs and the experimental frame.

For the ABM M (such as the ABM part of CONNECTING), with a set of parameters P_M, a set of variables V_M, which is executed for each household (or individual) within a synthetic population (potentially for several time steps), a concrete instance M^u can be defined. P_M contains, e.g., calibrated parameters of individual choice models, while V_M contains the random draws for individual choice models. For a concrete instance M^u the set Ω_{M^u} contains the defined parameter values. A set s_v, containing random seeds for each potential random draw during a simulation, can be used to create a result instance $r_{M^u_{s_v}}$ of M^u. The nominal concrete instance of M is defined as $M^*_{s_v}$ where each parameter in P_M takes the nominal value in Ω_{M^*}. In addition, $M^*_{s_*}$ is defined as the nominal concrete instance of M, where each random choice event results in its most likely outcome.

The nomenclature of a LCA model L (such as the LCA part of CONNECTING) can be defined analogously, with a set of parameters P_L containing all elements of the technosphere, biosphere and characterisation matrices (as well as potentially additional parameters modelling dependencies between different process parameters). For a concrete instance L^w the set Ω_{L^w} contains the defined parameter values. Unlike M, L does usually not encompass any random elements, thus for a concrete instance L^w one and only one result instance r_{L^w} can be computed. The nominal concrete instance of L is defined as L^*, with each parameters in P_L taking its value defined in Ω_{L^*}.

Both M and L can have inputs describing, e.g., outside drivers affecting the modelled system. The definition of such inputs is of course dependent on the perspective, e.g., from the perspective of the sub-model L the set $r_{M^u_{s_v}}$ contains inputs, while from the perspective of the sub-model M they are outputs. Taking the perspective of the ABM/LCA coupled model a set I is defined, containing the inputs considered exogenous to both models. Similar to the parameters, concrete instances of input vectors can be defined and the same holds true for decisions taken in the experimental frame.

Figure 5.1 illustrates the nomenclature for one concrete instance of an ABM/LCA coupled
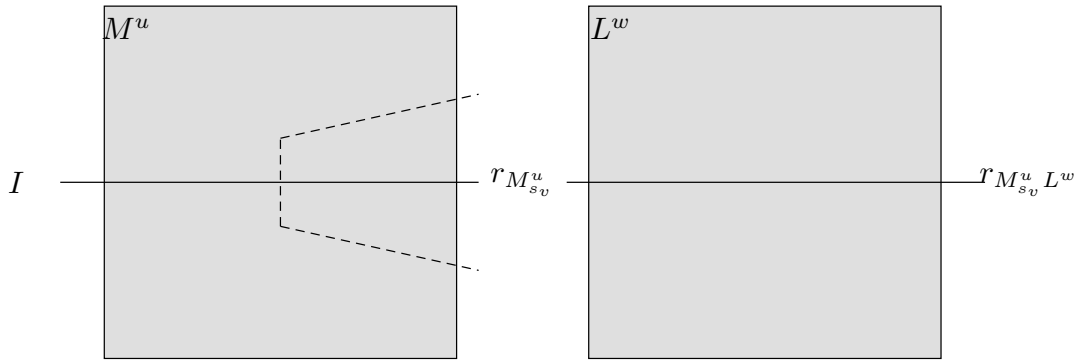
Figure 5.1: The execution of a model run for one concrete instance of an ABM/LCA coupled model is represented. Given a set of inputs I and a set s_v containing random seeds for each potential random choice M^u produces a set of ABM results $r_{M^u_{s_v}}$ (i.e., activity-travel pattern for a synthetic population). The model outputs of M^u become inputs to the LCA model part L^w which allows to produce a set of final model outputs $r_{M^u_{s_v} L^w}$.

model. The flow of information (from left to right) is represented by edges passing through the sub-models represented by squares. The stochastic nature of the ABM part is represented by the forking of the information path (where alternative possible "paths" are represented by dashed lines). The results of the ABM part are reproducible by re-using the same set of random seeds s_v. The nominal concrete instance of an ABM/LCA coupled model corresponds to both sub-models in their nominal concrete instance state.

Building on this nomenclature, the UA framework is presented in the following. The three steps of uncertainty characterisation, uncertainty propagation and uncertainty communication are presented.

5.3 Uncertainty characterisation

The focus of the proposed framework is on model uncertainty stemming from measured parameters and the simulation error. Other uncertainty locations will be discussed at the end of this section.

5.3.1 ABM sub-model

The ABM part of CONNECTING is an utility-based ABM composed of logistic and Cox-hazard models. Each of these models aims at representing a choice component as a result of a human decision-making process. The ABM generates individual DAPs in time and space. Decisions include whether or not to conduct an activity, when to start an activity, where to conduct an activity and which mode of transport to use to arrive at the activity location. These choice models are generally composed of explanatory variables, calibrated parameters and (in case of logistic models) error terms, and allow to determine the state of a dependent variable (Castiglione et al., 2015). A detailed description of all choice models is presented in chapter 4.

Realistically, choices can only be predicted up to a probability of occurrence and in consequence choice models are not deterministic models (predicting one crisp choice) but rather choice probabilities for possible outcomes (Castiglione et al., 2015). In case of some logistic models (i.e., MNL modelling) the Independence of Irrelevant Alternatives (IIA) assumption is applied, where

choice probabilities are assumed independent of other "irrelevant" alternatives.

For all MNL models of the CONNECTING model presented in chapter 4 the following general expression can be formulated (Castiglione et al., 2015):

$$U_{out} = \boldsymbol{\beta_{out}} \cdot \boldsymbol{x_i} = \beta_{0,out} + \beta_{1,out} \cdot x_{1,i} + \ldots + \beta_{e,out} \cdot x_{e,i} + \ldots + \epsilon_{out} \tag{5.1}$$

where U_{out} is understood to be the utility of outcome out, $x_{e,i}$ represents the eth explanatory variable for observation i, $\beta_{e,out}$ is the marginal utility associated with the eth explanatory variable and outcome out, and ϵ_{out} is the error term capturing to impact of unobserved variables on outcome out. Applying the assumption that error terms are independent and identically distributed (i.i.d.) random variables following an extreme value type 1 (EV 1) distribution, the probability of outcome out can be derived (Castiglione et al., 2015):

$$P(Y_i = out) = P(U_{out} + \epsilon_{out} > U_{alt} + \epsilon_{alt}, \forall alt \neq out) = \frac{e^{\boldsymbol{\beta_{out}} \cdot \boldsymbol{x_i}}}{\sum_{\forall alt} e^{\boldsymbol{\beta_{alt}} \cdot \boldsymbol{x_i}}} \tag{5.2}$$

where ϵ_{out} and ϵ_{alt} are the error terms for alternative outcomes alt. Probabilities for conditional logistic models can be formulated is similar fashion, as done in Mariante (2017) for the CONNECTING model.

The second group of models used in the ABM part of CONNECTING is the Cox-hazard model to determine activity and travel durations. Again a general expression can be formulated (Mariante, 2017):

$$\lambda_{ab}(t, X_i) = \lambda_0(t) e^{\boldsymbol{\alpha} \cdot \boldsymbol{x_i}} \tag{5.3}$$

where $\boldsymbol{x_i}$ is a set containing explanatory variables for observation i and $\boldsymbol{\alpha}$ contains the estimated parameters associated with each explanatory variable and representing the relative risk against the baseline hazard. Survival functions can be derived (Mariante, 2017):

$$P(X_i > t) = e^{-\Lambda_{ab}(t))} \tag{5.4}$$

where Λ_{ab} is the cumulative hazard function:

$$\Lambda_{ab}(t) = \int_0^t \lambda_{ab}(x) dx \tag{5.5}$$

5.3.2 LCA sub-model

Focussing on the LCA part of the CONNECTING model, the main locations of uncertainty to be addressed are the elements (i.e., measured parameters) of the technosphere and biosphere matrices representing the inputs and outputs of the unit process data, describing the transport modes and related processes.

Chapter 4 introduces the measured parameters of the unit process data and details data sources. In total 63 unit processes are modelled with 1'803 inputs and outputs representing exchanges among each other, the background database (i.e., ecoinvent) and the environment. Their large number makes it impractical to derive detailed uncertainty distributions for all parameters. The so-called pedigree approach, which builds on a set of DQIs, allows to efficiently estimate uncertainty distributions for such a large number of quantities.

The original approach was adapted for LCA and introduced in Weidema and Wesnæs (1996). The underlying premise is that the reliability of LCA results depends on the uncertainty present in data, as well as the quality of the data. Therefore data quality management must be an

integral part the analysis. Data quality is assessed and reported for each set of data using a set of DQIs, which are subsequently interpreted as additional uncertainty. Some indicators might be unit process specific (e.g., age related indicators), while others are specific to individual flows.

In this thesis five semi-quantitative DQIs, each having levels $\in [1, 2, 3, 4, 5]$, are applied to the measured parameters of the CONNECTING LCI (exceptions include, e.g., market shares which have to sum 1 and for which more advanced methods would be required). These five indicators are based on the original indicators advanced in Weidema and Wesnæs (1996) and are also applied to the most recent versions of ecoinvent database (Muller et al., 2014):

- reliability

- completeness

- temporal correlation (temporal)

- geographic correlation (geographic)

- further technological correlation (technological),

Where the reliability indicator relates to the data source, acquisition methods and verification procedures. Data could be acquired by empirical measurements or expert judgement implying different levels of quality. E.g., in the CONNECTING LCI, fuel consumption data from official driving cycle measurements are corrected to account for the bias compared to real world emissions. The reliability of data sources for emissions and correction factors are assessed.

The completeness indicator relates to the representativeness of the sample. Data could be available for the entire population or only a subset. E.g., in CONNECTING fuel consumption data is available for almost every vehicle in the Luxembourgish car fleet, implying a high completeness.

The temporal indicator relates to the correlation between the year of data collection and the year of the LCA study. Data could be available from recent studies adequately capturing current industrial efficiency levels, or older data failing to do so. E.g., in the CONNECTING LCI fuel consumption data for cars are based on the most recently available Luxembourgish car fleet data. For transit modes ecoinvent data is used, which have been collected several years prior to the CONNECTING study period, implying a slightly lower temporal correlation.

The geographical indicator relates to the correlation between the location of data collection and the defined data location in the goal and scope definition phase of the study. Data might be available for the defined data location or for a location with more or less similar conditions. In CONNECTING, Luxembourgish fuel consumption data is used to describe the car fleet of the French CBC population, as no location (or population) specific data is available, implying a slightly lower geographical correlation.

Finally, the technological indicator relates to the correlation between the data of the measured process and the defined process. Data might be available for the investigated process or a similar process. E.g., in the CONNECTING LCI the emission data for vehicles falling under the EURO6 emission standard are largely based on the data from EURO5 vehicles (correcting for specific differences of both emission standards), since EURO6 datasets were not available during the data collection phase of the project, implying a slightly lower technological correlation.

For each indicator and level $\in [1, 2, 3, 4, 5]$ a so-called uncertainty factor (UF) has to be determined quantifying the additional uncertainty due to the data quality. Uncertainty factor values for the five DQIs have been published and updated for the ecoinvent database and the most recent values are summarised in table 5.1.

These uncertainty factors are usually referred to as additional uncertainty factors, either added to the empirically derived uncertainty of a flow or (in case empirical data is not available) to uncertainty derived from the basic uncertainty factors shown in table 5.2.

To calculate the Geometric Standard Deviation (GSD) of a flow from both types of uncertainty (basic and additional) the following equation can be applied:

$$\sigma_g^2 = e^{\sqrt{(ln(UF_1)^2 + ln(UF_2)^2 + ln(UF_3)^2 + ln(UF_4)^2 + ln(UF_5)^2 + ln(UF_{base})^2)}}, \tag{5.6}$$

where UF_1, UF_2, ... UF_5 correspond to the five additional uncertainty factor values (e.g., table 5.1) and UF_{base} to the basic uncertainty factor value (e.g., table 5.2).

Following the initial publication of these expert-based uncertainty factors, several authors have published there own empirical-based factors, i.e., Ciroth et al. (2013) and Muller et al. (2016), where Bayesian inference is used to update the original expert-based factors by systematically combining them with other information (e.g., stemming from other databases). In Muller et al. (2016) these factors are published and compared to the original values. Furthermore, additional uncertainty factors are published not only for generic processes, but also for specific process categories (e.g., agriculture, combustion, transportation, etc.).

Of particular interest are the categories of combustion and transportation processes. Table 5.3 presents the updated additional uncertainty factors for combustion processes, where increasing (red) and decreasing (green) values compared to the generic expert factors are highlighted.

Table 5.4 presents the updated additional uncertainty factors for transportation processes, again highlighting increasing (red) and decreasing (green) values.

The implications of the differences between both sources of uncertainty factors on the model output uncertainty will be evaluated in this thesis. A python data package is developed containing both expert-based and empirical-based uncertainty factors. To apply the different categories (e.g., combustion, transport, agricultural, etc.) of basic and additional uncertainty factors to corresponding LCI processes, a mapping between the International Standard Industrial Classification of all economic activities (ISIC)[1] and the uncertainty factor categories (e.g., transportation, agricultural or manufacturing) is used.

After attributing data quality levels to the five indicators for all data in the CONNECTING LCI, uncertainty distributions can be derived. First formula 5.6 allows to derive the GSD. Following Muller et al. (2014), log-normal distributions (the most common distribution type in the CONNECTING LCI) are then defined by:

$$f(x, \mu_g, \sigma_g) = \frac{\exp(\frac{-(\ln x - \ln \mu_g)^2}{2 \ln^2 \sigma_g})}{\sqrt{2\pi} \ln \sigma_g}, \tag{5.7}$$

where σ_g is the GSD and μ_g the geometric mean.

Finally, a relevant aspect revealed during the literature review in chapter 3 is the dependency among inputs and outputs of unit processes of transport modes, in particular during the use phase where fuel consumptions and airborne tailpipe emissions (e.g., CO_2) can be strongly correlated.

Table 5.1: Ecoinvent default additional uncertainty factors as contribution to the square of the Geometric Standard Deviation (GSD).

Indicator level	1	2	3	4	5
Reliability (UF_1)	1.00	1.05	1.10	1.20	1.50
Completeness (UF_2)	1.00	1.02	1.05	1.10	1.20
Temporal (UF_3)	1.00	1.03	1.10	1.20	1.50
Geographic (UF_4)	1.00	1.01	1.02	1.05	1.10
Technological (UF_5)	1.00	1.05	1.20	1.50	2.00

---

[1]https://ilostat.ilo.org/resources/methods/classification-economic-activities/

To account for the effect of these dependencies two separate sampling types are employed, one where uncertainty is independently sampled for inputs and outputs of unit processes (referred to as *independent sampling*) and one where fuel related emissions for all transport modes with internal combustion engines are derived from sampled fuel consumptions and emission factors defined per mass of burned fuel (referred to as *dependent sampling*). Fuel dependent emissions include the afore mentioned carbon dioxide, sulphur dioxide, dinitrogen monoxide, ammonia, heavy metals (e.g., cadmium, copper, chromium, lead, mercury, nickel, selenium and zinc) and Polycyclic Aromatic Hydrocarbons (PAH).

Table 5.2: Ecoinvent basic uncertainty factors (UF_{base}); c: combustion emissions; p: process emissions; a: agricultural emissions. "NA" is used to designates "Not applicable".

input / output group	c	p	a
demand of:			
Thermal energy, electricity, semi-finished products, material, waste	1.05	1.05	1.05
Transport	2.00	2.00	2.00
Infrastructure	3.00	3.00	3.00
resources:			
Primary energy carriers, metals, salt	1.05	1.05	1.05
Land use occupation	1.50	1.50	1.10
Land use transformation	2.00	2.00	1.20
pollutants emitted to water:			
BOD, COD, TOC, DOC, inorganic compounds (NH_4, PO_4, NO_3, Cl, Na, etc)	NA	1.50	NA
Individual hydrocarbons, PAH	NA	3.00	NA
Heavy metals	NA	5.00	1.80
Pesticides	NA	NA	1.50
NO_3, PO_4	NA	NA	1.50
pollutants emitted to soil:			
Oil, hydrocarbons total	NA	1.50	NA
Heavy metals	NA	1.50	1.50
Pesticides	NA	NA	1.50
pollutants emitted to air:			
CO_2	1.05	1.05	NA
SO_2	1.05	NA	NA
NMVOC total	1.50	NA	NA
CO_2	1.50	NA	NA
NO_x, N_2O	1.50	NA	1.40
CH_4, NH_3	1.50	NA	1.20
Individuals hydrocarbons	1.50	2.00	NA
PM>10	1.50	1.50	NA
PM10	2.00	2.00	NA
PM2.5	3.00	3.00	NA
Polycyclic aromatic hydrocarbons (PAH)	3.00	NA	NA
CO, heavy metals	5.00	NA	NA
Inorganic emissions, others	NA	1.50	NA
Radionuclides (e.g., Radon-222	NA	3.00	NA

5.3.3   Other locations

While the focus of this thesis is on dealing with parameter uncertainty and the simulation error (the most addressed locations for both sub-models) other locations outlined in the classification proposed in chapter 3 will be qualitatively discussed here.

One prominent source of uncertainty in the experimental frame is the sampling error occurring for many ABMs, due to running the model with only a fraction of the population. This has been extensively investigated in literature, e.g., by Kwak et al. (2012), Manzo et al. (2015), and Petrik et al. (2018). In case of the CONNECTING model however all simulations are based on the entire synthetic population, following the projections of CBCs living in France and working in Luxembourg from 2015 until 2025.

To some extent input uncertainty is investigated through the scenarios (e.g., share of EVs in the CBC population's car fleet and projections of CBCs over the study period). However, uncertainty of other inputs (e.g., changes in future socio-demographic variables) can significantly contribute to output uncertainty as shown in de Jong et al. (2007). Uncertainty in these inputs can be addressed by means of scenario analysis or stochastic modelling (if appropriate distributions can be derived), similar to the stochastic propagation schemes advanced in section 5.4. At the interface of the ABM and LCA part of CONNECTING, the output uncertainty of the ABM becomes input uncertainty to the LCA. This uncertainty is characterised by means of uncertainty treatment (i.e., the uncertainty propagation schemes presented in section 5.4).

Another uncertainty location not addressed in the present work is ABM estimation (i.e., calibrated parameters of individual choice models). This has been addressed for ABMs in Petrik et al. (2018), deriving uncertainty distributions for all estimated parameters and performing stochastic modelling. Their findings together with the framework advanced in the present thesis provide a basis to address uncertainty in ABM parameters for ABM/LCA coupled models.

Finally, there is model specification uncertainty (e.g., about the functional form of the ABM and LCA part of CONNECTING as well as the integrating structure) as an uncertainty location. Different types of discrete choice models and different sets of selected explanatory variables

Table 5.3: Updated values for additional uncertainty factors of combustion processes based on Muller et al. (2016), as contribution to the square of the GSD.

Indicator level	1	2	3	4	5
Reliability (UF_1)	1.00	1.06	1.12	1.18	1.69
Completeness (UF_2)	1.00	1.02	1.05	1.10	1.20
Temporal (UF_3)	1.00	1.08	1.27	1.72	1.75
Geographic (UF_4)	1.00	1.08	1.11	1.66	1.65
Technological (UF_5)	1.00	1.04	1.04	1.50	1.89

Table 5.4: Updated values for additional uncertainty factors of transportation processes based on Muller et al. (2016), as contribution to the square of the GSD.

Indicator level	1	2	3	4	5
Reliability (UF_1)	1.00	1.05	1.10	1.20	1.50
Completeness (UF_2)	1.00	1.02	1.05	1.10	1.20
Temporal (UF_3)	1.00	1.16	1.26	1.26	1.15
Geographic (UF_4)	1.00	1.01	1.02	1.05	1.10
Technological (UF_5)	1.00	1.05	1.20	1.50	2.00

would results in different sets of predicted activity-travel patterns. At the beginning of the CONNECTING project different types of mode choice modelling (e.g., using Bayesian networks) have been tested and Mariante (2017) also tests various types of econometric modelling options and constraints, however the current selection of models are considered to be the best fit. With regard to model specification of the LCI of CONNECTING, the overarching structure follows the matrix approach outlined in chapter 2. Uncertainty with regard to this overarching structure (such as uncertainty resulting from the simplistic assumption of linearity) is beyond the scope of this thesis.

5.4 Uncertainty treatment

Uncertainty propagation using stochastic modelling is used as the most appropriate and feasible method. To this end sampling needs to be somewhat coordinated, for which a so-called random seed factory is defined in section 5.4.1.

In total three uncertainty propagation schemes are then outlined in this section to propagate parameter uncertainty (scheme 1), the simulation error (scheme 2) and both locations simultaneously (scheme 3). These schemes serve to answer questions about the magnitude of uncertainty stemming from these locations and affecting the model outputs (i.e., the QOIs defined in chapter 4).

5.4.1 Random seed factory

When running UA for multiple scenario an issue arises: how can one make sure that differences between scenarios are not a result of different random seeds being passed to model components, but purely a result of differences between the scenarios themselves. To this end, a seed generating structure (hereafter referred to as "random seed factory") is used, building on the work of Bowman et al. (2006) and Vovsha et al. (2008). The purpose of the random seed factory is to make model runs reproducible and solve the above mentioned issue.

For each random draw, e.g., to simulate the jth activity type choice of the ith individual, the same random seed should be applied for this choice across all scenarios for the same model run. To assure this, the random seed factory first randomly generates seeds (in case of the CONNECTING model random integers) for each model run based on an initial master seed. Subsequently, the factory uses these seeds to generate seeds for each choice model and ultimately for each potential choice of each individual i. Using the same initial seed for each scenario will assure that for each individual choice of a model run the same seed is used. Figure 5.2 illustrates the seed generation.

Similarly, when running LCA simulations for ABM results of different scenarios, again the difference among final results should not be due to different random samples of parameter values in the technosphere and biosphere matrices, but due to the differences in the scenarios. To assure this, seeds are used in a manner that the same concrete instances of L are generated in the same order for the UA of each scenario. This is done using the python package presamples[2] which is compatible with the brightway2 package (Mutel, 2017) used to perform the LCA calculations.

5.4.2 Sampling

While for the LCA sub-model of CONNECTING, sampling can be conducted simply by randomly drawing values from the probability distributions of technosphere and biosphere

---

[2]https://presamples.readthedocs.io/en/latest/index.html

Activity 1
seed

Activity type
model seed ___ . . .

Activity 7
seed

Run 1
seed

Activity duration
model seed   - . . .

. . .

. . .

Initial seed

Activity 1
seed

Activity type
model seed ___ . . .

Activity 7
seed

Run N
seed

Activity duration
model seed   - . . .

. . .
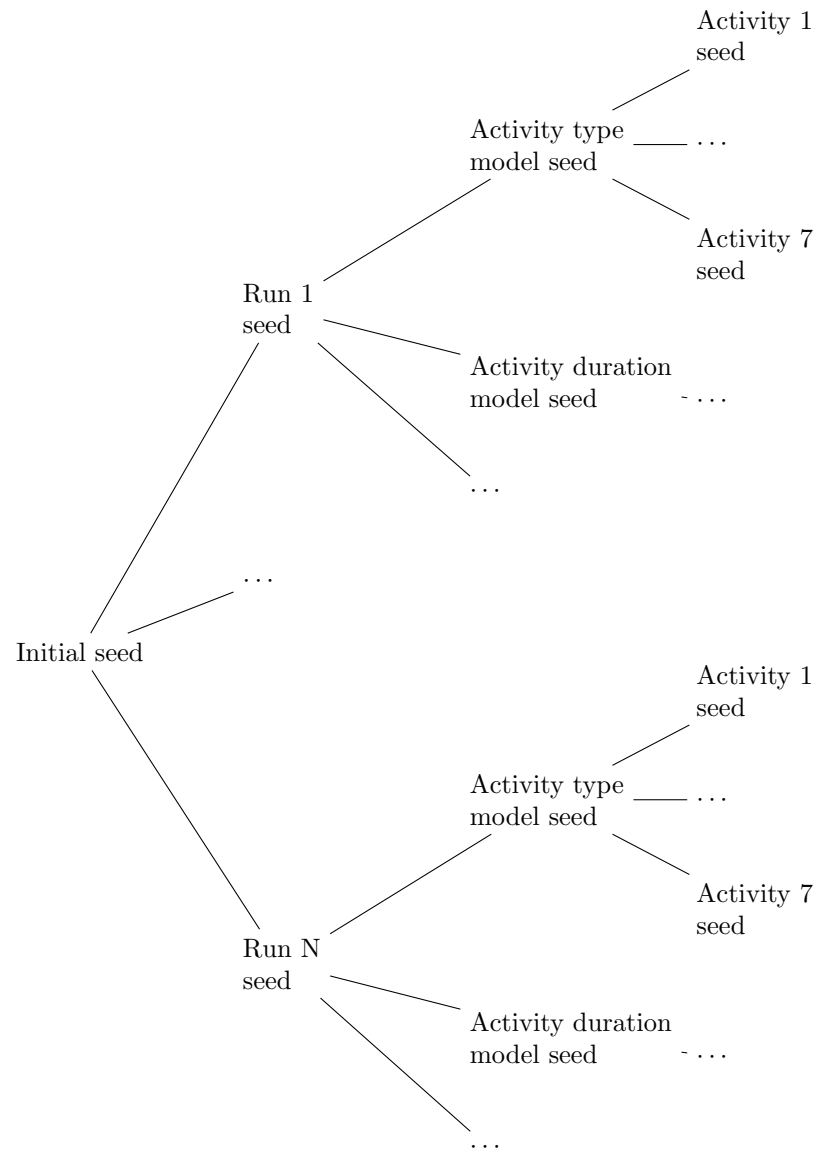
Figure 5.2: Random seed generation by seed factory. Based on an initial seed, seeds are generated for each model run, then for each individual choice model and ultimately for each potential choice. The same seeds are generated across scenarios by using the same initial seed.

flows, sampling from the individual choice models of the ABM part of CONNECTING is more challenging.

Helder et al. (2015) describe two alternative ways of sampling individual choices when performing a microsimulation. In the following a brief description of both alternative sampling methods is provided, based on Helder et al. (2015).

The first sampling method proceeds by sampling directly from the distributions of the error terms (i.e., EV 1) for each possible outcome *out*, and then chooses the outcome with the highest

utility U_{out}. This is repeated for each individual using the random seeds provided for each choice (see section 5.4.1).

The second sampling method proceeds by determining all choice probabilities $P(Y_i = out)$ for an individual according to equation 5.2. The probabilities of all possible outcomes allow then to form a cumulative distribution function for that individual. Next, a random draw is made from a standard uniform distribution, which is mapped onto the cumulative distribution function, determining the individual's choice. Similar to the first sampling method, this is repeated for each individual using the random seed provided by the seed factory (see section 5.4.1) for each choice. The present work applies this second method.

5.4.3   Scheme 1: Simulation error

The first scheme aims at propagation the simulation error from the stochastic choice models of the ABM. It builds on the body of literature found in chapter 3 proposing methodologies to propagate the simulation error, e.g., Rasouli and Timmermans (2013a), while adapting these efforts to the new context of ABM/LCA coupled models. The following steps are applied. First, the synthetic population is initialized for the study region (this step is perform using the same random seed for each model run, thus always resulting in the identical population). Next the uncertainty propagation starts:

1. The seed factory is initialised creating N sets s_v of random seeds with $v \in [1, ..., N]$, containing seeds for each potential choice of each choice model

2. Choice models are calibrated based on the survey data creating one nominal concrete instance M^*

3. The ABM is run N times (once for each set of random seeds)

4. For each output $r_{M^*_{s_v}}$ of the ABM a LCA is run using the nominal concrete instance L^*

5. The output uncertainty measures are computed for each QOI

As noted above, the entire synthetic population is used for each model run (and each time step), where the total number of model runs N is set to be 500 (which is consistent with what has been observed in the literature review of ABM studies in chapter 3). Figure 5.3 illustrates the general structure of the first scheme based on the nomenclature presented in section 5.2.

While previous efforts, e.g., Rasouli and Timmermans (2013a), have primarily focussed to propagate the simulation error from all choice facets simultaneously, three sub-schemes of scheme 1 are defined in the following to allow for propagation of uncertainty from (1) individual ABM sub-models, (2) combinations of 2 ABM sub-models and (3) all ABM sub-models.

Scheme 1-1   The first sub-scheme aims at investigating the uncertainty from individual choice models. To this end one of the four ABM sub-models takes its stochastic state, with the remaining sub-models taking their deterministic state (nominal concrete instance). This sub-scheme is repeated for all four sub-models resulting in a total of 4·500 model runs.

Scheme 1-2   To investigate potential interaction effects among ABM sub-models with regard to uncertainty, the second sub-scheme is repeated for all combinations of two ABM sub-models taking their stochastic state, with the remaining two sub-models taking their deterministic state. This sub-scheme is repeated for all six possible combinations resulting in a total of 6·500 model runs.
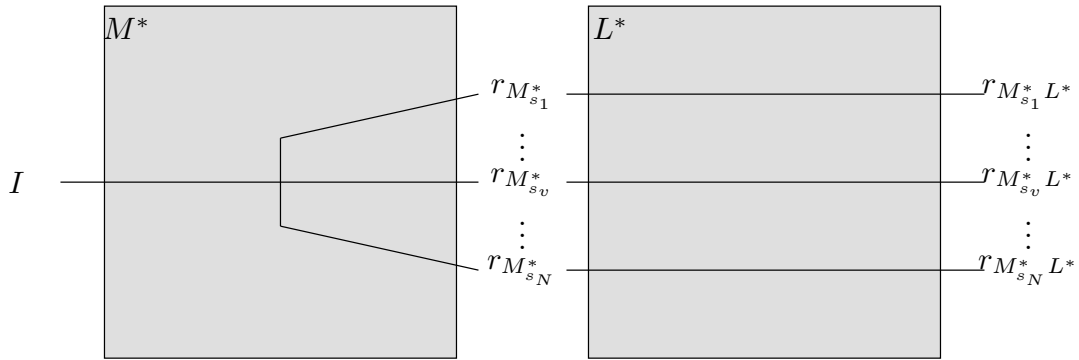
Figure 5.3: Scheme 1: Given a set of inputs I and N sets s_v containing random seeds for each potential random choice M^* produces a set of ABM results $r_{M^*_{s_v}}$. The model outputs of M^* become inputs to the LCA model part L^* which allows to produce a set of final model outputs $r_{M^*_{s_v} L^*}$ for each set s_v.

Scheme 1-3 This final sub-scheme follows the general description of scheme 1, with all ABM sub-models (activity type, duration, location and mode choices) taking their stochastic state. To this end 500 model runs are required.

Figure 5.4 shows all scheme 1 sub-schemes, where in the Venn diagram the four coloured rectangles represent each choice model being run stochastically. The intersections represent multiple sub-models being run stochastically, i.e., scheme 1-3 is represented where all four rectangles intersect.

5.4.4 Scheme 2: Parameter uncertainty

The second scheme aims at propagation the uncertainty of parameters of the LCA sub-models. Stochastic modelling in LCA dates back to the work of Kennedy et al. (1996) and has been applied to LCA in the context of mobility as shown in chapter 3 (e.g., Cox et al. (2018)). For scheme 2 the following steps are applied during each model run. First, the synthetic population is initialized for the study region (this step is performed using the same random seed for each model run, thus always resulting in the identical population). Next the uncertainty propagation starts:

1. The seed factory is initialised creating N random seeds

2. Choice models are calibrated based on the survey data creating one nominal concrete instance $M^*_{s_*}$

3. The nominal concrete instance $M^*_{s_*}$ of the ABM is run one time, where for each execution of each choice model the most likely outcome is used

4. For the output $r_{M^*_{s_*}}$ N LCA model runs are conducted, each time creating a new concrete instance L^w by sampling all LCA parameters values according to the corresponding random seed and the derived uncertainty distributions

5. The output uncertainty measures are computed for each QOI

Again, the entire synthetic population is used for each ABM run, while the total number of model runs N is set to be 1'000 (which is at the lower end of what has been observed in the
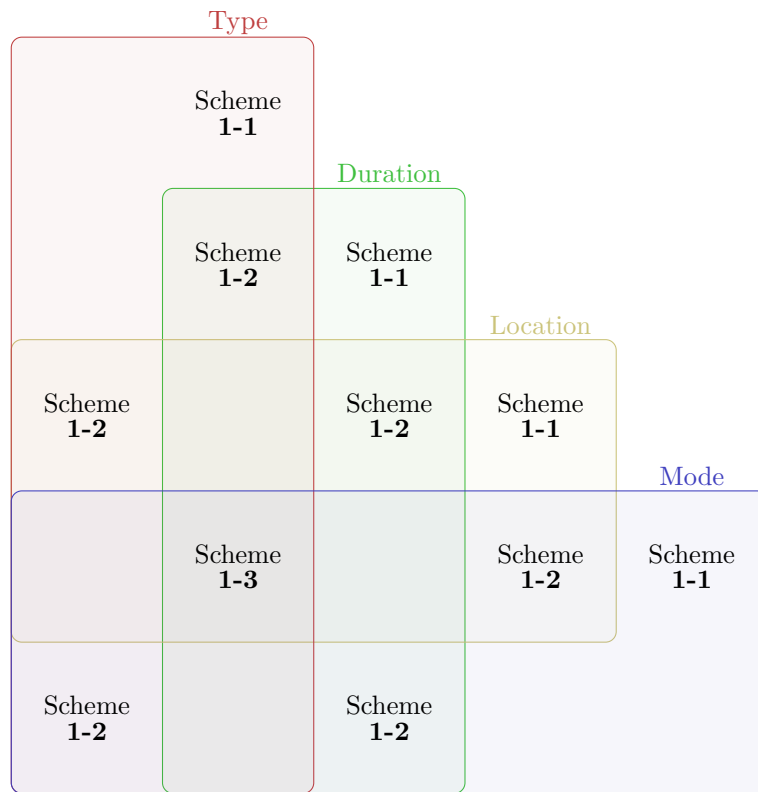
Figure 5.4: Venn diagram showing the three sub-schemes of scheme 1
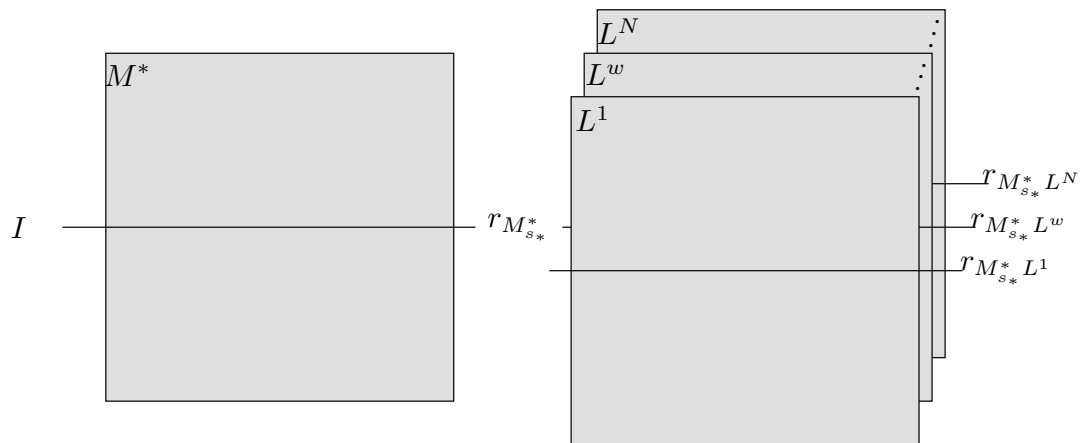
Figure 5.5: Scheme 2: Given a set of inputs I and N random seeds M^* produces one simulation result r_{M^*}. The model output of M^* becomes the input to N concrete instances of the LCA model part L, which allows to produce a set of final model outputs $r_{M^*L^w}$ for each wth seed.

literature review of LCA studies in chapter 3). Figure 5.5 illustrates the general structure of the
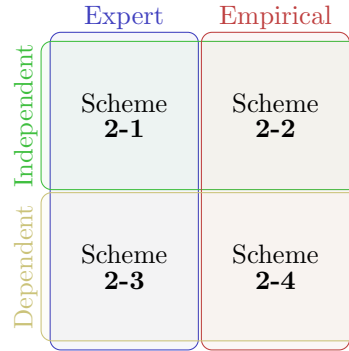
Figure 5.6: Venn diagram showing the four sub-schemes of scheme 2

second scheme based on the nomenclature presented in section 5.2.

Four sub-schemes of scheme 2 are defined to assess the impact of the two sets of uncertainty factor values (expert and empirical factors presented in section 5.3.2), as well as the impact of accounting for dependencies among fuel consumption and tailpipe emissions (similar to e.g., Boureima et al. (2009)) on the uncertainty of both QOIs. The four sub-schemes correspond to all possible combinations of uncertainty factors (referred to as *expert* and *empirical*) and sampling methods (referred to as *independent sampling* and *dependent sampling*). For all four sub-schemes in total 4·1'000 model runs are conducted.

5.4.5   Scheme 3: Simulation error and parameter uncertainty

Finally, the third scheme aims at propagating both the simulation error and the uncertainty from parameters of the LCA. This is the first attempt to align MC runs of such coupled models. The following steps are applied during each model run. First, the synthetic population is initialized for the study region (this step is performed using the same random seed for each model run, thus always resulting in the identical population). Next the uncertainty propagation starts:

1. The seed factory is initialised creating R sets s_v of random seeds with $v \in [1, ..., R]$, containing seeds for each potential choice of each choice model and N random seeds for the LCA

2. Choice models are calibrated based on the survey data creating one nominal concrete instance M^*

3. The ABM is run R times (once for each set s_v of random seeds)

4. Using bootstrapping with replacement, N ABM outputs are sampled from the R original results and for each a corresponding concrete instance L^w is created by sampling all LCA parameters values according to the corresponding random seed to conduct N LCA model runs

5. The output uncertainty measures are computed for each QOI

Again, the entire synthetic population is used for the ABM runs, while the number of ABM runs R is set to be 500 and the number of LCA model runs N is set to be 1'000. The bootstrapping of step 4 allows to address the disparity of the feasible number of model runs between both sub-models. In practice this means that 1'000 $r_{M^*_{s_v}}$ are randomly chosen (with replacement) out
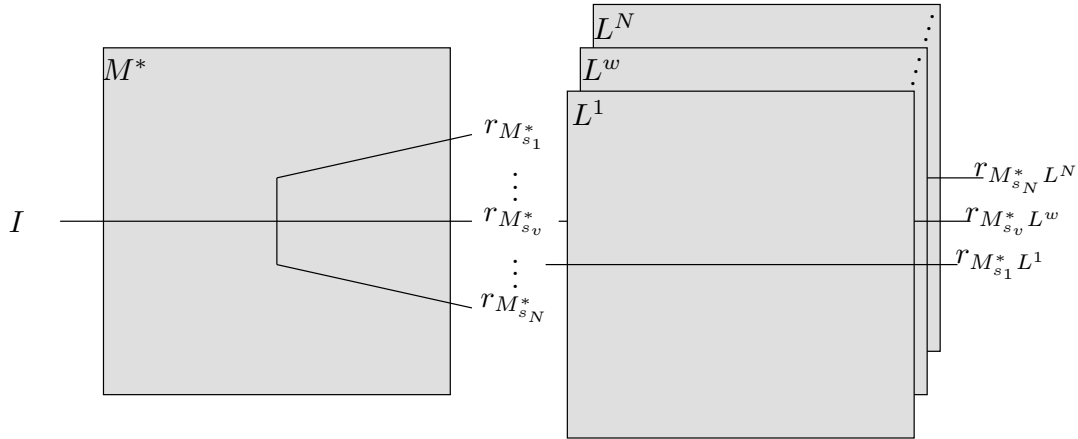
Figure 5.7: Scheme 3: Given a set of inputs I and R sets s_v containing random seeds for each potential random choice, $M^*_{s_v}$ produces a set of ABM results $r_{M^*_{s_v}}$. Next N random seeds are generated to create N concrete instances of the LCA L^w and using bootstrapping with replacement N corresponding ABM results are selected, allowing to produce a set of final model outputs $r_{M^*_{s_v} L^w}$ for each wth seed in N.

of the 500 original results. These 1'000 bootstrapped results then serve as inputs to the 1'000 subsequent LCA model runs. The impact of this bootstrapping will be assessed in order to assure that it does not cause major changes in the mean or spread of results.

This third scheme is only run for the setup where all choice models are set to their stochastic state, the expert uncertainty factors and the independent sampling. Figure 5.7 illustrates the general structure of the third scheme based on the nomenclature presented in section 5.2.

5.5 Uncertainty communication

Finally, uncertainty communication aims at communicating key findings of the UA to stakeholders.

Three different objectives can be formulated and the corresponding uncertainty measures can be introduced. As a first, when assessing the effect of uncertainty on a single scenario to evaluate magnitude of different uncertainty locations the CV has been chosen, as it is normalised by the mean (making it a comparable measure between QOI, scenarios and schemes).

The second objective is to assess the adequate number of model runs to perform for each scheme. To this end, the convergence (percentage difference of the CV compared to the CV after N model runs) is chosen. Rasouli (2016) has applied a similar approach, formulating a threshold for the percentage difference of the CV compared to the CV after N model runs. This approach however does not allow a conclusion whether or not convergence has been reached, as the relative difference will always drop to zero after N model runs.

To further advance the state-of-the-art it is here proposed to add a second condition to the approach of Rasouli (2016), where it is considered that convergence is reached if the percentage difference of the CV is consistently lower than 5% prior to $N/2$ model runs. It has to be acknowledge that both the threshold of 5% and the number of model runs by which this threshold should be reached are arbitrary, however they can be set according to the wisdom of the modeller or potentially requirements defined during the project definition phase. Using the second condition,

there is now a real possibility of concluding that convergence in not reached and that potentially additional model runs should be performed.

Finally, when applying UA in a comparative assertion to multiple scenarios, a variety of measures have been proposed. Based on the measures applied and reviewed by Mendoza Beltran et al. (2018a) it is chosen to use the modified Null Hypothesis Significance Test (NHST), the Bhattacharyya coefficient and the discernibility score for all scenarios.

The modified NHST proposed by Mendoza Beltran et al. (2018a) builds on regular NHST, which investigates if the mean (or median) of the relative impacts of two scenarios are statistically significantly different from each other. A pair-wise difference per MC runs is computed for each pair of scenarios and a paired t-test is performed to determine whether the mean of the distribution of differences is significantly different from zero (which is the hypothesised mean of the null hypothesis). The null hypothesis is then rejected or not, depending on the p-value and the predefined significance level α. The modification to the standard NHST proposed by Mendoza Beltran et al. (2018a) addresses the limitation of the null hypothesis which is theoretically always rejected by simply increasing the sample size (in this case the number of MC runs). While for standard NHST the null hypothesis assumes no difference between mean (or median) values, the modified NHST includes an "at least as different as" in the null hypothesis, requiring a standardized difference of means of at least 0.2.

A second complimentary measure applied in this thesis is the Bhattacharyya coefficient, which is first proposed by Mendoza Beltran et al. (2018a) and applied by Heijungs (2021). It is a measure of the amount of overlap between two statistical samples. To make the Bhattacharyya coefficient operational, the values of the two samples that are being compared are split into a chosen number of partitions (par), and the number of members of each sample in each partition is computed. The Bhattacharyya coefficient can then be computed as follows:

$$BC(\mathbf{p}, \mathbf{q}) = \sum_{\forall par} \sqrt{p_{par} q_{par}} \tag{5.8}$$

Where $\mathbf{p}$ and $\mathbf{q}$ are the two samples and p_{par} and q_{par} the numbers of members of each partition par of $\mathbf{p}$ and $\mathbf{q}$ respectively.

Finally, a widely applied measure of uncertainty in comparative LCA is the discernibility score, where a pair-wise comparison per MC run is made for each pair of scenarios, assessing whether the results of one scenario are higher or lower than those of another scenario. The results are expressed as, e.g., a percentage of MC runs for which a scenario has higher results than another scenario.

5.6 Summary

This chapter introduces the uncertainty framework and research designs applied for the CONNECTING model.

The main locations of uncertainty identified from the literature reviews are determined and a new nomenclature for ABM/LCA coupled models is introduced. The nomenclature introduces the notion of a (nominal) concrete instance of a model, which can be associated to a specific result. The main purpose of this notion is to make specific mode runs traceable and reproducible.

For both sub-models, the uncertainty characterisation is outlined. For the ABM part of CONNECTING the formulas to derive choice probabilities for the main types of choice models are presented. For the LCA the broadly applied pedigree approach is introduced, and two sources of uncertainty factors (expert-based and empirical-based) are compare, which are applied to the CONNECTING LCI.

Three schemes for the UA of the ABM simulation error (scheme 1), parameter uncertainty in the LCA (scheme 2) and a combination of both (scheme 3) are detailed building on the newly introduced nomenclature. These schemes and various sub-schemes allow for an in depth investigation of these uncertainty locations.

Finally, based on the findings of the literature review in chapter 3 two additional issues and their respective solutions are highlighted: (1) the proper usage of a random seed factory for UA of multiple scenarios; (2) the investigation of parameter dependencies among inputs and outputs of LCI unit processes.

Chapter 6

Results of scheme 1 - ABM model uncertainty

6.1   Introduction

As presented in chapter 3, both sub-models of the CONNECTING model have relevant uncertainty locations that need to be systematically addressed. To this end, chapter 5 presented a nomenclature and three schemes (with various sub-schemes) that allow to propagate model uncertainty. This chapter will report on the results of scheme 1, which focusses on ABM uncertainty.

Although model uncertainty encompasses uncertainty from model specification (e.g., uncertainty about the functional form), model estimation (e.g., uncertainty about measures and calibrated parameters) and the simulation error, this thesis will focus only on the simulation error of the ABM part of CONNECTING. This choice is motivated by the fact that this is the most addressed location found in the literature review in chapter 3 for ABMs.

As seen in chapter 4, the ABM part of CONNECTING can be classified as an utility-based model, with error terms present in the utility functions. For each model run, random draws from choice models can cause variations in the model output (i.e., different choices being made by individuals in the synthetic population). The distributions of error terms depend on the assumptions underlying the specific modelling chosen for a choice facet (as described in chapter 5).

The focus is set on uncertainty of system level outputs (rather than individual or sub-regional outputs), namely the QOIs quantifying climate change related impacts (*GWP100*) and respiratory effects related impacts (*R-E*) for which uncertainty will be quantified and communicated as outlined in section 5.5.

All schemes are applied to the CONNECTING model for two scenarios (*BAU* and *GREEN*) of the PT system (reflecting two levels of investment into PT) and two scenarios describing the evolution of electric mobility (*ADEME* and *TIR*) within the private car fleet. All combinations of both scenario families are evaluated in the following, resulting in the four scenarios: *BAU-ADEME*, *BAU-TIR*, *GREEN-ADEME* and *GREEN-TIR*.

In sections 6.2 a brief description of the nominal CONNECTING model results is presented, showing the single score deterministic results for all scenarios. These results serve as a reference for this and subsequent result chapters. Sections 6.3-6.4 will present the results of the three sub-schemes of scheme 1, before a short summary is provided in section 6.5.

6.2   Nominal model results

In this section a brief description of the results of the nominal model for the four policy scenarios is provided. To this end a nominal concrete instance of both CONNECTING sub-models is created, where "nominal concrete instance" (see nomenclature in chapter 5) is a model where all model parameters take their nominal value and where each random choice event results in its most likely outcome. This nominal concrete instance is run once resulting in the deterministic results of the CONNECTING model.

6.2.1   ABM results

First, the intermediate results of the ABM are presented. The ABM part of CONNECTING predicts a DAP for each individual in the synthetic population, where the two PT scenarios affect individual choices, aiming at decreasing the usage of cars and increasing the usage of PT. Note, that the two scenarios with regard to EVs (*TIR* and *ADEME*) are not presented in this section, as the share of powertrains in the car fleet will only affect the LCA and not the intermediate ABM results.

Figure 6.1 shows the results of the ABM part of CONNECTING. To make the ABM results (and subsequent LCA results) more relatable, the average travelled distances per individual are calculated. In figure 6.1 the distances travelled by the two PT modes (bus and train), by car and by slow mobility are shown. In 2015 the model predicts that per individual 64 kilometres (or 79% of daily travel distances) are travelled by the mode of car, while bus, train and slow mobility only account for a smaller share (together 21% of daily travel distances). Both scenarios achieve a decrease of car usage. While the *BAU* scenario decreases the daily travelled distances by car to around 58 kilometres (or 72% of daily travel distances) by 2025, the *GREEN* scenario achieves a more substantial reduction to around 51 kilometres (or 65% of daily travel distances). Both PT scenarios thus achieve a reduction of car usage, with the *GREEN* scenario showing a more substantial reduction.

At the same time, the usage of bus and train increases for both scenario, with the *GREEN* scenario (figure 6.1 (b)) showing a stronger increase than the *BAU* scenario (figure 6.1 (a)). The mode of slow mobility remains unattractive for CBCs for both scenarios throughout the study period, only accounting for a marginal share of the travelled distances. This is not surprising as CBCs usually need to travel long distances to arrive at their work place, which is impractical with slow mobility.

6.2.2   LCA results

Next, the CONNECTING model outputs (more specifically both QOIs) can be calculated (shown in figure 6.2) using the travelled distances as inputs to the LCA part of CONNECTING. In 2015 all scenarios show identical results, as the PT system and car fleets are identical as well. 2015 is thus the reference year after which scenarios diverge.

In figure 6.2 (a) one can see that all scenarios presented earlier in chapter 4 translate into a reduction of the environmental burden with regard to *GWP100*. While in 2015, GHG emissions are still above 17 kg per CBC for a all daily travels, the *BAU-ADEME* scenario can achieve a reduction of 3% in 2020 and 8% in 2025. The *BAU-TIR* scenario shows a stronger reduction of 4% and 13% in 2020 and 2025 respectively. The highest reduction is achieved by the *GREEN-TIR* scenario, for which impacts are reduced by 8% and 17% in 2020 and 2025 respectively.

The *GREEN* scenario thus systematically results in lower *GWP100* impacts compared to the *BAU* scenario, all else equal. However, in 2025 a lower investment in PT can be compensated by a higher share of EVs, as the *BAU-TIR* scenario shows lower impacts (15.20 $kgCO_2 - Eq$ per
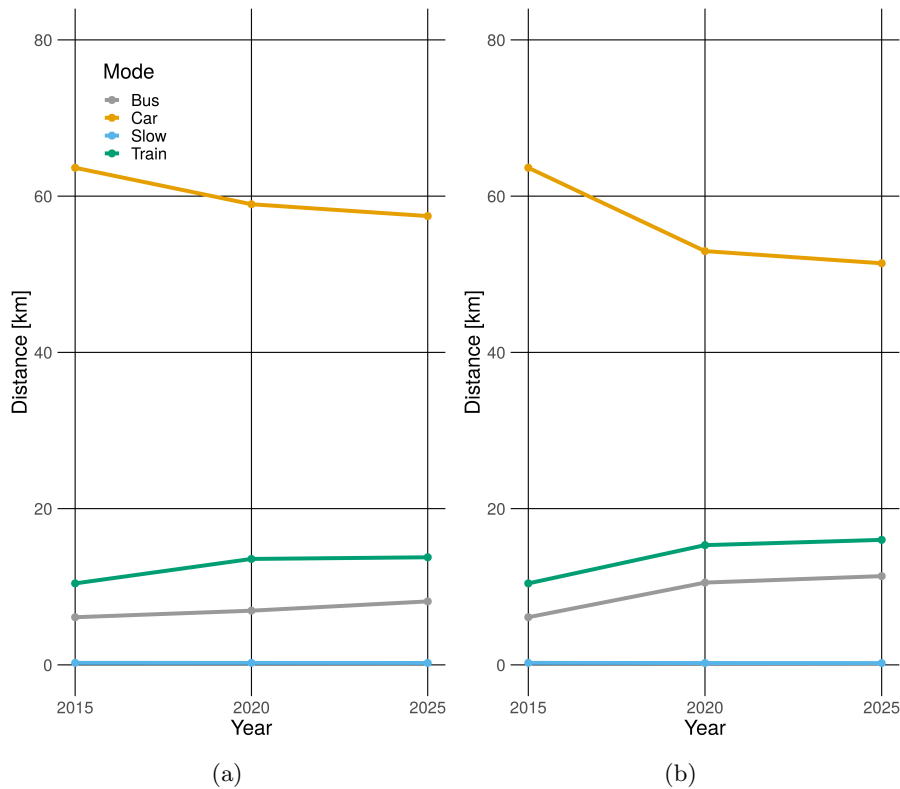
Figure 6.1: Evolution of travel demand per CBC by transport mode. The mode "Car" encompasses all powertrains. (a) shows the results for the *BAU* scenario. (b) shows the results for the *GREEN* scenario.

commuter) than the *GREEN-ADEME* scenario (15.27 $kgCO_2 - Eq$ per commuter) in figure 6.2 (a).

The *TIR* scenario also systematically results in lower *GWP100* impacts compared to the scenario *ADEME*, all else equal. This suggests that a higher share of EVs can in fact reduce GHG emissions of a transport system from a life cycle perspective. However, the impact of electric mobility only becomes apparent in 2025. In 2020 impacts of *TIR* scenarios are on average only 0.10 $kgCO_2 - Eq$ lower than *ADEME* scenarios, all else equal. In 2025 they are on average 0.85 $kgCO_2 - Eq$ lower. This can be explained by the differences in the car fleet shares between the *TIR* and *ADEME* scenario, which are only marginal up to 2020, but increase for later study years, as shown in figure 4.4.

In Figure 6.2 (b) the results for *R-E*, the second QOI, are shown. One can see that the impacts per CBC are decreasing over the course of the study period for all scenarios, with the *GREEN* scenario systematically showing lower *R-E* impacts compared to the *BAU* scenario. Both *BAU* scenarios achieve impact reductions of 12% and 20% in 2020 and 2025 respectively. Both *GREEN* scenarios achieve impact reductions of 14% and 22% in 2020 and 2025 respectively.

The *TIR* and *ADEME* scenarios seem to have no significant influence. In part this results from the small differences between the fleet shares, as noted above for *GWP*. In addition, while EVs do not have tailpipe emissions, they are responsible for emissions occurring during the electricity production to charge the battery and emissions occurring during the raw material
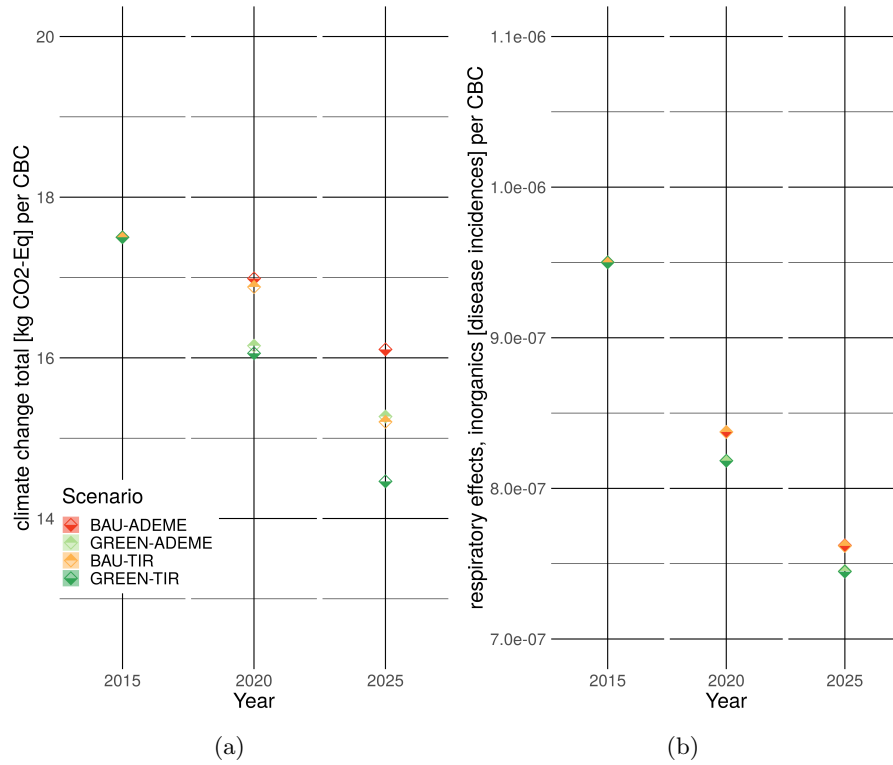
Figure 6.2: Nominal model outputs for both QOIs. (a) shows *GWP100* per CBC. (b) shows *R-E* per CBC.

extraction (e.g., for battery components).

Based on the single score results in figure 6.2 decisions seem rather clear cut. Higher investments in PT and higher shares of EVs in car fleets can reduce environmental impacts. However, without an indication of the confidence that one can put into these results some investments might ultimately be ill advised and not result in the desired outcomes. The following sections will show how different uncertainty locations can affect both QOIs.

Following the results of the nominal model, the following sections 6.3-6.4 will present the results of the three sub-schemes of scheme 1.

6.3   Sub-scheme 1-1: Separate treatment

Sub-scheme 1-1 focusses on individual choice facets of the ABM part of CONNECTING. For each of the four choice models presented in chapter 4 a concrete instance of the CONNECTING model is created and run 500 times. Each time one choice model is set run stochastically (with changing random number seeds for each model run), while all other choice models are set to their deterministic state (corresponding to their nominal concrete instance) where each random choice event results in its most likely outcome.

6.3.1 Output distributions

Tables 6.1 and 6.2 provide the descriptive statistics of the model outputs for both QOIs respectively. Each table is sub-divided into sections for each ABM choice model, containing the results of sub-scheme 1-1 for that choice model being run stochastically. For each model the median, mean, SD and CV are provided. In 2015, the reference year, these statistics are identical for all scenarios, while for later years they diverge increasingly.

A first notable aspect of the results in table 6.1 is, that mean and median values change for different choice models being set to run stochastically.

Taking the nominal results presented in figure 6.2 as a reference, running the activity type model stochastically results in (on average) -1.6% lower mean values, while running the location model stochastically results in (on average) 2.8% higher mean values. For other choice models similar behaviours can be observed, but to a lesser extend. Similar results are also observed for the second QOI, *R-E* in table 6.2.

This phenomena can be explained in part by the definition of the nominal concrete instance of the ABM part of CONNECTING, where each execution of a choice model results in the most likely outcome (i.e., option with the highest utility). Taking the location model as an example,

Table 6.1: Descriptive statistics of uncertainty distributions of *GWP100* scores in [kg CO2-eq] for sub-scheme 1-1. Values are provided for each of the four ABM sub-models.

	BAU-ADEME			BAU-TIR			GREEN-ADEME			GREEN-TIR		
	2015	2020	2025	2015	2020	2025	2015	2020	2025	2015	2020	2025
Activity type model												
Median	17.3	16.7	15.8	17.3	16.6	15.0	17.3	15.9	15.0	17.3	15.8	14.2
Mean	17.3	16.7	15.8	17.3	16.6	15.0	17.3	15.9	15.0	17.3	15.8	14.2
SD	0.020	0.017	0.016	0.020	0.017	0.015	0.020	0.017	0.015	0.020	0.017	0.014
CV [%]	0.118	0.102	0.100	0.118	0.102	0.099	0.118	0.105	0.102	0.118	0.105	0.100
Duration model												
Median	17.5	17.0	16.1	17.5	16.9	15.2	17.5	16.2	15.3	17.5	16.1	14.5
Mean	17.5	17.0	16.1	17.5	16.9	15.2	17.5	16.2	15.3	17.5	16.1	14.5
SD	0.014	0.012	0.011	0.014	0.012	0.011	0.014	0.012	0.011	0.014	0.012	0.011
CV [%]	0.081	0.073	0.071	0.081	0.072	0.069	0.081	0.076	0.075	0.081	0.076	0.073
Location model												
Median	17.9	17.4	16.6	17.9	17.3	15.7	17.9	16.7	15.8	17.9	16.6	14.9
Mean	17.9	17.4	16.6	17.9	17.3	15.7	17.9	16.7	15.8	17.9	16.6	14.9
SD	0.006	0.006	0.006	0.006	0.006	0.006	0.006	0.006	0.006	0.006	0.006	0.006
CV [%]	0.035	0.037	0.039	0.035	0.037	0.038	0.035	0.038	0.039	0.035	0.038	0.039
Mode choice model												
Median	17.8	17.2	16.3	17.8	17.1	15.4	17.8	16.0	15.2	17.8	15.9	14.4
Mean	17.8	17.2	16.3	17.8	17.1	15.4	17.8	16.0	15.2	17.8	15.9	14.4
SD	0.011	0.009	0.010	0.011	0.009	0.009	0.011	0.009	0.009	0.011	0.009	0.009
CV [%]	0.059	0.055	0.059	0.059	0.055	0.056	0.059	0.056	0.059	0.059	0.056	0.056

running it stochastically increases impacts compared to the nominal model. One explanation for this could be, that the location model reduces utility for locations causing a longer detour from the home-work axis of the individual (as seen in chapter 4). Thus, the most likely choice tends to be close to the home-work axis, while running the location model stochastically will allow individuals to choose any possible location (not necessarily the most likely one) with a certain probability, even locations further away from the home-work axis. The stochastic model can thus potentially result in longer detours for commuters, which will results in overall longer travel distances and in consequence higher impacts.

A second notable aspect of the results in table 6.1 is that different choice models cause different levels of uncertainty in the model outcome. The activity type model shows the highest CV values (0.099%-0.118%), followed by the duration model (0.069%-0.081%) and the mode choice model (0.059%-0.055%). The activity location model shows the lowest CV values (0.035%-0.039%) compared to the other choice models. This ranking is confirmed by results in table 6.2 for the R-E impacts, where the activity type model shows the highest CV values (0.095%-0.117%), followed by the duration model (0.065%-0.080%) and the mode choice model (0.045%-0.057%). The activity location model shows the lowest CV values (0.035%-0.035%).

These values can be in part explained by choice probabilities for a logit models derived

Table 6.2: Descriptive statistics of uncertainty distributions of R-E scores in 10^{-7} [disease incidences] for sub-scheme 1-1. Values are provided for each of the four ABM sub-models.

	BAU-ADEME			BAU-TIR			GREEN-ADEME			GREEN-TIR		
	2015	2020	2025	2015	2020	2025	2015	2020	2025	2015	2020	2025
Activity type model												
Median	9.4	8.3	7.6	9.4	8.3	7.6	9.4	8.1	7.4	9.4	8.1	7.4
Mean	9.4	8.3	7.6	9.4	8.3	7.6	9.4	8.1	7.4	9.4	8.1	7.4
SD	0.011	0.008	0.007	0.011	0.008	0.007	0.011	0.008	0.007	0.011	0.008	0.007
CV [%]	0.117	0.100	0.095	0.117	0.100	0.095	0.117	0.100	0.095	0.117	0.100	0.095
Duration model												
Median	9.5	8.4	7.6	9.5	8.4	7.6	9.5	8.2	7.5	9.5	8.2	7.4
Mean	9.5	8.4	7.6	9.5	8.4	7.6	9.5	8.2	7.5	9.5	8.2	7.4
SD	0.008	0.006	0.005	0.008	0.006	0.005	0.008	0.006	0.005	0.008	0.006	0.005
CV [%]	0.080	0.069	0.065	0.080	0.069	0.065	0.080	0.071	0.067	0.080	0.071	0.066
Location model												
Median	9.7	8.6	7.8	9.7	8.6	7.8	9.7	8.4	7.6	9.7	8.4	7.6
Mean	9.7	8.6	7.8	9.7	8.6	7.8	9.7	8.4	7.6	9.7	8.4	7.6
SD	0.003	0.003	0.003	0.003	0.003	0.003	0.003	0.003	0.003	0.003	0.003	0.003
CV [%]	0.035	0.036	0.036	0.035	0.036	0.036	0.035	0.036	0.036	0.035	0.036	0.036
Mode choice model												
Median	9.6	8.5	7.8	9.6	8.5	7.8	9.6	8.3	7.6	9.6	8.3	7.6
Mean	9.6	8.5	7.8	9.6	8.5	7.8	9.6	8.3	7.6	9.6	8.3	7.6
SD	0.005	0.004	0.004	0.005	0.004	0.004	0.005	0.004	0.003	0.005	0.004	0.003
CV [%]	0.057	0.045	0.045	0.057	0.045	0.045	0.057	0.046	0.045	0.057	0.046	0.045

according to equation 5.2. If all options in a choice set have similar utility to an individual, they will also have similar probabilities of choice, while if some options have a higher utility compared to other options they will have a higher probability of choice. If there is a high disparity among the utilities (and in consequence the probabilities of choice) this will cause similar choices across model runs and in consequence low variability among DAPs (especially if one option is significantly more likely than all other options).

Taking the location model as an example, locations providing a high level of services will have a significantly higher utility and in consequence higher probability of choice than locations with a low level of services. In the study region there are only a few such locations, mainly the cities of Luxembourg, Thionville and Metz. These locations will thus have a high probability of choice, causing little variation among model runs. In addition, CBCs are more constrained by their mandatory work activity which has a fixed location, thus causing no variation at all for work location choices. In consequence, the location model exhibits a low level of uncertainty.

In case of the activity type model, choices can have similar levels of utility (and probability of choice) to an individual, potentially resulting in longer or shorter DAPs. This causes a relatively higher level of variation among DAPs and translates into a higher level of uncertainty in the model outcomes (i.e., both QOIs).

A third notable aspect of the results in tables 6.1-6.2 is that for three of the four models (activity type, duration and mode choice) the SD and CV values decrease for later simulation years. This could be a result of increasing population numbers, similar to the effect of the simulation error, where a larger sample of the population leads to a lower variability observed in the model output.

Finally, a fourth notable aspect of the results in tables 6.1-6.2 is that the overall level of uncertainty is low compared to the mean and median values, with all CV values being well below 1%. Individually, choice models do not cause high levels of variation in the systems environmental impacts for CBCs.

6.3.2   Convergence

Following the descriptive statistics of both QOIs, next the convergence of CV values for individual ABM choice models is investigated.

Convergence of activity type model   The CV values for the activity type model are presented as a function of the number of model runs in figure 6.3. After 500 runs, CV values in figure 6.3 correspond to the values previously shown in tables 6.1-6.2 for the activity type model. The CV values are provided every 25 runs starting after 25 runs.

It can be observed that in absolute terms, the CV values do not exhibit much fluctuation or strong upward or downward trends for any scenario or year. It seems that only a few runs are necessary to arrive at reasonable estimates for CV values.

As these visual impressions can be misleading, a new convergence metric has been suggested in chapter 5 of the present thesis. Similar to Rasouli (2016) it is assumed that convergence of a measure is reached, once its percentage difference compared to the value of that measure after N model runs is consistently lower than a selected threshold. As indicator of convergence, the lowest number of runs required to reach convergence can be compared.

However, as noted in chapter 5 convergence will eventually always be reached (at the latest for N runs), regardless of the chosen threshold. Therefore, a second condition was suggested in this thesis: in order to assert that for a specific measure the model output has *converged*, the lowest number of runs required must be lower than $N/2$.

Tables 6.3-6.4 show the lowest number of runs required to reach convergence of the activity
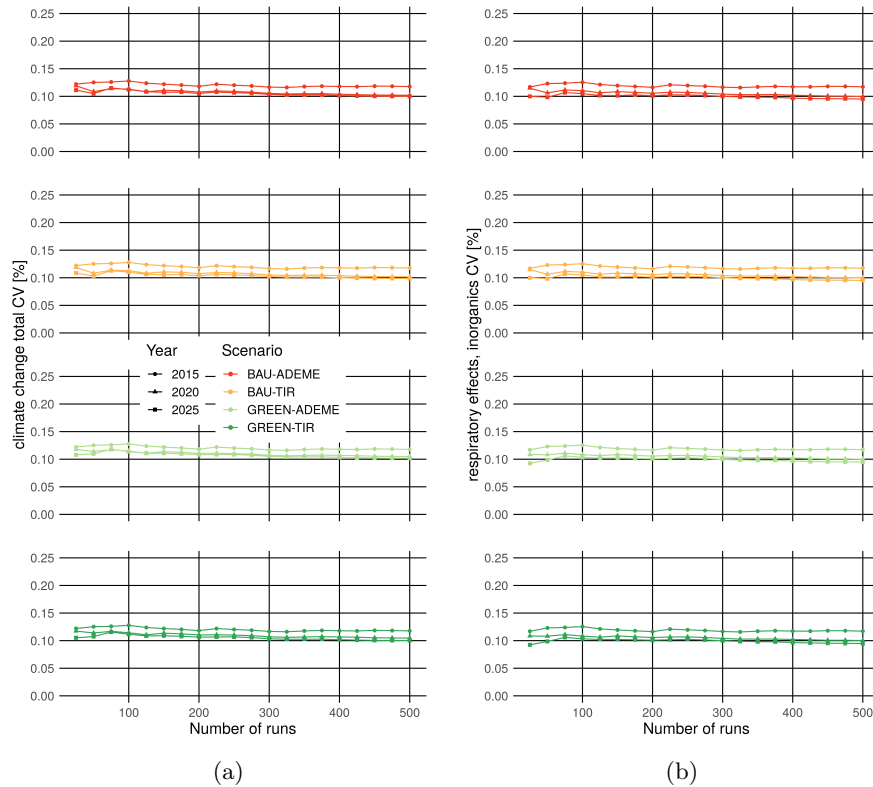
Figure 6.3: CV as a function of the number of model runs for sub-scheme 1-1 of the activity type model. (a) shows the CV values for *GWP100*. (b) shows the CV values for *R-E*.

type model for both QOIs, using thresholds of 1% up to 10% relative difference. While for 2015 we can assert that the CV values have converged according to our criteria (i.e., reaching 5% threshold within $N/2$ mode runs), both for 2020 and 2025 the criteria are not satisfied. Such a claim could only be made for higher thresholds.

Convergence of duration model   Next, convergence of the CV of both QOIs for sub-scheme 1-1 of the duration model is assessed. Figure 6.4 shows the CV as a function of the number of model runs. As seen in the previous section, CV values are lower compared to those of the activity type model. For the first 175 runs, CV values show a slight downwards trend before stabilising around their final values.

Tables 6.5-6.6 show the lowest number of runs required to reach convergence of the duration model. In contrast to the type model, we can assert that CV values have converged for all years and scenarios and both QOIs as our criteria are always satisfied.

Convergence of location choice model   Next, convergence of the CV of both QOIs for sub-scheme 1-1 of the location model is assessed. Figure 6.5 shows the CV as a function of the number of model runs. While CV values are the lowest among all choice models, there is a slight upward trend that can be observed at least until 425 model runs.

Tables 6.7-6.8 show the lowest number of runs required to reach convergence of the location model. Confirming the visual impression, the location model converges significantly slower than

Table 6.3: Convergence for thresholds of 1-10% for *GWP100*, for sub-scheme 1-1 with activity type sub-model is being run stochastically.

	BAU-ADEME			BAU-TIR			GREEN-ADEME			GREEN-TIR		
	2015	2020	2025	2015	2020	2025	2015	2020	2025	2015	2020	2025
1	372	428	432	372	428	431	372	433	435	372	433	432
2	268	407	388	268	407	388	268	417	394	268	417	393
3	253	381	346	253	381	346	253	285	334	253	285	334
4	130	333	295	130	333	295	130	277	285	130	277	285
5	126	278	278	126	278	278	126	258	277	126	258	278
6	120	270	268	120	270	269	120	196	257	120	196	257
7	107	254	248	107	254	248	107	191	194	107	191	230
8	103	176	126	103	176	125	103	152	189	103	152	189
9	95	150	124	95	150	123	95	103	150	95	101	150
10	41	103	120	41	103	112	41	99	122	41	98	120

Table 6.4: Convergence for thresholds of 1-10% for *R-E*, for sub-scheme 1-1 with activity type sub-model is being run stochastically.

	BAU-ADEME			BAU-TIR			GREEN-ADEME			GREEN-TIR		
	2015	2020	2025	2015	2020	2025	2015	2020	2025	2015	2020	2025
1	372	449	466	372	449	466	372	432	466	372	432	466
2	263	413	397	263	413	397	263	412	400	263	412	400
3	237	388	381	237	388	381	237	382	385	237	382	385
4	122	343	347	122	343	347	122	288	346	122	288	346
5	111	284	334	111	284	334	111	279	303	111	279	303
6	105	275	281	105	275	281	105	271	280	105	271	280
7	101	264	275	101	264	275	101	256	275	101	256	275
8	94	247	254	94	247	254	94	188	255	94	188	255
9	32	150	115	32	150	115	32	95	122	32	95	121
10	18	103	101	18	103	101	18	93	97	18	93	97

Table 6.5: Convergence for thresholds of 1-10% for *GWP100*, for sub-scheme 1-1 with duration sub-model is being run stochastically.

	BAU-ADEME			BAU-TIR			GREEN-ADEME			GREEN-TIR		
	2015	2020	2025	2015	2020	2025	2015	2020	2025	2015	2020	2025
1	453	447	445	453	447	417	453	380	460	453	380	460
2	363	364	405	363	364	405	363	310	376	363	310	376
3	343	356	364	343	356	364	343	205	362	343	205	362
4	121	143	362	121	143	362	121	201	187	121	201	188
5	117	128	149	117	128	150	117	149	152	117	149	152
6	115	120	146	115	120	147	115	143	148	115	143	148
7	96	117	143	96	117	143	96	138	143	96	138	143
8	68	114	137	68	114	138	68	129	138	68	129	138
9	67	99	128	67	99	128	67	125	122	67	125	125
10	66	88	117	66	88	119	66	119	117	66	119	118
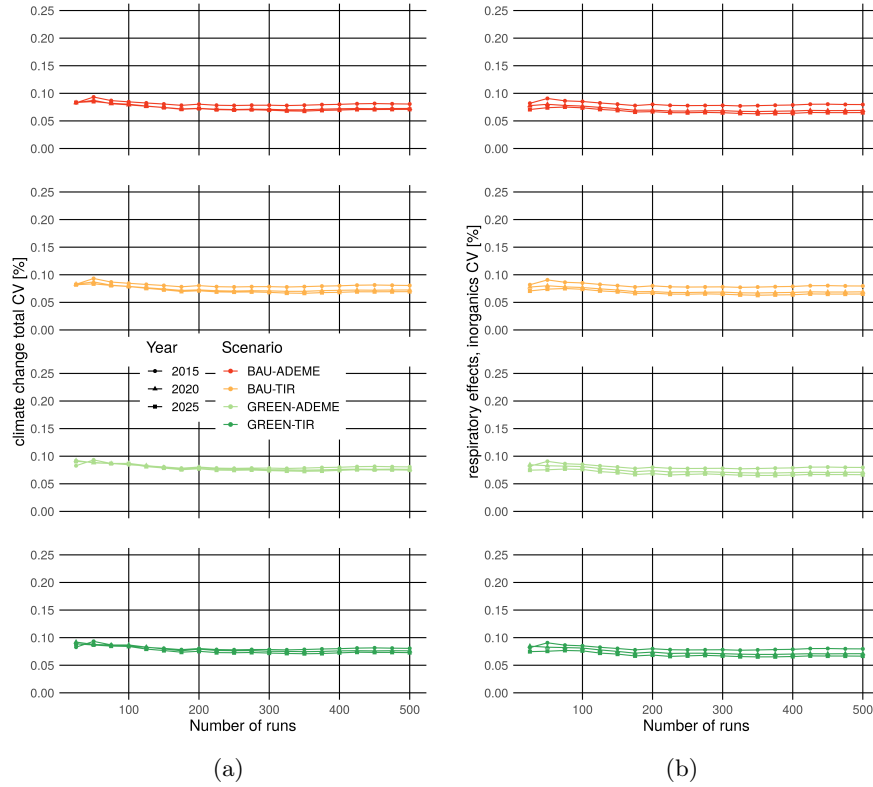
Figure 6.4: CV as a function of the number of model runs for sub-scheme 1-1 of the duration model. (a) shows the CV values for *GWP100*. (b) shows the CV values for *R-E*.

the activity type and duration models.

The location model does not satisfy the convergence criteria set for this thesis, as convergence for a 5% threshold is only reached significantly after $N/2$ mode runs for all scenarios and years.

Table 6.6: Convergence for thresholds of 1-10% for *R-E*, for sub-scheme 1-1 with duration sub-model is being run stochastically.

	BAU-ADEME			BAU-TIR			GREEN-ADEME			GREEN-TIR		
	2015	2020	2025	2015	2020	2025	2015	2020	2025	2015	2020	2025
1	449	447	417	449	447	417	449	446	405	449	446	405
2	362	385	408	362	385	408	362	356	364	362	356	364
3	326	356	362	326	356	362	326	205	200	326	205	200
4	129	155	166	129	155	166	129	201	158	129	201	158
5	121	150	156	121	150	156	121	157	154	121	157	154
6	119	147	151	119	147	151	119	150	149	119	150	149
7	115	137	148	115	137	148	115	147	146	115	147	146
8	99	127	144	99	127	144	99	143	143	99	143	143
9	96	119	138	96	119	138	96	137	137	96	137	137
10	62	115	119	62	115	119	62	125	115	62	125	115
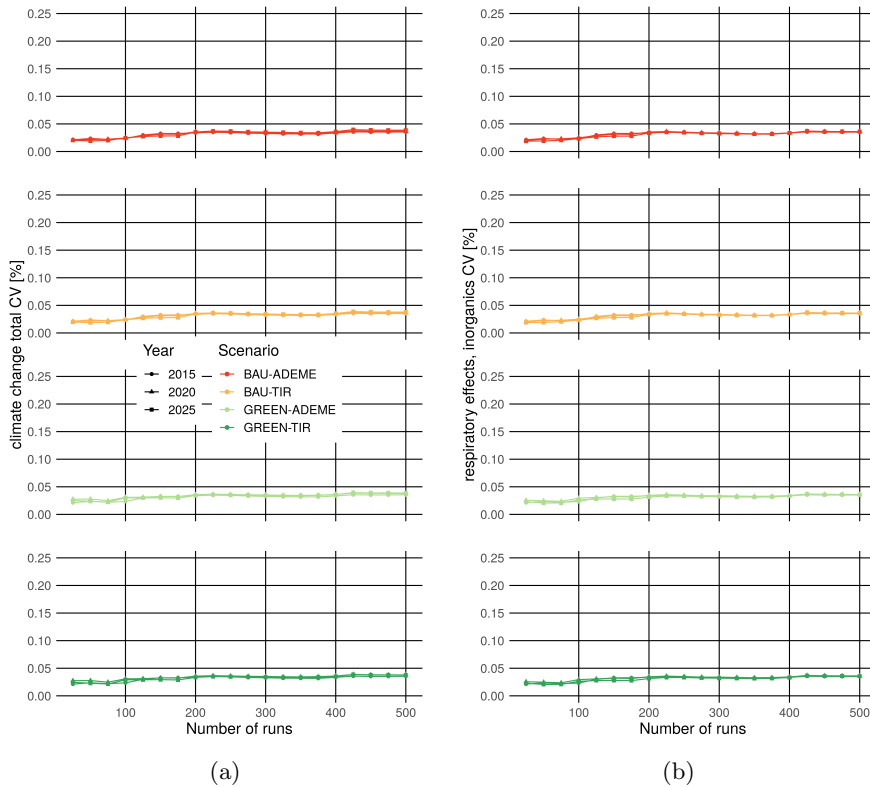
Figure 6.5: CV as a function of the number of model runs for sub-scheme 1-1 of the location model. (a) shows the CV values for *GWP100*. (b) shows the CV values for *R-E*.

Convergence of mode choice model Finally, convergence of the mode choice model is assessed. Figure 6.6 shows the CV as a function of the number of model runs. CV values are stabilising quickly after around 75 model runs for all scenarios and years.

Table 6.7: Convergence for thresholds of 1-10% for *GWP100*, for sub-scheme 1-1 with location sub-model is being run stochastically.

	BAU-ADEME			BAU-TIR			GREEN-ADEME			GREEN-TIR		
	2015	2020	2025	2015	2020	2025	2015	2020	2025	2015	2020	2025
1	470	469	444	470	469	442	470	451	442	470	451	439
2	408	408	431	408	408	430	408	431	428	408	431	427
3	405	407	407	405	407	407	405	406	408	405	406	408
4	404	405	405	404	405	406	404	404	407	404	404	407
5	403	404	404	403	404	405	403	400	406	403	400	406
6	400	402	403	400	402	403	400	396	404	400	397	404
7	383	400	400	383	400	400	383	382	401	383	382	401
8	381	382	397	381	382	398	381	366	398	381	366	398
9	378	380	383	378	380	383	378	352	382	378	352	382
10	377	376	381	377	376	381	377	191	380	377	191	380

(a)   (b)
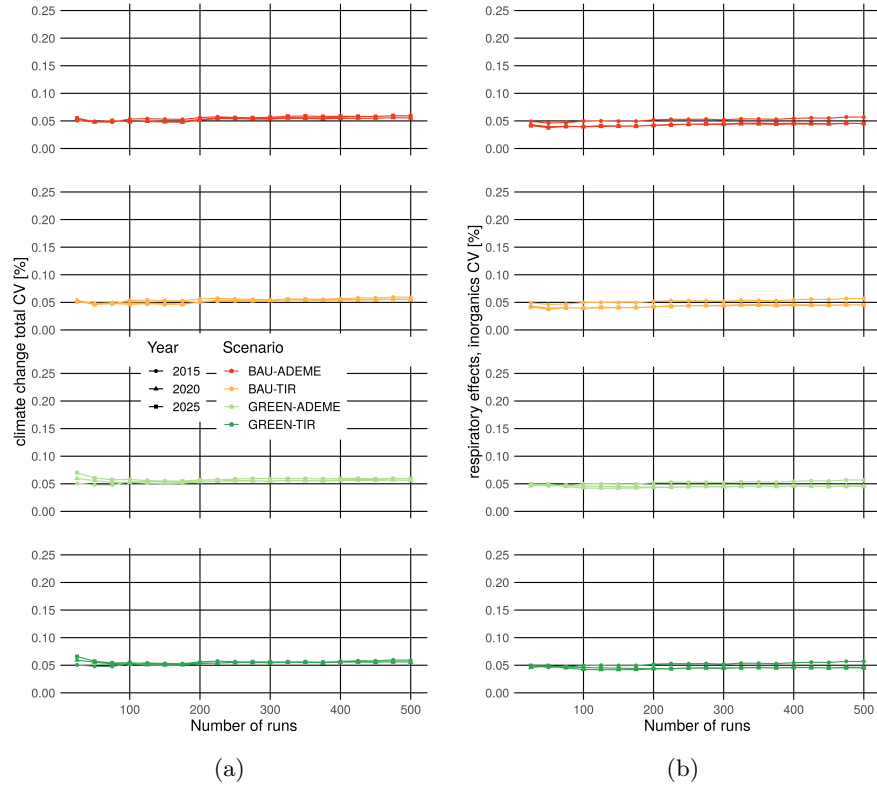
Figure 6.6: CV as a function of the number of model runs for sub-scheme 1-1 of the mode choice model. (a) shows the CV values for *GWP100*. (b) shows the CV values for *R-E*.

Tables 6.9-6.10 show the lowest number of runs required to reach convergence of the mode choice model. While in 2015 the model does not satisfy the convergence criteria set for this thesis, for *GWP100* the convergence criteria are satisfied in 2020 for all scenarios and in 2025 for the

Table 6.8: Convergence for thresholds of 1-10% for *R-E*, for sub-scheme 1-1 with location sub-model is being run stochastically.

T (%)	*BAU-ADEME*			*BAU-TIR*			*GREEN-ADEME*			*GREEN-TIR*		
	2015	2020	2025	2015	2020	2025	2015	2020	2025	2015	2020	2025
1	469	469	446	469	469	446	469	450	436	469	450	436
2	407	426	433	407	426	433	407	431	425	407	431	425
3	405	407	407	405	407	407	405	406	408	405	406	408
4	403	405	405	403	405	405	403	405	407	403	405	407
5	400	404	404	400	404	404	400	401	406	400	401	406
6	383	402	403	383	402	403	383	399	404	383	399	404
7	382	400	401	382	400	401	382	381	401	382	381	401
8	380	382	397	380	382	397	380	376	400	380	376	400
9	377	380	382	377	380	382	377	355	381	377	355	381
10	376	377	380	376	377	380	376	190	378	376	190	378

GREEN scenarios. For *R-E* they are satisfied for all scenarios in 2020 and 2025.

Overall, it seems that choice facets associated with higher levels of uncertainty, such as activity type and duration, converge faster than choice facets with lower levels of uncertainty, such as location and mode choices.

6.4 Sub-schemes 1-2 and 1-3: Simultaneous treatment

Following the results of sub-scheme 1-1, the results of schemes 1-2 and 1-3 are presented in this section. For both sub-schemes combinations of choice models are set to run stochastically, with (in case of sub-scheme 1-2) remaining choice models set to their deterministic state.

6.4.1 Output distributions

First, the empirical output distributions of sub-scheme 1-3 for both QOIs are shown in figure 6.7, along with the median value indicators. Results of this sub-scheme are of particular importance as this sub-scheme will be reused for scheme 3 (for which results are presented in

Table 6.9: Convergence for thresholds of 1-10% for *GWP100*, for sub-scheme 1-1 with mode choice sub-model is being run stochastically.

	BAU-ADEME			BAU-TIR			GREEN-ADEME			GREEN-TIR		
	2015	2020	2025	2015	2020	2025	2015	2020	2025	2015	2020	2025
1	456	482	476	456	482	476	456	486	378	456	486	378
2	451	396	308	451	396	307	451	378	250	451	378	250
3	404	301	307	404	301	307	404	227	227	404	227	227
4	399	289	300	399	289	291	399	209	209	399	209	209
5	380	210	285	380	210	283	380	203	180	380	203	180
6	379	206	235	379	206	215	379	193	180	379	193	180
7	307	206	215	307	206	215	307	180	179	307	180	179
8	301	196	210	301	196	210	301	180	175	301	180	175
9	180	192	209	180	192	209	180	180	160	180	180	160
10	177	182	206	177	182	206	177	180	34	177	180	34

Table 6.10: Convergence for thresholds of 1-10% for *R-E*, for sub-scheme 1-1 with mode choice sub-model is being run stochastically.

	BAU-ADEME			BAU-TIR			GREEN-ADEME			GREEN-TIR		
	2015	2020	2025	2015	2020	2025	2015	2020	2025	2015	2020	2025
1	461	477	473	461	477	473	461	478	431	461	478	431
2	456	435	282	456	435	282	456	451	412	456	451	412
3	451	376	272	451	376	272	451	318	209	451	318	209
4	400	220	236	400	220	236	400	301	75	400	301	75
5	396	209	235	396	209	235	396	226	74	396	226	74
6	379	206	215	379	206	215	379	208	72	379	208	72
7	374	194	215	374	194	209	374	193	71	374	193	71
8	301	185	206	301	185	206	301	180	69	301	180	69
9	209	181	192	209	181	192	209	180	67	209	180	68
10	192	180	181	192	180	181	192	169	49	192	169	49
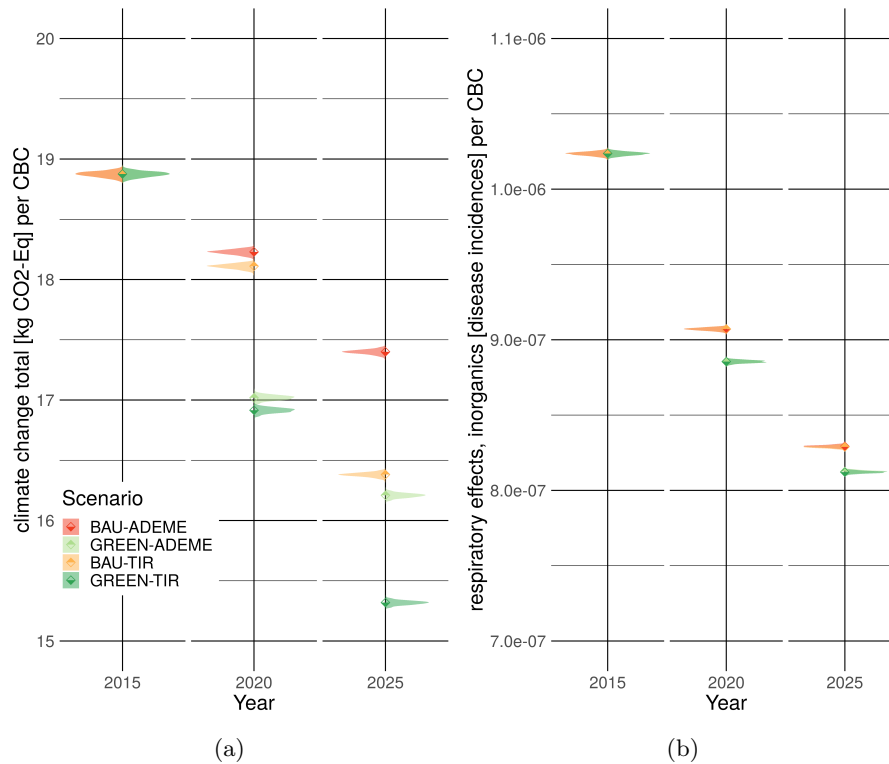
Figure 6.7: Empirical distributions of both QOIs for sub-scheme 1-3. (a) shows *GWP100* per CBC. (b) shows *R-E* per CBC.

chapter 8) where both uncertainties of the LCA and ABM part are simultaneously propagated. In both figures 6.7 (a) and (b) *BAU* scenario distributions are plotted towards the left, while *GREEN* scenario distributions are plotted towards the right. In 2015 all distributions are identical, as all model inputs, parameters and the sets of random number seeds are identical as well.

Figure 6.7 (a) shows the distributions for *GWP100* impacts, with table 6.11 containing the descriptive statistics. In 2020 and 2025 the distributions increasingly diverge with regard to their median values, similar to the results shown in section 6.2 for the nominal concrete instance of the CONNECTING model.

However, while the results of the nominal model in section 6.2 showed that in 2025 the *GREEN-ADEME* has a higher *GWP100* impacts than the *BAU-TIR* scenario, table 6.11 shows a reversed ranking of median values for both scenarios in 2025.

Table 6.11 also shows that mean and median values for all years and scenarios are very close, suggesting that all distributions are close to being symmetrical. CV values in table 6.11 range from 0.109% to 0.127%. The *GREEN* scenarios show slightly higher CV values in 2020 and 2025 compared to the *BAU* scenarios.

Figure 6.7 (b) show the distributions for *R-E* impacts, with table 6.12 presenting the descriptive statistics. While median values of *BAU* and *GREEN* scenarios diverge from each other in 2020 and 2025, *ADEME* and *TIR* scenarios show little divergence, all else equal. As seen for *GWP100* distributions, mean and median values for each distribution are very close, suggesting that all distributions are close to being symmetrical.

CV values in table 6.12 are very close to CV values in table 6.11, suggesting that uncertainty from choice models equally affects both QOIs. CV values also seem to behave similarly across scenarios over time for *R-E* impacts.

Overall, *GWP100* median values are on average 7% higher than results of the nominal model shown in section 6.2 and *R-E* median values are on average 8% higher. This results from the combined effect of choice models being run stochastically.

Besides the effects discussed in section 6.3, compared to sub-scheme 1-3 a higher share of short (i.e., home-work-home) DAPs is present in results of nominal model. Short DAPs with no discretionary activities result in shorter distances travelled over the course of the day and in consequence lower associated environmental impacts. One explanation for the higher share of short DAPs could be that in our nominal model each random choice event results in its most likely outcome, even if probabilities are very close. Short DAPs are the most prominent in the survey data of CBCs and often the most likely outcome chosen by the nominal model, while for the stochastic model there is always a chance of generating a longer DAP.

For sub-scheme 1-3, one can conclude that for *GWP100* the observed spread is often small compared to the difference between scenarios, with the exception of the year 2020, where *ADEME* and *TIR* scenarios overlap to some extent as shown in figure 6.7 (a). For *R-E*, *ADEME* and *TIR* scenarios overlap almost entirely, all else equal, as shown in figure 6.7 (b).

Figures 6.8 and 6.9 show the CV values for all sub-schemes of scheme 1 using Venn diagrams. In addition to previous results of sub-scheme 1-1 (shown in tables 6.1 and 6.2) and sub-scheme 1-3 (shown in tables 6.11 and 6.12) the results of sub-scheme 1-2 where combinations of two choice models are set to their stochastic state are included. When results are encompassed in a rectangle of a specific sub-model, this indicates that the sub-model was set to run stochastically. Figure 5.4 shown in the previous chapter further specifies which elements belong to which sub-scheme. To give a visual impression of the magnitude of the uncertainty observed for each sub-schemes, spheres are used, where the diameter is scaled according to the CV. In addition, a label indicating the CV is provided underneath each sphere.

In figures 6.8 CV values for *GWP100* are shown. A first notable aspect is that the results of

Table 6.11: Descriptive statistics of uncertainty distributions of *GWP100* scores in [kg CO2-eq] for sub-scheme 1-3.

	BAU-ADEME			BAU-TIR			GREEN-ADEME			GREEN-TIR		
	2015	2020	2025	2015	2020	2025	2015	2020	2025	2015	2020	2025
Median	18.9	18.2	17.4	18.9	18.1	16.4	18.9	17.0	16.2	18.9	16.9	15.3
Mean	18.9	18.2	17.4	18.9	18.1	16.4	18.9	17.0	16.2	18.9	16.9	15.3
SD	0.023	0.021	0.019	0.023	0.020	0.018	0.023	0.022	0.019	0.023	0.021	0.018
CV [%]	0.124	0.113	0.109	0.124	0.113	0.107	0.124	0.127	0.120	0.124	0.126	0.117

Table 6.12: Descriptive statistics of uncertainty distributions of *R-E* scores in 10^{-7} [disease incidences] for sub-scheme 1-3.

	BAU-ADEME			BAU-TIR			GREEN-ADEME			GREEN-TIR		
	2015	2020	2025	2015	2020	2025	2015	2020	2025	2015	2020	2025
Median	10.2	9.1	8.3	10.2	9.1	8.3	10.2	8.9	8.1	10.2	8.9	8.1
Mean	10.2	9.1	8.3	10.2	9.1	8.3	10.2	8.9	8.1	10.2	8.9	8.1
SD	0.013	0.010	0.008	0.013	0.010	0.008	0.013	0.010	0.008	0.013	0.010	0.008
CV [%]	0.123	0.109	0.101	0.123	0.109	0.101	0.123	0.114	0.104	0.123	0.114	0.104
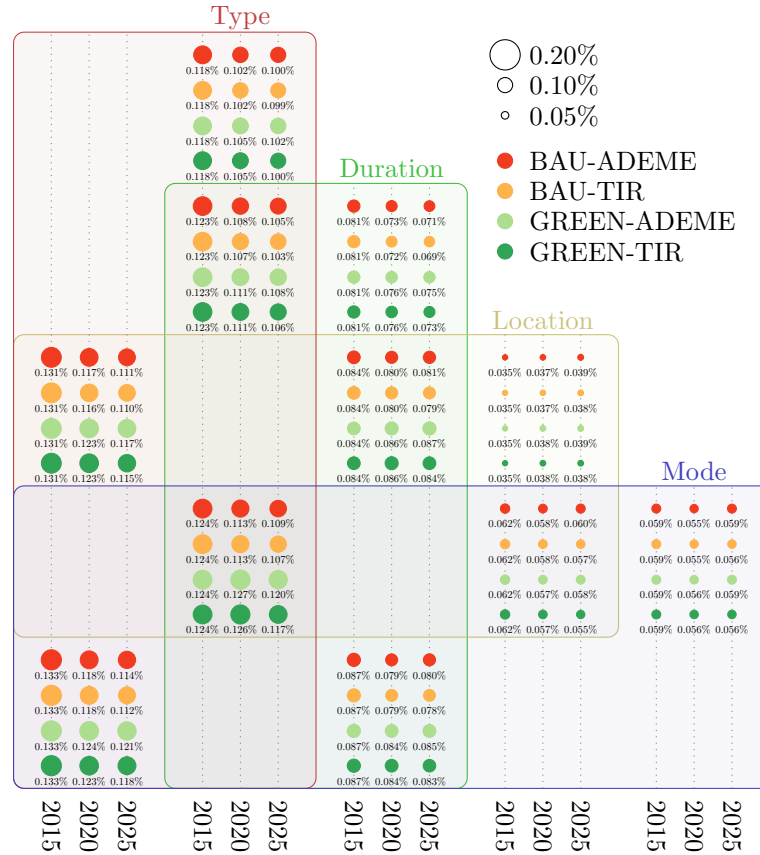
Figure 6.8: Venn diagram showing the CV for *GWP100*, for sub-scheme 1-1, 1-2 and 1-3.

sub-scheme 1-3 suggest that uncertainty stemming from individual choice models is not additive, but that there are damping effects when all choice models are set to run stochastically. Specifically, the sum of CV (or SD) values of sub-scheme 1-1 of the four individual choice models, is more than twice as large as the CV (or SD) values of sub-scheme 1-3 where all choice models are simultaneously set to run stochastically.

For all results of sub-scheme 1-2 similar conclusions can be drawn. Taking the sub-scheme 1-2 where the activity type and duration models are set to run stochastically as an example, CV values in figures 6.8 are only marginally larger than for sub-scheme 1-1 where only the activity type model is set to run stochastically. In some cases of sub-scheme 1-2 (e.g., when the activity type and mode choice models are set to run stochastically) CV values are even higher than those of sub-scheme 1-3 when all choice models are set to run stochastically.

While such damping effects have been observed for four-step models in the past, this is the first time a similar effect has been observed for ABMs of travel demand.

The results for the second QOI, *R-E*, in figure 6.9 are very similar to those of *GWP100*.

6.4.2 Convergence

Next, the convergence of the CV values is investigated for both QOIs focussing on sub-scheme 1-3. The CV values are presented as a function of the number of model runs in figure 6.10. After
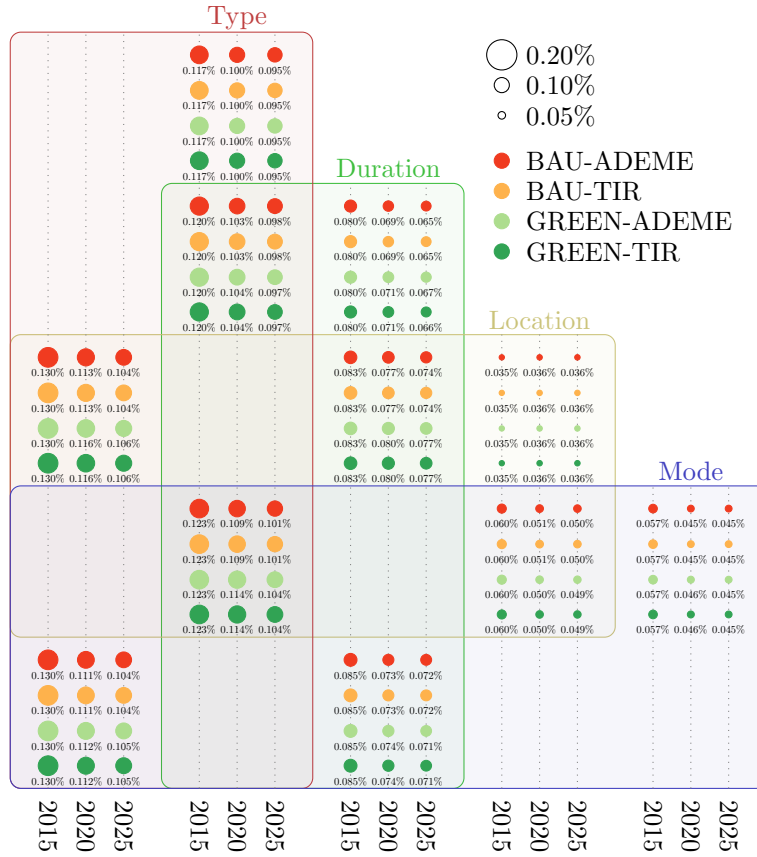
Figure 6.9: Venn diagram showing the CV for *R-E*, for sub-scheme 1-1, 1-2 and 1-3.

500 model runs, CV values range from 0.109%-0.127% and 0.101%-0123% for *GWP100* and *R-E* respectively, as previously shown in tables 6.11-6.12.

For all scenarios shown in figure 6.10, CV values stabilise quickly after only a couple of hundred model runs, showing little fluctuation and no strong upward or downward trends afterwards. One can see the effect of the seed factory, which keeps seeds coherent across scenarios and years, resulting in a similar shape of all curves when comparing them for one QOI.

Table 6.13 shows the lowest number of model runs required to reach convergence for *GWP100*, where thresholds for 1% up to 10% are used. For a threshold of 5% convergences is reached for at most 193 model runs across scenarios, thus satisfying the convergence criteria.

Table 6.14 shows the lowest number of model runs required to reach convergence for *R-E*. For a threshold of 5% convergences is reached for 113 (i.e., *GREEN-ADEME* and *GREEN-TIR* in 2020) up to 297 model runs (i.e., *BAU-ADEME* and *BAU-TIR* in 2025). While for the *GREEN* scenarios, we can assert that CV values have converged, for the *BAU* scenarios in 2020 and 2025 our criteria are not satisfied. However, due to the high computational burden of the ABM part of CONNECTING, increasing *N* is impractical.
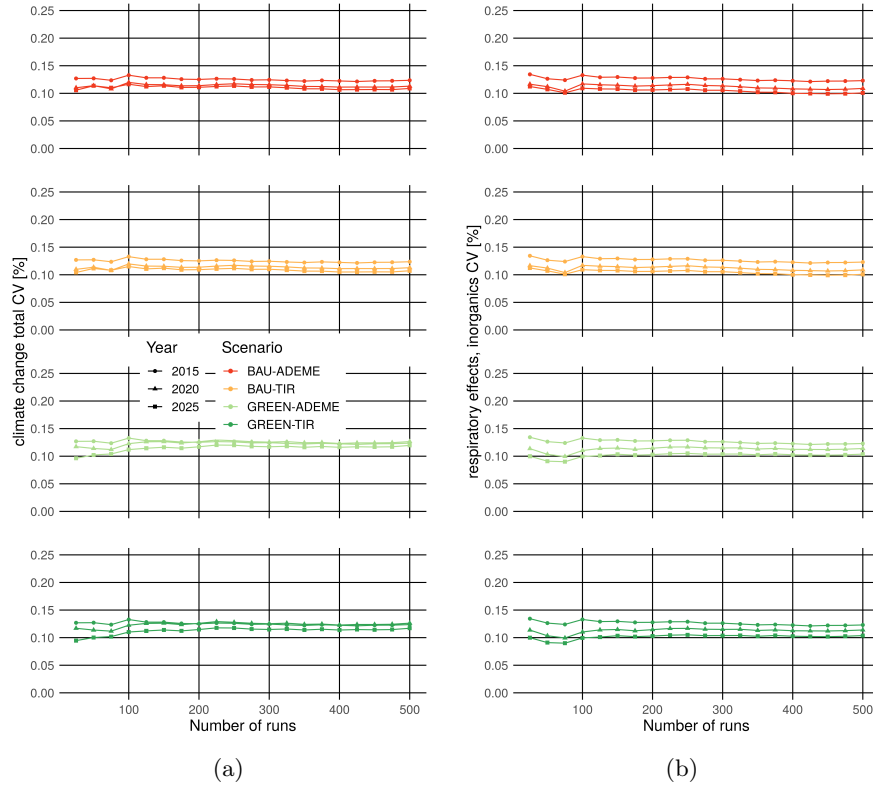
Figure 6.10: CV as a function of the number of model runs for sub-scheme 1-3. (a) shows the CV values for *GWP100*. (b) shows the CV values for *R-E*.

6.4.3   Further insights

Given the results of this chapter, we can now proceed by evaluating how much the simulation error stemming from the stochastic choice models in the ABM could potentially affect policy choices given the four alternatives. To this end we compute the three measures introduced in

Table 6.13: Convergence of *GWP100* CV values for thresholds of 1-10% for sub-scheme 1-3.

T (%)	*BAU-ADEME*			*BAU-TIR*			*GREEN-ADEME*			*GREEN-TIR*		
	2015	2020	2025	2015	2020	2025	2015	2020	2025	2015	2020	2025
1	461	476	476	461	476	476	461	476	477	461	476	476
2	444	440	475	444	440	475	444	474	476	444	474	476
3	215	267	267	215	267	267	215	414	414	215	414	414
4	156	256	256	156	256	255	156	114	193	156	114	193
5	128	127	154	128	127	154	128	90	193	128	90	193
6	119	101	102	119	101	104	119	90	114	119	90	114
7	104	32	99	104	32	101	104	86	114	104	86	114
8	19	16	16	19	16	16	19	86	114	19	86	114
9	16	16	16	16	16	16	16	85	90	16	85	90
10	16	16	16	16	16	16	16	85	88	16	85	88
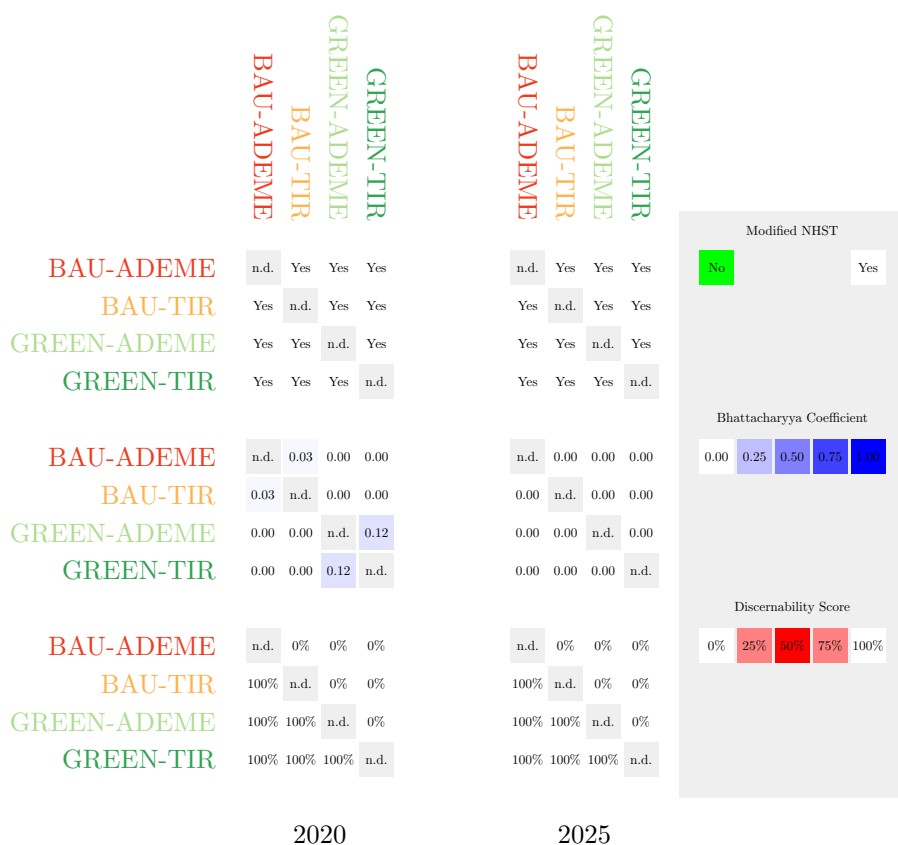
Figure 6.11: Uncertainty communication measures for *GWP100* for 2020 and 2025 are presented for sub-scheme 1-3. The presentation has been adapted from Mendoza Beltran et al. (2018a).

section 5.5. Figures 6.11-6.12 show the results for sub-scheme 1-3. These measures and their representation is based largely on Mendoza Beltran et al. (2018a).

Table 6.14: Convergence of *R-E* CV values for thresholds of 1-10% for sub-scheme 1-3.

T (%)	BAU-ADEME			BAU-TIR			GREEN-ADEME			GREEN-TIR		
	2015	2020	2025	2015	2020	2025	2015	2020	2025	2015	2020	2025
1	461	476	476	461	476	476	461	476	476	461	476	476
2	317	461	449	317	461	449	317	440	457	317	440	457
3	271	324	326	271	324	326	271	114	193	271	114	193
4	264	307	310	264	307	310	264	114	114	264	114	114
5	224	275	297	224	275	297	224	113	114	224	113	114
6	155	260	260	155	260	260	155	90	114	155	90	114
7	137	255	254	137	255	254	137	86	90	137	86	90
8	101	129	136	101	129	136	101	86	90	101	86	90
9	34	19	127	34	19	127	34	86	86	34	86	86
10	25	16	35	25	16	35	25	85	86	25	85	86

Figure 6.12: Uncertainty communication measures for *R-E* for 2020 and 2025 are presented for sub-scheme 1-3.

In the upper part of the figures 6.11-6.12 the results of the modified NHST are shown. For each years, a matrix shows the comparison of each scenario (row) against every other scenario (column), with the diagonal cells remaining empty (n.d.) as scenarios are not compared against themselves. The modified NHST allows to assert whether or not differences in mean values of two scenarios are statistically significant. Specifically, if one can reject the null hypothesis (that mean values are the same) for a pair-wise comparison in figure 6.11, the matrix will state "Yes", otherwise the cell will state "No". For both QOIs one can always assert the scenario mean results are significantly different.

Next in the middle part of the figures 6.11-6.12 the Bhattacharyya coefficients are shown, representing the overlap of distributions, where a coefficient of 0 means that the distributions do not overlap at all, while a coefficient of 1 means that they overlap completely. While for *GWP100* (figure 6.11) in 2020 only the *GREEN-ADEME* and *GREEN-TIR* show a slight overlap, for *R-E* (figure 6.12) *ADEME* and *TIR* scenarios completely overlap, all else equal, showing scores of 1 or close to 1.

Finally, the discernibility scores are shown in the bottom part of both figures. This measures builds on a pair-wise comparison per MC run expressing the percentage of runs for which a scenario (row) has lower results than another scenario (column). Discernibility scores can range from 0% to 100%. For both QOIs results are clear cut, where *GREEN* scenarios have lower

impacts than *BAU* scenarios for 100% of model runs and *TIR* scenarios have lower impacts than *ADEME* scenarios for 100% of model runs, all else equal.

These measures are complementary, capturing different aspects of uncertainty relevant to decision making. The modified NHST allows to assess the statistical significance of the difference of mean values. The Bhattacharyya coefficients captures only the extent of the difference of two distributions. Finally, the discernibility score complements both measures by indicating the consistency of one scenario showing lower impacts than another scenario.

6.5 Summary

In this chapter the results of scheme 1, investigating the uncertainty of the ABM part of CONNECTING have been presented. Three sub-schemes of scheme 1 were defined in chapter 5 with sub-scheme 1-1 propagating the uncertainty from individual choices models (i.e., activity type, duration, location and mode choice). For sub-scheme 1-2 the simultaneous propagation of uncertainty from two choice models is investigated, with the remaining choice models set to their deterministic state (always resulting in the most likely choice for each individual). Finally sub-scheme 1-3 propagated uncertainty from all four choice models simultaneously.

There are several notable aspects of the results of sub-scheme 1-1. As a first, running choice models stochastically can lead to a shift in median (or mean) values compared to the results of the nominal concrete instance. This has been observed for all four choice models. A second notable aspect is that, with regard to the QOIs chosen, the level of uncertainty observed varies across choice models, with the activity type model showing the highest level of uncertainty and the location model showing the lowest level of uncertainty. A third notable aspect is that for the present case study both SD and CV values decrease for later simulation years.

The most notable aspect of the results of sub-scheme 1-2 (confirmed by the results of scheme 1-3) is that uncertainty of individual choice models is not additive, where running two or more choice models stochastically does not lead to the CV (or SD) values to be equal to the sum of the CV (or SD) values of sub-schemes where the same individual choice models are set to run stochastically. There seem to be damping effects for all combinations of choice models.

Finally, the most notable aspect of the results of sub-scheme 1-3 is the low overall level of uncertainty observed for the ABM part of CONNECTING. CV values are consistently much lower that one percentage point and uncertainty measures relevant for decision making (i.e., the modified NHST, the Bhattacharyya coefficient and the discernibility score) show that in most cases (with the exception of *R-E* impacts of *ADEME* and *TIR* scenarios) clear conclusions can be drawn.

Chapter 7

Results of scheme 2 - LCA parameter uncertainty

7.1 Introduction

Following the results of scheme 1 presented in chapter 6, the present chapter will present the results of scheme 2 (with its four sub-schemes), which aims at propagating uncertainty stemming from the LCA part of CONNECTING.

While various uncertainty locations were classified for LCA in chapter 3, parameter uncertainty showed to be the most addressed location in the quantitative review. For this reason it was decided to focus on this location, more specifically on measured parameters present in the technosphere and biosphere matrices.

To characterise parameter uncertainty in the LCA part of CONNECTING, the so-called pedigree approach is applied. In literature, this approach often builds on expert based uncertainty factors to derived uncertainty distributions based on DQIs (see chapter 5 for a more detailed description of the methodology). More recently however, empirically based uncertainty factors have been published for various process types (e.g., transport, combustion, etc.) to update these expert based factors (Ciroth et al., 2013; Muller et al., 2016). The influence of using both types of factors will be tested in this chapter.

The propagation of LCA parameter uncertainty builds on the results of the nominal concrete instance of the ABM presented in chapter 6. Building on the findings of chapter 3, two types of sampling are employed: sampling where tailpipe emissions are independently sampled from fuel consumption (hereafter referred to a *independent sampling*) and sampling where fuel dependent tailpipe emissions (e.g., carbon dioxide) are derived from the sampled fuel consumption values (hereafter referred to a *dependent sampling*).

The four sub-schemes of scheme 2 result from combining different uncertainty factors and sampling schemes. The sub-scheme 2-1 is uses the expert uncertainty factors from ecoinvent shown in tables 5.2 and 5.1, where all technosphere and biosphere exchanges are sampled independently. Sub-scheme 2-2 employs independent sampling, yet uses the expert uncertainty factors shown in tables 5.3 and 5.4 to derive distributions. Sub-scheme 2-3 employs dependent sampling while using expert uncertainty factors. Finally, sub-scheme 2-4 employs dependent sampling while using empirical uncertainty factors. Figure 5.6 summarises the combinations of sampling and uncertainty factors applied for the different sub-schemes. The number of runs for each sub-scheme is chosen to be 1000. Across all sub-schemes the same random seeds are used for each LCI

exchange. This allows to compare results across scenarios and years similar to the random seed factory used for scheme 1.

Similar to the previous chapter, the focus is set on uncertainty of system level outputs, namely the QOIs quantifying climate change related impacts (*GWP100*) and respiratory effects related impacts (*R-E*) for which uncertainty will be quantified and communicated as outlined in section 5.5.

In the following sections 7.2-7.5 will present the results for the four propagation sub-schemes of scheme 2 before a short summary is provided in section 7.6.

7.2   Sub-scheme 2-1

First, results of sub-scheme 2-1 are presented. These can be considered a reference for subsequent results, as they build on the widely applied expert uncertainty factors and independent sampling applied for most studies (as identified in chapter 3). Section 7.2.1 presents the output distributions and statistics, section 7.2.2 presents the convergence of CV values and finally section 7.2.3 presents the uncertainty communication measures. This section structure will be retained for subsequent sub-schemes.

7.2.1   Distributions

Figure 7.1 shows the empirical output distributions for all scenarios for sub-scheme 2-1. As seen for scheme 1, *BAU* scenario distributions are plotted towards the left while *GREEN* scenario distributions are plotted towards the left. In 2015 all distributions (and median values) are identical, as all seeds and all model inputs and parameters are identical. For later years the distributions and median values diverge. However, in contrast to results of scheme 1, figure 7.1 shows that there is substantial overlap of distributions in 2020 and 2025.

Table 7.1 provides the descriptive statistics for *GWP100* distributions. One can see that mean values are systematically larger than median values, indicating that distributions are right skewed. This can also be seen visually in figure 7.1 (a), as distributions have a so-called "fat" right tail. One reason for this could be that many parameters in LCI databases are modelled using log-normal distributions, which are right skewed. CV values range from 5.49%-6.15% and tend to decrease in 2020 (compared to 2015) before increasing again in 2025. SD values show a similar behaviour for *ADEME* scenarios, while decreasing steadily for *TIR* scenarios.

Table 7.2 provides the descriptive statistics for *R-E* distributions. Again, mean values are systematically larger than median values indicating that distributions are right skewed. CV values are larger than for *GWP100* ranging from 19.3%-21.8% and increase steadily for later study years. However, this increase can be explained by the decreasing mean values, as the CV is the ratio of the SD and the mean. While the SD values slightly decrease with time, so do the mean values.

Table 7.1: Descriptive statistics of uncertainty distributions of *GWP100* scores in [kg CO2-eq] for sub-scheme 2-1.

|	BAU-ADEME			BAU-TIR			GREEN-ADEME			GREEN-TIR		
	2015	2020	2025	2015	2020	2025	2015	2020	2025	2015	2020	2025
Median	19.2	18.6	17.6	19.2	18.5	16.7	19.2	17.7	16.7	19.2	17.6	15.9
Mean	19.3	18.7	17.8	19.3	18.6	16.8	19.3	17.7	16.8	19.3	17.6	16.0
SD	1.11	1.05	1.09	1.11	1.04	1.01	1.11	0.98	1.01	1.11	0.97	0.93
CV [%]	5.77	5.64	6.15	5.77	5.62	5.98	5.77	5.51	5.98	5.77	5.49	5.82
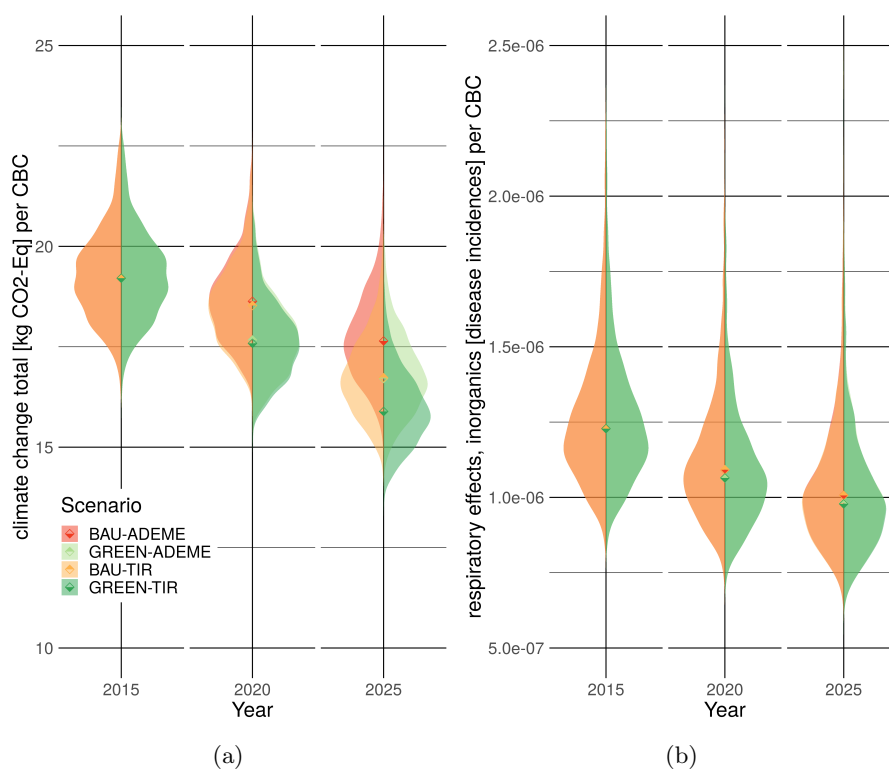
Figure 7.1: Empirical distributions for both QOIs for sub-scheme 2-1. (a) shows *GWP100* per CBC. (b) shows *R-E* per CBC.

While in figure 6.7 (a) distributions of *GWP100* are diverging somewhat for later years, in figure 6.7 (b) the differences in median values of *R-E* among all scenarios seem small compared to the observed spread. Uncertainty communication measures presented in section 7.2.3 will provide further insights on scenario comparison.

7.2.2 Convergence

Next, the convergence of the CV values is investigated for both QOIs and for all scenarios and years. In contrast to what was observed for uncertainty stemming from ABM sub-models,

Table 7.2: Descriptive statistics of uncertainty distributions of *R-E* scores in 10^{-7} [disease incidences] for sub-scheme 2-1.

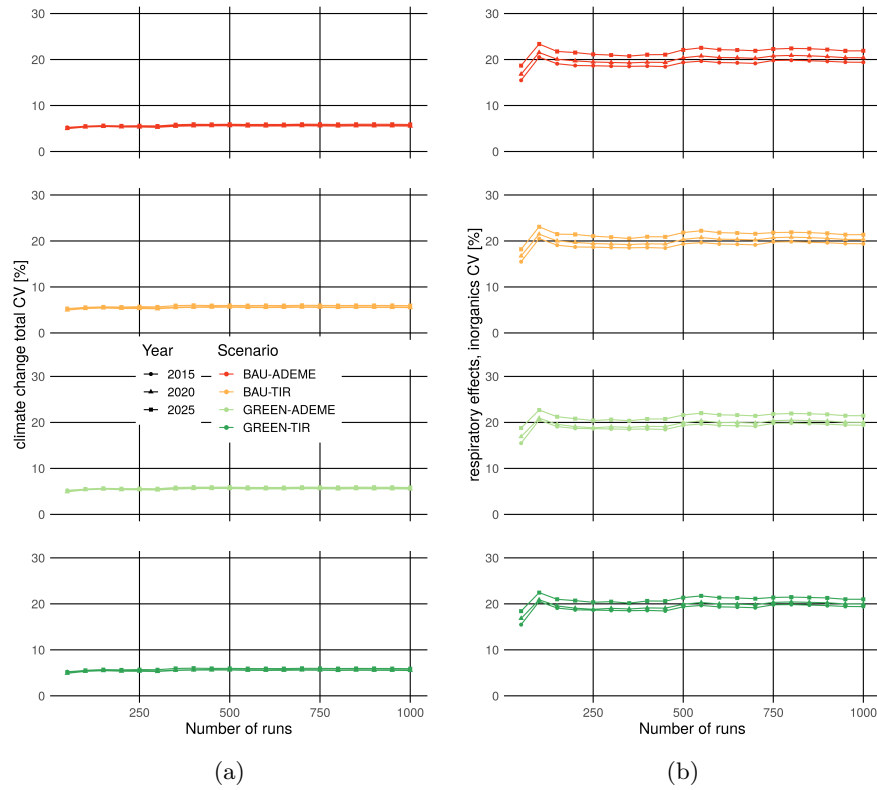|	*BAU-ADEME*			*BAU-TIR*			*GREEN-ADEME*			*GREEN-TIR*		
	2015	2020	2025	2015	2020	2025	2015	2020	2025	2015	2020	2025
Median	12.3	10.9	10.1	12.3	10.9	10.1	12.3	10.6	9.8	12.3	10.6	9.8
Mean	12.8	11.4	10.5	12.8	11.4	10.5	12.8	11.1	10.2	12.8	11.1	10.2
SD	2.46	2.32	2.30	2.46	2.31	2.23	2.46	2.20	2.18	2.46	2.20	2.12
CV [%]	19.3	20.4	21.8	19.3	20.3	21.3	19.3	19.9	21.3	19.3	19.8	20.8

Figure 7.2: CV as a function of the number of model runs for sub-scheme 2-1. (a) shows the CV values for *GWP100*. (b) shows the CV values for *R-E*.

both QOIs show different levels of uncertainty with *GWP100* showing CV values around 6% after 1000 model runs, while CV values for *R-E* are around 20% after 1000 model runs.

    CV values of *GWP100* in figure 7.2 (a) stabilise after a couple of hundred model runs, showing little fluctuation and no strong upward or downward trends afterwards. However, CV values of *R-E* in figure 7.2 (b) are still fluctuating somewhat after 500 and even 750 model runs. For both QOIs one can see that curves have similar shapes resulting from controlling seeds across years and scenarios.

    These visual impressions are confirmed when computing the lowest number of model runs required to reach convergence for thresholds from 1% up to 10%, shown in table 7.3 for *GWP100*. For a threshold of, e.g., 10% convergence is reached for at most 141 model runs across scenarios. For the more rigorous threshold of 5% chosen for this thesis, convergences reached for at most 341 model runs across scenarios.

    Table 7.4 shows the lowest number of model runs required to reach convergence for *R-E*. For a threshold of 10% convergence is reached for at most 118 model runs across scenarios. For the more rigorous threshold of 5% convergences is reached for at most 472 model runs. We can thus assert that the convergence criteria set for this thesis (i.e., reaching 5% threshold within $N/2$ model runs) are reached for both QOIs.

7.2.3 Further insights

We can now proceed to evaluating how much the uncertainty stemming from the measured parameters of the LCA affect policy choices given the four scenarios. To this end we compute the three uncertainty communication measures introduced in chapter 5 in figures 7.3-7.4, for sub-scheme 2-1.

Looking at the modified NHST, we can see that mean scenario values are significantly different with the exception of *GWP100* for *BAU-TIR* and *GREEN-ADEME* in 2025 (highlighted green in figure 7.3). While for results of scheme 1 in chapter 6 the modified NHST always allowed to assert that mean values are significantly different, this is thus not the case for scheme 2-1.

The Bhattacharyya Coefficient in the middle parts of figures 7.3-7.4 shows that there is a strong overlap of between output distributions. This is especially true for *R-E* (showing values close to one), but also for *GWP100* (showing values consistently higher than 0.60). Overall the differences between *BAU* and *GREEN* scenarios are larger than the differences between *ADEME* and *TIR* scenarios, all else equal.

Finally, discernibility scores complete the comparison, where for *GWP100* the results show that *BAU-TIR* and *GREEN-ADEME* in 2025 are almost indistinguishable (confirming results of the modified NHST). For *R-E* discernibility scores complement the modified NHST, providing further detail. When comparing *TIR* to *ADEME* scenarios (all else equal), the higher shares of

Table 7.3: Convergence for thresholds of 1-10% for *GWP100*, for sub-scheme 2-1.

	BAU-ADEME			BAU-TIR			GREEN-ADEME			GREEN-TIR		
	2015	2020	2025	2015	2020	2025	2015	2020	2025	2015	2020	2025
1	935	942	946	935	941	941	935	941	945	935	940	940
2	302	345	621	302	345	464	302	345	624	302	345	624
3	220	338	371	220	338	345	220	338	381	220	338	371
4	220	220	345	220	220	345	220	337	345	220	317	345
5	127	141	341	127	141	337	127	141	341	127	141	338
6	112	136	317	112	136	220	112	136	337	112	136	220
7	64	127	178	64	127	178	64	127	176	64	127	172
8	63	127	172	63	127	171	63	127	172	63	112	171
9	60	76	141	60	76	141	60	76	141	60	76	141
10	59	76	141	59	76	141	59	76	141	59	76	141

Table 7.4: Convergence for thresholds of 1-10% for *R-E*, for sub-scheme 2-1.

	BAU-ADEME			BAU-TIR			GREEN-ADEME			GREEN-TIR		
	2015	2020	2025	2015	2020	2025	2015	2020	2025	2015	2020	2025
1	905	909	918	905	909	919	905	918	919	905	924	924
2	843	856	858	843	856	859	843	843	856	843	843	856
3	777	771	769	777	771	770	777	766	765	777	766	765
4	472	472	472	472	472	550	472	472	470	472	472	363
5	472	472	363	472	472	344	472	470	363	472	470	344
6	344	359	344	344	344	133	344	363	344	344	359	293
7	83	344	122	83	344	130	83	344	293	83	344	124
8	81	81	116	81	82	124	81	293	84	81	81	122
9	81	81	84	81	81	122	81	81	82	81	81	118
10	81	81	82	81	81	118	81	81	81	81	81	94

Figure 7.3: Uncertainty communication measures for *GWP100* for 2020 and 2025 are presented for sub-scheme 2-1.

EVs in the car fleet cause a decrease in *R-E* impacts for around 65% of model runs, with 35% of model runs suggesting the opposite. Comparisons of *BAU* and *GREEN* scenarios show higher disparities, with *GREEN* scenarios showing lower *R-E* impacts in 84%-90% of model runs.

As seen for scheme 1, the complementarity of the three measures is shown, where the modified NHST allows to identify that in the long term, there is no significant difference between *BAU-TIR* and *GREEN-ADEME* with regard to *GWP100*. The Bhattacharyya coefficient shows that differences of a somewhat larger extent can only be observed when comparing *BAU-ADEME* to the *GREEN-TIR* scenario (at least for *GWP100*). Finally the discernibility scores confirm the results of the modified NHST for *GWP100*, but also highlight that no scenario has consistently lower or higher *R-E* impacts than any given competing scenario.

7.3 Sub-scheme 2-2

Sub-scheme 2-2 presented in this section focusses on the influence of using the updated empirical uncertainty factors published by Ciroth et al. (2013) and Muller et al. (2016), while still independently sampling fuel consumptions and tailpipe emissions.
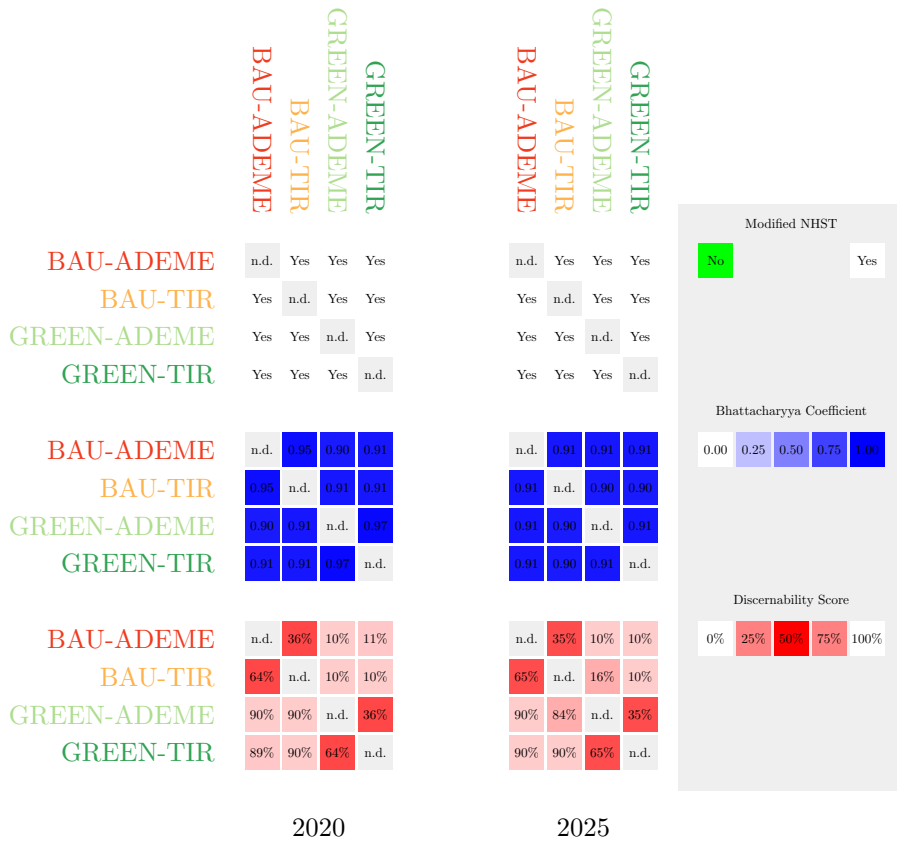
Figure 7.4: Uncertainty communication measures for *R-E* for 2020 and 2025 are presented for sub-scheme 2-1.

7.3.1 Distributions

Figure 7.5 shows the empirical output distributions of all scenarios for sub-scheme 2-2. Visually, distributions are similar to those of sub-scheme 2-1 shown in figure 7.1. For both QOIs prior to 2025 distributions overlap significantly. In 2025, at least for *GWP100* in figure 7.5 (a), one can see distributions diverge somewhat.

Table 7.5 provides the descriptive statistics for *GWP100* distributions. Similar to what has been noted for sub-scheme 1-2, mean values are systematically larger than median values indicating that distributions are right skewed. CV values range from 6.00%-6.87% thus showing a slightly higher level of uncertainty compared to sub-scheme 2-1 in table 7.1.

Table 7.6 provides the descriptive statistics for *R-E* distributions. Distributions are right skewed, as seen before, while CV values ranging from 19.4%-21.9%. Sub-scheme 2-2 thus shows higher CV (and SD) values for *R-E* compared to sub-scheme 2-1 in table 7.2.

7.3.2 Convergence

Next, the convergence of sub-scheme 2-2 is presented. Figure 7.6 shows CV values as a function of model runs. Visually there are no notable differences to results of sub-scheme 2-1 in figure 7.2.
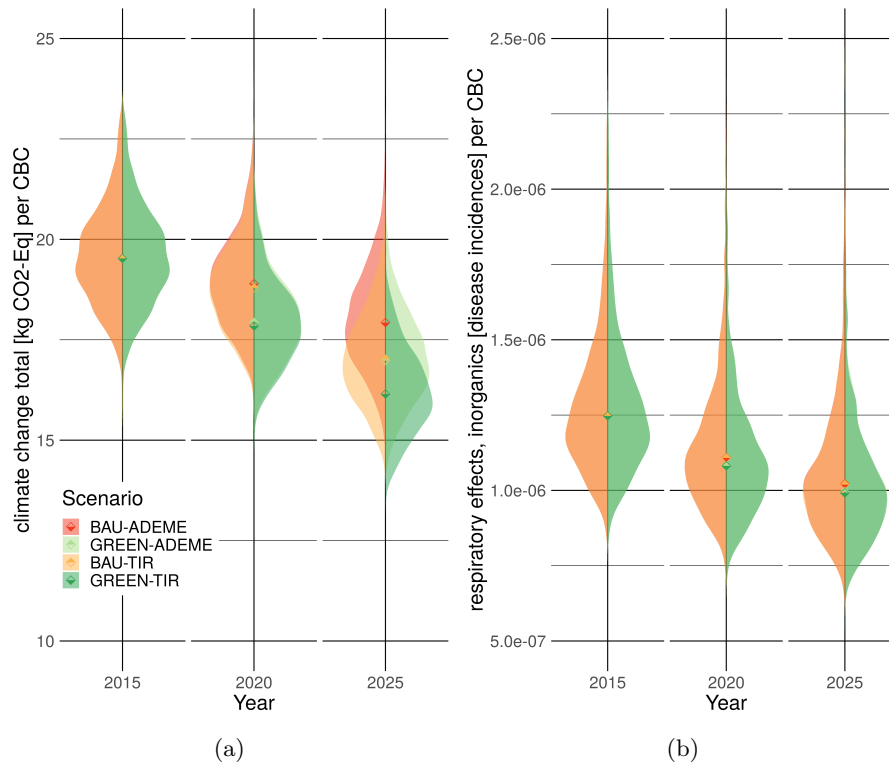
Figure 7.5: Empirical distributions for both QOIs for sub-scheme 2-2. (a) shows *GWP100* per CBC. (b) shows *R-E* per CBC.

The lowest number of model runs required to reach convergence for sub-scheme 2-2 is shown in tables 7.7-7.8. Comparing these values to those of sub-scheme 2-1, for a threshold of 5%, convergence is reached slightly faster for sub-scheme 2-2. However for most scenarios differences are small.

7.3.3   Further insights

Finally, the three uncertainty communication measures are computed for sub-scheme 2-2, shown in figures 7.7-7.8.

Table 7.5: Descriptive statistics of uncertainty distributions of *GWP100* scores in [kg CO2-eq] for sub-scheme 2-2.

	BAU-ADEME			*BAU-TIR*			*GREEN-ADEME*			*GREEN-TIR*		
	2015	2020	2025	2015	2020	2025	2015	2020	2025	2015	2020	2025
Median	19.5	18.9	17.9	19.5	18.8	17.0	19.5	17.9	17.0	19.5	17.8	16.1
Mean	19.6	19.0	18.0	19.6	18.9	17.1	19.6	18.0	17.1	19.6	17.9	16.2
SD	1.24	1.16	1.24	1.24	1.15	1.16	1.24	1.08	1.15	1.24	1.07	1.08
CV [%]	6.31	6.10	6.87	6.31	6.08	6.77	6.31	6.02	6.73	6.31	6.00	6.63
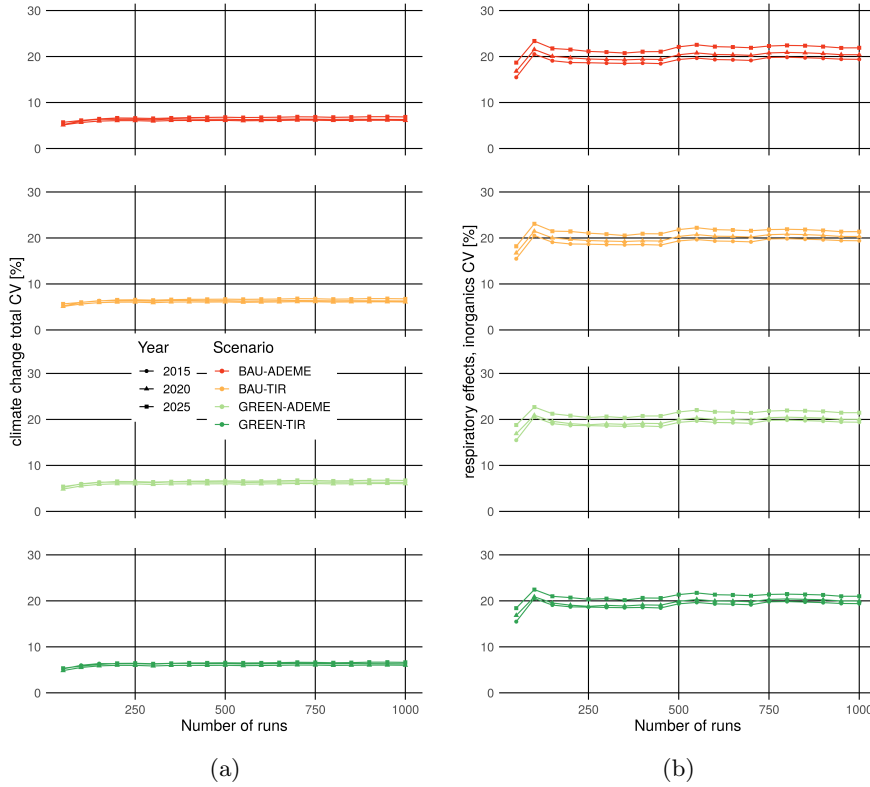
Figure 7.6: CV as a function of the number of model runs for sub-scheme 2-2. (a) shows the CV values for *GWP100*. (b) shows the CV values for *R-E*.

Uncertainty communication measures for *GWP100* in figure 7.7 show no notable differences to the results of sub-scheme 2-1 shown figure 7.3. While CV (and SD) values have increased slightly for sub-scheme 2-2, the modified NHST shows identical results. The Bhattacharyya Coefficients in the middle part of figure 7.7 show that the distribution overlap has increased for sub-scheme 2-2 compared to sub-scheme 2-1. Changes in discernibility scores are very small, showing only a slight change when comparing *BAU-TIR* and *GREEN-ADEME* in 2025.

Uncertainty communication measures for *R-E* in figure 7.8 show that there are a few notable differences to the results of sub-scheme 2-1 shown figure 7.4. The most significant difference can be observed for the modified NHST. While for sub-scheme 2-1 mean scenario values are

Table 7.6: Descriptive statistics of uncertainty distributions of *R-E* scores in 10^{-7} [disease incidences] for sub-scheme 2-2.

	BAU-ADEME			*BAU-TIR*			*GREEN-ADEME*			*GREEN-TIR*		
	2015	2020	2025	2015	2020	2025	2015	2020	2025	2015	2020	2025
Median	12.5	11.1	10.2	12.5	11.1	10.2	12.5	10.8	10.0	12.5	10.8	9.9
Mean	12.9	11.5	10.7	12.9	11.5	10.6	12.9	11.2	10.4	12.9	11.2	10.3
SD	2.51	2.35	2.33	2.51	2.34	2.27	2.51	2.25	2.22	2.51	2.24	2.17
CV [%]	19.4	20.4	21.9	19.4	20.3	21.4	19.4	20.0	21.5	19.4	20.0	21.0

always significantly different from each other, for sub-scheme 2-2 the null hypothesis is rejected when comparing *ADEME* and *TIR* scenarios, all else equal. The results of the Bhattacharyya Coefficients are only marginally different from results shown for sub-scheme 2-1. Discernibility scores are consistent with the shift observed for the modified NHST, where for comparisons of *ADEME* and *TIR* scenarios, scores move closer to 50%.

Comparing results of sub-schemes 2-1 and 2-2 shows that using different uncertainty factors can lead to changes in the observed model output uncertainty. For the CONNECTING case study results, updated empirical uncertainty factors increase uncertainty in the model outputs. This increase in model output uncertainty can alter conclusions based on uncertainty communication measures. Specifically, while we can assert for sub-scheme 2-1 that *TIR* scenarios lead to statistically significant lower *R-E* impacts than *ADEME* scenarios, all else equal, this is not the case for sub-scheme 2-2.

Table 7.7: Convergence for thresholds of 1-10% for *GWP100*, for sub-scheme 2-2.

	BAU-ADEME			BAU-TIR			GREEN-ADEME			GREEN-TIR		
	2015	2020	2025	2015	2020	2025	2015	2020	2025	2015	2020	2025
1	881	941	945	881	940	940	881	938	941	881	937	937
2	390	338	624	390	338	549	390	338	625	390	338	624
3	136	317	381	136	317	345	136	317	383	136	317	374
4	127	141	345	127	141	338	127	141	371	127	141	341
5	114	136	338	114	136	317	114	140	338	114	136	317
6	112	136	178	112	131	176	112	136	317	112	136	176
7	76	127	172	76	127	172	76	127	172	76	127	172
8	76	77	145	76	77	144	76	113	147	76	112	145
9	70	76	141	70	76	140	70	77	141	70	77	141
10	63	76	134	63	76	134	63	77	136	63	77	136

Table 7.8: Convergence for thresholds of 1-10% for *R-E*, for sub-scheme 2-2.

	BAU-ADEME			BAU-TIR			GREEN-ADEME			GREEN-TIR		
	2015	2020	2025	2015	2020	2025	2015	2020	2025	2015	2020	2025
1	905	917	919	905	918	920	905	924	924	905	924	925
2	842	856	859	842	856	859	842	843	856	842	842	856
3	771	771	770	771	771	770	771	766	765	771	766	764
4	472	472	470	472	472	550	472	472	364	472	472	363
5	470	472	363	470	470	130	470	470	363	470	363	293
6	344	344	344	344	344	124	344	344	344	344	344	122
7	81	344	116	81	81	121	81	344	293	81	293	118
8	81	81	82	81	81	117	81	81	81	81	81	82
9	81	81	81	81	81	82	81	81	81	81	81	81
10	81	81	81	81	81	81	81	81	81	81	81	81

Figure 7.7: Uncertainty communication measures for *GWP100* for 2020 and 2025 are presented for sub-scheme 2-2.
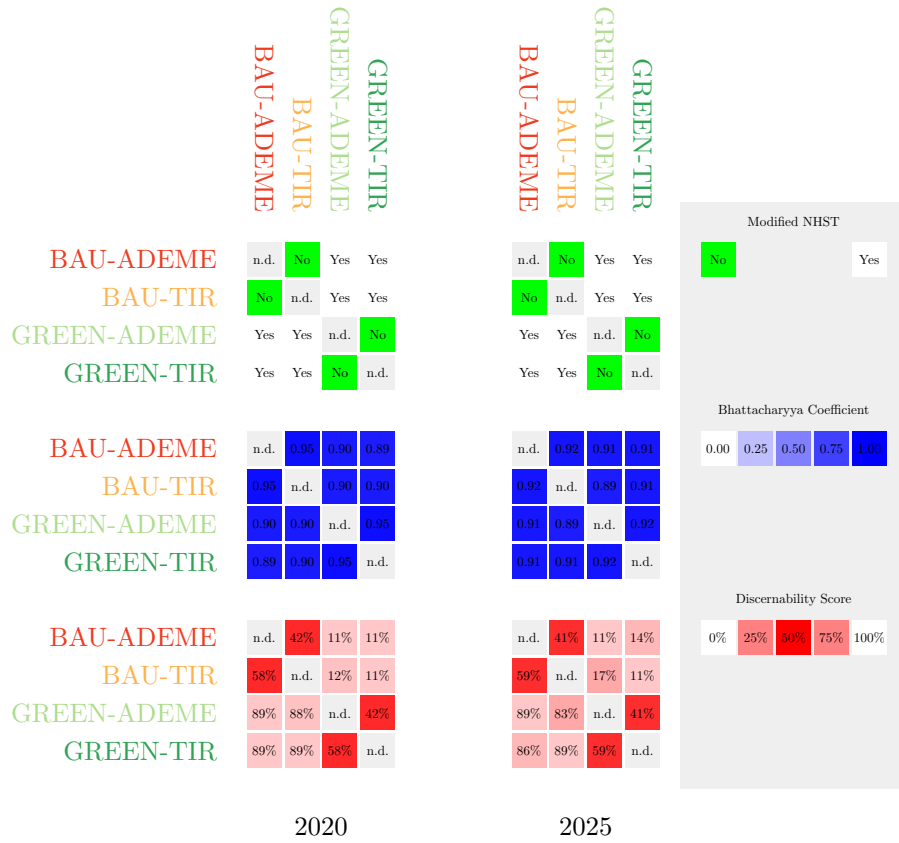
Figure 7.8: Uncertainty communication measures for *R-E* for 2020 and 2025 are presented for sub-scheme 2-2.
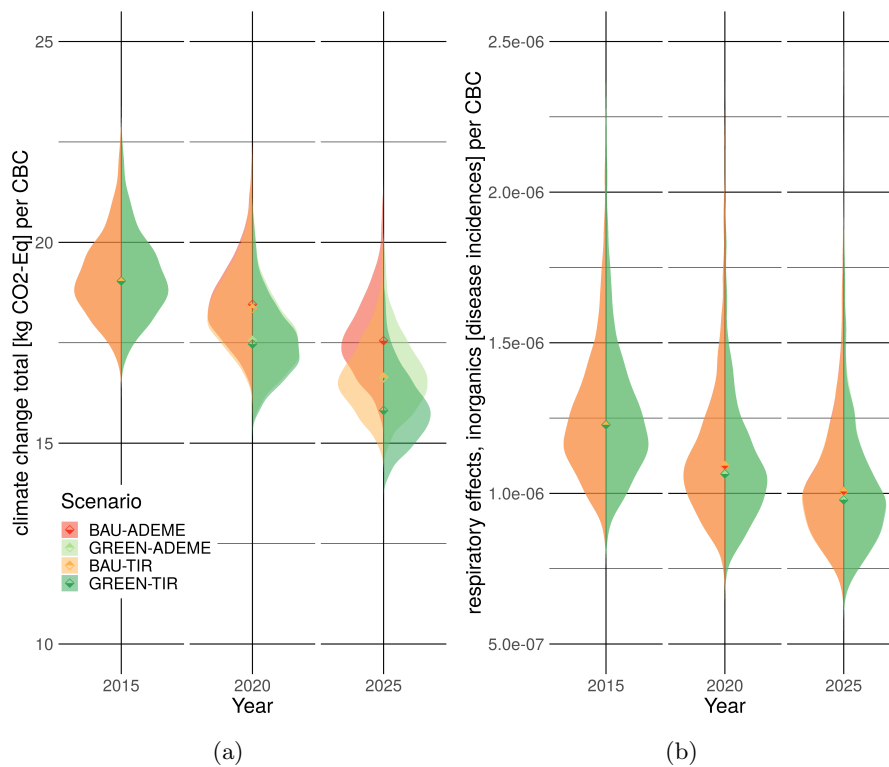
Figure 7.9: Empirical distributions for both QOIs for sub-scheme 2-3. (a) shows *GWP100* per CBC. (b) shows *R-E* per CBC.

7.4   Sub-scheme 2-3

Sub-scheme 2-3 presented in this section focusses on the influence of dependently sampling fuel consumptions and tailpipe emissions, while using the expert uncertainty factors.

7.4.1   Distributions

Figure 7.9 shows the empirical output distributions of all scenarios for sub-scheme 2-3. Again, visually distributions are similar to those of sub-scheme 2-1 shown in figure 7.1 and sub-scheme 2-2 shown in figure 7.5.

Table 7.9 provides the descriptive statistics for *GWP100* distributions. Similar to what has been noted for sub-schemes 1-2 and 2-2, mean values are systematically larger than median values indicating that distributions are right skewed. CV values range from 5.20%-5.57% thus showing a slightly lower level of uncertainty compared to sub-scheme 2-1 in table 7.1.

Table 7.10 provides the descriptive statistics for *R-E* distributions. Distributions are right skewed, as seen before, while CV values range from 19.3%-21.8%. These values are very close to those seem for sub-scheme 2-1, suggesting that dependent sampling of fuel dependent emissions does not influence uncertainty levels for *R-E* impacts. To some extent this results from the chosen method, for which fuel dependent emissions are less relevant, than emissions that are not derived from fuel consumption (i.e., nitrogen oxide emissions).

It thus shows that dependent sampling, where fuel dependent emissions (i.e., carbon dioxide emissions) result from the sampled values of fuel consumption, can reduce the level of uncertainty of some model outputs (i.e., *GWP100*) while other outputs remain unaffected (i.e., *R-E*).

7.4.2   Convergence

Next, the convergence of sub-scheme 2-3 is presented. Figure 7.10 shows CV values as a function of model runs. Visually, results resemble those of sub-schemes 2-1 and 2-2.

The lowest number of model runs required to reach convergence using dependent sampling is shown in tables 7.11-7.12. As seen for the CV values in table 7.10, there is no impact for *R-E*. For *GWP100* and a threshold of 5%, convergence is slower in 2015 and 2020, in 2025 (with a higher share of EVs in the car fleet that do not have tailpipe emissions) convergence is similar and in some cases faster than seen for to sub-scheme 2-1. The convergence criteria set for this thesis are always satisfied.

7.4.3   Further insights

Finally, for sub-scheme 2-3 the three uncertainty communication measures are computed and shown in figures 7.11-7.12.

With regard to *GWP100* shown in figure 7.11 there are only minor differences compared to results of sub-scheme 2-1 shown figure 7.3. While the results of the modified NHST are identical to those of sub-scheme 2-1, the Bhattacharyya Coefficients suggest that the distribution overlap has slightly decreased for sub-scheme 2-3 compared to sub-scheme 2-1. Changes in discernibility scores are only marginal compared to sub-scheme 2-1.

With regard to the second QOI, *R-E* shown in figure 7.12 results are identical to those of sub-scheme 2-1 shown figure 7.4. This is coherent with what has been seen for the uncertainty distributions and convergence of *R-E* for sub-scheme 2-3.

Sampling fuel dependent tailpipe emissions in accordance with fuel consumptions can thus

Table 7.9: Descriptive statistics of uncertainty distributions of *GWP100* scores in [kg CO2-eq] for sub-scheme 2-3.

	BAU-ADEME			BAU-TIR			GREEN-ADEME			GREEN-TIR		
	2015	2020	2025	2015	2020	2025	2015	2020	2025	2015	2020	2025
Median	19.0	18.5	17.6	19.0	18.4	16.6	19.0	17.6	16.6	19.0	17.5	15.8
Mean	19.1	18.6	17.7	19.1	18.5	16.7	19.1	17.6	16.7	19.1	17.6	15.9
SD	1.03	0.99	0.98	1.03	0.98	0.92	1.03	0.92	0.91	1.03	0.91	0.85
CV [%]	5.40	5.32	5.57	5.40	5.30	5.49	5.40	5.21	5.44	5.40	5.20	5.36

Table 7.10: Descriptive statistics of uncertainty distributions of *R-E* scores in 10^{-7} [disease incidences] for sub-scheme 2-3.

	BAU-ADEME			BAU-TIR			GREEN-ADEME			GREEN-TIR		
	2015	2020	2025	2015	2020	2025	2015	2020	2025	2015	2020	2025
Median	12.3	10.9	10.1	12.3	10.9	10.1	12.3	10.6	9.8	12.3	10.6	9.8
Mean	12.8	11.4	10.5	12.8	11.4	10.5	12.8	11.1	10.2	12.8	11.1	10.2
SD	2.46	2.32	2.30	2.46	2.31	2.23	2.46	2.20	2.18	2.46	2.20	2.12
CV [%]	19.3	20.4	21.8	19.3	20.3	21.3	19.3	19.9	21.3	19.3	19.8	20.8

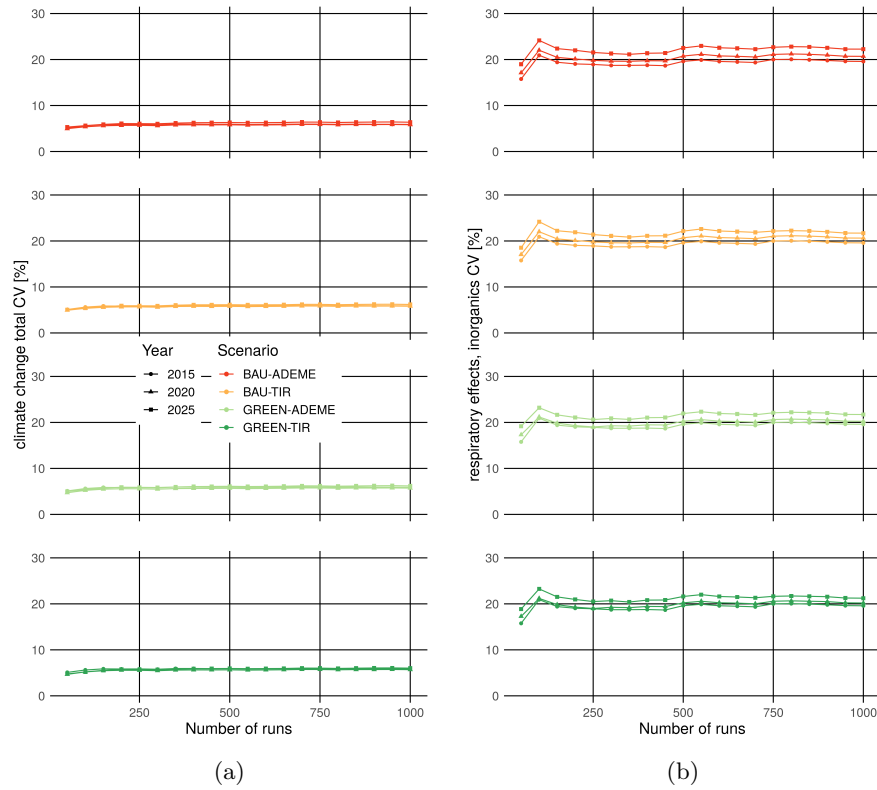(a)   (b)

Figure 7.10: CV as a function of the number of model runs for sub-scheme 2-3. (a) shows the CV values for *GWP100*. (b) shows the CV values for *R-E*.

affect uncertainty levels of *GWP100*, however not to an extent that uncertainty communication measures would lead to different conclusions with regard to the ranking of scenarios.

Table 7.11: Convergence for thresholds of 1-10% for *GWP100*, for sub-scheme 2-3.

	BAU-ADEME			*BAU-TIR*			*GREEN-ADEME*			*GREEN-TIR*		
	2015	2020	2025	2015	2020	2025	2015	2020	2025	2015	2020	2025
1	941	942	943	941	942	941	941	942	943	941	942	941
2	345	346	352	345	346	345	345	345	346	345	345	345
3	341	345	345	341	345	341	341	341	345	341	341	341
4	338	341	341	338	341	341	338	340	341	338	340	340
5	220	338	340	220	337	337	220	337	338	220	337	317
6	59	220	337	59	220	234	59	127	234	59	127	220
7	59	127	225	59	127	147	59	64	220	59	64	127
8	55	64	127	55	64	127	55	64	127	55	64	127
9	21	59	127	21	59	127	21	59	127	21	59	127
10	18	59	127	18	59	127	18	59	64	18	59	64
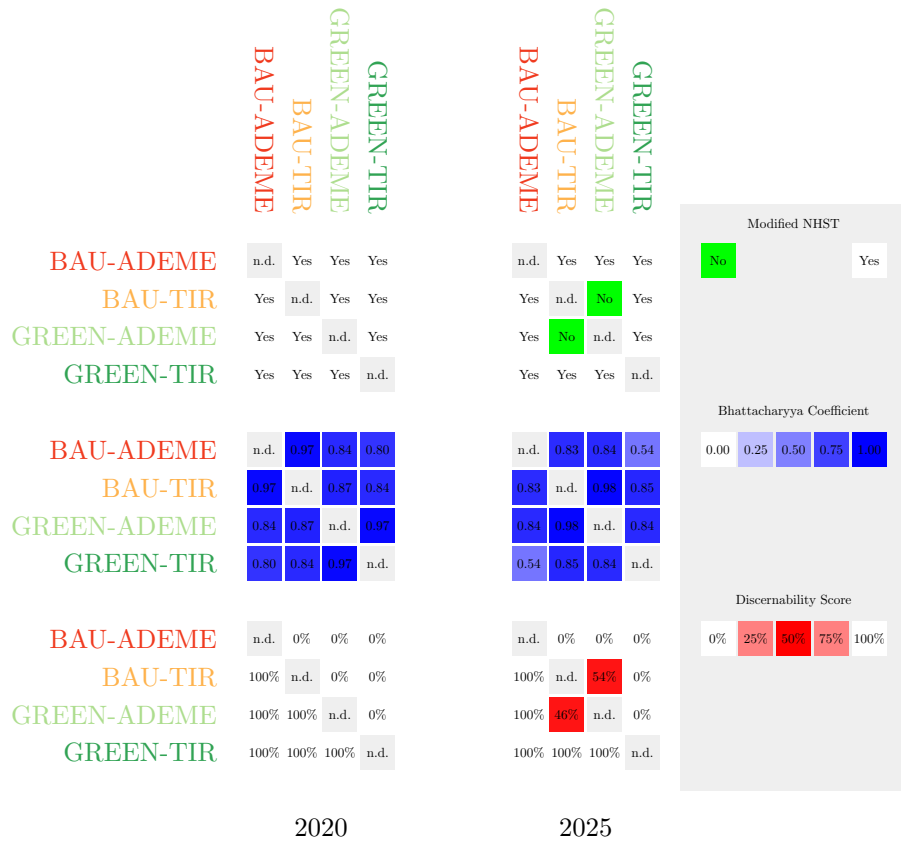
Figure 7.11: Uncertainty communication measures for *GWP100* for 2020 and 2025 are presented for sub-scheme 2-3.

Table 7.12: Convergence for thresholds of 1-10% for *R-E*, for sub-scheme 2-3.

	BAU-ADEME			*BAU-TIR*			*GREEN-ADEME*			*GREEN-TIR*		
	2015	2020	2025	2015	2020	2025	2015	2020	2025	2015	2020	2025
1	905	909	918	905	909	919	905	918	919	905	924	924
2	843	856	858	843	856	859	843	843	856	843	843	856
3	777	771	769	777	771	770	777	766	765	777	766	765
4	472	472	472	472	472	550	472	472	470	472	472	363
5	472	472	363	472	472	344	472	470	363	472	470	344
6	344	359	344	344	344	133	344	363	344	344	359	293
7	83	344	122	83	344	130	83	344	293	83	344	124
8	81	81	116	81	82	124	81	293	84	81	81	122
9	81	81	84	81	81	122	81	81	82	81	81	118
10	81	81	82	81	81	118	81	81	81	81	81	85

132

Figure 7.12: Uncertainty communication measures for *R-E* for 2020 and 2025 are presented for sub-scheme 2-3.

7.5 Sub-scheme 2-4

Finally, sub-scheme 2-4 uses both the empirical uncertainty factors and employs dependent sampling.

7.5.1 Distributions

Figure 7.13 shows the empirical output distributions of all scenarios for sub-scheme 2-4. Distributions are visually similar those of previous sub-schemes of scheme 2.

Table 7.13 provides the descriptive statistics for *GWP100* distributions. CV values range from 5.51%-5.94% thus showing a slightly lower level of uncertainty compared to sub-scheme 2-1 in table 7.1. Overall, values are closer to those of sub-scheme 2-3 (applying dependent sampling) than 2-2 (using empirical uncertainty factors).

Table 7.14 provides the descriptive statistics for *R-E* distributions. CV values range from 19.4%-21.9%. These values are identical to those of 2-2. For both QOI distributions are right skewed.

Overall, results of sub-scheme 2-4 show that dependent sampling of fuel consumption and tailpipe emissions has a stronger effect on uncertainty of *GWP100*, while for uncertainty of *R-E*
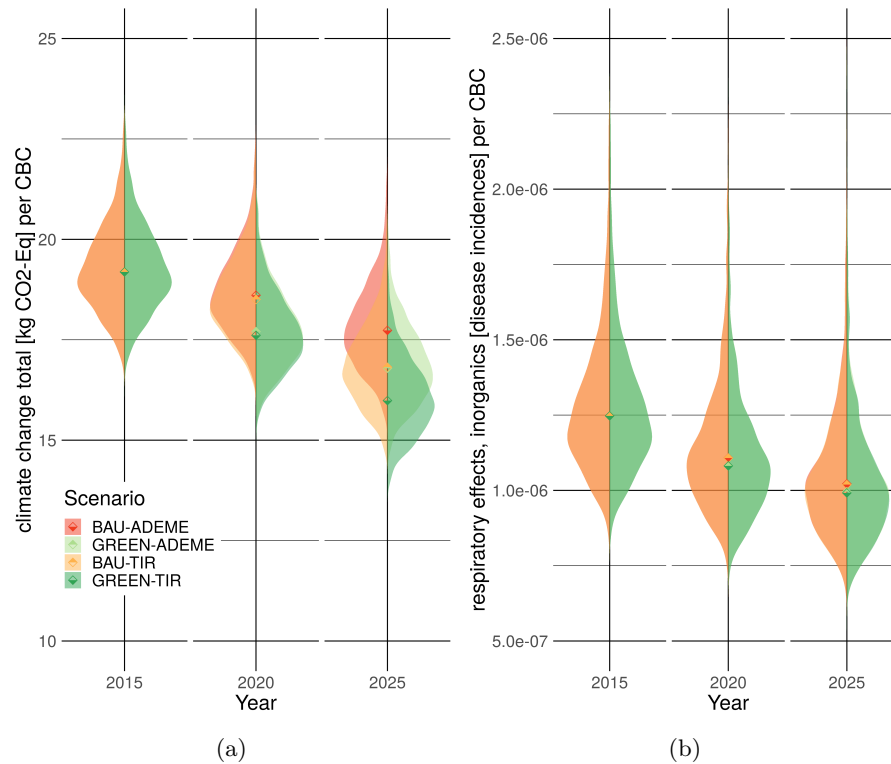
Figure 7.13: Empirical distributions for both QOIs for sub-scheme 2-4. (a) shows *GWP100* per CBC. (b) shows *R-E* per CBC.

using empirical uncertainty factors shows a stronger effect.

To summarize, figure 7.14 shows CV values for *GWP100* contrasting dependent and independent sampling, as well as both sets of uncertainty factors for all sub-schemes, where results are encompassed in the rectangle indicating the specific sampling schemes and set of uncertainty factors chosen. Figure 7.15 shows the CV values for *R-E* for all sub-schemes.

Table 7.13: Descriptive statistics of uncertainty distributions of *GWP100* scores in [kg CO2-eq] for sub-scheme 2-4.

| | *BAU-ADEME* | | | *BAU-TIR* | | | *GREEN-ADEME* | | | *GREEN-TIR* | | |
	2015	2020	2025	2015	2020	2025	2015	2020	2025	2015	2020	2025
Median	19.2	18.6	17.7	19.2	18.5	16.8	19.2	17.7	16.8	19.2	17.6	16.0
Mean	19.3	18.7	17.8	19.3	18.6	16.9	19.3	17.8	16.9	19.3	17.7	16.1
SD	1.08	1.03	1.05	1.08	1.03	1.00	1.08	0.98	0.99	1.08	0.97	0.95
CV [%]	5.62	5.52	5.88	5.62	5.51	5.94	5.62	5.52	5.85	5.62	5.51	5.91
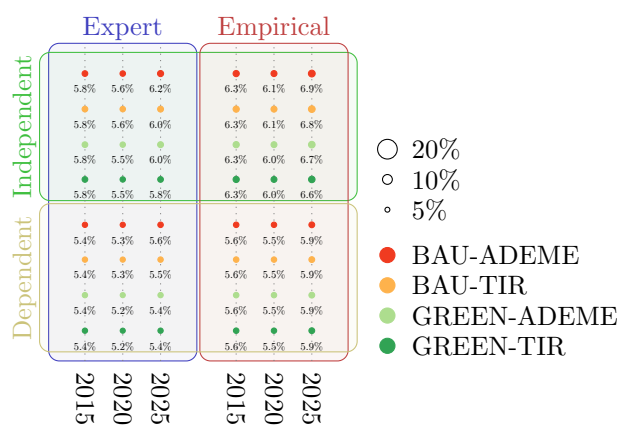
Figure 7.14: The CV for *GWP100*.
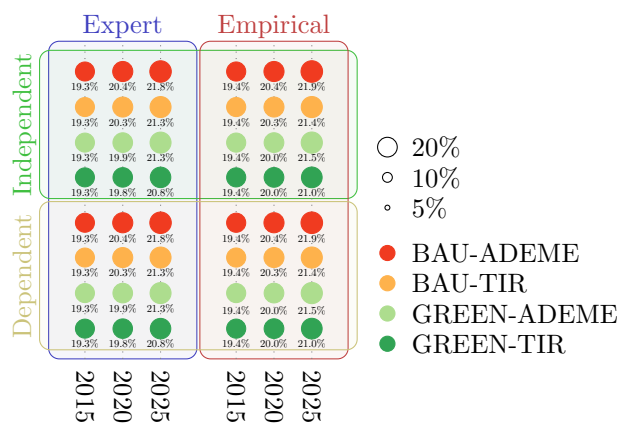
Figure 7.15: The CV for *R-E*.

7.5.2 Convergence

Next, the convergence of sub-scheme 2-4 results is presented. Figure 7.16 shows CV values as a function of model runs.

The lowest number of model runs required to reach convergence is shown in tables 7.15-7.16.

Table 7.14: Descriptive statistics of uncertainty distributions of *R-E* scores in 10^{-7} [disease incidences] for sub-scheme 2-4.

	BAU-ADEME			*BAU-TIR*			*GREEN-ADEME*			*GREEN-TIR*		
	2015	2020	2025	2015	2020	2025	2015	2020	2025	2015	2020	2025
Median	12.5	11.1	10.2	12.5	11.1	10.2	12.5	10.8	10.0	12.5	10.8	9.9
Mean	12.9	11.5	10.7	12.9	11.5	10.6	12.9	11.2	10.4	12.9	11.2	10.3
SD	2.51	2.35	2.33	2.51	2.34	2.27	2.51	2.25	2.22	2.51	2.24	2.17
CV [%]	19.4	20.4	21.9	19.4	20.3	21.4	19.4	20.0	21.5	19.4	20.0	21.0

Figure 7.16: CV as a function of the number of model runs for sub-scheme 2-4. (a) shows the CV values for *GWP100*. (b) shows the CV values for *R-E*.

The convergence criteria set for this thesis are satisfied for all scenarios and years.

Table 7.15: Convergence for thresholds of 1-10% for *GWP100*, for sub-scheme 2-4.

	BAU-ADEME			BAU-TIR			GREEN-ADEME			GREEN-TIR		
	2015	2020	2025	2015	2020	2025	2015	2020	2025	2015	2020	2025
1	940	943	942	940	942	938	940	943	943	940	943	939
2	514	512	345	514	513	341	514	514	341	514	515	421
3	340	341	341	340	341	341	340	340	341	340	340	337
4	337	340	341	337	338	337	337	334	337	337	317	317
5	64	334	338	64	317	317	64	127	317	64	127	220
6	59	127	317	59	127	220	59	64	127	59	64	127
7	59	64	127	59	64	127	59	64	127	59	64	127
8	58	64	127	58	64	127	58	64	127	58	64	127
9	55	64	127	55	64	127	55	64	64	55	64	65
10	16	59	64	16	59	64	16	59	64	16	59	64
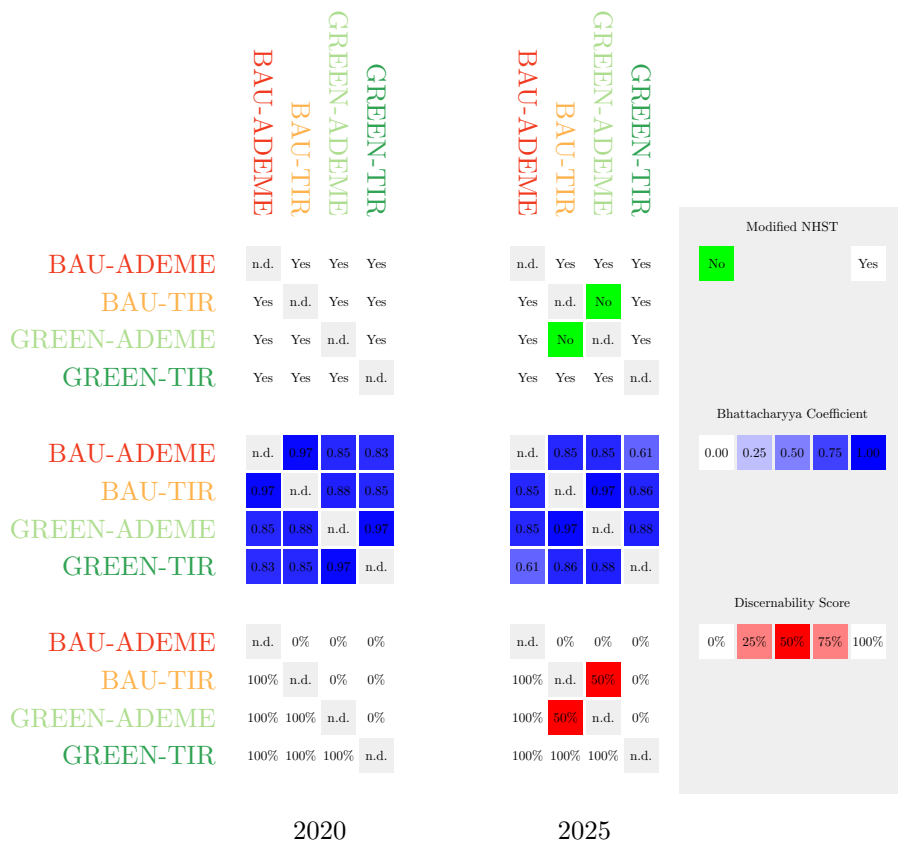
Figure 7.17: Uncertainty communication measures for *GWP100* for 2020 and 2025 are presented for sub-scheme 2-4.

Table 7.16: Convergence for thresholds of 1-10% for *R-E*, for sub-scheme 2-4.

	BAU-ADEME			*BAU-TIR*			*GREEN-ADEME*			*GREEN-TIR*		
	2015	2020	2025	2015	2020	2025	2015	2020	2025	2015	2020	2025
1	905	917	919	905	918	920	905	924	924	905	924	925
2	842	856	859	842	856	859	842	843	856	842	842	856
3	771	771	770	771	771	770	771	766	765	771	766	764
4	472	472	470	472	472	550	472	472	364	472	472	363
5	470	472	363	470	470	130	470	470	363	470	363	293
6	344	344	344	344	344	124	344	344	344	344	344	122
7	81	344	116	81	81	121	81	344	293	81	293	118
8	81	81	82	81	81	117	81	81	81	81	81	82
9	81	81	81	81	81	82	81	81	81	81	81	81
10	81	81	81	81	81	81	81	81	81	81	81	81

Figure 7.18: Uncertainty communication measures for *R-E* for 2020 and 2025 are presented for sub-scheme 2-4.

7.5.3   Further insights

Finally, for sub-scheme 2-4 the three uncertainty communication measures are computed, shown in figures 7.17-7.18.

With regard to *GWP100* shown in figure 7.17, results of sub-scheme 2-4 are very similar to those of sub-scheme 2-1. The combined effect of employing dependent sampling and using empirical uncertainty factors thus shows little influence on the chosen uncertainty communication measures.

With regard to the second QOI, *R-E*, shown in figure 7.18, the most relevant differences to results of sub-scheme 2-1 can be observed for the modified NHST. Results of sub-scheme 2-4 are identical to those of sub-scheme 2-2 suggesting that this QOI is sensitive to empirical uncertainty factors, while showing little sensitivity to the sampling applied.

7.6   Summary

This chapter investigated the results of scheme 2, focussing on parameter uncertainty of the LCA part of CONNECTING. More specifically, the chapter reported on the results of four sub-schemes of scheme 2 investigating the influence of different uncertainty factors (expert based

and empirical based) used for the uncertainty characterisation and two different sampling methods (independent and dependent sampling of fuel consumptions and tailpipe emissions).

There are notable aspects of the results that were observed for both QOIs. As a first, uncertainty of LCA parameters results in higher CV values for both QOIs than shown for scheme 1 which aimed at propagating uncertainty stemming from random choice models. While for scheme 1 CV values were lower than 1%, scheme 2 showed CV values around 5% and 20% for *GWP100* and *R-E* respectively.

Results of sub-scheme 2-2 reveal a second notable aspect. The usage of empirical uncertainty factors rather than using the broadly applied expert factors for uncertainty characterisation, can have a measurable impact on the model output uncertainty and ultimately on the conclusions of uncertainty communication measures. This suggests that expert uncertainty factors cause an underestimation of the level of model output uncertainty.

Similarly, a third notable aspect of results of scheme 2 is, that dependently sampling fuel consumption and fuel dependent tailpipe emissions for ICEVs can change model output uncertainty levels. Specifically, sub-scheme 2-3 applied dependent sampling, showing that this leads to a decrease of CV values for *GWP100*, as carbon dioxide emissions for vehicles are now derived from the sampled fuel consumption values. However, this does not lead to relevant changes in the conclusions that can be drawn from the uncertainty communication measures.

Chapter 8

Results of scheme 3 - ABM/LCA combined uncertainty

8.1   Introduction

This chapter will present the results of scheme 3, the final uncertainty propagation scheme advanced by this thesis. The scheme aims at simultaneously propagating uncertainty stemming from the ABM and LCA parts of CONNECTING (or in general from an ABM/LCA coupled model).

Scheme 3 build on previously applied schemes 1 and 2. More specifically, for the ABM sub-scheme 1-3 is applied, where uncertainty is coming from all choice models (activity type, duration, location and mode choice). For the LCA sub-scheme 2-1 is adopted using the expert uncertainty factors for uncertainty characterisation and independent sampling.

However, a challenge arises as for schemes 1 and 2 the number of model runs is different. Scheme 1 is constrained by the high computational burden of the ABM and therefore only 500 model runs were considered feasible. The review in chapter 3 shows that this is consistent with recent efforts to propagate uncertainty of ABMs. Chapter 6 however indicates that when applying the convergence criteria advanced by this thesis, a higher number of iterations would be preferable. Scheme 2 is less constrained, as the computational burden of the LCA would allow for even higher numbers of model runs. However, as seen in chapter 7, the convergence criteria set for this thesis are satisfied using 1'000 model runs for scheme 2.

Scheme 3 advanced in chapter 5 proposes a simple solution to align model runs of the ABM and LCA, building on a bootstrapping procedure. To this end, model runs from sub-scheme 1-3 are bootstrapped (with replacement) to reach the number of model runs applied for sub-scheme 2-1. Then, each ABM run is associated to a LCA model run, resulting in 1'000 model outputs.

Similar to the previous chapters, the focus is set on uncertainty of system level outputs, namely the QOIs quantifying climate change related impacts ($GWP100$) and respiratory effects related impacts ($R\text{-}E$) for which uncertainty will be quantified and communicated as outlined in section 5.5.

In sections 8.2 the results of the bootstrapping procedure will be evaluated and compared to results of sub-scheme 1-3, to assert that relevant statistics are not affected. Then, section 8.3 will present the results of scheme 3, before a short summary is provided in section 8.4.
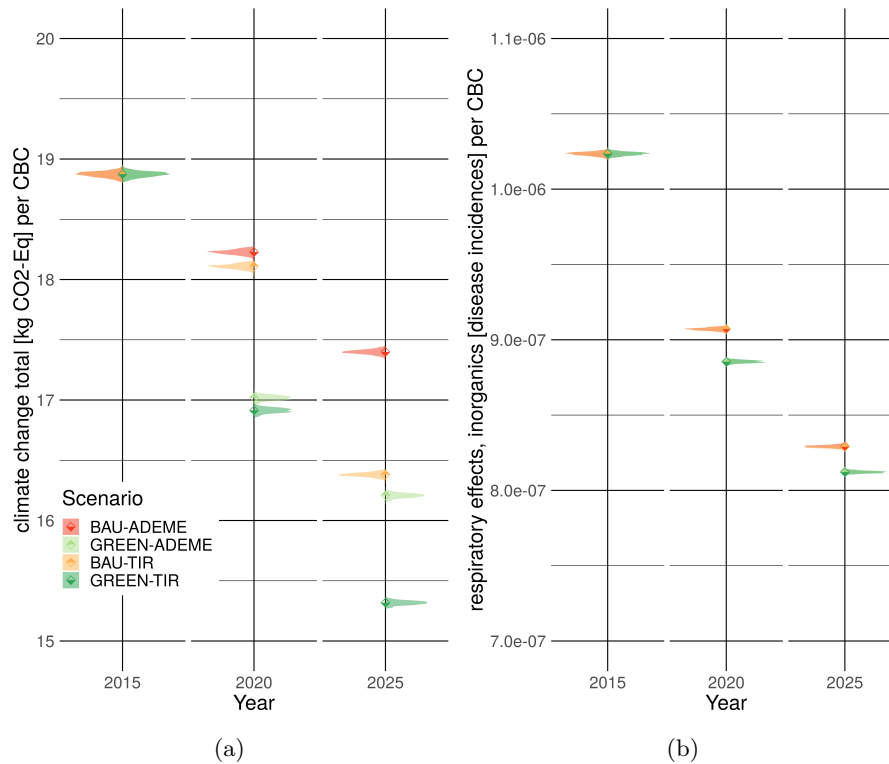
Figure 8.1: Empirical distributions for both QOIs following bootstrapping of sub-scheme 1-3. (a) shows *GWP100* per CBC. (b) shows *R-E* per CBC

8.2   Bootstrapping

This section will report on the model outputs, after applying the bootstrapping procedure to the ABM results of sub-scheme 1-3. The bootstrapping sampled 1'000 from the 500 model runs with replacement. To calculate the QOIs, the nominal concrete instance of the LCA is used.

8.2.1   Distributions

Figure 8.1 shows the empirical distributions for both QOIs. When comparing the shapes to those of figure 6.7 only small changes can be observed. Both the median and the spread seem to be conserved.

In table 8.1 the descriptive statistics for *GWP100* are provided. Mean and median values are identical to those in table 6.11 for sub-scheme 1-3. Uncertainty measures show marginal differences with some SD and CV values increasing slightly after bootstrapping.

In table 8.2 the descriptive statistics for *R-E* are provided. Again, mean and median values are identical to those in table 6.12 for sub-scheme 1-3. Uncertainty measures also show marginal differences, with some SD and CV values decreasing slightly after bootstrapping.

Overall, one can assert that bootstrapping did not strongly alter output uncertainty distributions.

8.2.2 Convergence

Next, the convergence after bootstrapping is assessed. It has to be noted that bootstrapping with replacement only inflates the number of model runs without adding new information. In addition, the original order of model runs is not retained as model runs are sampled randomly from the original 500 runs.

Figure 8.2 shows the CV values as a function of sampled model runs. Similar to what has been observed for sub-scheme 1-3, CV values stabilize quickly showing no strong upwards or downwards trends.

Tables 8.3-8.4 show the lowest number of model runs required to reach convergence for both QOIs. The convergence criteria set for this thesis are reached for all scenarios are years.

Table 8.1: Descriptive statistics of uncertainty distributions of *GWP100* scores in [kg CO2-eq] following bootstrapping of sub-scheme 1-3.

	BAU-ADEME			BAU-TIR			GREEN-ADEME			GREEN-TIR		
	2015	2020	2025	2015	2020	2025	2015	2020	2025	2015	2020	2025
Median	18.9	18.2	17.4	18.9	18.1	16.4	18.9	17.0	16.2	18.9	16.9	15.3
Mean	18.9	18.2	17.4	18.9	18.1	16.4	18.9	17.0	16.2	18.9	16.9	15.3
SD	0.023	0.021	0.019	0.023	0.020	0.018	0.023	0.022	0.020	0.023	0.022	0.018
CV [%]	0.124	0.113	0.109	0.124	0.113	0.108	0.124	0.128	0.121	0.124	0.128	0.118

Table 8.2: Descriptive statistics of uncertainty distributions of *R-E* scores in 10^{-7} [disease incidences] following bootstrapping of sub-scheme 1-3.

	BAU-ADEME			BAU-TIR			GREEN-ADEME			GREEN-TIR		
	2015	2020	2025	2015	2020	2025	2015	2020	2025	2015	2020	2025
Median	10.2	9.1	8.3	10.2	9.1	8.3	10.2	8.9	8.1	10.2	8.9	8.1
Mean	10.2	9.1	8.3	10.2	9.1	8.3	10.2	8.9	8.1	10.2	8.9	8.1
SD	0.013	0.010	0.008	0.013	0.010	0.008	0.013	0.010	0.008	0.013	0.010	0.008
CV [%]	0.123	0.108	0.101	0.123	0.108	0.101	0.123	0.113	0.102	0.123	0.113	0.102

Table 8.3: Convergence of *GWP100* CV values for thresholds of 1-10% following bootstrapping of sub-scheme 1-3.

T (%)	BAU-ADEME			BAU-TIR			GREEN-ADEME			GREEN-TIR		
	2015	2020	2025	2015	2020	2025	2015	2020	2025	2015	2020	2025
1	892	709	622	892	709	622	892	892	923	892	892	923
2	448	239	182	448	239	181	448	574	366	448	574	366
3	198	136	96	198	136	92	198	380	362	198	380	362
4	107	108	86	107	108	64	107	364	331	107	364	331
5	78	108	64	78	108	64	78	360	138	78	360	328
6	78	66	42	78	66	41	78	328	92	78	328	41
7	76	64	41	76	64	40	76	64	41	76	64	40
8	33	64	40	33	64	39	33	64	40	33	64	40
9	32	37	39	32	37	38	32	64	37	32	64	37
10	32	35	38	32	35	38	32	30	37	32	30	36

(a)   (b)
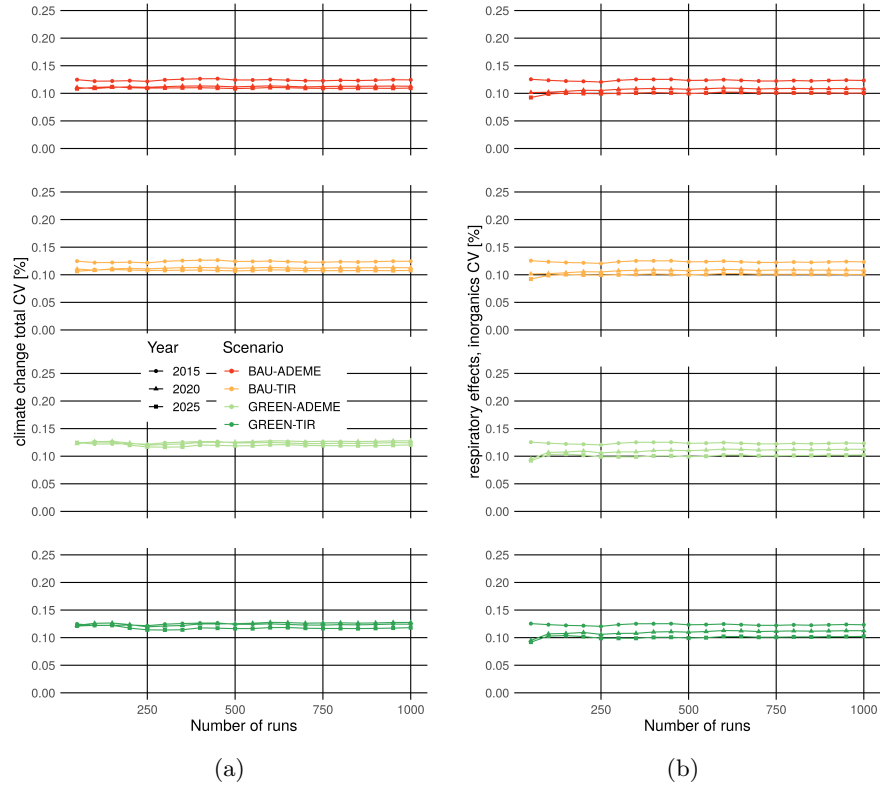
Figure 8.2: CV as a function of the number of model runs following bootstrapping of sub-scheme 1-3. (a) shows the CV values for *GWP100*. (b) shows the CV values for *R-E*.

8.2.3   Further insights

Finally, to investigate the influence of bootstrapping on the uncertainty communication measures figures 8.3-8.4 show the results for the bootstrapped simulations. Comparing all measures

Table 8.4: Convergence of *R-E* CV values for thresholds of 1-10% following bootstrapping of sub-scheme 1-3.

T (%)	*BAU-ADEME*			*BAU-TIR*			*GREEN-ADEME*			*GREEN-TIR*		
	2015	2020	2025	2015	2020	2025	2015	2020	2025	2015	2020	2025
1	619	815	677	619	815	677	619	863	890	619	863	890
2	447	257	613	447	257	613	447	574	576	447	574	576
3	239	244	200	239	244	200	239	369	535	239	369	535
4	87	235	124	87	235	124	87	364	361	87	364	361
5	76	149	84	76	149	84	76	360	85	76	360	85
6	41	137	80	41	137	80	41	244	85	41	244	85
7	41	124	78	41	124	78	41	133	85	41	133	85
8	34	107	77	34	107	77	34	85	84	34	85	84
9	33	66	75	33	66	75	33	84	80	33	84	80
10	32	64	64	32	64	64	32	80	77	32	80	77
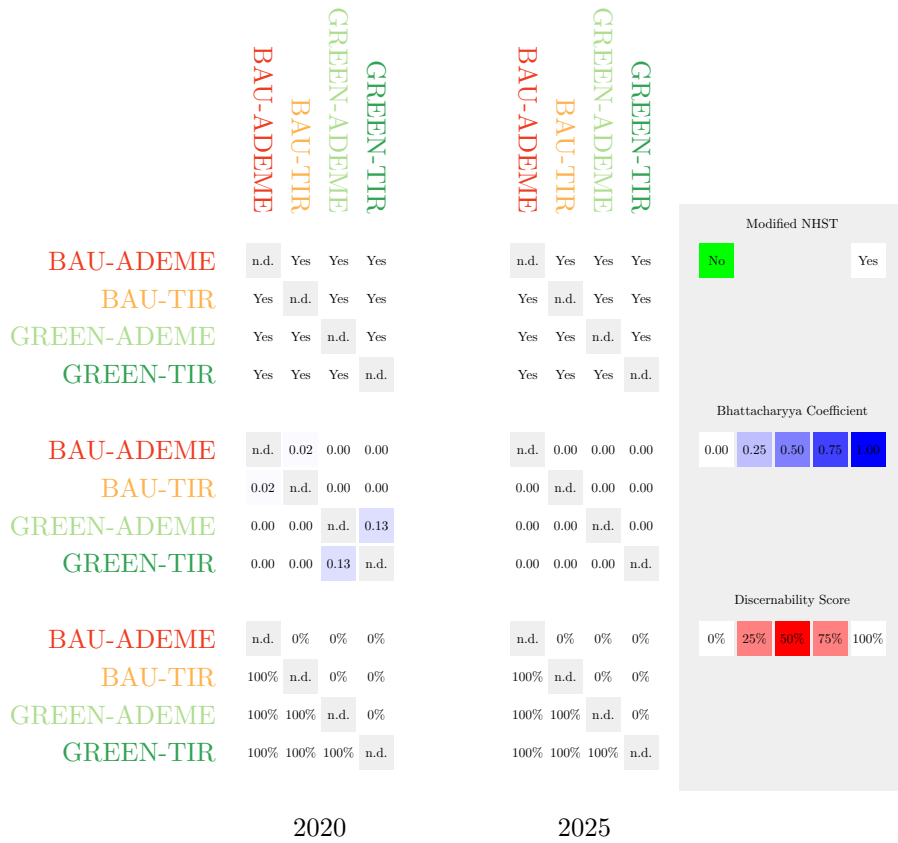
Figure 8.3: Uncertainty communication measures for *GWP100* for 2020 and 2025 are presented following bootstrapping of sub-scheme 1-3

to those of figures 6.11-6.12 for sub-scheme 1-3 one can notice only marginal differences for the Bhattacharyya coefficients.

8.3 Scheme 3: Combined ABM/LCA uncertainty

Following the description of bootstrapped results of sub-scheme 1-3, the results of scheme 3 can be presented, which combines the bootstrapped ABM simulations with LCA simulations of sub-scheme 2-1.

In order to combine uncertainty for both sub-models, each sampled ABM run is associated to a LCA model run from sub-scheme 2-1.

Figure 8.4: Uncertainty communication measures for R-E for 2020 and 2025 are presented following bootstrapping of sub-scheme 1-3

8.3.1 Distributions

Figure 8.5 shows the empirical distributions results from scheme 3. Overall, one can see that results change compared to those of sub-scheme 2-1. While the spread seems less affected, running the ABM stochastically has an effect on the median values (as outlined in chapter 6).

Table 8.5 shows the descriptive statistics for *GWP100*. Compared to results of sub-scheme 2-1, there is a slight increase in SD and CV values. Consistent with what has been observed for sub-scheme 1-3 mean and median values increase with choice models being run stochastically compared to sub-scheme 2-1 (which build on the nominal results of the ABM).

Table 8.6 shows the descriptive statistics for *R-E*. Similar conclusions as for *GWP100* can be drawn: there is a slight increase in SD and CV values as well as the expected increase in mean an median values. For both QOIs one can observe that distributions are right skewed as seen before for results of scheme 2. When comparing SD values of scheme 3 to those of sub-scheme 2-1 and 1-3 it seems that uncertainties stemming from the ABM and LCA are close to additive.

8.3.2 Convergence

Next convergence is assessed. CV only slightly increase due to the additional uncertainty stemming from the ABM in figure 8.6 after 1000. Convergence seems to behave similarly to what
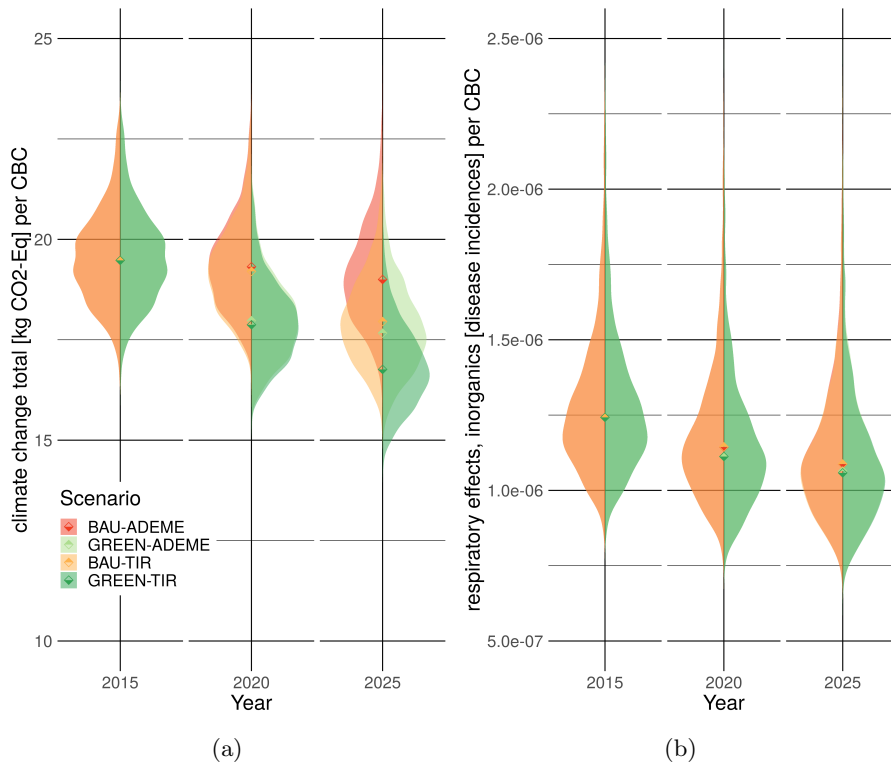
Figure 8.5: Empirical distributions for scheme 3 for both QOIs. (a) shows *GWP100* per CBC. (b) shows *R-E* per CBC

has been observed for scheme 2.

Tables 8.7-8.8 show the lowest number of iterations required to reach convergence for *GWP100* and *R-E* respectively. The convergence criteria set for this thesis are satisfied for both QOIs.

8.3.3 Further insights

We can now proceed by evaluating how much the uncertainty stemming from both sub-models could potentially affect policy choices given the four policy scenarios as seen for previous schemes. To this end we again compute the three uncertainty communication measures.

Table 8.5: Descriptive statistics of uncertainty distributions of *GWP100* scores in [kg CO2-eq] for scheme 3.

| | *BAU-ADEME* | | | *BAU-TIR* | | | *GREEN-ADEME* | | | *GREEN-TIR* | | |
	2015	2020	2025	2015	2020	2025	2015	2020	2025	2015	2020	2025
Median	19.5	19.3	19.0	19.5	19.2	18.0	19.5	18.0	17.7	19.5	17.9	16.8
Mean	19.6	19.4	19.1	19.6	19.3	18.0	19.6	18.0	17.8	19.6	17.9	16.8
SD	1.15	1.13	1.22	1.15	1.12	1.12	1.15	1.03	1.10	1.15	1.02	1.01
CV [%]	5.89	5.83	6.37	5.89	5.81	6.20	5.89	5.71	6.16	5.89	5.69	6.03

(a)   (b)

Figure 8.6: CV as a function of the number of model iterations for scheme 3. (a) shows the CV values for *GWP100*. (b) shows the CV values for *R-E*.

The results for the modified NHST indicate that mean scenario values are all significantly different from each other, including the comparison of *BAU-TIR* and *GREEN-ADEME* where the null hypothesis could not be rejected for sub-scheme 2-1 in 2025.

The Bhattacharyya coefficient shows slightly lower values compared to scheme 2, especially for *GWP100*. This suggests that distributions overlap less when taking into account uncertainty from all sub-models.

Finally, the discernibility scores for *GWP100* in 2020 confirm the changes compared to scheme 2, where *GREEN-ADEME* now shows lower values than *BAU-TIR* for 95% of model runs. This suggests that in the long term higher investments in PT perform consistently better

Table 8.6: Descriptive statistics of uncertainty distributions of *R-E* scores in 10^{-7} [disease incidences] for scheme 3.

	BAU-ADEME			BAU-TIR			GREEN-ADEME			GREEN-TIR		
	2015	2020	2025	2015	2020	2025	2015	2020	2025	2015	2020	2025
Median	12.4	11.4	10.9	12.4	11.5	10.9	12.4	11.1	10.6	12.4	11.1	10.6
Mean	12.9	12.0	11.4	12.9	12.0	11.4	12.9	11.6	11.1	12.9	11.6	11.0
SD	2.53	2.48	2.54	2.53	2.47	2.47	2.53	2.35	2.41	2.53	2.34	2.35
CV [%]	19.6	20.7	22.3	19.6	20.6	21.7	19.6	20.2	21.7	19.6	20.2	21.2

than fostering a higher share of EVs in the car fleet.

8.4   Summary

.

   In this chapter the third and final uncertainty propagation scheme presented in chapter 5 is applied to the CONNECTING model. Scheme 3 allows to combine propagation for both sub-models of CONNECTING.

   Prior to applying scheme 3 however, a bootstrapping procedure is used to increase the number of model runs of the ABM to match the number of model runs of the LCA. The evaluation of model outputs of the bootstrapped model runs shows that output distributions and uncertainty communication measures are only marginally changed.

   For results of scheme 3, both the effects of running ABM choice models stochastically observed for scheme 1 and the effects running the LCA model stochastically seen for scheme 2

Table 8.7: Convergence for thresholds of 1-10% for *GWP100*, for scheme 3.

T (%)	BAU-ADEME			BAU-TIR			GREEN-ADEME			GREEN-TIR		
	2015	2020	2025	2015	2020	2025	2015	2020	2025	2015	2020	2025
1	936	942	947	936	942	942	936	942	946	936	941	942
2	234	345	621	234	345	621	234	345	625	234	345	625
3	220	338	352	220	338	345	220	341	373	220	341	371
4	220	337	345	220	317	341	220	337	345	220	337	345
5	114	220	338	114	220	337	114	220	341	114	141	338
6	112	141	317	112	141	220	112	141	337	112	141	317
7	64	136	178	64	136	178	64	136	178	64	136	178
8	60	127	172	60	127	172	60	127	172	60	127	172
9	59	76	145	59	76	147	59	112	147	59	112	147
10	59	76	141	59	76	141	59	76	141	59	76	141

Table 8.8: Convergence for thresholds of 1-10% for *R-E*, for scheme 3.

T (%)	BAU-ADEME			BAU-TIR			GREEN-ADEME			GREEN-TIR		
	2015	2020	2025	2015	2020	2025	2015	2020	2025	2015	2020	2025
1	905	924	919	905	924	924	905	926	926	905	926	928
2	847	858	860	847	858	860	847	855	857	847	855	856
3	779	778	777	779	778	777	779	767	765	779	767	765
4	472	472	470	472	472	554	472	470	363	472	470	363
5	470	470	363	470	470	141	470	363	363	470	363	293
6	344	344	344	344	344	135	344	344	344	344	344	293
7	94	84	123	94	84	131	94	293	293	94	293	124
8	82	81	118	82	82	125	82	293	84	82	81	122
9	81	81	85	81	81	123	81	81	82	81	81	118
10	81	81	82	81	81	119	81	81	81	81	81	85
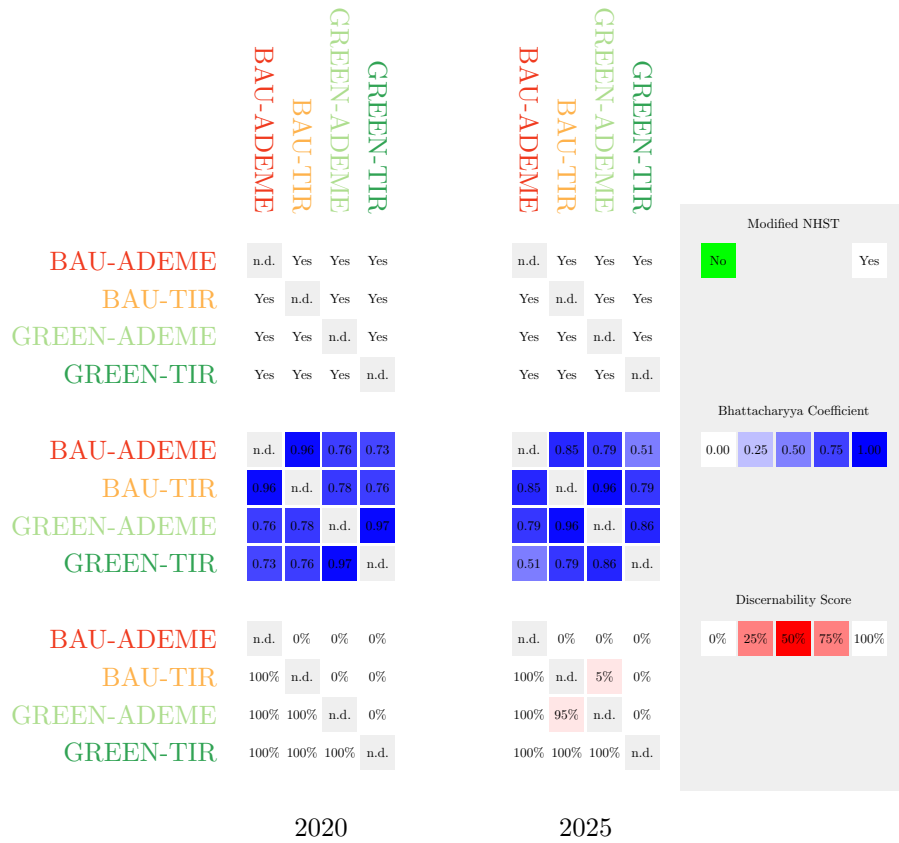
Figure 8.7: The discernibility scores for *GWP100* for 2020 and 2025 are presented for scheme 3. The discernibility score indicates the percentage of iterations for which a scenario (row) has a lower score than a given reference scenario (column).

can be observed. SD values observed for scheme 3 are close to the sum of SD values observed for sub-scheme 1-4 and sub-scheme 2-1. Compared to scheme 2, mean and median values increase (resulting from running choice model stochastically).

Finally, uncertainty communication measures for scheme 3 are altered compared to schemes 1 and 2. This suggests that only including both (and ultimately all) uncertainty locations can provide a good assessment of model output uncertainty to decision makers.
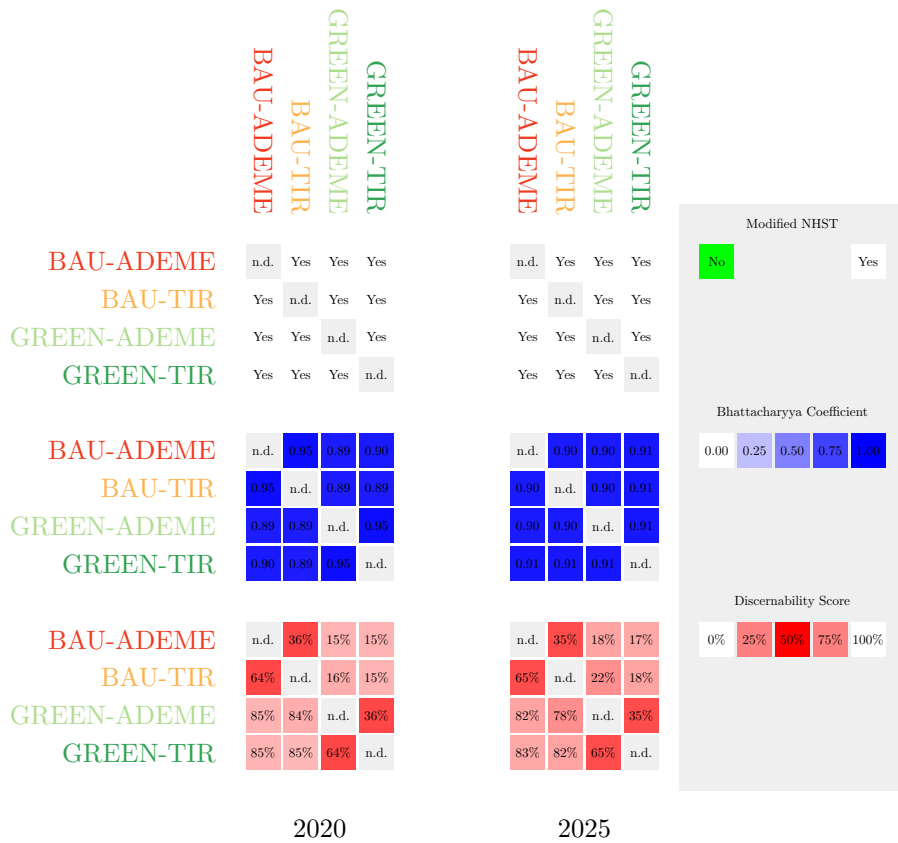
Figure 8.8: The discernibility scores for *R-E* for 2020 and 2025 are presented for scheme 3. The discernibility score indicates the percentage of iterations for which a scenario (row) has a lower score than a given reference scenario (column).

Chapter 9

Conclusions

9.1   Introduction

In a context, where ever more complex C-LCA modelling approaches are being applied to increasingly complex case studies, there are increasing concerns about whether or not such endeavours can still allow to produce scientific outputs that can be trusted by decision makers eager to identify robust policy measures. One broadly accepted tool to increase the trust that can be placed in a model, is the systematic analysis of uncertainty that can potentially affect the model output and in consequence the decision of a policy maker. The present thesis aims at going beyond the state-of-the-art, by proposing an UA framework for C-LCA models, where the consequential aspect is generated by an ABM approach of travel demand.

More specifically, the thesis is part of a larger multi-disciplinary project – the CONNECTING project – which aims at developing such an ABM/LCA coupled model, where the ABM part focusses on the CBC population living in France and working in Luxembourg and the LCA part focusses on the available transportation modes, allowing these commuters to participate in their daily activities. It is this model and the related case study that allows to apply the UA framework developed in this thesis.

The CONNECTING model (much like all models) is merely the attempt to create an isomorphic image of a perceived source system and each execution of the model is subject to uncertainties. A single model execution allows to evaluate only one possible trajectory of the modelled system, where uncertainties of epistemological and ontological nature affect both the ABM part of the model, where thousands of individuals make choices about their DAPs, as well as the LCA part of the model representing thousands of interconnected processes and their exchanges with the natural environment. Only a large set of model executions allows to provide a robust answer to the questions that decisions makers have about the behaviour of the modelled system. UA is the organisation of these model executions, ultimately allowing to describe the uncertainty in the model outputs.

ABM/LCA coupled models, such as the CONNECTING model, allow to generate a DAP for each individual in the CBC population, determining what activities an individual conducts when, where and which transport modes the individual uses to reach each activity location. While these individual DAPs can be themselves evaluated, in case of the CONNECTING model they are aggregated in time and space to compute the system's demand for transport processes modelled in the LCA part of the CONNECTING model. Using the matrix inversion approach of LCA the demand can be translated into related impacts such as impacts on the environment, impacts on human health or impacts on resource depletion. These are the QOIs of the CONNECTING

project intended to be communicated to decision makers and in consequence the model outputs for which uncertainty shall be quantified.

While the CONNECTING model is the first attempt to couple an ABM and LCA, it only links both models at an aggregated scale, where only the total distances travelled at the population level are currently used as inputs to the LCA. This limitation has some implications for the UA, where uncertainty of the DAPs at a more disaggregated scale do not necessarily translate into uncertainty of the chosen QOIs. Uncertainties at lower levels of aggregation however were considered out of the scope of the present thesis.

Similarly, coupling ABMs and LCA opens up the possibility to not only assess the effect of travel demand by coupling the ABM with the LCI but also assess coupling the ABM to the LCIA (e.g., by modelling air quality and assessing exposure). This would imply that uncertainty of the ABM would affect both LCA phases, however such a coupling was considered beyond the scope of the CONNECTING project and can thus not be assessed in the present thesis.

In the following, the conclusions of the UA applied to the CONNECTING model and case study will be structures according to two distinct subjects. As a first, section 9.2 will focus on the UA framework and its application. Section 9.3 will focus on the implications of the uncertainty in a decision making context. At the end a few final comments are provided to outline further research.

9.2 Uncertainty analysis of ABM/LCA coupled models

Prior to proceeding with the analysis of uncertainty by performing model runs, the present thesis dedicates a large portion to the description of ABM/LCA coupled models in general, the CONNECTING model in particular and the review of UA of such models. While a re-iteration of the first two subjects is of lesser interest to the conclusions of the present thesis, the conclusions of the review of UA will allow to set the stage for the conclusions regarding the UA results.

In both fields individually, scholars have advanced frameworks for all steps of performing UA, starting with the location and identification of uncertainty within the model, the characterisation and treatment of that uncertainty to its communication. It goes without saying that a failure at the uncertainty location and identification stage of UA will propagate to subsequent steps and can potentially cause for irrelevant results, as important uncertainties are disregarded from the outset. A proper set of uncertainty locations (elements of the model where the uncertainty manifests itself), a description of uncertainty nature (epistemic or ontic) and level is thus primordial to a successful UA. While uncertainty nature and level are already covered by generic classifications such as Walker et al. (2003), uncertainty locations are usually more model specific and such classifications have been advance both for LCA and ABMs. However, there is no such classification for ABM/LCA coupled models and thus chapter 3 proceeds by proposing the first classification, building on prior work of both fields. Going beyond ABM/LCA coupled models, especially in the field of LCA the prominent classifications of so-called uncertainty sources are often ignorant of the different dimensions of uncertainty (nature, location and level) as proposed by Walker et al. (2003) and thus propose classifications that conflate these terms and concepts. While the classification presented in the current thesis aims at being specific to ABM/LCA coupled models, it could also be applied to textbook LCA studies proposing the following uncertainty locations: experimental frame, inputs, model and outputs. Model uncertainty is used as an umbrella term encompassing model specification, model estimation and the simulation error.

The present thesis thus evaluates uncertainty locations of the CONNECTING model, where the most relevant locations are selected based on their prevalence in literature of UA for both fields. This prevalence is assessed based on a quantitative and systematic literature review of

UA of LCA studies of transport modes and of ABM case studies. The extensive and systematic literature reviews on both subjects build on the screening more than 1'000 records each. The most prevalent uncertainty locations are the simulation error of ABMs, as well as the measured parameters of LCA present in the technosphere and biosphere matrices. Both are addressed for over 90% of studies in the respective literature reviews and are thus selected to be made operational by the uncertainty propagation schemes advanced by this thesis. It has to be noted that the selection based on prevalence in the literature review can be questioned, and a selection of locations potentially contributing most to the overall output uncertainty could also have been made. However, the present thesis aims at catering to the largest possible audience by trying to address the uncertainty locations that practitioners have focused on most.

Several other relevant aspects have been identified during the literature review, especially with regard to the current uncertainty characterisation and treatment practice, and the implications for the estimation of output uncertainties.

More specific to LCA, while many studies apply the pedigree approach to deal with the impracticability of characterising the uncertainty of thousands of flows in the technosphere and biosphere matrix only few studies assess the sensitivity towards competing uncertainty factors used to derive uncertainty distributions. The present thesis presents the first case study assessment of the impacts of two sets of uncertainty factors present in literature on the output uncertainty.

In addition, the literature review has revealed that only few studies have investigated the impact of dependencies among uncertainty locations on the output uncertainty. Especially, LCA parameters of unit processes can exhibit strong dependencies (i.e., fuel consumption and CO_2 emissions). The present thesis presents one of the first fleet level case studies assessing the impact of dependencies among fuel consumption and fuel related emissions on the output uncertainty.

Finally, while several studies assess the uncertainty of ABM outputs stemming from all choice facets simultaneously, the present thesis investigates the uncertainty stemming from individual choice models of the CONNECTING ABM on the QOIs, as well as stemming from combinations of choice models, where other models are set to being run deterministically. No prior study has attempted to systematically investigate uncertainty of individual and combinations of ABM sub-models in this manner.

Three uncertainty schemes representing specific research designs are advanced by this thesis propagating: (1) uncertainty from the ABM; (2) uncertainty from the LCA; and (3) uncertainty from both the ABM and the LCA sub-model simultaneously. Next the three advanced schemes are briefly described (a detailed description is presented in chapter 5):

Scheme 1   First, the synthetic population is generated always using the same random number seed. Next, random seeds are generated for each potential decision of each individual of the synthetic population to be fed to the choice models of the ABM, for each mode run. ABM sub-models are calibrated based on the survey data. Next the ABM is executed N times and for each execution a deterministic LCA is run to produce the QOIs. Finally, uncertainty measures are computed for the outputs.

Scheme 2   First, the synthetic population is generated always using the same random number seed. Next, N random seeds are generated, one for each planned model execution. ABM sub-models are calibrated based on the survey data. Next the ABM is executed one time where each sub-model is set to run deterministically. Then N LCA iterations are run using the N random seeds and producing N model outputs. Finally, uncertainty measures are computed for the outputs.

Scheme 3   First, the synthetic population is generated always using the same random number seed. Next, R random seeds are generated for each potential decision of each individual of the synthetic population to be fed to the choice models of the ABM, for each mode run. Next, N random seeds are generated, one for each planned LCA model execution. ABM sub-models are calibrated based on the survey data. Next the ABM is executed R times. Using bootstrapping with replacement, N model runs are sampled from the original R ABM runs. Then, for each sampled ABM run a stochastic LCA is run to produce the QOIs. Finally, uncertainty measures are computed for the outputs.

Two main output measures are used to assess the uncertainty in QOIs: (1) the CV defined as the ratio of the sample SD and the sample mean; (2) the convergence where it is considered that convergence is reached if the percentage difference of the CV after n iterations compared to the CV after N simulations is consistently lower to a selected threshold.

The threshold for the convergence is set to 5%. The convergence measure is complemented with a second condition in addition the threshold, where it is argued that in order for the convergence measure to be able to arrive at the conclusion that a model has not converged, it needs to be defined by which share of the executions the defined threshold has to be consistently met. Here this share is conveniently set to $N/2$.

The results of scheme 1 for both measures allow for the drawing of following conclusions:

1. The simulation error of the ABM is relatively small (i.e., compared to the uncertainty from LCA parameters), with CV values being consistently lower than 0.13%

2. The location choice model seems to contribute only marginally to the observed output uncertainty of scheme 1, while the activity type and duration models contribute the most. It seems that commuters are more constrained in their location choices or QOIs are less sensitive to the uncertainty of these choices, at least at the aggregated scale.

3. With regard to the convergence, when all models are run stochastically the criteria are met most of the time, while for individual models (especially the location choice model) convergence seems significantly slower potentially requiring additional model runs.

4. Uncertainty does not seem to be additive in the sense that the sum of CV (or SD) values when individual ABM sub-models are being investigated does not result in the CV (or SD) values when all ABM sub-models are being run stochastically. This suggests that there could be a damping effect due one or the combination of ABM sub-models being set to a certain state (stochastic or deterministic).

5. ABM sub-models being set to run deterministically (or stochastically) can affect mean (or median) values of output distributions. This results from the definition of the deterministic state of a model (where deterministic means that the options with the highest utility are chosen for each individual).

The results of scheme 2 allow for the drawing of following conclusions:

1. The uncertainty from the parameters of the LCA sub-model is substantially larger than the simulation error stemming from the ABM. This suggests that the QOIs are more sensitive to the uncertainty about the transport mode data, than to the uncertainty about individual DAPs.

2. With regard to the two QOIs used throughout this thesis, uncertainty is larger for *R-E* than for *GWP100*. This suggests that *R-E* is more sensitive to variations in emissions relevant to human health, or that these emissions are more uncertain in the LCI or both.

3. Output uncertainty for both QOIs (in terms of CV values and convergence) is not very sensitive towards alternative uncertainty factor definitions or dependent sampling. The current practice of using expert factors and independently sampling fuel consumption and fuel related emissions does not significantly over- or underestimate the overall uncertainty.

4. However, uncertainty communication measures (which might be more relevant to decision makes), i.e., modified NHST, Bhattacharyya coefficients and discernibility scores, can show different outcomes especially with regard to the two sets of uncertainty factors used.

Finally, the results of scheme 3 allow for the drawing of following conclusions:

1. Bootstrapping the results of the ABM iterations of scheme 1, by increasing the amount of outputs by a factor of 2 does not show significant impacts on the model outputs, their uncertainty or the convergence of CV values. It seems thus appropriate to inflate the number of model runs of the ABM part artificially to a certain degree if need be.

2. Comparing results of scheme 3 to those of scheme 1 and scheme 2 suggests the overall uncertainty is close to being additive.

3. Uncertainty communication measures suggest that even though the uncertainty magnitude from the ABM is small, running the ABM stochastically (rather than deterministically as done for scheme 2) can have substantial effects due to changes in mean and median values.

4. Overall, the results of scheme 3 show that only the combination of multiple uncertainty locations (stemming from both sub-models) allow to accurately present the reliability of the model outputs.

9.3 Decision making under uncertainty

Following the conclusions with regard to the UA framework and application, this section focusses on the conclusions with regard to decision making under uncertainty for ABM/LCA coupled models.

The present thesis builds on uncertainty communication measures designed to facilitate decision making based on UA of comparative LCA studies, where the selected measures (the modified null hypothesis significance test, the Bhattacharyya coefficient and the discernibility score) each cover different aspects of the effect of output uncertainty on decision making.

These measures are systematically applied to all possible scenario comparisons for the 4 policy scenarios (*BAU-ADEME*, *BAU-TIR*, *GREEN-ADEME* and *GREEN-TIR*) defined in chapter 4. The modified NHST first proposed by Mendoza Beltran et al. (2018a) is a measure that allows to assess the statistical significance of scenario means. It thus covers the *significance* dimension of scenario comparison. The Bhattacharyya coefficient is a measure for the overlap of output distributions, thus covering the *extent* dimension of scenario differences. Finally, the discernibility score provides the percentage of iterations for which one scenario performs better (i.e., shows a lower impact for a QOI) compared to another scenario covering the *consistency* dimension of the scenario difference.

Based on the results of scheme 1, it can be concluded that the simulation error of the ABM is only policy relevant to a lesser extent. Both the modified NHST and the discernibility score allow for clear cut decisions, similar to the nominal results of the CONNECTING model. Only the Bhattacharyya coefficient (or in other words the extent of differences among scenarios) suggests that at least for comparisons of *ADEME* and *TIR* scenarios for *R-E*, these uncertainty sources could potentially affect decision making.

Results of scheme 2 point towards the opposite conclusions for uncertainty from LCA parameters. While all measures identify policy relevant uncertainties, especially the comparison of the *BAU-TIR* and *GREEN-ADEME* scenario for *GWP100* point towards an interesting trade-off that is identified by all three measures. For many other comparisons often only one measure points towards policy relevant uncertainties suggesting that only in the combination these measures are robust, while single measures might lead to overlooking policy relevant uncertainty and making an uninformed choice.

Finally, the uncertainty communication measures computed for scheme 3 reveal that even though the simulation error stemming from the ABM is marginal, the effect of running the model stochastically on the mean (or median) results can cause shifts in the relevance of output uncertainties. In the present case, scheme 3 allows for more clear cut decisions compared to scheme 2.

9.4   Final comments

While the present thesis has presented a substantial amount of results produced under high computational burden it has only partially addresses the subject of UA of ABM/LCA coupled models (or even AgBM/LCA coupled models). A large portion of the work went into the conceptualisation of ABM/LCA coupled models necessary for UA, the literature review to establish the state-of-the-art, as well as the more technical aspects regarding the implementation of UA. In consequence the present thesis leaves much room for further work on the subject. In the following a few research pathways will be outlined.

As a first, the present thesis deals with uncertainty locations most prevalent in literature which are by no means the most relevant in terms of impact on the output or relevance to policy makers. To identify the most relevant uncertainty locations (or key issues) SA methods have been developed and successfully applied to a broad range of models (including ABMs, AgBMs and LCA). Uncertainty locations such as inputs (i.e., transport system data), estimated parameters or the model's functional form could be systematically screened and/or their CTV could be assessed by means of GSA.

While the focus of the present thesis is UA, model development of ABM/LCA coupled approaches has only just begone, with much work left to be done. The current coupling of both approaches, using aggregated system level outputs of the ABM to compute LCA results represents only a fraction of the potential that could be reached. One concrete next step would be to assess occupancy rates of transport modes at the ABM side and use them as inputs to LCA transport mode processes. This could allow to assess policies aiming at increasing car sharing or assess the efficiency of additional bus or train lines from an environmental point of view. A second step could be to couple air quality models (which have already been coupled to ABM and LCA respectively) to both models to further develop the coupling towards the LCIA phase. Finally a third step could be to include long term choices such as car purchasing or disposal into the system's demand, allowing to couple more stages of the vehicle life cycle to the ABM.

A final research pathway outlined here is a focus on decision making based on UA outputs of complex C-LCA models such as the CONNECTING model. While UA might be able to increase the trust in such approaches, decision making requires additional methods and measures. In the present thesis a few such measures have been presented, applied and interpreted. However several other interesting concepts where considered out of scope. Robust decision making is such a tool, which has yet to be applied to a LCA case study to steer decision makers towards an informed choice.

Bibliography

Abdul-Manan, A. F. N. (2015). Uncertainty and differences in GHG emissions between electric and conventional gasoline vehicles with implications for transport policy making. In: *Energy Policy* 87, pp. 1–7. DOI: 10.1016/j.enpol.2015.08.029.

Adnan, M., F. C. Pereira, C. M. L. Azevedo, K. Basak, M. Lovric, S. Raveau, Y. Zhu, J. Ferreira, C. Zegras, and M. E. Ben-Akiva (2016). Simmobility: A multi-scale integrated agent-based simulation platform. In: *95th Annual Meeting of the Transportation Research Board Forthcoming in Transportation Research Record.*

Alfaro, J. F., B. E. Sharp, and S. A. Miller (2010). Developing LCA techniques for emerging systems: Game theory, agent modeling as prediction tools. In: *Proceedings of the 2010 IEEE International Symposium on Sustainable Systems and Technology.* Arlington, VA: IEEE, pp. 1–6. DOI: 10.1109/ISSST.2010.5507728.

Arentze, T. A. and H. J. P. Timmermans (2004). A learning-based transportation oriented simulation system. In: *Transportation Research Part B: Methodological* 38.7, pp. 613–633. DOI: 10.1016/j.trb.2002.10.001.

Aven, T. (2010). Some reflections on uncertainty analysis and management. In: *Reliability Engineering & System Safety* 95.3, pp. 195–201. DOI: 10.1016/j.ress.2009.09.010.

Aven, T. and E. Zio (2011). Some considerations on the treatment of uncertainties in risk assessment for practical decision making. In: *Reliability Engineering & System Safety* 96.1, pp. 64–74. DOI: 10.1016/j.ress.2010.06.001.

Axhausen, K. W. and T. Gärling (1992). Activity-based approaches to travel analysis: conceptual frameworks, models, and research problems. In: *Transport Reviews* 12.4, pp. 323–341.

Axhausen, K. W., A. Horni, and K. Nagel (2016). *The multi-agent transport simulation MATSim.* Ubiquity Press.

Axtell, R. L., C. J. Andrews, and M. J. Small (2001). Agent-based modeling and industrial ecology. In: *Journal of Industrial Ecology* 5.4, pp. 10–14.

Bao, Q., B. Kochan, T. Bellemans, D. Janssens, and G. Wets (2013). Activity-Based Travel Demand Forecasting Using Micro-Simulation: Stochastic Error Investigation of FEATHERS Framework. In: *Data Science and Simulation in Transportation Research.* IGI Global, pp. 167–181.

Bao, Q., B. Kochan, T. Bellemans, D. Janssens, and G. Wets (2015). Investigating micro-simulation error in activity-based travel demand forecasting: a case study of the FEATHERS framework. In: *Transportation Planning and Technology* 38.4. Publisher: Taylor & Francis, pp. 425–441. DOI: 10.1080/03081060.2015.1026102.

Bao, Q., B. Kochan, Y. Shen, L. Creemers, T. Bellemans, D. Janssens, and G. Wets (2018). Applying FEATHERS for travel demand analysis: model considerations. In: *Applied Sciences* 8.2, p. 211. DOI: 10.3390/app8020211.

Bastin, L., D. Cornford, R. Jones, G. B. Heuvelink, E. Pebesma, C. Stasch, S. Nativi, P. Mazzetti, and M. Williams (2013). Managing uncertainty in integrated environmental modelling: The UncertWeb framework. In: *Environmental Modelling & Software* 39, pp. 116–134. DOI: 10.1016/j.envsoft.2012.02.008.

Bauer, C., J. Hofer, H.-J. Althaus, A. Del Duce, and A. Simons (2015). The environmental performance of current and future passenger vehicles: Life cycle assessment based on a novel scenario analysis framework. In: *Applied Energy* 157, pp. 871–883. DOI: 10.1016/j.apenergy.2015.01.019.

Baustert, P. and E. Benetto (2017). Uncertainty analysis in agent-based modelling and consequential life cycle assessment coupled models: A critical review. In: *Journal of Cleaner Production* 156, pp. 378–394. DOI: 10.1016/j.jclepro.2017.03.193.

Baustert, P., B. Othoniel, B. Rugani, and U. Leopold (2018). Uncertainty analysis in integrated environmental models for ecosystem service assessments: Frameworks, challenges and gaps. In: *Ecosystem Services*. DOI: 10.1016/j.ecoser.2018.08.007.

Baustert, P., T. Navarrete Gutiérrez, T. Gibon, L. Chion, T.-Y. Ma, G. L. Mariante, S. Klein, P. Gerber, and E. Benetto (2019). Coupling Activity-Based Modeling and Life Cycle Assessment—A Proof-of-Concept Study on Cross-Border Commuting in Luxembourg. In: *Sustainability* 11.15, p. 4067. DOI: 10.3390/su11154067.

Bekhor, S., L. Kheifits, and M. Sorani (2014). Stability analysis of activity-based models: case study of the Tel Aviv transportation model. In: *European Journal of Transport and Infrastructure Research* 14.4. DOI: 10.18757/ejtir.2014.14.4.3039.

Ben-Akiva, M. E. and J. L. Bowman (1998). Activity based travel demand model systems. In: *Equilibrium and Advanced Transportation Modelling*. Springer, pp. 27–46.

Beven, K., R. Lamb, D. Leedal, and N. Hunter (2015). Communicating uncertainty in flood inundation mapping: a case study. In: *International Journal of River Basin Management* 13.3, pp. 285–295. DOI: 10.1080/15715124.2014.917318.

Bhat, C. R. and F. S. Koppelman (1999). Activity-based modeling of travel demand. In: *Handbook of Transportation Science*. Springer, pp. 35–61.

Bhat, C. R., J. Guo, S. Srinivasan, and A. Sivakumar (2004). Comprehensive Econometric Microsimulator for Daily Activity-Travel Patterns. In: *Transportation Research Record: Journal of the Transportation Research Board* 1894, pp. 57–66. DOI: 10.3141/1894-07.

Bi, Z., G. A. Keoleian, and T. Ersal (2018). Wireless charger deployment for an electric bus network: A multi-objective life cycle optimization. In: *Applied Energy* 225, pp. 1090–1101. DOI: 10.1016/j.apenergy.2018.05.070.

Bichraoui-Draper, N., M. Xu, S. A. Miller, and B. Guillaume (2015). Agent-based life cycle assessment for switchgrass-based bioenergy systems. In: *Resources, Conservation and Recycling* 103, pp. 171–178. DOI: 10.1016/j.resconrec.2015.08.003.

Björklund, A. E. (2002). Survey of approaches to improve reliability in LCA. In: *The International Journal of Life Cycle Assessment* 7.2, pp. 64–72. DOI: http://dx.doi.org/10.1007/BF02978849.

Boulanger, P.-M. and T. Bréchet (2005). Models for policy-making in sustainable development: The state of the art and perspectives for research. In: *Ecological Economics* 55.3, pp. 337–350. DOI: 10.1016/j.ecolecon.2005.07.033.

Boureima, F.-S., M. Messagie, J. Matheys, V. Wynen, N. Sergeant, J. Van Mierlo, M. de Vos, and B. de Caevel (2009). Comparative LCA of electric, hybrid, LPG and gasoline cars in Belgian context. In: *World Electric Vehicle Journal* 3.3, pp. 469–476. DOI: 10.3390/wevj3030469.

Bowman, J. L. (2004). A comparison of population synthesizers used in microsimulation models of activity and travel demand. In: *Unpublished working paper. http://jbowman. net.*

Bowman, J. L. and M. E. Ben-Akiva (2001). Activity-based disaggregate travel demand model system with activity schedules. In: *Transportation Research Part A: Policy and Practice* 35.1, pp. 1–28. DOI: 10.1016/S0965-8564(99)00043-9.

Bowman, J. L., M. A. Bradley, and J. Gibb (2006). The Sacramento activity-based travel demand model: estimation and validation results. In: *European Transport Conference*. Strasbourg , France.

Bradley, M. A. and J. L. Bowman (2006). A summary of design features of activity-based microsimulation models for US MPOs. In: *White Paper for the Conference on Innovations in Travel Demand Modeling*. Austin, TX, USA.

Bradley, M. A., J. L. Bowman, and B. Griesenbeck (2010). SACSIM: An applied activity-based model system with fine-level spatial and temporal resolution. In: *Journal of Choice Modelling* 3.1, pp. 5–31. DOI: 10.1016/S1755-5345(13)70027-7.

Brandão, M., R. Clift, A. Cowie, and S. Greenhalgh (2014). The Use of Life Cycle Assessment in the Support of Robust (Climate) Policy Making: Comment on "Using Attributional Life Cycle Assessment to Estimate Climate-Change Mitigation..." In: *Journal of Industrial Ecology* 18.3, pp. 461–463. DOI: 10.1111/jiec.12152.

Cai, H. and M. Q. Wang (2014). Consideration of Black Carbon and Primary Organic Carbon Emissions in Life-Cycle Analysis of Greenhouse Gas Emissions of Vehicle Systems and Fuels. In: *Environmental Science & Technology* 48.20, pp. 12445–12453. DOI: 10.1021/es503852u.

Cai, H., M. Q. Wang, A. Elgowainy, and J. Han (2013). Life-Cycle Greenhouse Gas and Criteria Air Pollutant Emissions of Electric Vehicles in the United States. In: *SAE International Journal of Alternative Powertrains* 2.2, pp. 325–336. DOI: 10.4271/2013-01-1283.

Cash, D. W., W. C. Clark, F. Alcock, N. M. Dickson, N. Eckley, D. H. Guston, J. Jäger, and R. B. Mitchell (2003). Knowledge systems for sustainable development. In: *Proceedings of the national academy of sciences* 100.14. 01945, pp. 8086–8091. DOI: 10.1073/pnas.1231332100.

Castiglione, J., J. Freedman, and M. A. Bradley (2003). Systematic investigation of variability due to random simulation error in an activity-based microsimulation forecasting model. In: *Transportation Research Record* 1831.1, pp. 76–88.

Castiglione, J., M. A. Bradley, and J. Gliebe (2015). *Activity-based travel demand models: A primer*. Transportation Research Board.

Chowdhury, S., P. Champagne, and P. J. McLellan (2009). Uncertainty characterization approaches for risk assessment of DBPs in drinking water: A review. In: *Journal of Environmental Management* 90.5, pp. 1680–1691. DOI: 10.1016/j.jenvman.2008.12.014.

Chu, Z., L. Cheng, and H. Chen (2012). A review of activity-based travel demand modeling. In: *CICTP 2012: Multimodal Transportation Systems—Convenient, Safe, Cost-Effective, Efficient*, pp. 48–59.

Ciroth, A., S. Muller, B. P. Weidema, and P. Lesage (2013). Empirically based uncertainty factors for the pedigree matrix in ecoinvent. In: *The International Journal of Life Cycle Assessment*, pp. 1–11. DOI: 10.1007/s11367-013-0670-5.

Consoli, F. (1994). Guidelines for Life-Cycle Assessment. In: *Environmental Science and Pollution Research* 1.55. DOI: 10.1007/BF02986927.

Cools, M., B. Kochan, T. Bellemans, D. Janssens, and G. Wets (2011). Assessment of the effect of micro-simulation error on key travel indices: Evidence from the activity-based model feathers. In: *Proceedings of the 90th Annual Meeting of the Transportation Research Board*. Washington, DC, USA.

Cox, B., C. L. Mutel, C. Bauer, A. Mendoza Beltran, and D. P. van Vuuren (2018). Uncertain Environmental Footprint of Current and Future Battery Electric Vehicles. In: *Environmental Science & Technology* 52.8, pp. 4989–4995. DOI: 10.1021/acs.est.8b00261.

Cox, D. R. (1972). Regression models and life-tables. In: *Journal of the Royal Statistical Society: Series B (Methodological)* 34.2, pp. 187–202. DOI: 10.1111/j.2517-6161.1972.tb00899.x.

Curran, M. A., M. K. Mann, and G. Norris (2005). The international workshop on electricity data for life cycle inventories. In: *Journal of Cleaner Production* 13.8, pp. 853–862. DOI: 10.1016/j.jclepro.2002.03.001.

Damm, D. (1979). Interdependencies in activity behavior. In: *Transportation Research Record: Journal of the Transportation Research Board* 750, pp. 33–40.

Dandres, T., C. Gaudreault, P. Tirado-Seco, and R. Samson (2011). Assessing non-marginal variations with consequential LCA: Application to European energy sector. In: *Renewable and Sustainable Energy Reviews* 15.6, pp. 3121–3132. DOI: 10.1016/j.rser.2011.04.004.

Davidson, W. A., R. Donnelly, P. Vovsha, J. Freedman, S. Ruegg, J. Hicks, J. Castiglione, and R. Picado (2007). Synthesis of first practices and operational research approaches in activity-based travel demand modeling. In: *Transportation Research Part A: Policy and Practice* 41.5, pp. 464–488. DOI: 10.1016/j.tra.2006.09.003.

Davidson, W. A., P. Vovsha, and J. Freedman (2011). New advancements in activity-based models. In: *Australasian Transport Research Forum*. Citeseer, pp. 28–30.

Davis, C., I. Nikolić, and G. P. Dijkema (2008). Integrating life cycle analysis with agent based modeling: Deciding on bio-electricity. In: *Proceedings of the First International Conference on Infrastructure Systems and Services: Building Networks for a Brighter Future (INFRA)*. Rotterdam, The Netherlands, pp. 1–6. DOI: 10.1109/INFRA.2008.5439641.

Davis, C., I. Nikolić, and G. P. Dijkema (2009). Integration of life cycle assessment into agent-based modeling. In: *Journal of Industrial Ecology* 13.2, pp. 306–325. DOI: 10.1111/j.1530-9290.2009.00122.x.

Davis, C., I. Nikolić, and G. P. Dijkema (2010). Infrastructure modelling 2.0. In: *International Journal of Critical Infrastructures* 6.2, pp. 168–186. DOI: 10.1504/IJCIS.2010.031073.

De Jong, G., A. Daly, M. Pieters, S. Miller, R. Plasmeijer, and F. Hofman (2007). Uncertainty in traffic forecasts: literature review and new results for The Netherlands. In: *Transportation* 34.4, pp. 375–395. DOI: 10.1007/s11116-006-9110-8.

Demazeau, Y. (1995). From interactions to collective behaviour in agent-based systems. In: *Proceedings of the first European Conference on Cognitive Science*. Saint-Malo, France, pp. 117–132.

Dijkema, G. P. and L. Basson (2009). Complexity and industrial ecology: Foundations for a Transformation From Analysis to Action. In: *Journal of Industrial Ecology* 13.2, pp. 157–164. DOI: 10.1111/j.1530-9290.2009.00124.x.

Dijkema, G. P., M. Xu, S. Derrible, and R. Lifset (2015). Complexity in Industrial Ecology: Models, Analysis, and Actions. In: *Journal of Industrial Ecology* 19.2, pp. 189–194. DOI: 10.1111/jiec.12280.

Dreier, D., S. Silveira, D. Khatiwada, K. V. O. Fonseca, R. Nieweglowski, and R. Schepanski (2018). Well-to-Wheel analysis of fossil energy use and greenhouse gas emissions for conventional, hybrid-electric and plug-in hybrid-electric city buses in the BRT system in Curitiba, Brazil. en. In: *Transportation Research Part D: Transport and Environment* 58, pp. 122–138. DOI: 10.1016/j.trd.2017.10.015.

Duchin, F. (1992). Industrial input-output analysis: implications for industrial ecology. In: *Proceedings of the National Academy of Sciences* 89, pp. 851–855. DOI: 10.1073/pnas.89.3.851.

Earles, J. M. and A. Halog (2011). Consequential life cycle assessment: a review. In: *The International Journal of Life Cycle Assessment* 16.5, pp. 445–453. DOI: 10.1007/s11367-011-0275-9.

EC (2010). ILCD Handbook - General Guide for Life Cycle Assessment-Detailed Guidance. English. Tech. rep. Luxembourg: European Commission, p. 417.

Edwards, R., V. Mahieu, J.-C. Griesemann, J.-F. Larivé, and D. J. Rickeard (2004). Well-to-wheels analysis of future automotive fuels and powertrains in the European context. In: *SAE Transactions*, pp. 1072–1084.

EEA (2018a). Air quality in Europe — 2018 report. Tech. rep. 12. European Environment Agency, p. 88.

EEA (2018b). Progress of EU transport sector towards its environment and climate objectives. Tech. rep. European Environment Agency, p. 12.

Ekvall, T. (2000). A market-based approach to allocation at open-loop recycling. In: *Resources, Conservation and Recycling* 29.1, pp. 91–109. DOI: 10.1016/S0921-3449(99)00057-9.

Ekvall, T. and B. P. Weidema (2004). System boundaries and input data in consequential life cycle inventory analysis. In: *The International Journal of Life Cycle Assessment* 9.3, pp. 161–171. DOI: 10.1007/BF02994190.

Ercan, T. and O. Tatari (2015). A hybrid life cycle assessment of public transportation buses with alternative fuel options. In: *The International Journal of Life Cycle Assessment* 20.9, pp. 1213–1231. DOI: 10.1007/s11367-015-0927-2.

Eurostat (2014). Air pollution fact sheet 2014 - Luxembourg. Tech. rep. Eurostat, p. 20.

Eurostat (2017a). Energy, transport and environment indicators — 2017 edition. Tech. rep. Luxembourg: European Commission, p. 244.

Eurostat (2017b). Eurostat regional yearbook — 2017 edition. Tech. rep. Luxembourg: European Commission, p. 274.

Fargione, J., J. Hill, D. Tilman, S. Polasky, and P. Hawthorne (2008). Land clearing and the biofuel carbon debt. In: *Science* 319.5867, pp. 1235–1238. DOI: 10.1126/science.1152747.

Finkbeiner, M., E. M. Schau, A. Lehmann, and M. Traverso (2010). Towards Life Cycle Sustainability Assessment. In: *Sustainability* 2.10, pp. 3309–3322. DOI: 10.3390/su2103309.

Finnveden, G., M. Z. Hauschild, T. Ekvall, J. B. Guinée, R. Heijungs, S. Hellweg, A. Koehler, D. W. Pennington, and S. Suh (2009). Recent developments in life cycle assessment. In: *Journal of environmental management* 91.1, pp. 1–21. DOI: 10.1016/j.jenvman.2009.06.018.

Fridstrøm, L., V. Østli, and K. W. Johansen (2016). A stock-flow cohort model of the national car fleet. en. In: *European Transport Research Review* 8.3, p. 22. DOI: 10.1007/s12544-016-0210-z.

Fritschi, L., L. Brown, R. Kim, D. Schwela, and S. Kephalopolous (2011). Burden of disease from environmental noise: quantification of healthy life years lost in Europe. Tech. rep. World Health Organisation (WHO).

Funtowicz, S. O. and J. R. Ravetz (1990). *Uncertainty and quality in science for policy*. Vol. 15. Springer Science & Business Media.

Gavankar, S., S. Anderson, and A. A. Keller (2015). Critical Components of Uncertainty Communication in Life Cycle Assessments of Emerging Technologies. In: *Journal of Industrial Ecology* 19.3, pp. 468–479. DOI: 10.1111/jiec.12183.

Geyer, R. (2008). Parametric assessment of climate change impacts of automotive material substitution. In: *Environmental Science & Technology* 42.18, pp. 6973–6979. DOI: 10.1021/es800314w.

Giang, P. H. (2015). Decision making under uncertainty comprising complete ignorance and probability. In: *International Journal of Approximate Reasoning* 62, pp. 27–45. DOI: 10.1016/j.ijar.2015.05.001.

Gilbert, G. N. (2008). *Agent-based models*. 153. London: Sage.

Golob, J. and T. F. Golob (1982). A Classification of Approaches to Travel-behaviour Analysis. In: *TRB Special Report* 201, pp. 83–107.

Guinée, J. B., R. Heijungs, G. Huppes, A. Zamagni, P. Masoni, R. Buonamici, T. Ekvall, and T. Rydberg (2010). Life cycle assessment: past, present, and future. In: *Environmental Science & Technology* 45.1, pp. 90–96. DOI: 10.1021/es101316v.

Haas, T. and F. Peltier (2017). Projections macroéconomiques et démographiques de long terme: 2017-2060. Tech. rep. Luxembourg-: Institut national de la statistique et des études économiques (STATEC), p. 52.

Hamby, D. M. (1994). A review of techniques for parameter sensitivity analysis of environmental models. In: *Environmental Monitoring and Assessment* 32.2, pp. 135–154. DOI: 10.1007/BF00547132.

Harris, A., D. Soban, B. M. Smyth, and R. Best (2018). Assessing life cycle impacts and the risk and uncertainty of alternative bus technologies. In: *Renewable and Sustainable Energy Reviews* 97, pp. 569–579. DOI: 10.1016/j.rser.2018.08.045.

Harris, A., D. Soban, B. M. Smyth, and R. Best (2020). A probabilistic fleet analysis for energy consumption, life cycle cost and greenhouse gas emissions modelling of bus technologies. In: *Applied Energy* 261, p. 114422. DOI: 10.1016/j.apenergy.2019.114422.

Hauschild, M. Z., R. K. Rosenbaum, and S. I. Olsen (2017). *Life Cycle Assessment: Theory and Practice.*

Hawkins, T. R., B. Singh, G. Majeau-Bettez, and A. H. Strømman (2013). Comparative Environmental Life Cycle Assessment of Conventional and Electric Vehicles. In: *Journal of Industrial Ecology* 17.1, pp. 53–64. DOI: 10.1111/j.1530-9290.2012.00532.x.

Heairet, A., S. Choudhary, S. A. Miller, and M. Xu (2012). Beyond life cycle analysis: Using an agent-based approach to model the emerging bio-energy industry. In: *Proceedings of 2012 IEEE International Symposium on Sustainable Systems and Technology (ISSST).* Boston, MA, USA, pp. 1–5.

Heijungs, R. (1994). A generic method for the identification of options for cleaner products. In: *Ecological Economics* 10.1, pp. 69–81. DOI: 10.1016/0921-8009(94)90038-8.

Heijungs, R. (1996). Identification of key issues for further investigation in improving the reliability of life-cycle assessments. In: *Journal of Cleaner Production* 4.3, pp. 159–166. DOI: 10.1016/S0959-6526(96)00042-X.

Heijungs, R. (2010). Sensitivity coefficients for matrix-based LCA. In: *The International Journal of Life Cycle Assessment* 15.5, pp. 511–520. DOI: 10.1007/s11367-010-0158-5.

Heijungs, R. (2021). Selecting the best product alternative in a sea of uncertainty. In: *The International Journal of Life Cycle Assessment.* DOI: 10.1007/s11367-020-01851-4.

Heijungs, R. and R. Frischknecht (1998). A special view on the nature of the allocation problem. In: *The International Journal of Life Cycle Assessment* 3.6, pp. 321–332. DOI: 10.1007/BF02979343.

Heijungs, R. and S. Suh (2002). *The computational structure of life cycle assessment.* Vol. 11. Dordrecht, The Netherlands.

Heijungs, R., J. B. Guinée, G. Huppes, R. M. Lankreijer, H. A. Udo de Haes, A. Wegener Sleeswijk, A. M. M. Ansems, P. G. Eggels, R. van Duin, and H. P. de Goede (1992). Environmental life cycle assessment of products: guide and backgrounds. Tech. rep. Leiden, The Netherlands: Centre of Environmental Science.

Helder, E., M. de Bok, and G. de Jong (2015). A Review of Theoretical and Practical Issues in Microsimulating Transport Demand. In: *European Transport Conference 2015.* Frankfurt , Germany.

Helton, J. C., J. D. Johnson, and W. L. Oberkampf (2004). An exploration of alternative approaches to the representation of uncertainty in model predictions. In: *Reliability Engineering & System Safety* 85.1, pp. 39–71. DOI: 10.1016/j.ress.2004.03.025.

Henriksson, P. J. G., J. B. Guinée, R. Heijungs, A. d. Koning, and D. M. Green (2014). A protocol for horizontal averaging of unit process data—including estimates for uncertainty. In: *The*

International Journal of Life Cycle Assessment 19.2, pp. 429–436. DOI: 10.1007/s11367-013-0647-4.

Hensher, D. A. and K. J. Button (2003). *Handbook of Transport and the Environment.*

Hong, J., S. Shaked, R. K. Rosenbaum, and O. Jolliet (2010). Analytical uncertainty propagation in life cycle inventory and impact assessment: application to an automobile front panel. In: *The International Journal of Life Cycle Assessment* 15.5, pp. 499–510. DOI: 10.1007/s11367-010-0175-4.

Hsu, D. D., D. Inman, G. A. Heath, E. J. Wolfrum, M. K. Mann, and A. Aden (2010). Life Cycle Environmental Impacts of Selected U.S. Ethanol Production and Use Pathways in 2022. In: *Environmental Science & Technology* 44.13, pp. 5289–5297. DOI: 10.1021/es100186h.

Hugosson, M. B. (2005). Quantifying uncertainties in a national forecasting model. In: *Transportation Research Part A: Policy and Practice* 39.6, pp. 531–547. DOI: 10.1016/j.tra.2005.02.010.

Huijbregts, M. A. J. (1998). A General Framework for the Analysis of Uncertainty and Variability in Life Cycle Assessment–Part I: A general Framework for the Analysis of Uncertainty and Variability in Life Cycle Assessment. In: *International Journal of Life Cycle Assessment* 3.5, pp. 273–280.

Huijbregts, M. A. J., G. Norris, R. Bretz, A. Ciroth, B. Maurice, B. von Bahr, B. P. Weidema, and A. S. de Beaufort (2001). Framework for modelling data uncertainty in life cycle inventories. In: *The International Journal of Life Cycle Assessment* 6.3, pp. 127–132. DOI: 10.1007/BF02978728.

Huijbregts, M. A. J., Z. J. N. Steinmann, P. M. F. Elshout, G. Stam, F. Verones, M. Vieira, M. Zijp, A. Hollander, and R. van Zelm (2017). ReCiPe2016: a harmonised life cycle impact assessment method at midpoint and endpoint level. In: *The International Journal of Life Cycle Assessment* 22.2, pp. 138–147. DOI: 10.1007/s11367-016-1246-y.

Huo, H., H. Cai, Q. Zhang, F. Liu, and K. He (2015). Life-cycle assessment of greenhouse gas and air emissions of electric vehicles: A comparison between China and the U.S. In: *Atmospheric Environment* 108, pp. 107–116. DOI: 10.1016/j.atmosenv.2015.02.073.

Hägerstrand, T. (1970). What about people in regional science? In: *Papers of the Regional Science Association.* Vol. 24.

Igos, E., E. Benetto, R. Meyer, P. Baustert, and B. Othoniel (2018). How to treat uncertainties in life cycle assessment studies? In: *The International Journal of Life Cycle Assessment.* DOI: 10.1007/s11367-018-1477-1.

IPCC (2015). Climate change 2014: Mitigation of climate change. Tech. rep. Intergovernmental Panel on Climate Change.

IPCC (2018). Special Report on Global Warming of 1.5 degree Celcius (SR15). Tech. rep. Intergovernmental Panel on Climate Change, p. 792.

ISO (2006a). ISO 14040. In: *Environmental management – Life cycle assessment – Principles and framework.*

ISO (2006b). ISO 14044. In: *Environmental management – Life cycle assessment – Requirements and guidelines.*

Janssens, D., G. Wets, H. J. P. Timmermans, and T. A. Arentze (2007). Modelling Short-Term Dynamics in Activity-Travel Patterns: Conceptual Framework of the Feathers Model. In: *11th World Conference on Transport ResearchWorld Conference on Transport Research Society*.

Jones, P. M. (1983). A new approach to understanding travel behaviour and its implications for transportation planning. PhD thesis. Imperial College London.

Jonnalagadda, N., J. Freedman, W. A. Davidson, and J. D. Hunt (2001). Development of Microsimulation Activity-Based Model for San Francisco: Destination and Mode Choice Models. In: *Transportation Research Record* 1777.1, pp. 25–35. DOI: 10.3141/1777-03.

Jørgensen, A., A. Le Bocq, L. Nazarkina, and M. Z. Hauschild (2007). Methodologies for social life cycle assessment. In: *The International Journal of Life Cycle Assessment* 13.2, p. 96. DOI: 10.1065/lca2007.11.367.

Kelly, J. C., J. L. Sullivan, A. Burnham, and A. Elgowainy (2015). Impacts of vehicle weight reduction via material substitution on life-cycle greenhouse gas emissions. In: *Environmental Science & Technology* 49.20. Publisher: ACS Publications, pp. 12535–12542. DOI: 10.1021/acs.est.5b03192.

Kennedy, D. J., D. C. Montgomery, D. A. Rollier, and J. B. Keats (1996). Data quality. Stochastic Environmental Life Cycle Assessment Modeling. In: *The International Journal of Life Cycle Assessment* 2.4, pp. 229–239. DOI: 10.1007/BF02978693.

Kitamura, R. (1988). An evaluation of activity-based travel analysis. In: *Transportation* 15.1-2, pp. 9–34. DOI: 10.1007/BF00167973.

Kitamura, R., C. Chen, R. M. Pendyala, and R. Narayanan (2000). Micro-simulation of daily activity-travel patterns for travel demand forecasting. In: *Transportation* 27.1, pp. 25–51. DOI: 10.1023/A:1005259324588.

Klir, G. (2013). *Facets of systems science*. Vol. 7. Springer Science & Business Media.

Kloprogge, P., J. P. van der Sluijs, and J. A. Wardekker (2007). Uncertainty communication: issues and good practice. Tech. rep. Copernicus Institute for Sustainable Development and Innovation.

Knight, F. (1921). *Risk, Uncertainty and Profit*. University of Chicago Press.

Kolkman, M. J., M. Kok, and A. van der Veen (2005). Mental model mapping as a new tool to analyse the use of information in decision-making in integrated water management. In: *Physics and Chemistry of the Earth, Parts A/B/C* 30.4, pp. 317–332. DOI: 10.1016/j.pce.2005.01.002.

Kraines, S. and D. Wallace (2006). Applying Agent-based Simulation in Industrial Ecology. In: *Journal of Industrial Ecology* 10.1-2, pp. 15–18. DOI: 10.1162/108819806775545376.

Kwak, M.-A., T. A. Arentze, E. de Romph, and S. Rasouli (2012). Activity-based dynamic traffic modeling: influence of population sampling fraction size on simulation error. In: *International Association of Travel Behavior Research Conference*. Toronto, Canada, pp. 1–17.

Kwakkel, J. H., W. E. Walker, and V. A. Marchau (2010). Classifying and communicating uncertainties in model-based policy analysis. In: *International Journal of Technology, Policy and Management* 10.4, pp. 299–315. DOI: 10.1504/IJTPM.2010.036918.

Lawe, S., J. Lobb, A. Sadek, S. Huang, and C. Xie (2009). TRANSIMS implementation in Chittenden County, Vermont: development, calibration, and preliminary sensitivity analysis. In: *Transportation Research Record: Journal of the Transportation Research Board* 2132, pp. 113–121. DOI: 10.3141/2132-13.

Lenntorp, B. (1979). Das PESASP-Modell: seine theoretische Grundlegung im Rahmen des zeitgeographischen Ansatzes und Anwendungsmöglichkeiten. In: *Geographische Zeitschrift* 67.4, pp. 336–353.

Leontief, W. (1986). *Input-output economics.* Oxford University Press.

Lesage, P. and S. Muller (2017). Life Cycle Inventory: An In-Depth Look at the Modeling, Data, and Available Tools. In: *Encyclopedia of Sustainable Technologies*, p. 267.

Lloyd, S. M. and R. Ries (2007). Characterizing, Propagating, and Analyzing Uncertainty in Life-Cycle Assessment: A Survey of Quantitative Approaches. In: *Journal of Industrial Ecology* 11.1, pp. 161–179. DOI: 10.1162/jiec.2007.1136.

Lu, Z., J. Han, M. Q. Wang, H. Cai, P. Sun, D. Dieffenthaler, V. Gordillo, J.-C. Monfort, X. He, and S. Przesmitzki (2016). Well-to-Wheels Analysis of the Greenhouse Gas Emissions and Energy Use of Vehicles with Gasoline Compression Ignition Engines on Low Octane Gasoline-Like Fuel. In: *SAE International Journal of Fuels and Lubricants* 9.3, pp. 527–545.

Macal, C. M. and M. J. North (2005). Tutorial on agent-based modeling and simulation. In: *Proceedings of the Winter Simulation Conference, 2005.* Orlando, FL, USA, 14–pp.

Manzo, S., O. A. Nielsen, and C. G. Prato (2015). How uncertainty in socio-economic variables affects large-scale transport model forecasts. In: *European Journal of Transport & Infrastructure Research* 15.3, pp. 304–316. DOI: 10.18757/ejtir.2015.15.3.3080.

Mariante, G. L. (2017). Econometric generation of individual daily travel and activity pattern. MA thesis. Katholieke Universiteit Leuven.

Marvuglia, A., G. Rios, and R. Wallace (2009). A New Approach to the Inventory Problem in Life Cycle Assessment. In: *First International Workshop on Constraint Reasoning and Optimization for Computational Sustainability.* Lisbon, Portugal.

Marvuglia, A., E. Benetto, S. Rege, and C. Jury (2013). Modelling approaches for consequential life-cycle assessment (C-LCA) of bioenergy: critical review and proposed framework for biogas production. In: *Renewable and Sustainable Energy Reviews* 25, pp. 768–781. DOI: 10.1016/j.rser.2013.04.031.

Marvuglia, A., S. Rege, T. Navarrete Gutiérrez, L. Vanni, D. Stilmant, and E. Benetto (2016). A return on experience from the application of agent-based simulations coupled with life cycle assessment to model agricultural processes. In: *Journal of Cleaner Production* 142.4, pp. 1539–1551. DOI: 10.1016/j.jclepro.2016.11.150.

McCleese, D. L. and P. T. LaPuma (2002). Using Monte Carlo simulation in life cycle assessment for electric and internal combustion vehicles. In: *The International Journal of Life Cycle Assessment* 7.4, pp. 230–236. DOI: 10.1007/BF02978878.

McKay, M. D., R. J. Beckman, and W. J. Conover (1979). Comparison of three methods for selecting values of input variables in the analysis of output from a computer code. In: *Technometrics* 21.2, pp. 239–245. DOI: 10.1080/00401706.2000.10485979.

McKay, M. D., J. D. Morrison, and S. C. Upton (1999). Evaluating prediction uncertainty in simulation models. In: *Computer Physics Communications* 117.1, pp. 44–51. DOI: 10.1016/S0010-4655(98)00155-6.

McNally, M. G. (1996). An activity-based microsimulation model for travel demand forecasting. In: *Conference on Activity-based Approaches, Eindhoven University of Technology*. Eindhoven, The Netherlands.

McNally, M. G. and C. R. Rindt (2007). The activity-based approach. In: *Handbook of Transport Modelling: 2nd Edition*, pp. 55–73.

MDDI (2012). Stratégie globale pour une mobilité durable pour les résidents et les frontaliers. French. Tech. rep. Luxembourg: Ministère du Développement Durable et des Infrastructures, p. 168.

MDDI (2018). Modu 2.0 Stratégie pour une mobilité durable. Tech. rep. Luxembourg: Département des Transports, Direction de la Planification de la Mobilité, p. 53.

Meadows, D. H., D. L. Meadows, J. Randers, and W. W. Behrens (1972). *The limits to growth*. Vol. 102. New York.

Mendoza Beltran, A., V. Prado, D. Font Vivanco, P. J. G. Henriksson, J. B. Guinée, and R. Heijungs (2018a). Quantified Uncertainties in Comparative Life Cycle Assessment: What Can Be Concluded? In: *Environmental Science & Technology*. DOI: 10.1021/acs.est.7b06365.

Mendoza Beltran, A., B. Cox, C. L. Mutel, D. P. v. Vuuren, D. F. Vivanco, S. Deetman, O. Y. Edelenbosch, J. B. Guinée, and A. Tukker (2018b). When the Background Matters: Using Scenarios from Integrated Assessment Models in Prospective Life Cycle Assessment. In: *Journal of Industrial Ecology* 24.1, pp. 64–79. DOI: 10.1111/jiec.12825.

Messagie, M., F.-S. Boureima, J. Matheys, N. Sergeant, L. Turcksin, C. Macharis, and J. van Mierlo (2010). Life Cycle Assessment of conventional and alternative small passenger vehicles in Belgium. In: *2010 IEEE Vehicle Power and Propulsion Conference*. Lille, France, pp. 1–5. DOI: 10.1109/VPPC.2010.5729233.

Messagie, M., F.-S. Boureima, T. Coosemans, C. Macharis, and J. V. Mierlo (2014). A range-based vehicle life cycle assessment incorporating variability in the environmental assessment of different vehicle technologies and fuels. In: *Energies* 7.3, pp. 1467–1482. DOI: 10.3390/en7031467.

Messagie, M., T. Coosemans, and J. Van Mierlo (2019). The Need for Uncertainty Propagation in Life Cycle Assessment of Vehicle Technologies. In: *2019 IEEE Vehicle Power and Propulsion Conference (VPPC)*. Hanoi, Vietnam, pp. 1–7. DOI: 10.1109/VPPC46532.2019.8952350.

Micolier, A., P. Loubet, F. Taillandier, and G. Sonnemann (2019). To what extent can agent-based modelling enhance a life cycle assessment? Answers based on a literature review. In: *Journal of Cleaner Production* 239, p. 118123. DOI: 10.1016/j.jclepro.2019.118123.

Miller, S. A., S. Moysey, B. E. Sharp, and J. F. Alfaro (2013). A stochastic approach to model dynamic systems in life cycle assessment. In: *Journal of Industrial Ecology* 17.3, pp. 352–362. DOI: 10.1111/j.1530-9290.2012.00531.x.

Mitchell, M. (2009). *Complexity: A guided tour*. Oxford University Press.

Morgan, M. G., M. Henrion, and M. J. Small (1990). *Uncertainty: a guide to dealing with uncertainty in quantitative risk and policy analysis*. Cambridge university press.

Muller, S., P. Lesage, A. Ciroth, C. L. Mutel, B. P. Weidema, and R. Samson (2014). The application of the pedigree approach to the distributions foreseen in ecoinvent v3. In: *The International Journal of Life Cycle Assessment*, pp. 1327–1337. DOI: 10.1007/s11367-014-0759-5.

Muller, S., P. Lesage, and R. Samson (2016). Giving a scientific basis for uncertainty factors used in global life cycle inventory databases: an algorithm to update factors using new information. In: *The International Journal of Life Cycle Assessment* 21.8, pp. 1185–1196. DOI: 10.1007/s11367-016-1098-5.

Mutel, C. L. (2017). Brightway: An open source framework for Life Cycle Assessment. In: *Journal of Open Source Software* 2.12, p. 236. DOI: 10.21105/joss.00236.

Navarrete Gutiérrez, T. (2012). Une architecture de contrôle de systèmes complexes basée sur la simulation multi-agent. These de doctorat. Université de Lorraine.

Navarrete Gutiérrez, T., S. Rege, and A. Marvuglia (2015a). Does having a green conscience necessarily lead to green outcomes? Results from an Agent Based Model for agriculture in Luxembourg. In: *Adjunct Proceedings of the 29th EnviroInfo and 3rd ICT4S Conference*. Copenhagen, Denmark.

Navarrete Gutiérrez, T., S. Rege, A. Marvuglia, and E. Benetto (2015b). Introducing LCA Results to ABM for Assessing the Influence of Sustainable Behaviours. In: *Trends in Practical Applications of Agents, Multi-Agent Systems and Sustainability*, pp. 185–196.

Nikolić, I. (2009). Co-evolutionary method for modelling large scale socio-technical systems evolution. PhD thesis. TU Delft, Delft University of Technology.

Noshadravan, A., L. Cheah, R. Roth, F. Freire, L. Dias, and J. Gregory (2015). Stochastic comparative assessment of life-cycle greenhouse gas emissions from conventional and electric vehicles. In: *The International Journal of Life Cycle Assessment* 20.6, pp. 854–864. DOI: 10.1007/s11367-015-0866-y.

Nowok, B., G. M. Raab, and C. Dibben (2016). synthpop: Bespoke creation of synthetic data in R. In: *J Stat Softw* 74.11, pp. 1–26.

O'Neill, B. C., E. Kriegler, K. Riahi, K. L. Ebi, S. Hallegatte, T. R. Carter, R. Mathur, and D. P. van Vuuren (2014). A new scenario framework for climate change research: the concept of shared socioeconomic pathways. In: *Climatic Change* 122.3, pp. 387–400. DOI: 10.1007/s10584-013-0905-2.

Pas, E. I. (1985). State of the art and research opportunities in travel demand: another perspective. In: *Transportation Research A* 19.5/6, pp. 460–464.

Paulsen, M., T. K. Rasmussen, and O. A. Nielsen (2018). Output variability caused by random seeds in a multi-agent transport simulation model. In: *Procedia Computer Science* 130, pp. 850–857. DOI: 10.1016/j.procs.2018.04.078.

PBL (2014). *Integrated Assessment of Global Environmental Change with IMAGE 3.0 - Model description and policy applications*. en. Text. Library Catalog: www.pbl.nl.

Perez, P., A. Banos, and C. Pettit (2017). Agent-Based Modelling for Urban Planning Current Limitations and Future Trends. In: *Agent Based Modelling of Urban Systems*. Singapore, Singapore, pp. 60–69. DOI: 10.1007/978-3-319-51957-9_4.

Petersen, A. C., P. H. M. Janssen, J. P. van der Sluijs, J. S. Risbey, J. R. Ravetz, J. A. Wardekker, and H. Martinson (2013). *Guidance for Uncertainty Assessment and Communication, second edition*. BPL Netherlands Environmental Assessment Agency.

Petrik, O., M. Adnan, K. Basak, and M. E. Ben-Akiva (2018). Uncertainty analysis of an activity-based microsimulation model for Singapore. In: *Future Generation Computer Systems* 110, pp. 350–363. DOI: 10.1016/j.future.2018.04.078.

Pigné, Y., T. Navarrete Gutiérrez, T. Gibon, T. Schaubroeck, E. Popovici, A. H. Shimako, E. Benetto, and L. Tiruta-Barna (2019). A tool to operationalize dynamic LCA, including time differentiation on the complete background database. In: *The International Journal of Life Cycle Assessment*, pp. 267–279. DOI: 10.1007/s11367-019-01696-6.

Pinjari, A. R. and C. R. Bhat (2011). Activity-based travel demand analysis. In: *A Handbook of Transport Economics* 10, pp. 213–248. DOI: 10.4337/9780857930873.00017.

Popper, K. R. (1962). On the Sources of Knowledge and of Ignorance. In: *Philosophy and Phenomenological Research*. DOI: 10.2307/2104935.

Pryshlakivsky, J. and C. Searcy (2017). Uncertainty analysis focusing on the variance of energy intensity of vehicle materials. In: *Journal of Cleaner Production* 143, pp. 1165–1182. DOI: 10.1016/j.jclepro.2016.12.004.

Querini, F. and E. Benetto (2013). Definition and influence of functional unit in LCA of electric and plug-in hybrid vehicles applied to implantation scenarios. In: *Proceddings of the 6th International Conference on Life Cycle Management – LCM*. Berlin, Germany.

Querini, F. and E. Benetto (2014). Agent-based modelling for assessing hybrid and electric cars deployment policies in Luxembourg and Lorraine. In: *Transportation Research Part A: Policy and Practice* 70, pp. 149–161. DOI: 10.1016/j.tra.2014.10.017.

Querini, F. and E. Benetto (2015). Combining Agent-Based Modeling and Life Cycle Assessment for the Evaluation of Mobility Policies. In: *Environmental Science & Technology* 49.3, pp. 1744–1751. DOI: 10.1021/es5060868.

Rasouli, S. (2016). Uncertainty in modeling activity-travel demand in complex urban systems. PhD thesis. TU Eindhoven.

Rasouli, S. and H. J. P. Timmermans (2012). Uncertainty in travel demand forecasting models: literature review and research agenda. In: *Transportation Letters* 4.1, pp. 55–73. DOI: 10.3328/TL.2012.04.01.55-73.

Rasouli, S. and H. J. P. Timmermans (2013a). Assessment of model uncertainty in destinations and travel forecasts of models of complex spatial shopping behaviour. In: *Journal of Retailing and Consumer Services* 20.2. Publisher: Elsevier, pp. 139–146. DOI: 10.1016/j.jretconser.2012.05.001.

Rasouli, S. and H. J. P. Timmermans (2013b). Probabilistic forecasting of time-dependent origin–destination matrices by a complex activity-based model system: effects of model uncertainty. In: *International Journal of Urban Sciences* 17.3, pp. 350–361. DOI: 10.1080/12265934.2013.835117.

Rasouli, S. and H. J. P. Timmermans (2013c). Uncertainty in Predicted Sequences of Activity Travel Episodes. In: *Transportation Research Record: Journal of the Transportation Research Board* 2382, pp. 46–53. DOI: 10.3141/2382-06.

Rasouli, S. and H. J. P. Timmermans (2014a). Activity-based models of travel demand: promises, progress and prospects. In: *International Journal of Urban Sciences* 18.1, pp. 31–60. DOI: 10.1080/12265934.2013.835118.

Rasouli, S. and H. J. P. Timmermans (2014b). Uncertain travel times and activity schedules under conditions of space-time constraints and invariant choice heuristics. In: *Environment and Planning B: Planning and Design* 41.6, pp. 1022–1030. DOI: 10.1068/b130062p.

Rasouli, S., T. A. Arentze, and H. J. P. Timmermans (2012). Analysis of Uncertainty in Performance Indicators of a Complex Activity-Based Model: The Case of the Albatross Model System. In: *Proceedings innovations in travel demand modelling conference*. Tampa, FL, USA.

Raykin, L., H. L. MacLean, and M. J. Roorda (2012). Implications of driving patterns on well-to-wheel performance of plug-in hybrid electric vehicles. In: *Environmental Science & Technology* 46.11, pp. 6363–6370. DOI: 10.1021/es203981a.

Rebitzer, G., T. Ekvall, R. Frischknecht, D. Hunkeler, G. Norris, T. Rydberg, W.-P. Schmidt, S. Suh, B. P. Weidema, and D. W. Pennington (2004). Life cycle assessment: Part 1: Framework, goal and scope definition, inventory analysis, and applications. In: *Environment international* 30.5, pp. 701–720. DOI: 10.1016/j.envint.2003.11.005.

Refsgaard, J. C., J. P. van der Sluijs, A. L. Højberg, and P. A. Vanrolleghem (2007). Uncertainty in the environmental modelling process–a framework and guidance. In: *Environmental Modelling & Software* 22.11, pp. 1543–1556. DOI: 10.1016/j.envsoft.2007.02.004.

Rich, J., O. A. Nielsen, C. Brems, and C. O. Hansen (2010). Overall design of the Danish national transport model. In: *Proceedings from the Annual Transport Conference at Aalborg University*. Issue: 1. Aalborg, Denmark. DOI: 10.5278/ojs.td.v17i1.5509.

Roy, C. and W. L. Oberkampf (2012). A Complete Framework for Verification, Validation, and Uncertainty Quantification in Scientific Computing. In: *48th AIAA Aerospace Sciences Meeting Including the New Horizons Forum and Aerospace Exposition*. Orlando, FL, USA. DOI: 10.2514/6.2010-124.

Russell, A., T. Ekvall, and H. Baumann (2005). Life cycle assessment–introduction and overview. In: *Journal of Cleaner Production* 13.13, pp. 1207–1210. DOI: 10.1016/j.jclepro.2005.05.008.

Saltelli, A. and P. Annoni (2010). How to avoid a perfunctory sensitivity analysis. In: *Environmental Modelling & Software* 25.12, pp. 1508–1517. DOI: 10.1016/j.envsoft.2010.04.012.

Saltelli, A., K. Chan, and E. M. Scott (2000). *Sensitivity analysis*. Vol. 1. Wiley New York.

Samaras, C. and K. Meisterling (2008). Life Cycle Assessment of Greenhouse Gas Emissions from Plug-in Hybrid Vehicles: Implications for Policy. In: *Environmental Science & Technology* 42.9, pp. 3170–3176. DOI: 10.1021/es702178s.

Schmitz, F. and P. Gerber (2011). Voiture ou transports en commun? Comment les frontaliers se rendent-ils au travail en 2010? In: *Vivre au Luxembourg* 78.

Schmitz, F., G. Drevon, and P. Gerber (2012). *La mobilité des frontaliers du Luxembourg: dynamiques et perspectives*. Esch-sur-Alzette: CEP/INSTEAD.

Searchinger, T., R. Heimlich, R. A. Houghton, F. Dong, A. Elobeid, J. Fabiosa, S. Tokgoz, D. Hayes, and T.-H. Yu (2008). Use of US croplands for biofuels increases greenhouse

gases through emissions from land-use change. In: *Science* 319.5867, pp. 1238–1240. DOI: `10.1126/science.1151861`.

Shiftan, Y., M. E. Ben-Akiva, K. Proussaloglou, G. de Jong, Y. Popuri, K. Kasturirangan, and S. Bekhor (2004). The Tel Aviv Activity Based Model System. In: *EIRASS. In: Conference on Progress in Activity-Based Analysis.* Maastricht, The Netherlands.

Smith, L., R. J. Beckman, and K. Baggerly (1995). TRANSIMS: Transportation analysis and simulation system. Tech. rep. Los Alamos National Lab., NM (United States).

Spielmann, M. and H.-J. Althaus (2007). Can a prolonged use of a passenger car reduce environmental burdens? Life Cycle analysis of Swiss passenger cars. In: *Journal of Cleaner Production.* The Automobile Industry & Sustainability 15.11, pp. 1122–1134. DOI: `10.1016/j.jclepro.2006.07.022`.

Spielmann, M., R. W. Scholz, O. Tietje, and P. d. Haan (2005). Scenario Modelling in Prospective LCA of Transport Systems. Application of Formative Scenario Analysis. In: *The International Journal of Life Cycle Assessment* 10.5, pp. 325–335. DOI: `10.1065/lca2004.10.188`.

Spielmann, M., P. de Haan, and R. W. Scholz (2008). Environmental rebound effects of high-speed transport technologies: a case study of climate change rebound effects of a future underground maglev train system. In: *Journal of Cleaner Production* 16.13. Publisher: Elsevier, pp. 1388–1398. DOI: `10.1016/j.jclepro.2007.08.001`.

STATEC (2018). Le Luxembourg en chiffres. Tech. rep. Institut national de la statistique et des études économiques (STATEC), p. 54.

STATEC (2019). Économie et statistiques N° 105/2019 Projections économiques à moyen terme 2019-2023. fr. Tech. rep. Luxembourg: Institut national de la statistique et des études économiques (STATEC), p. 30.

Stevens, S. S. (1946). On the theory of scales of measurement. In: *Science* 103, pp. 677–680.

Subramanyan, K., Y. Wu, U. M. Diwekar, and M. Q. Wang (2008). New stochastic simulation capability applied to the GREET model. In: *The International Journal of Life Cycle Assessment* 13.3, pp. 278–285. DOI: `10.1065/lca2007.07.354`.

Suh, S. and G. Huppes (2005). Methods for Life Cycle Inventory of a product. In: *Journal of Cleaner Production* 13.7, pp. 687–697. DOI: `10.1016/j.jclepro.2003.04.001`.

Swarr, T. E., D. Hunkeler, W. Klöpffer, H.-L. Pesonen, A. Ciroth, A. C. Brent, and R. Pagan (2011). Environmental life-cycle costing: a code of practice. In: *The International Journal of Life Cycle Assessment* 16.5, pp. 389–391. DOI: `10.1007/s11367-011-0287-5`.

Thompson, M., R. Ellis, and A. Wildavsky (2018). *Cultural Theory.* Routledge.

Tillman, A.-M. (2000). Significance of decision-making for LCA methodology. In: *Environmental Impact Assessment Review* 20.1, pp. 113–123. DOI: `10.1016/S0195-9255(99)00035-9`.

Transport & Environment (2018). Electric buses arrive on time. Marketplace, economic, technology, environmental and policy perspectives for fully electric buses in the EU. Tech. rep. Brussels: Transport & Environment, p. 35.

Vedung, E. (2017). Policy instruments: typologies and theories. In: *Carrots, sticks and sermons.* Routledge, pp. 21–58.

Veldhuisen, J., H. J. P. Timmermans, and L. Kapoen (2000a). Microsimulation Model of Activity-Travel Patterns and Traffic Flows: Specification, Validation Tests, and Monte Carlo Error. In: *Transportation Research Record* 1706.1, pp. 126–135. DOI: 10.3141/1706-15.

Veldhuisen, J., H. J. P. Timmermans, and L. Kapoen (2000b). RAMBLAS: A Regional Planning Model Based on the Microsimulation of Daily Activity Travel Patterns. In: *Environment and Planning A: Economy and Space* 32.3, pp. 427–443. DOI: 10.1068/a325.

Vermeulen, I., J. van Caneghem, C. Block, J. Baeyens, and C. Vandecasteele (2011). Automotive shredder residue (ASR): Reviewing its production from end-of-life vehicles (ELVs) and its recycling, energy or chemicals' valorisation. In: *Journal of Hazardous Materials* 190.1, pp. 8–27. DOI: 10.1016/j.jhazmat.2011.02.088.

Verán-Leigh, D., G. Larrea-Gallegos, and I. Vázquez-Rowe (2019). Environmental impacts of a highly congested section of the Pan-American highway in Peru using life cycle assessment. In: *The International Journal of Life Cycle Assessment* 24.8, pp. 1496–1514. DOI: 10.1007/s11367-018-1574-1.

Vigon, B. W., B. W. Vigon, and C. L. Harrison (1993). *Life-cycle assessment: Inventory guidelines and principles.* Cincinnati, Ohio.

Vovsha, P., R. Donnelly, and S. Gupta (2008). Network equilibrium with activity-based microsimulation models: the New York experience. In: *Transportation Research Record* 2054.1, pp. 102–109. DOI: 10.3141/2054-12.

Vázquez-Rowe, I., S. Rege, A. Marvuglia, J. Thénie, A. Haurie, and E. Benetto (2013). Application of three independent consequential LCA approaches to the agricultural sector in Luxembourg. In: *The International Journal of Life Cycle Assessment* 18.8, pp. 1593–1604. DOI: 10.1007/s11367-013-0604-2.

Walker, W. E., P. Harremoës, J. Rotmans, J. P. van der Sluijs, M. B. van Asselt, P. H. M. Janssen, and M. P. Krayer von Krauss (2003). Defining uncertainty: a conceptual basis for uncertainty management in model-based decision support. In: *Integrated Assessment* 4.1, pp. 5–17. DOI: 10.1076/iaij.4.1.5.16466.

Wang, M. Q. (2002). Fuel choices for fuel-cell vehicles: well-to-wheels energy and emission impacts. In: *Journal of Power Sources* 112.1, pp. 307–321. DOI: 10.1016/S0378-7753(02)00447-0.

Wardekker, J. A., J. P. van der Sluijs, P. H. M. Janssen, P. Kloprogge, and A. C. Petersen (2008). Uncertainty communication in environmental assessments: views from the Dutch science-policy interface. In: *Environmental Science & Policy* 11.7, pp. 627–641. DOI: 10.1016/j.envsci.2008.05.005.

Warmink, J. J., J. Janssen, M. J. Booij, and M. S. Krol (2010). Identification and classification of uncertainties in the application of environmental models. In: *Environmental Modelling & Software* 25.12, pp. 1518–1527. DOI: 10.1016/j.envsoft.2010.04.011.

Weidema, B. P. (1993). Market aspects in product life cycle inventory methodology. In: *Journal of Cleaner Production* 1.3, pp. 161–166. DOI: http://dx.doi.org/10.1016/0959-6526(93)90007-X.

Weidema, B. P. (2003). *Market information in life cycle assessment.* Vol. 863. Environmental Project No. 863. Copenhagen, Denmark: Danish Environmental Protection Agency.

Weidema, B. P. and M. S. Wesnæs (1996). Data quality management for life cycle inventories—an example of using data quality indicators. In: *Journal of Cleaner Production* 4.3, pp. 167–174. DOI: 10.1016/S0959-6526(96)00043-1.

Weidema, B. P., N. Frees, and A.-M. Nielsen (1999). Marginal production technologies for life cycle inventories. In: *The International Journal of Life Cycle Assessment* 4.1, pp. 48–56. DOI: 10.1007/BF02979395.

Whitefoot, K. S., H. G. Grimes-Casey, C. E. Girata, W. R. Morrow, J. J. Winebrake, G. A. Keoleian, and S. J. Skerlos (2011). Consequential life cycle assessment with market-driven design. In: *Journal of Industrial Ecology* 15.5, pp. 726–742. DOI: 10.1111/j.1530-9290.2011.00367.x.

Wigan, M. R. and J. M. Morris (1981). The transport implications of activity and time budget constraints. In: *Transportation Research Part A: General* 15.1, pp. 63–86. DOI: 10.1016/0191-2607(83)90017-1.

Wu, Y., M. Q. Wang, P. B. Sharer, and A. Rousseau (2006). Well-to-Wheels Results of Energy Use, Greenhouse Gas Emissions, and Criteria Air Pollutant Emissions of Selected Vehicle/Fuel Systems. In: *SAE Transactions* 115, pp. 210–222. DOI: 10.4271/2006-01-0377.

Ziems, S. E., B. Sana, J. Plotz, and R. M. Pendyala (2011). Stochastic variability in microsimulation modeling results and convergence of corridor-level characteristics. In: *90th Annual Meeting of the Transportation Research Board*. Washington, DC, USA.

Author index

Cools, M. 29, 43, 46
Coosemans, T. 36, 38, 40
Cornford, D. 33
Cowie, A. 16
Cox, B. 35, 38, 39, 86
Cox, D. R. 64
Creemers, L. 47
Curran, M. A. 16

Daly, A. 28, 82
Damm, D. 17, 18
Dandres, T. 16
Davidson, W. A. 3, 17, 18, 42
Davis, C. 21, 23
de Beaufort, A. S. 33
de Bok, M. 84
de Caevel, B. 38, 39, 88
de Goede, H. P. 8
de Haan, P. 35, 37–39
de Jong, G. 28, 42, 82, 84
de Romph, E. 42, 43, 47, 82
de Vos, M. 38, 39, 88
Deetman, S. 38
Del Duce, A. 3
Demazeau, Y. 20
Derrible, S. 20, 21
Dias, L. 37, 38
Dibben, C. 63
Dickson, N. M. 5
Dieffenthaler, D. 37
Dijkema, G. P. 20, 21, 23
Diwekar, U. M. 37, 39
Dong, F. 16
Donnelly, R. 3, 17, 18, 43, 45, 47, 83
Dreier, D. 35, 37
Drevon, G. 55
Duchin, F. 13

Earles, J. M. 16
Ebi, K. L. 33
EC 2, 3, 8, 9
Eckley, N. 5
Edelenbosch, O. Y. 38
Edwards, R. 35, 37
EEA 2
Eggels, P. G. 8
Ekvall, T. 3, 8, 16
Elgowainy, A. 35, 37, 38
Ellis, R. 36
Elobeid, A. 16

Elshout, P. M. F. 36
Ercan, T. 35, 37
Ersal, T. 35, 37
Eurostat 1, 3, 4

Fabiosa, J. 16
Fargione, J. 16
Ferreira, J. 42
Finkbeiner, M. 8
Finnveden, G. 3
Fonseca, K. V. O. 35, 37
Font Vivanco, D. xiii, 35, 90, 111, 155
Freedman, J. 3, 17, 18, 42, 43, 46, 47
Frees, N. 16
Freire, F. 37, 38
Fridstrøm, L. 71
Frischknecht, R. 15, 16
Fritschi, L. 2
Funtowicz, S. O. 5, 25, 33

Gaudreault, C. 16
Gavankar, S. 35
Gerber, P. xii, xv, 6, 49, 55, 58, 69–72, 75
Geyer, R. 35, 38
Giang, P. H. 31
Gibb, J. 43, 45, 47, 83
Gibon, T. xii, xv, 6, 13, 49, 58, 69–72, 75
Gilbert, G. N. 20
Girata, C. E. 5
Gliebe, J. 69, 77, 78
Golob, J. 17
Golob, T. F. 17
Gordillo, V. 37
Green, D. M. 34
Greenhalgh, S. 16
Gregory, J. 37, 38
Griesemann, J.-C. 35, 37
Griesenbeck, B. 42
Grimes-Casey, H. G. 5
Guillaume, B. 22
Guinée, J. B. xiii, 3, 8, 34, 35, 38, 90, 111, 155
Guo, J. 19
Gupta, S. 43, 45, 47, 83
Guston, D. H. 5
Gärling, T. 17, 18

Haan, P. d. 35, 37–39
Haas, T. 69
Hallegatte, S. 33
Halog, A. 16

Hamby, D. M. 34
Han, J. 37
Hansen, C. O. 42
Harremoës, P. 25, 26, 28–32, 47, 152
Harris, A. 35, 38
Harrison, C. L. 8
Haurie, A. 16
Hauschild, M. Z. xi, 3, 8, 27–29, 32, 33
Hawkins, T. R. 3
Hawthorne, P. 16
Hayes, D. 16
He, K. 37
He, X. 37
Heairet, A. 22
Heath, G. A. 35, 37
Heijungs, R. xiii, 3, 8, 11, 13, 15, 31, 34, 35, 59,
    60, 90, 111, 155
Heimlich, R. 16
Helder, E. 84
Hellweg, S. 3
Helton, J. C. 33
Henriksson, P. J. G. xiii, 34, 35, 90, 111, 155
Henrion, M. 5, 29, 31, 33
Hensher, D. A. 2
Heuvelink, G. B. 33
Hicks, J. 3, 17, 18
Hill, J. 16
Hofer, J. 3
Hofman, F. 28, 82
Hollander, A. 36
Hong, J. 34
Horni, A. 42
Houghton, R. A. 16
Hsu, D. D. 35, 37
Huang, S. 47
Hugosson, M. B. 29
Huijbregts, M. A. J. 27, 29, 31, 33, 36
Hunkeler, D. 8, 16
Hunt, J. D. 42
Hunter, N. 33
Huo, H. 37
Huppes, G. 8, 13
Hägerstrand, T. 18, 19
Højberg, A. L. 5, 26, 33

Igos, E. 31, 34, 35
Inman, D. 35, 37
IPCC 2
ISO xi, 3, 8–10, 49

Janssen, J. 26, 33
Janssen, P. H. M. 25, 26, 28–32, 35, 47, 152
Janssens, D. 29, 42, 43, 46, 47
Johansen, K. W. 71
Johnson, J. D. 33
Jolliet, O. 34
Jones, P. M. 1, 17–19
Jones, R. 33
Jonnalagadda, N. 42
Jury, C. 4, 16
Jäger, J. 5
Jørgensen, A. 8

Kapoen, L. 42, 43, 47
Kasturirangan, K. 42
Keats, J. B. 86
Keller, A. A. 35
Kelly, J. C. 35, 38
Kennedy, D. J. 86
Keoleian, G. A. 5, 35, 37
Kephalopolous, S. 2
Khatiwada, D. 35, 37
Kheifits, L. 42, 43, 47
Kim, R. 2
Kitamura, R. 17, 18
Klein, S. xii, xv, 6, 49, 58, 69–72, 75
Klir, G. 29
Kloprogge, P. 5, 35
Klöpffer, W. 8
Knight, F. 30
Kochan, B. 29, 43, 46, 47
Koehler, A. 3
Kok, M. 5
Kolkman, M. J. 5
Koning, A. d. 34
Koppelman, F. S. 17, 18
Kraines, S. 21
Krayer von Krauss, M. P. 25, 26, 28–32, 47, 152
Kriegler, E. 33
Krol, M. S. 26, 33
Kwak, M.-A. 42, 43, 47, 82
Kwakkel, J. H. 26, 30

Lamb, R. 33
Lankreijer, R. M. 8
LaPuma, P. T. 35, 38
Larivé, J.-F. 35, 37
Larrea-Gallegos, G. 35
Lawe, S. 47
Le Bocq, A. 8

Leedal, D. 33
Lehmann, A. 8
Lenntorp, B. 19
Leontief, W. 13
Leopold, U. xi, 5, 6, 31, 32
Lesage, P. xv, 12, 79, 80, 82, 115, 120
Lifset, R. 20, 21
Liu, F. 37
Lloyd, S. M. 29, 34
Lobb, J. 47
Loubet, P. 21, 22
Lovric, M. 42
Lu, Z. 37

Ma, T.-Y. xii, xv, 6, 49, 58, 69–72, 75
Macal, C. M. 20
Macharis, C. 38
MacLean, H. L. 58
Mahieu, V. 35, 37
Majeau-Bettez, G. 3
Mann, M. K. 16, 35, 37
Manzo, S. 32, 42–45, 47, 82
Marchau, V. A. 26, 30
Mariante, G. L. xii, xv, 6, 49, 58, 62, 63, 69–72, 75, 78, 83
Martinson, H. 35
Marvuglia, A. 4, 15, 16, 21, 23
Masoni, P. 8
Matheys, J. 38, 39, 88
Mathur, R. 33
Maurice, B. 33
Mazzetti, P. 33
McCleese, D. L. 35, 38
McKay, M. D. 29, 34
McLellan, P. J. 33
McNally, M. G. 17, 18
MDDI 4, 69
Meadows, D. H. 8
Meadows, D. L. 8
Meisterling, K. 35, 38
Mendoza Beltran, A. xiii, 35, 38, 39, 86, 90, 111, 155
Messagie, M. 36, 38–40, 88
Meyer, R. 31, 34, 35
Micolier, A. 21, 22
Mierlo, J. V. 38
Miller, S. 28, 82
Miller, S. A. 22, 23
Mitchell, M. 20

Mitchell, R. B. 5
Monfort, J.-C. 37
Montgomery, D. C. 86
Morgan, M. G. 5, 29, 31, 33
Morris, J. M. 17
Morrison, J. D. 29
Morrow, W. R. 5
Moysey, S. 23
Muller, S. xv, 12, 79, 80, 82, 115, 120
Mutel, C. L. 35, 38, 39, 68, 79, 80, 83, 86

Nagel, K. 42
Narayanan, R. 18
Nativi, S. 33
Navarrete Gutiérrez, T. xii, xv, 6, 13, 21, 23, 49, 58, 69–72, 75, 76
Nazarkina, L. 8
Nielsen, A.-M. 16
Nielsen, O. A. 32, 42–45, 47, 82
Nieweglowski, R. 35, 37
Nikolić, I. 21, 23
Norris, G. 16, 33
North, M. J. 20
Noshadravan, A. 37, 38
Nowok, B. 63

Oberkampf, W. L. 33
Olsen, S. I. xi, 27–29, 32, 33
Othoniel, B. xi, 5, 6, 31, 32, 34, 35
O'Neill, B. C. 33

Pagan, R. 8
Pas, E. I. 17, 18
Paulsen, M. 47
PBL 38
Pebesma, E. 33
Peltier, F. 69
Pendyala, R. M. 18, 47
Pennington, D. W. 3, 16
Pereira, F. C. 42
Perez, P. 20
Pesonen, H.-L. 8
Petersen, A. C. 35
Petrik, O. 29, 30, 42–47, 75, 82
Pettit, C. 20
Picado, R. 3, 17, 18
Pieters, M. 28, 82
Pigné, Y. 13
Pinjari, A. R. 17
Plasmeijer, R. 28, 82

41–43, 46, 47, 75, 85, 86
Tirado-Seco, P. 16
Tiruta-Barna, L. 13
Tokgoz, S. 16
Transport & Environment 58
Traverso, M. 8
Tukker, A. 38
Turcksin, L. 38

Udo de Haes, H. A. 8
Upton, S. C. 29

van Asselt, M. B. 25, 26, 28–32, 47, 152
van Caneghem, J. 2
van der Sluijs, J. P. 5, 25, 26, 28–33, 35, 47, 152
van der Veen, A. 5
van Duin, R. 8
van Mierlo, J. 38
van Vuuren, D. P. 33, 35, 38, 39, 86
van Zelm, R. 36
Vandecasteele, C. 2
Vanni, L. 23
Vanrolleghem, P. A. 5, 26, 33
Vedung, E. 2
Veldhuisen, J. 42, 43, 47
Vermeulen, I. 2
Verones, F. 36
Verán-Leigh, D. 35
Vieira, M. 36
Vigon, B. W. 8
Vivanco, D. F. 38
von Bahr, B. 33
Vovsha, P. 3, 17, 18, 43, 45, 47, 83
Vuuren, D. P. v. 38

Vázquez-Rowe, I. 16, 35

Walker, W. E. 25, 26, 28–32, 47, 152
Wallace, D. 21
Wallace, R. 15
Wang, M. Q. 37, 39
Wardekker, J. A. 5, 35
Warmink, J. J. 26, 33
Wegener Sleeswijk, A. 8
Weidema, B. P. 16, 33, 34, 78–80, 115, 120
Wesnæs, M. S. 34, 78, 79
Wets, G. 29, 42, 43, 46, 47
Whitefoot, K. S. 5
Wigan, M. R. 17
Wildavsky, A. 36
Williams, M. 33
Winebrake, J. J. 5
Wolfrum, E. J. 35, 37
Wu, Y. 37, 39
Wynen, V. 38, 39, 88

Xie, C. 47
Xu, M. 20–22

Yu, T.-H. 16

Zamagni, A. 8
Zegras, C. 42
Zhang, Q. 37
Zhu, Y. 42
Ziems, S. E. 47
Zijp, M. 36
Zio, E. 33

Østli, V. 71

Curriculum Vitae

Paul Baustert was born on 31-10-1988 in Friesach, Austria.

After finishing his études secondaires classiques in 2008 at the Lycée Hubert Clément in Esch-sur-Alzette, Luxembourg, he studied environmental engineering at the Swiss Federal Institute of Technology in Zurich, Switzerland. In 2015 he graduated within the Ecological Systems Design group on "How quickly can we restore the biodiversity of aquatic habitats? A meta analysis". From 2015-2021 he started a PhD project at Technische Universiteit Eindhoven at Eindhoven, Netherlands of which the results are presented in this dissertation. Since 2015 he is employed at Luxembourg Institute of Science and Technology.